



UNIVERSITÀ DEGLI STUDI DI PADOVA

DIPARTIMENTO DI INGEGNERIA INDUSTRIALE

CORSO DI LAUREA MAGISTRALE IN
INGEGNERIA ELETTRICA

TESI DI LAUREA MAGISTRALE

**Decoupled On-Load Tap-Changer
Transformer in a Danish Low Voltage Grid
with Unbalanced Distributed Generation**

RELATORE: Prof. Roberto Turri

Dipartimento di Ingegneria Industriale

CORRELATORE: Research Scientist Mattia Marinelli

Department of Electrical Engineering – Technical University of Denmark

CORRELATORE: Ing. Massimiliano Coppo

Dipartimento di Ingegneria Industriale

LAUREANDO: Antonio Zecchino - 1058554

ANNO ACCADEMICO 2014/2015

Ringraziamenti

Questa tesi rappresenta per me un traguardo importantissimo, che senza l'aiuto fondamentale di alcune persone non sarei sicuramente riuscito a raggiungere, tantomeno con stessa serenità, grinta e determinazione.

Ringrazio in primis i miei genitori e mia sorella: mi hanno permesso di intraprendere e portare a termine questo percorso senza alcuna preoccupazione di altro tipo, consentendomi sempre di poter dedicare alla causa tutto il tempo che io avessi ritenuto necessario. Senza il loro apporto emotivo e la loro pazienza quotidiana ritengo che questa méta sarebbe stata sicuramente più difficile, se non impossibile.

Un ringraziamento speciale va ovviamente ad Elena, con la quale ho trascorso assieme tutti e cinque gli anni del mio percorso accademico, condividendo sia gioie che sacrifici. La ringrazio per essere sempre riuscita a starmi vicino nonostante i numerosi periodi di lontananza per studio e per essere sempre stata pronta a dispensarmi saggi consigli e pareri sempre molto utili.

Riservo inoltre un caloroso ringraziamento a mia nonna Gianna: la sua vicinanza e il suo supporto non si sono fatti mancare dal primo all'ultimo giorno di questa avventura; sempre pronta a rivolgermi un pensiero o una preghiera, la ringrazio davvero di cuore.

Infine vorrei dedicare un pensiero a tutte le persone, parenti ed amici, che hanno gioito per i risultati da me ottenuti e che sono state orgogliose di me.

Abstract

The increasing penetration of fluctuating photovoltaic generation brings operational challenge for distribution system operators such as introducing voltage rise problem. The situation is worse in presence of single-phase generation unevenly connected on the phases. To address this problem, distribution transformers with single-phase tapping capability and automatic reactive power management systems are under development. This thesis presents modeling and analysis on the benefits of coordinated actions of a decoupled three-phase on-load tap-changer and a reactive power control by photovoltaic inverters in distribution system, for accommodating more renewable generations in the grid. 24-hours root-mean-square simulation studies have been carried out in DIgSILENT PowerFactory software environment with time-step of 1 second using 10-mins resolution consumption and production profiles. A merely passive real Danish low voltage distribution network is used for the grid topology as well as for the characterization of loads profiles, while the production ones are empirically defined under specific assumptions in scenarios with different level of photovoltaic penetration. A first set of simulations without any reactive power provided by photovoltaic inverters show that power distribution transformer with on-load tap-changer control on each phase significantly improves the photovoltaic hosting capacity in the analyzed unbalanced scenarios without side effects such as causing additional power losses, or significant neutral voltage rising or worsening of the voltage unbalance factor. The second set of simulations is based on coordinated actions of the two control systems: a further improve of the photovoltaic hosting capacity is allowed, since the phase-neutral voltage deviations and the neutral potential are reduced without worsening of the power losses. Negative effects will be found on the voltage unbalance factor, which is not controlled by the two control logics and should hence be considered elsewhere by the distribution system operator.

Contents

| | | |
|-----------|--|-----------|
| 1. | Introduction | 1 |
| 1.1. | Project Goals | 1 |
| 1.2. | Problem Statement | 2 |
| 1.3. | Background to unbalance conditions | 7 |
| 1.4. | Background to Power Quality | 13 |
| 1.5. | Background to OLTC and similar products | 20 |
| 1.6. | Power system simulation tool | 25 |
| 2. | Network Modeling | 27 |
| 2.1. | Real Danish network layout | 27 |
| 2.2. | Multiphase system modeling | 29 |
| 2.3. | Loads and PVs modeling | 30 |
| 2.4. | Transformer modeling..... | 34 |
| 2.4.1. | <i>Tapping Logic</i> | 38 |
| 2.5. | Dynamics analysis – RMS Simulation in DIgSILENT PowerFactory | 42 |
| 2.6. | Grid elements modeling in PowerFactory..... | 49 |
| 2.6.1. | <i>Transformer Controller</i> | 49 |
| 2.6.2. | <i>Passive Loads</i> | 51 |
| 2.6.3. | <i>Active Loads</i> | 51 |
| 2.6.4. | <i>Active Loads with Q regulation</i> | 53 |
| 3. | Scenarios and Indexes Definition | 55 |
| 3.1. | Testing scenarios..... | 55 |
| 3.1.1. | <i>Phase-neutral voltages at each bus</i> | 57 |
| 3.1.2. | <i>Phase- ground voltages at the secondary side of the transformer</i> | 58 |

| | | |
|-----------|--|------------|
| 3.1.3. | <i>Neutral conductor potential at each bus</i> | 58 |
| 3.1.4. | <i>Voltage Unbalance Factor – VUF – at the bus in the worst phase-neutral voltages conditions</i> | 59 |
| 3.1.5. | <i>Absolute and relative line power losses for each phase and the total ones</i> | 59 |
| 3.2. | PV cases | 60 |
| 3.3. | PV reactive power regulation | 64 |
| 3.4. | Italian and German technical standards..... | 66 |
| 3.4.1. | <i>Italian Technical Standard CEI 0-21 – Rules for passive and active users</i> | 66 |
| 3.4.2. | <i>German Technical Standard VDE-AR-N 4105 – Power generation systems connected to the LV distribution network</i> | 71 |
| 3.5. | VUF calculation | 75 |
| 3.6. | Power losses calculation..... | 77 |
| 4. | Simulation Results | 81 |
| 4.1. | Without Q regulation cases: plots and numerical results | 82 |
| 4.1.1. | <i>PV10% – 35 kW – phase a</i> | 83 |
| 4.1.2. | <i>PV30% – 105 kW – phases a and b</i> | 89 |
| 4.1.3. | <i>PV40% – 140 kW – phases a and b</i> | 96 |
| 4.1.4. | <i>PV50% – 175 kW – phases a and b</i> | 102 |
| 4.1.5. | <i>PV40% – 140 kW – phases a, b and c</i> | 109 |
| 4.1.6. | <i>PV50% – 175 kW – phases a, b and c</i> | 115 |
| 4.1.7. | <i>PV60% – 210 kW – phases a, b and c</i> | 122 |
| 4.1.8. | <i>PV70% – 245 kW – phases a, b and c</i> | 128 |
| 4.1.9. | <i>PV80% – 280 kW – phases a, b and c</i> | 135 |
| 4.2. | Without Q regulation cases: results comments and analysis | 142 |
| 4.3. | With Q regulation cases: plots and numerical results..... | 155 |
| 4.3.1. | <i>PV40% – 140 kW – phases a and b</i> | 156 |
| 4.3.2. | <i>PV50% – 175 kW – phases a and b</i> | 160 |
| 4.3.3. | <i>PV70% – 245 kW – phases a, b and c</i> | 165 |
| 4.3.4. | <i>PV80% – 280 kW – phases a, b and c</i> | 169 |
| 4.4. | With Q regulation cases: results comments and analysis | 176 |
| 5. | Conclusions..... | 183 |
| 6. | Bibliography | 187 |

Chapter 1

Introduction

Contents

| | |
|---|-----------|
| 1.1. Project Goals | 1 |
| 1.2. Problem Statement..... | 2 |
| 1.3. Background to unbalance conditions | 7 |
| 1.4. Background to Power Quality | 13 |
| 1.5. Background to OLTC and similar products | 20 |
| 1.6. Power system simulation tool..... | 25 |

1.1. Project Goals

Aim of this thesis is the development of the feasibility study of a new device for stabilizing the low voltage supply grid: the decoupled three-phase On-Load-Tap-Changer MV/LV transformer.

The research project which the thesis is based on is called 'Energy saving By Voltage Management – ESVM'. Developed at DTU, it has been run in collaboration with PSS Energy Group, a Danish energy consultancy company.

Basically the device is supposed to be added to a normal transformer, to make it provided with a secondary side windings selector, which permits to change the transformation ratio and consequently to change the secondary side voltage basing on direct voltage measurements. This technology is usually called OLTC – On Load Tap Changer – therefore

henceforth this acronym will be used. It can operate in the three phases simultaneously or independently: aim of the project is to analyze the differences which will appear without considering any tapping and with simultaneous-independent tap actions.

In order to test the technical feasibility of the device, different grid configurations have been studied. Each one has been analyzed three times, according to the OLTC tapping logic: without tapping, with three-phase simultaneous tapping and with phase-wise tapping.

The three representative grid configuration cases are defined:

- only passive load;
- passive and active loads;
- passive and active loads with reactive power regulation control system by the PV plants.

In this feasibility study, a real Danish low voltage network from Dong Eldistribution has been modeled in the software PowerFactory DIgSilent. With the support of the software, it has been possible to analyze the effects of this device in the network, comparing different operating scenarios in different grid configurations.

The measured data of the real Dong Eldistribution low voltage network have been analyzed and the resulting loading profiles in terms of active and reactive power have been used for the analysis. Mainly, the voltage characteristics of the distribution system including voltage profiles of each buses and the voltage unbalance are investigated as well as the line power losses.

1.2. Problem Statement

It is common in Denmark to have three-phase connection available even for relatively small residential users and, depending on the layout of the household electrical installation, concurrent loads may be concentrated on just one phase. Moreover, the increasing presence of small single-phase distributed energy resources like photovoltaic (PV) and new storage-capable loads (e.g., plug-in hybrid electric vehicles), is leading into uncorrelated voltage

variations along the feeder: it may happen that one phase voltage is increasing along the feeder, while the others are decreasing.

Therefore, since low voltage networks host both single- and three-phase 'pro-sumers' (customers which are both producers and users), the different power flow on the phases may lead to voltage unbalances that can interfere with the conservation voltage reduction control strategy and lead to Power Quality decreasing.

For this reason it can be considered that the increasing popularity of solar cells and the possibility of delivering excess energy production to the national grid are creating huge challenges for supply companies.

Network operators nowadays face difficult challenges as the insurance of a stable voltage in the low voltage grid and at the same time to integrate an increasing amount of renewable energy. According to European standard EN 50160, the range of variation of the r.m.s (root mean square) magnitude of the supply voltage, whether line to neutral or line to line to phase, are within the range $\pm 10\%$ for 95% of a week. In practice, the r.m.s value could be determined over a fixed interval of 20 milliseconds and the basic measurement could be made by determining the average of these values over a period of 10 minutes. The assessment of compliance over an observation period of one week, including Saturday and Sunday, could be then performed checking that 95% of the ten minutes values fall within the specified range [1]–[5].

In the practice, a maximum voltage rise of 3-5% percent is available to renewable energies in the low voltage grid since the rest is reserved for the medium voltage grid, voltage drops, and the setting imprecisions. As example, Figure 1.1 shows the situations within the current setting up; the potential problems faced by the network operator without OLTC technology is presented.

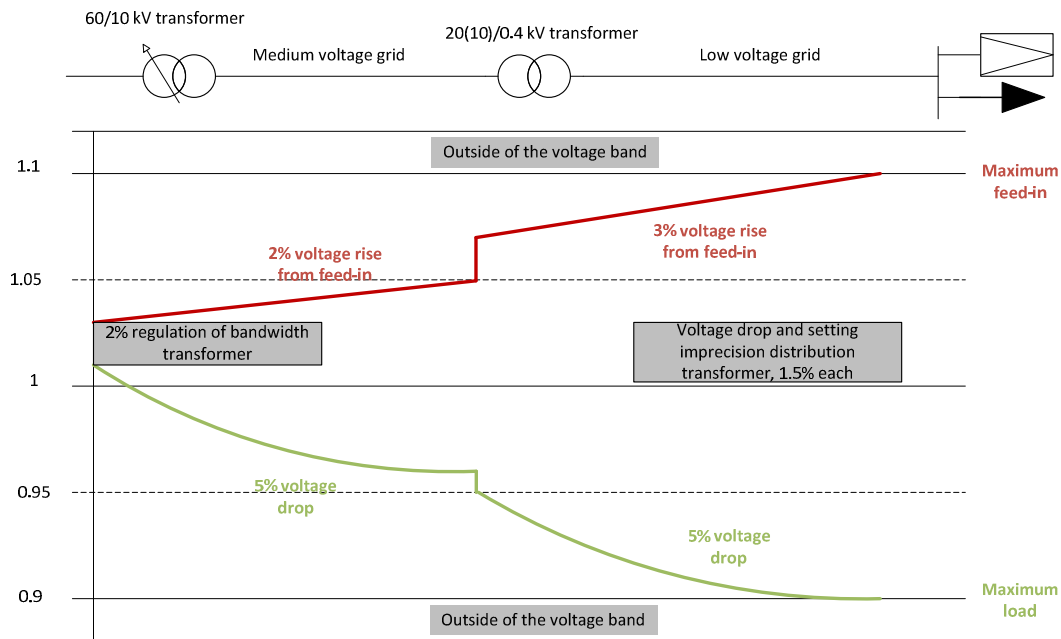


Figure 1.1. Potential problems faced by the network operator in the absence of OLTC

The increasing penetration of PVs will raise the risk of violation of the voltage band. Network operators are being forced into expensive expansion work even though the capacities of their operating equipment are far from exhausted. Besides the voltage band violation problem, voltage unbalance problem could also assume more importance in the near future, considering the increasing penetration of PV connected to single phases of the distribution grid. According to European standards, under normal operating conditions, during each period of one week, 95% of the 10 min mean r.m.s. values of the negative phase sequence component (fundamental) of the supply voltage shall be within the range 0% to 2% (the extreme acceptable limit is set at 3%) of the positive phase sequence component (fundamental) – this value is also known as Voltage Unbalance Factor or VUF.

To address the mentioned problems, this study aims to develop and demonstrate a new energy optimization unit whose objective is basically the improvement of distribution network power quality: the decoupled tap selector, which is for use in the distribution networks, precisely installed at the secondary side of the MV/LV (10/0.4 kV) distribution transformer.

The two main topics to take into account are:

- The 10/04-distribution transformer is the link between the energy supplier and the end-user. It converts the high voltage from the plant into low voltage for consumption in a fixed interval, ensuring that the end user is supplied with a maximum of 253 V closest to the transformer and minimum 207 V furthest from the transformer, so values within the $\pm 10\%$ of 230V, the nominal phase to neutral voltage;
- The OLTC technology makes it possible for the supply company to monitor, control and regulate the voltage in the supply grid, following the principles of voltage optimization.

As example, by using the OLTC in the network analyzed in Figure 1.1, the network operator could increase the grid capabilities by dynamically adapting the voltage, decoupling the voltages of low voltage and medium voltage grid. This may result in an 11 percent rather than a 3 percent voltage rise being available in the low voltage grid for feed-in from renewable energies. This kind of action may help improving the hosting capacity without expensive grid expansion investments.

In Figure 1.2 the PV hosting capacity increasing advantage offered to the network operator by the OLTC technology is depicted.

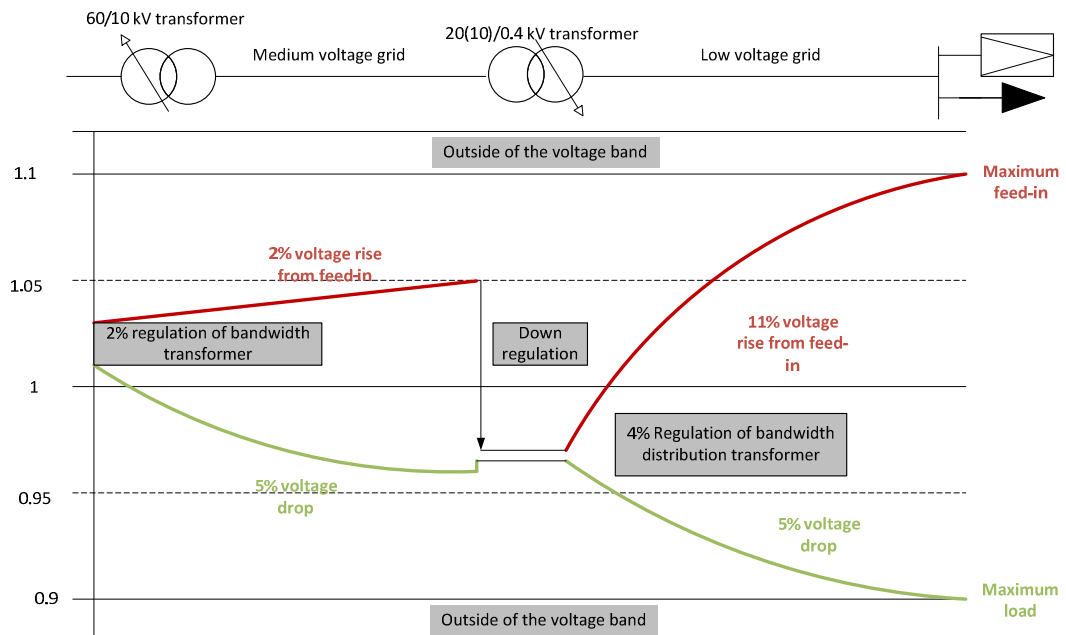


Figure 1.2. Advantages offered to the network operator by the OLTC

The novelty of the proposed approach is the utilization of a decoupled On Load Tap Changer (OLTC) MV/LV transformer, which is capable of regulating each single phase tap changer in a different way.

As previously said, this device can be part of the Smart Grid, and help stabilizing the fluctuations and subsequently secure the stability of the power supply.

So, summarizing, the positive effects which the device could lead to are:

- it enables to increase the renewable sources plants hosting capacity in the low voltage grid;
- it enables the suppliers to monitor voltage levels in the low voltage grid;
- it permits them to regulate the voltage;
- it permits to balance the three phases;
- it provides the ability to control and in case of an emergency to turn off parts of the power consumption.

It is the goal of the Danish government that Denmark will be free of fossil fuels for energy production by 2050, meaning that in less than 40 years Denmark will be independent of oil, gas and coal [6]. The independence of fossil fuels will entail that Denmark will:

- Maintain high energy security;
- Contribute significantly to stem the global warming;
- Enable green growth and employment.

The aims towards the fulfilment of the energy political 2050 goal are:

- Denmark will be a green, sustainable society;
- Denmark will be among the top 3 countries in the world that increases its use of renewable energy the most up until 2020;
- Denmark will be among the top 3 countries in OECD (Organization for Economic Cooperation and Development) regarding energy efficiency.

Thanks to the development of the decoupled three phase OLTC transformer, the grid hosting capacity of distributed generation plants from renewable resource could be increased, reducing the reliance on fossil fuels (or fuels in general) for energy production, thereby reducing the negative impact on the environment.

Therefore the introduction of this new technology will support the strike to make Denmark a green, sustainable society, with an increased level of renewable energy in the energy supply system.

Summarizing, the present work aims at providing, by evaluating achievements in term of voltage unbalances and losses reduction on a LV feeder, the feasibility analysis of the OLTC transformer with both synchronized and decoupled tap capability. The tap changers can regulate the single phase voltage $\pm 5\%$ the nominal value, by changing physically the transformation ratio.

Moreover a coordinated reactive power provision by PV is considered and further situations are analyzed to study the cooperation of the two control systems [7]–[10].

1.3. Background to unbalance conditions

The modern three-phase distribution systems supply a great diversity of customers; among them, those having single-phase, two-phase and unbalanced three-phase loads have become preponderant. The operation of these consumers imposes to the distribution network a permanent unbalanced running state, characterized by different parameters of the three phases. The unequal distribution of loads between the three phases of the supply system determines the flow of unbalanced currents that produce unbalanced voltage drops on the electric lines; as a result, the voltage system within the supply network becomes also unbalanced.

In addition, unsymmetrical generation (e.g. small photovoltaic generators) lead to voltage unbalance too. Voltage unbalance is not only a concern as such (e.g. degradation of the performance of three-phase machines due to torque pulsations, overheating due to the negative sequence) but also a concern for complying with the voltage limits as stated in the European standard EN 50160. Indeed, the unsymmetrical infeed leads to a disproportionate increase of the voltage in one phase which might exceed the limit.

In power systems supplying asymmetrical (unbalanced) loads, appear supplementary negative and/or zero sequence currents that cause additional power losses and faults in the electric power system and the unacceptable overheating of three-phase asynchronous machines belonging to different customers.

Contrary to some other disturbances in electrical power systems, for which the performance is evident for the ordinary customer, voltage unbalance belongs to those disturbances in which their perceptible effects are produced in the long run. Voltage unbalance leads to a sharp decrease on the efficiency of three-phase induction motors. Since induction motors represent the largest portion of industrial loads, it is seen that the voltage unbalance should be carefully studied and controlled.

Voltage unbalance in three-phase distribution systems regards the changing in phase angles and/or in the magnitude of voltage phasors. As said, the main causes leading to voltage unbalance are the following ones:

- Unsymmetrical distribution systems, which equipment and phase conductors present different impedance values.
- Unsymmetrical loads, such as arc furnaces, single and double phase loads;
- Different voltage drops due to differences in mutual impedances between phase conductors and between phase conductors and ground. This depends on the spatial configuration of conductors.

To study the unbalanced operation of a power system, the symmetrical components theory is used. According to Stokvis- Fortescue theorem, every three-phase asymmetrical system of phasors can be decomposed into three symmetrical systems of positive, negative and zero sequence respectively, as can be seen in [11] and [12]. This aspect can be seen in Figure 1.3, where every sequence system contains three phasors characterized by equal magnitudes; in the case of positive and negative sequences, components are rotated between them with 120 electrical degrees in counter-clockwise direction and negative clockwise direction, respectively. In the case of zero sequence components, there is no rotation between phasors.

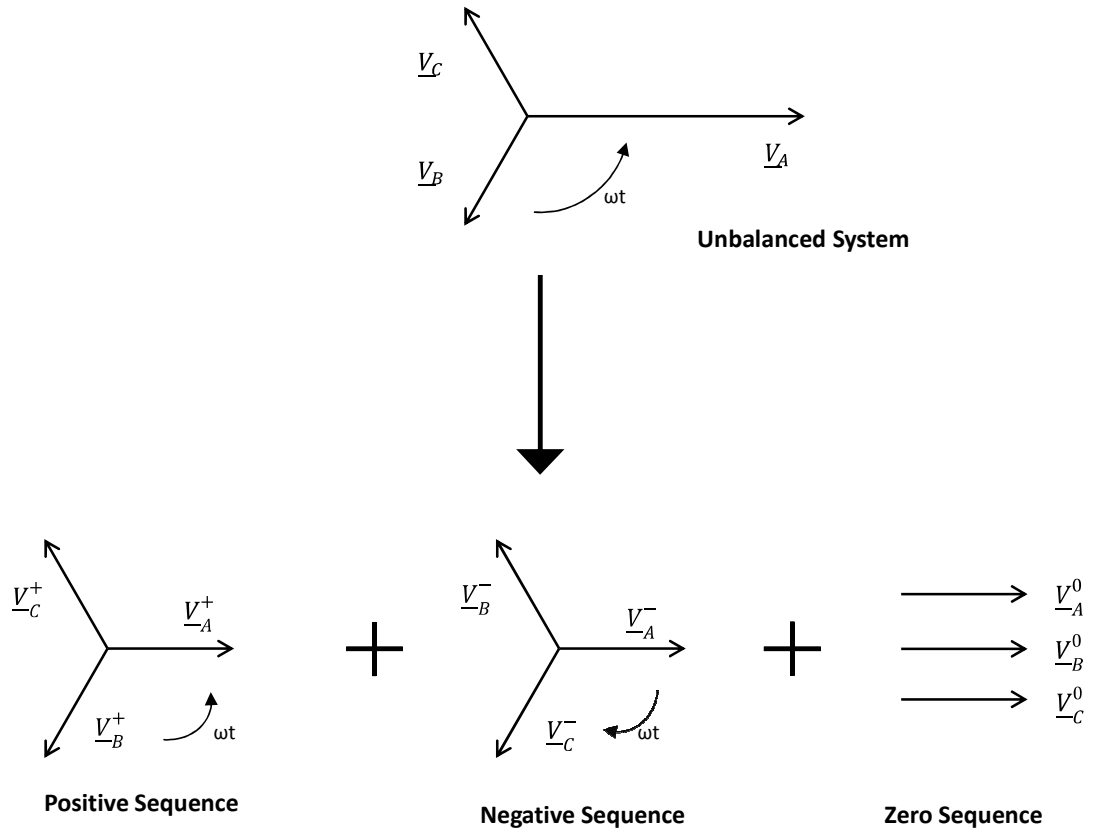


Figure 1.3. Schematic representation of the symmetrical components theory

If an asymmetrical phase to phase voltages system is taken into consideration, the relationship between the initial system and the symmetrical sequence systems can be written as in equation 1.1:

$$\begin{bmatrix} \underline{V}_A \\ \underline{V}_B \\ \underline{V}_C \end{bmatrix} = \begin{bmatrix} 1 & 1 & 1 \\ 1 & a^2 & a \\ 1 & a & a^2 \end{bmatrix} \begin{bmatrix} \underline{V}^+ \\ \underline{V}^- \\ \underline{V}^0 \end{bmatrix} \quad (1.1)$$

Where \underline{V}_A , \underline{V}_B and \underline{V}_C are the phase to phase voltage phasors, while \underline{V}^+ , \underline{V}^- and \underline{V}^0 are respectively the positive, negative and zero symmetrical systems. $a = e^{j120^\circ}$ is the rotation operator.

The reverse relationship is reported in equation 1.2:

$$\begin{pmatrix} \underline{V}^+ \\ \underline{V}^- \\ \underline{V}^0 \end{pmatrix} = \frac{1}{3} \begin{pmatrix} 1 & a & a^2 \\ 1 & a^2 & a \\ 1 & 1 & 1 \end{pmatrix} \begin{pmatrix} \underline{V}_A \\ \underline{V}_B \\ \underline{V}_C \end{pmatrix} \quad (1.2)$$

These sequence systems are not only theoretical, since they correspond to the reality: the positive sequence components are created by the synchronous or asynchronous generators while the negative and zero sequence components appear at the place of unbalance. Each of them can be separately measured and influences in a different way the power system. For example, in the case of motors, the positive sequence components produce the useful torque while the negative sequence components produce fields that create braking torques. On other hand, the zero sequence components is the one that get involved in the cases of interferences between the electric and the telecommunication transmission lines.

Other influences on balanced elements (generators and loads) connected to the power system are as follows:

- Negative sequence currents can produce the overheating of synchronous generator rotors, the transformers saturation and ripples in rectifiers;
- Zero sequence currents cause excessive power losses in neutral conductors and interferences with protection systems;
- In unbalanced electric systems, power losses grow and the loading capacity of the transmission networks diminishes.

Nevertheless the main effects of unbalanced voltages on a three-phase low voltage network are on three-phase induction motors [13].

Three-phase induction motors are designed and manufactured so that all three phases of the winding are carefully balanced with respect to the number of turns, placement of the winding, and winding resistance. When line voltages applied to a three-phase induction motor are not exactly the same, unbalanced currents will flow in the stator winding, whose magnitude depends upon the amount of unbalance. A small amount of voltage unbalance may increase

the current an excessive amount. The effect on the motor can be severe and the motor may overheat to the point of burnout.

Thus it is common to study the behavior of the positive and negative sequence components of the unbalanced supply voltage to understand the effect of an unbalance on the motor.

The effect of unbalanced voltages on three-phase induction motors is equivalent to the introduction of a negative sequence component having a rotation opposite to that occurring with balanced voltages. The positive sequence voltage produces a positive torque, whereas the negative sequence voltage gives rise to an air gap flux rotating against the forward rotating field, thus generating a detrimental reversing torque. Therefore, when neglecting non-linearities for instance due to saturation, the motor behaves like a superposition of two separate motors, one running at slip s with a certain terminal voltage per phase and the other running with a slip of $(2-s)$ and a different terminal voltage. The result is that the net torque and speed are reduced and torque pulsations and acoustic noise may be registered. Also, due to the low negative sequence impedance, the negative sequence voltage gives rise to large negative sequence currents. At normal operating speeds, the unbalanced voltages cause the line currents to be unbalanced in the order of 6 to 10 times the voltage unbalance. This introduces a complex problem in selecting the proper overload protective devices, particularly since devices selected for one set of unbalanced conditions may be inadequate for a different set of unbalanced voltages.

In addition to the torques issues, the other main consequences on the three-phase induction motors are related to temperature rising and load carrying capacity, full-load speed and currents.

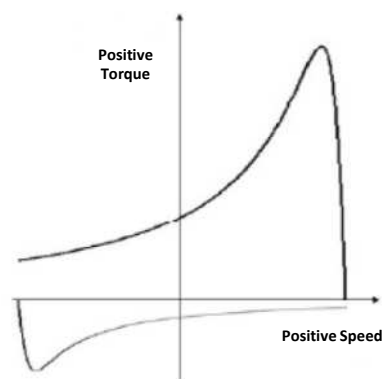


Figure 1.4. Graphical representation of the positive and negative sequence torques of an induction motor subjected to unbalanced supply voltages

From Figure 1.4 it is clear that the entire torque-speed curve is reduced. In that context, three points of particular interest on the resulting curve are the starting, the breakdown and the full load torque. It is clear that the motor takes longer to speed up in this case. This changes the thermal behavior of the motor and leads to decreased service life if not early failure. It has to be noticed that this is due to the negative torque and/or the reduced positive torque. Moreover, if full load is still demanded, the motor is forced to operate with a higher slip, increasing rotor losses and thus heat dissipation; the reduction of peak torques will compromise the ability of the motor to ride through dips and sags.

A motor often continues to operate with unbalanced voltages; however, its efficiency gets reduced because of both current increase and resistance increase due to heating. The increase in resistance and current 'stack up' to contribute to an exponential increase in motor heating. Essentially, this means that as the resulting losses increase, the heating intensifies rapidly. This may lead to a condition of uncontrollable heat rise, called 'thermal runaway', which results in a rapid deterioration of the winding insulation concluding with failure of the winding.

Premature failure can only be prevented by derating the machine according to standards, allowing it to operate within its thermal limitations: when voltage unbalance exceeds 1%, a motor needs to be derated for it to operate successfully. The derating curve, shown in Figure 1.5, indicates that at the 5% limit established by NEMA (National Electrical Manufacturers Association) for unbalance, a motor would be substantially derated, to only about 75% of its nameplate horsepower rating.

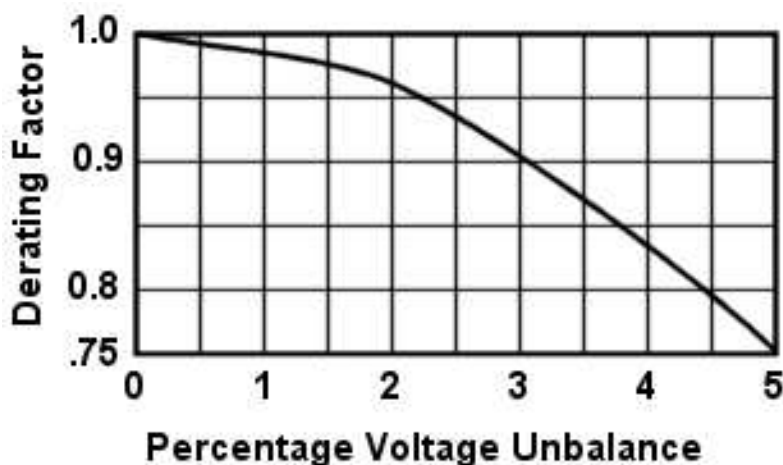


Figure 1.5. Induction motor derating curve

In addition to the torques issues, the other main consequences on the three-phase induction motors are related to: temperature rising and load carrying capacity, full-load speed and currents.

A relatively small unbalance in voltage will cause a considerable increase in temperature rise. In the phase with the highest current, the percentage increase in temperature rise will be approximately two times the square of the percentage voltage unbalance. The increase in losses and consequently, the increase in average heating of the whole winding will be slightly lower than the winding with the highest current.

To illustrate the severity of this condition, an approximate 3.5 percent voltage unbalance will cause an approximate 25 percent increase in temperature rise.

An Automatic Voltage Regulator (AVR) can be used to correct under-voltage and over-voltage, as well as voltage unbalance. As an active device, the AVR automatically compensates for all voltage fluctuations, providing that the input voltage to the AVR is within its range of magnitude and speed of adjustment. Although high power AVRs are available, it is usually more feasible to install a number of smaller units for the various circuits to be protected, as opposed to one large unit possibly at the plant service entrance.

To quantify the amount of unbalance, a set of different parameters is implemented. More details will be furnished in the chapter ‘VUF Calculation’ (Chapter 3.5), where different voltage unbalance factor definitions are described.

1.4. Background to Power Quality

Ideally, the best electrical supply would be a constant magnitude and frequency sinusoidal voltage waveform. However, because of the non-zero impedance of the supply system, of the large variety of loads that may be encountered and of other phenomena such as transients and outages, the reality is often different [14]. The Power Quality of a system expresses to which degree a practical supply system resembles the ideal supply system.

- If the Power Quality of the network is ‘good’ then any loads connected to it will run satisfactory and efficiently. Installation running costs and carbon footprint (i.e. environmental impact) will be minimal;

- If the Power Quality of the network is ‘bad’ then loads connected to it will fail or will have a reduced lifetime, and the efficiency of the electrical installation will reduce. Installation running costs and carbon footprint will be high and/or operation may not be possible at all.

In order to characterize the Power Quality, different indices have been defined.

Since nowadays the electricity is a good which can be bought and/or sold, it must satisfy some requirements, which are a sort of quality guaranty both to the grid supplier and to the grid users.

Power quality problems occur due to various types of electrical disturbances. Most of the PQ disturbances depend on amplitude or frequency or on both frequency and amplitude. Based on the duration of existence of PQ disturbances, events can be divided into short, medium or long type. The disturbances causing power quality degradation arising in a power system and their classification mainly include:

- *Interruption and under/over-voltage*: these are very common type disturbances. During power interruption, voltage level of a particular bus goes down to zero. The interruption may occur for short or medium or long period. Under- and over-voltage are fall and rise of voltage levels of a particular bus with respect to standard bus voltage. Sometimes under- and over-voltages of little percentage is allowable; but when they cross the limit of desired voltage level, they are treated as disturbances. Such disturbances are increasing the amount of reactive power absorption or deliver by a system, insulation problems and voltage stability. An interruption may occur when $\frac{\Delta U}{U_n} > 0.99$.
- *Voltage/Current unbalance*: voltage and current unbalance may occur due to the unbalance in drop in the generating system or transmission system and unbalanced loading. During unbalance, negative sequence components appear. They change the system performances and losses as well and in some cases it may hamper voltage stability.
- *Harmonics*: harmonics are the alternating components having frequencies other than fundamental present in voltage and current signals. There are various reasons for harmonics generation like non linearity, excessive use of semiconductor based

switching devices, different design constrains, etc. Harmonics have adverse effects on generation, transmission and distribution system as well as on consumer equipment also. Harmonics are classified as integer harmonics, sub harmonics and inter harmonics. Integer harmonics have frequencies which are integer multiple of the fundamental one, sub harmonics have frequencies which are smaller than the fundamental one and inter harmonics have frequencies which are greater than the fundamental one. Among these entire harmonics, integer and inter harmonics are very common in power system, since occurrence of sub harmonics is comparatively smaller than others. Sometimes harmonics are classified: time harmonics and spatial (space) harmonics. Obviously their causes of occurrence are different. It is clear that harmonics in general are not welcome and desirable. For the evaluation of harmonics content in power system applications, they are assessed with respect to fundamental. For this purpose different distortion factors with respect to the fundamental have been introduced.

- *Transients*: transients may generate in the system itself or may come from the other system. Transients are classified into two categories: DC transient and AC transient. AC transients are further divided into two categories: single cycle and multiple cycles.
- *Voltage dip*: it is a short duration disturbance. During voltage sag, r. m. s. voltage falls to a very low level for short period of time: $0.1 < \frac{\Delta U}{U_n} < 0.99$ with $10 \text{ ms} < \Delta t < 600 \text{ ms}$.
- *Voltage swell*: it is a short duration disturbance. During voltage swell, r. m. s. voltage increases to a very high level for short period of time: $1.1 < \frac{\Delta U}{U_n} < 1.8$ with $10 \text{ ms} < \Delta t < 600 \text{ ms}$.
- *Flicker*: it is an undesired variation of system frequency. It is a visible change in brightness of a lamp due to rapid fluctuations in the voltage of the power supply. It is caused by quick succession of short-time voltage dips.
- *Ringling waves*: oscillatory disturbances of decaying magnitude for short period of time is known as ringing wave. It may be called a 'special type transient'. The frequency of a flicker may or may not be same with the system frequency.

- *Outage*: it is special type of interruption where power cut has occurred for not more than 60 s.

All these phenomena are related to voltage alterations, since the supplier is able to manage only the voltage, not the current, which only depends on the loads. So it is commonly possible to talk about Voltage Quality instead of Power Quality.

Power Quality worsening potentially leads to inefficient running of installations, system down time and reduced equipment life and consequently high installation running costs [15], [16]. Poor Power Quality can be described as any event related to the electrical network that ultimately results in a financial loss.

Possible consequences of poor Power Quality include:

- Unexpected power supply failures (breakers tripping, fuses blowing);
- Equipment failure or malfunctioning;
- Equipment overheating (transformers, motors, ...) leading to their lifetime reduction;
- Damage to sensitive equipment (PC's, production line control systems, ...);
- Electronic communication interferences;
- Increase of system losses;
- Need to oversize installations to cope with additional electrical stress with consequential increase of installation and running costs and associated higher carbon footprint;
- Penalties imposed by utilities because the site pollutes the supply network too much;
- Connection refusal of new sites because the site would pollute the supply network too much;
- Impression of unsteadiness of visual sensation induced by a light stimulus whose luminance or spectral distribution fluctuates with time (flicker);
- Health issues with and reduced efficiency of personnel.

As example, common damages on transformers and motors are depicted in Figure 1.6.



Figure 1.6. Common damages on transformers and motors

If due to poor Power Quality the production is stopped, major costs are incurred. Table 1.1 gives an overview of typical financial loss due to a Power Quality incident (stop) in electrical installations for various industries, according to "The cost of poor power quality," Copper Development Association November 2001.

| Industry | Financial loss per incident |
|--------------------------|-----------------------------|
| Semiconductor production | 3,800,000 € |
| Financial trading | 6,000,000 € per hour |
| Computer center | 750,000 € |
| Telecommunications | 30,000 € per minute |
| Steel industry | 350,000 € |
| Glass industry | 250,000 € |
| Offshore platforms | 250,000-750,000 € per day |

Table 1.1. Financial loss caused by voltage sags

In addition to financial loss due to 'production stops', another factor of the cost of poor Power Quality can be identified by analyzing the extra kWh losses that exist due to the presence of harmonic pollution in typical network components such as transformers, cables and motors. As this loss has to be supplied by the utility power plants, a financial loss and CO₂ emissions can be assigned to it. Exact values of this loss depend on the local situation

of kWh tariffs and ways that the electrical power is generated (e.g. nuclear power plants have almost no CO₂ footprint per kWh generated as opposed to coal power plants for which the footprint is large at around 900-1000 g/kWh produced).

One possible method to quantify theoretically the extra losses introduced by harmonics in transformers is to use the IEEE C57.110 standard. The calculated impact will depend on the local situation but figures like a few thousands Euro/year are easily reached. This corresponds to a few tens of CO₂ emissions/year. Consequently, it may be concluded that in installations where significant harmonic polluting loads are present, the running costs can be significant.

Most harmonic pollution nowadays is created as harmonic current produced by loads in individual installations. This harmonic current, injected into the network impedance transfers into harmonic voltage, (Ohm's law); which gets applied to all the loads within that user's installation. As a result the user employing harmonic loads may suffer from Power Quality problems. In addition however, the harmonic current produced by one installation without filters is also flowing through the feeding transformers into the utility supply and creates harmonic voltage distortion on the public network too. As a result, any utility user connected to the same supply will become affected by the pollution created by another utility customer and could suffer operational consequences in his own installation due to this.

In order to limit this type of problems most utilities have adopted Power Quality standards/regulations that shall be respected by the users of the supply network. In extreme cases, non-compliance with these regulations leads to a connection refusal of a new installation, which in turn can have a significant impact on the production and revenue loss of the company.

In Table 1.2 the electric norms regarding the Power Quality standards are presented.

| Standard | Topic |
|-----------------|--|
| IEC 60038 | Standard voltages |
| IEC 60816 | Guides on methods of measurement of short-duration transients on low-voltage power and signal lines. Equipment susceptible to transients |
| IEC 60868 | Flicker meter: functional and design specifications |
| IEC 60868-0 | Flicker meter: evaluation of flicker severity; evaluates the severity of voltage fluctuation on the light flicker |
| IEC 1000-3-2 | Electromagnetic compatibility Part 3: Limits Section 2: Limits for harmonic current emissions (equipment absorbed current <16 A per phase) |
| IEC 1000-3-6 | Electromagnetic compatibility Part 3: Limits Section 6: Emission limits evaluation for perturbing loads connected to MV and HV networks |
| IEC 1000-4 | Electromagnetic compatibility Part 4: Sampling and metering techniques |
| EN 50160 | Voltage characteristics of electricity supplied by public distribution systems |
| IEC 61000 | Electromagnetic compatibility (EMC) |

Table 1.2. European standard on Power Quality

1.5. Background to OLTC and similar products

Power transformers equipped with on-load tap changers (OLTCs) have been the main components of electrical networks and industrial applications for nearly 90 years. OLTCs enable voltage regulation and/or phase shifting by varying the transformer ratio under load without interruption [17], [18].

On-load tap-changers (OLTCs) are indispensable in regulating power transformers used in electrical energy networks and industrial applications. Historically, as their classical application they have been mainly used as equipment to the primary station transformers, i.e. the ones which connect the high voltage transmission lines to the medium voltage ones.

Because of the high powers flowing through HV/MV transformers, the tap selector needs to be installed at the primary side, where, thanks to the higher voltage, currents flowing through the windings are much smaller than the ones at the secondary side. In this way it is possible to avoid the origin of electric arcs.

The OLTC changes the ratio of a transformer by adding or subtracting to and turns from either the primary or the secondary winding. The transformer is therefore equipped with a regulating or tap winding which is connected to the OLTC.

Figure 1.7 shows the principle winding arrangement of a 3-phase regulating transformer, with the OLTC located at the wye-delta-connection in the high voltage winding.

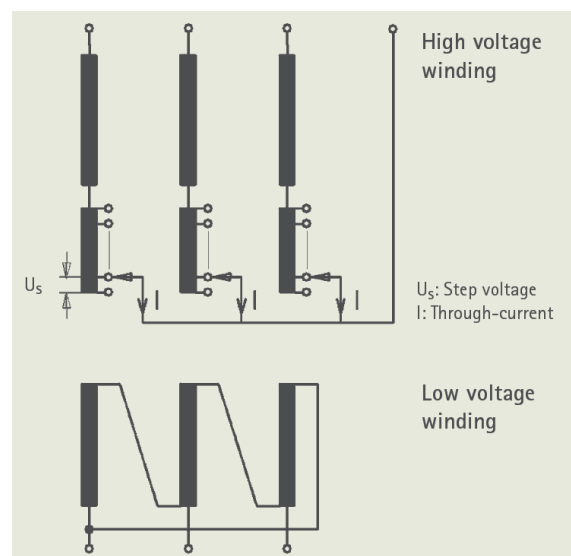


Figure 1.7. Principle winding arrangement of a regulating transformer in wye-delta-connection

Simple changing of taps during an energized status is unacceptable due to momentary loss of system load during the switching operation (Figure 1.8).

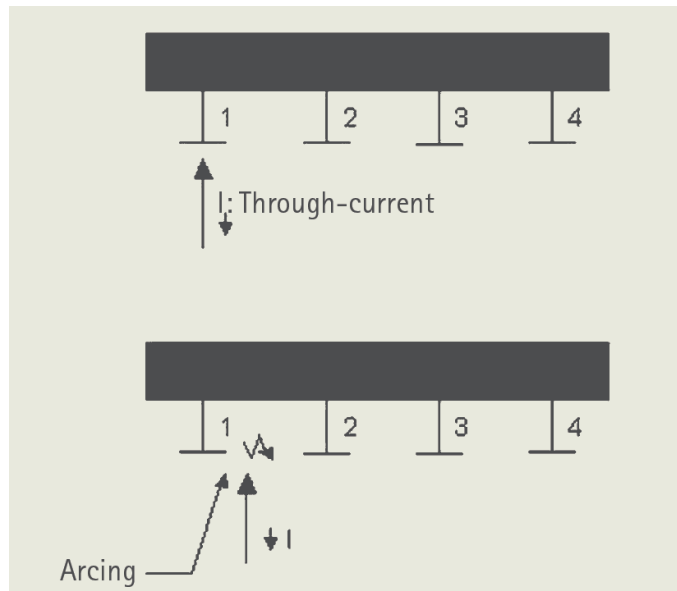


Figure 1.8. Simple contact switching

The ‘make (2) before break (1) contact concept’, shown in Figure 1.9, is therefore the basic design for all OLTCs. The transition impedance in the form of a resistor or reactor consists of one or more units that bridge adjacent taps for the purpose of transferring load from one tap to the other without interruption or appreciable change in the load current. At the same time they limit the circulating current (I_C) for the period when both taps are used. Normally, reactor-type OLTCs use the bridging position as a service position and the reactor is therefore designed for continuous loading.

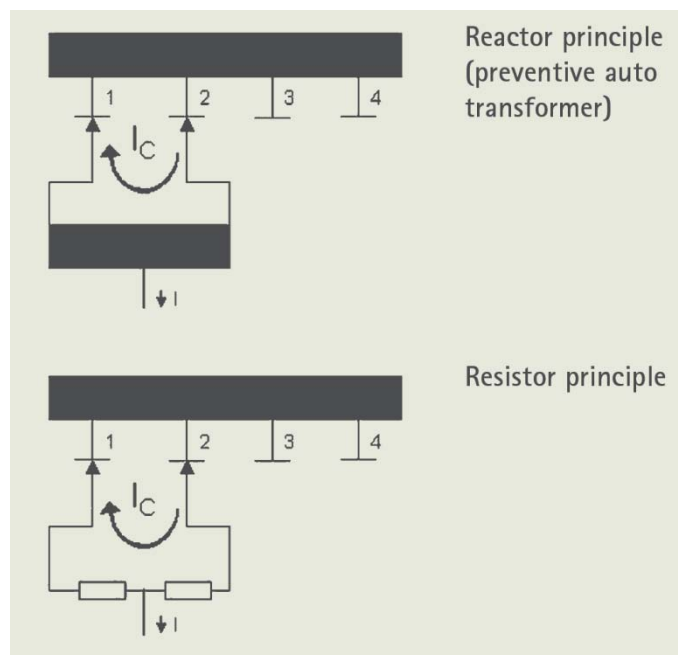


Figure 1.9. Basic switching principle “make (2) before break (1)” using transition impedances

The voltage between the taps mentioned above is the ‘step voltage’, which normally lies between 0.8% and 2.5% of the rated voltage of the transformer.

The main components of an OLTC are contact systems for make and break currents as well as carrying currents, transition impedances, gears, spring energy accumulators and a drive mechanism. Depending on the various winding arrangements and OLTC-designs, separate selector switches and change-over selectors (reversing or coarse type) are also used.

The following basic arrangements of tap windings are mainly used:

- Linear arrangement;
- Single reversing change-over selector;
- Double reversing change-over selector;
- Single coarse change-over selector;
- Multiple coarse change-over selector.

These different arrangements are depicted in Figure 1.10.

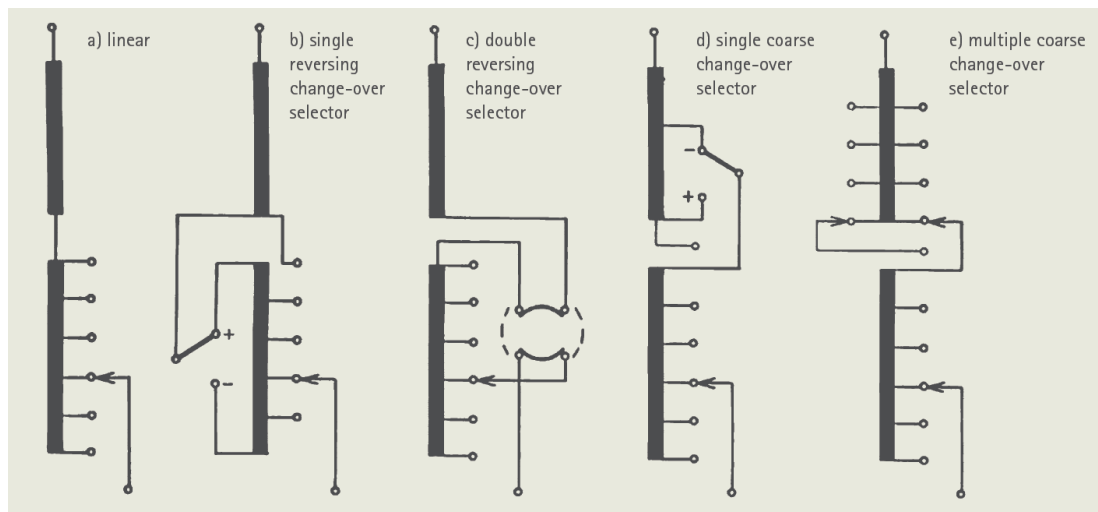


Figure 1.10. Basic connections of tap windings

Linear arrangement (Figure 1.10 a) is generally used on power transformers with moderate regulating ranges up to a maximum of 20%. The tapped turns are added in series with the main winding so that the transformer ratio is changed. The rated position can be any one of the tap positions: it can rationally be set by the operator.

With a reversing change-over selector (Figure 1.10 b) the tap winding is added to or subtracted from the main winding so that the regulating range can be doubled or the number of taps reduced. During this operation, the tap winding is disconnected from the main winding. The greatest copper losses occur, however, in the position with the minimum number of effective turns. This reversing operation is realized using a change-over selector which is part of the tap selector or of the selector switch (arcing tap switch).

The rated position is normally the mid position or neutral position.

The double reversing change-over selector (Figure 1.10 c) avoids the disconnection of tap winding during the change-over operation. In phase-shifting transformers (PST) this apparatus is called the advance-retard switch (ARS).

Using a coarse change-over selector (Figure 1.10 d) the tap winding is connected either to the plus or minus tapping of the coarse winding. During coarse selector operation, the tap winding is disconnected from the main winding (special winding arrangements can cause the same disconnection problems as described above; in addition the series impedance of coarse

winding/tap winding must be checked). In this case, the copper losses are lowest in the position of the lowest effective number of turns.

This advantage, however, places higher demands on insulation material and requires a larger number of windings.

The multiple coarse change-over selector (Figure 1.10 e) enables multiplication of the regulating range. It is mainly used for industrial process transformers (rectifier/furnace transformers). The coarse change-over selector is also part of the OLTC.

Which of these basic winding arrangements is used in each individual case depends on the system and operating requirements. These arrangements are applicable to two winding transformers as well as to autotransformers and to phase-shifting transformers (PST).

Where the tap winding and therefore the OLTC is inserted in the windings (high voltage or low voltage side) depends on the transformer design and customer specifications. As said it is clear that in the traditional applications (HV/MV transformers) the OLTC is installed at the high voltage side, because it is necessary to prevent electric arc phenomena which could take place because of the high amount of power. On the other hand, if the OLTC unit is installed on a MV/LV transformer, as it is in this thesis project, it could easily be installed at the low voltage side since the flowing powers, and consequently the currents, are not so high to origin electric arcs.

Two similar products available in the market are now shortly introduced: **GRIDCON® Transformer** from Maschinenfabrik Reinhausen GmbH and **FITformer® REG 2.0** from SIEMENS. Both of them are specifically designed for voltage regulation in the low voltage grid and are equipped with a 3-phase OLTC technology [19], [20].

GRIDCON® Transformer provides different features to deal with autonomous voltage regulation in distribution networks. Its main tasks are:

- The transformation function transforms upper voltage into lower voltage;
- The on-load switching function allows the ratio between the upper and lower voltage in the transformer to be dynamically adjusted under load, thanks to 5, 7 or 9 possible operating positions;
- The drive function guarantees reliable switching;

- The regulator function – including sensors – measures the voltage and derives the switching operations required.

The FITformer® REG 2.0 ensures ease of use thanks to separation of the regulation and control technology. Its main features are:

- Fluid-immersed distribution transformer;
- Power range up to 630 kVA;
- Maximum operating voltage: 36 kV;
- Low voltage load regulation range in three stages;
- Operating characteristics and dimensions correspond to conventional distribution transformers;
- Additional high-voltage tapping range for optimum operation.

1.6. Power system simulation tool

The routine to perform the simulations is implemented in the commercially available power system simulation tool DIgSILENT PowerFactory.

The calculation program PowerFactory, as written by DIgSILENT, is a computer aided engineering tool for the analysis of transmission, distribution, and industrial electrical power systems. It has been designed as an advanced integrated and interactive software package dedicated to electrical power system and control analysis in order to achieve the main objectives of planning and operation optimization.

“DIgSILENT” is an acronym for “**DIgital SIMuLation of Electrical NeTworks**”. That interactive single-line diagram included drawing functions, editing capabilities and all relevant static and dynamic calculation features.

PowerFactory uses a hierarchical, object-oriented database. All the data, which represents power system Elements, Single Line Diagrams, Study Cases, system Operation Scenarios, calculation commands, program Settings etc., are stored as objects inside a hierarchical set of

folders. The folders are arranged in order to facilitate the definition of the studies and optimize the use of the tools provided by the program.

The objects are grouped according to the kind of element that they represent. These groups are known as 'Classes' within the PowerFactory environment.

All data which defines a power system model is stored in "Project" folders within the database. Inside a "Project" folder, "Study Cases" are used to define different studies of the system considering the complete network, parts of the network, or variations on its current state. This 'project and study case' approach is used to define and manage power system studies in a unique application of the object-oriented software principle.

Chapter 2

Network Modeling

Contents

| | | |
|---------------|---|-----------|
| 2.1. | Real Danish network layout | 27 |
| 2.2. | Multiphase system modeling | 29 |
| 2.3. | Loads and PVs modeling | 30 |
| 2.4. | Transformer modeling..... | 34 |
| 2.4.1. | <i>Tapping Logic</i> | 38 |
| 2.5. | Dynamics analysis – RMS Simulation in DIgSILENT PowerFactory | 42 |
| 2.6. | Grid elements modeling in PowerFactory | 49 |
| 2.6.1. | <i>Transformer Controller</i> | 49 |
| 2.6.2. | <i>Passive Loads</i> | 51 |
| 2.6.3. | <i>Active Loads</i> | 51 |
| 2.6.4. | <i>Active Loads with Q regulation</i> | 53 |

2.1. Real Danish network layout

The real network considered for the analysis is a DONG Energy network located in Bistrup, a village around 20 km out of Copenhagen [21]. It is a 12- bus low voltage feeder connected to the MV network through a 10/0.4 kV transformer, as shown in Figure 2.1. The short circuit power of the main network is 20 MVA [22].

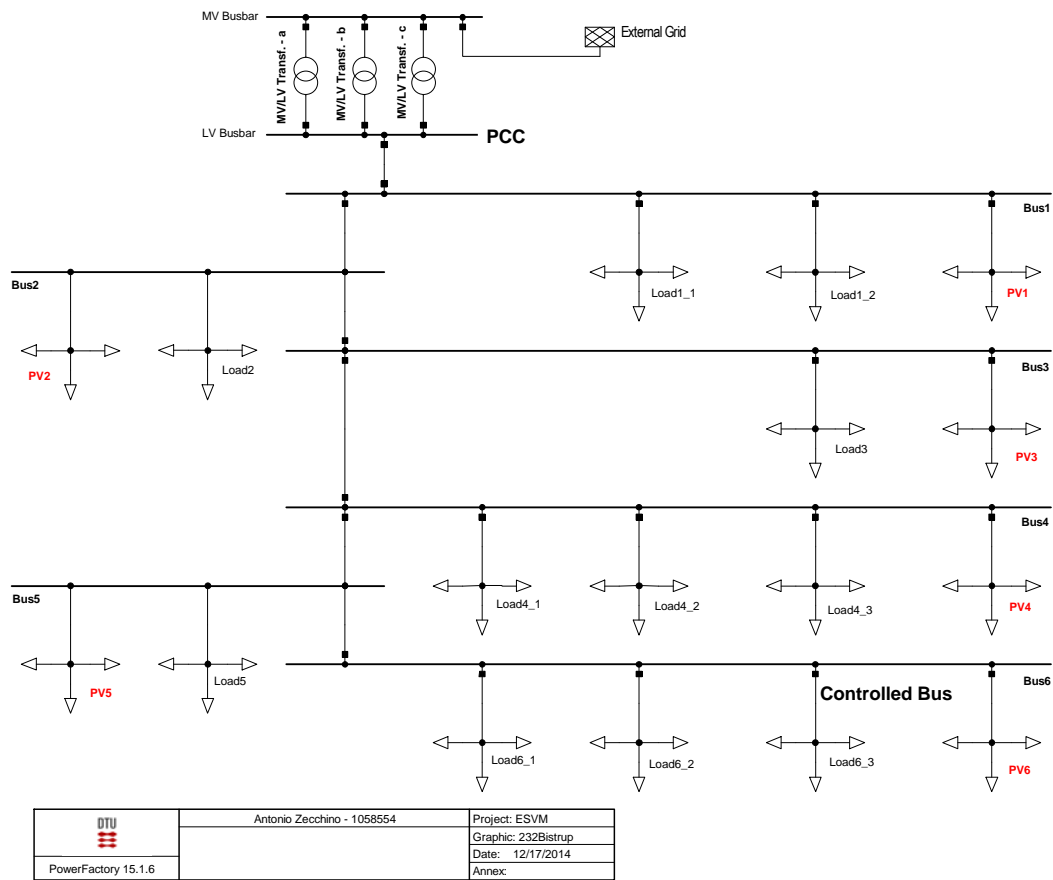


Figure 2.1. Single line diagram representation of the real Danish LV network

Measurements data on the real system allowed characterizing the power consumption of the 33 single phase loads during a 24-hours interval which resulted to be about 740 kWh, with a mean power of 30.8 kW. The daily energy losses amount amounted to 8.9 kWh, i.e. the 1.2% of the total energy absorbed from the MV grid. The total load energy and mean power amounts for each phase are reported in Table 2.1.

| | Phase a | Phase b | Phase c |
|------------------------|---------|---------|---------|
| Energy [kWh] | 295.5 | 201.2 | 242.4 |
| Mean Power [kW] | 12.4 | 8.4 | 10.2 |

Table 2.1. Total load energy (during 24 hours) and mean power value

The 18 single-phase PV plants work under different conditions in the different scenarios considered; after all the reference power injection is related to a real typical daily production of a 1kWp reference PV plant – see Chapter 3.2.

Finally a detailed description of each branch of the grid is reported in the table in Figure 2.2: information about length, section, material and absolute and kilometric resistance and reactance.

| Name | Grid | Terminal i Busbar | Terminal j Busbar | Length m | R(AC,20°C) Ohm/km | X' Ohm/km | R1 Ohm | X1 Ohm | Name |
|-------------------|------------|-------------------|-------------------|----------|-------------------|-----------|---------|---------|-----------|
| Line | 232Bistrup | Bus3 | PV3 | 100, | 0,159 | 0,081 | 0,0159 | 0,0081 | 150AL-MAL |
| Line(1) | 232Bistrup | Bus2 | PV2 | 100, | 0,159 | 0,081 | 0,0159 | 0,0081 | 150AL-MAL |
| Line(3) | 232Bistrup | Bus4 | PV4 | 100, | 0,159 | 0,081 | 0,0159 | 0,0081 | 150AL-MAL |
| Line(4) | 232Bistrup | Bus1 | PV1 | 100, | 0,159 | 0,081 | 0,0159 | 0,0081 | 150AL-MAL |
| Line(5) | 232Bistrup | Bus6 | PV6 | 100, | 0,159 | 0,081 | 0,0159 | 0,0081 | 150AL-MAL |
| Line(6) | 232Bistrup | Bus5 | PV5 | 100, | 0,159 | 0,081 | 0,0159 | 0,0081 | 150AL-MAL |
| Line1-2 | 232Bistrup | FCC | Bus1 | 98, | 0,159 | 0,081 | 0,01558 | 0,00793 | 150AL-PSP |
| Line10-11 | 232Bistrup | Bus5 | Bus6 | 71, | 0,159 | 0,081 | 0,01128 | 0,00575 | 150AL-MAL |
| Line11-12 | 232Bistrup | Bus6 | Bus6_Load6 | 39, | 0,159 | 0,081 | 0,00620 | 0,00315 | 150AL-MAL |
| Line11-13 | 232Bistrup | Bus6 | Bus6_Load6 | 18, | 0,159 | 0,081 | 0,00286 | 0,00145 | 150AL-MAL |
| Line2-3 | 232Bistrup | Bus1 | Bus1_Load1 | 167, | 0,159 | 0,081 | 0,02655 | 0,01352 | 150AL-MAL |
| Line2-4 | 232Bistrup | Bus1 | Bus2 | 74, | 0,159 | 0,081 | 0,01176 | 0,00599 | 150AL-MAL |
| Line4-5 | 232Bistrup | Bus2 | Bus3 | 74, | 0,159 | 0,081 | 0,01176 | 0,00599 | 150AL-MAL |
| Line5-6 | 232Bistrup | Bus3 | Bus4 | 159, | 0,098 | 0,079 | 0,01558 | 0,01256 | 240AL-MAL |
| Line6-10 | 232Bistrup | Bus4 | Bus5 | 74, | 0,159 | 0,081 | 0,01176 | 0,00599 | 150AL-MAL |
| Line6-8 | 232Bistrup | Bus4 | Bus4_Load4 | 98, | 0,247 | 0,083 | 0,02420 | 0,00813 | 95AL-PSP |
| Line_Bus1_Load1_2 | 232Bistrup | Bus1 | Bus1_Load1 | 1, | 0,159 | 0,081 | 0,00015 | 0,00008 | 150AL-MAL |
| Line_Bus2_Load2 | 232Bistrup | Bus2 | Bus2_Load2 | 1, | 0,159 | 0,081 | 0,00015 | 0,00008 | 150AL-MAL |
| Line_Bus3_Load3 | 232Bistrup | Bus3 | Bus3_Load3 | 1, | 0,159 | 0,081 | 0,00015 | 0,00008 | 150AL-MAL |
| Line_Bus4_Load4_1 | 232Bistrup | Bus4 | Bus4_Load4 | 1, | 0,159 | 0,081 | 0,00015 | 0,00008 | 150AL-MAL |
| Line_Bus4_Load4_2 | 232Bistrup | Bus4 | Bus4_Load4 | 1, | 0,159 | 0,081 | 0,00015 | 0,00008 | 150AL-MAL |
| Line_Bus5_Load5 | 232Bistrup | Bus5 | Bus5_Load5 | 1, | 0,159 | 0,081 | 0,00015 | 0,00008 | 150AL-MAL |
| Line_Bus6_Load6_2 | 232Bistrup | Bus6 | Bus6_Load6 | 1, | 0,159 | 0,081 | 0,00015 | 0,00008 | 150AL-MAL |

Figure 2.2. Grid lines characterization branch by branch

2.2. Multiphase system modeling

In order to perform the analysis in a LV distribution network, a power flow tool able to deal with asymmetrical systems has been needed. The method adopted for this work has been classified as a ‘Current Injection’ method and has allowed carrying out power flow analysis on multi-phase systems [22].

The principle leading to the composition of the potentially asymmetrical system is depicted in Figure 2.3, where the network admittance matrix is composed starting from the branches definition (self and mutual admittances) including lines and transformers.

The system is then integrated with the shunt elements (whether they are loads or generators, considered as active loads) which are represented as a parallel of constant admittances and variable current injectors, so the total current contribution depends on both terms and gives the possibility to change the models' voltage dependency according to the ZIP theory, described in Chapter 2.3.

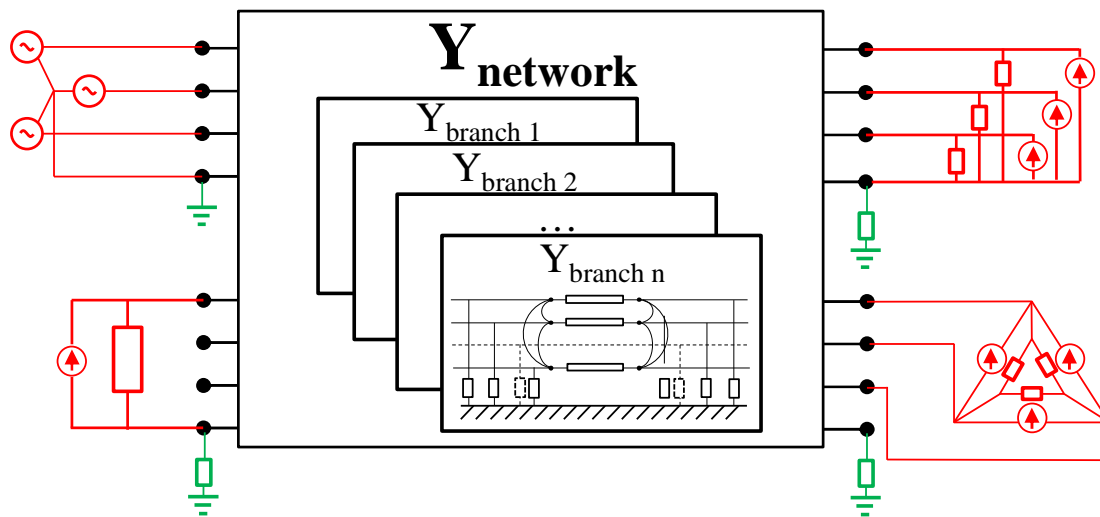


Figure 2.3. System representation for the asymmetrical power flow analysis

2.3. Loads and PVs modeling

The load profiles have been characterized by using single-phase measurement data on voltages, currents and active powers with a 10 minutes resolution during a 24-hours interval. In order to simulate the real behavior of both passive and active loads (i.e. PV plants), it has been necessary to link all the loads in the single line diagram to the real measurement data. Measurement data located in several text files have been used to calculate the absorbed active and reactive power amounts and read as input data of the loads in the schematic. This logic procedure is schematized in Figure 2.4.

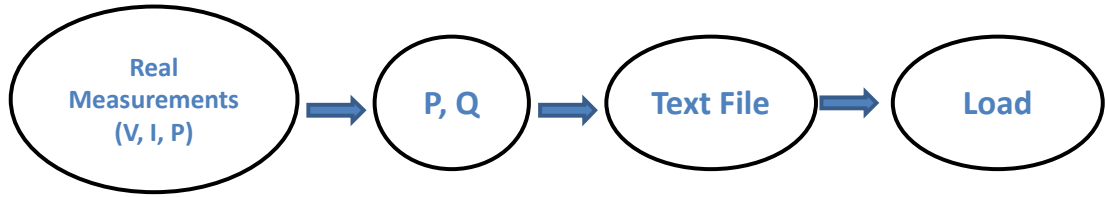


Figure 2.4. Passive load logical model

It has been noticed that there was no perfect correspondence between the measured power absorption and the input power data of the text files. Probably it was due to the ‘constant-impedance’ load model when running RMS simulations instead of a ‘constant-power’ model. At this point it has been necessary to define a standard load configuration – both for active and passive loads – that could be assumed in the simulation model of our project.

If on the one hand household loads could have been assumed as ‘constant-impedance’ loads, on the other hand the same assumption has not been valid for active loads, since PV generation plants in this work should have been considered as ‘constant-power’ active loads. With reference to these considerations, it has been important to base on a theory able to allow defining each specific load behavior: the ZIP theory.

According to it, each real load could be modeled with reference to its nature: it could simply be a ‘constant-power’, a ‘constant-voltage’ or a ‘constant-impedance’ load, or it could be represented as a mix of the previous characteristics.

In order to define the behavior, equation 2.1 is used:

$$P = P_0 \left[a_1 \left(\frac{V}{V_0} \right)^2 + a_2 \left(\frac{V}{V_0} \right) + a_3 \right] \quad (2.1)$$

It is clear that the three coefficients a_1, a_2, a_3 represent, respectively, the shares of the constant-impedance, constant-voltage and constant-power contributions.

Another possible model is based on the Exponential Model theory, which considers a simple exponential law where the exponent α is an index related the load nature (equation 2.2). The three extreme load cases – ‘constant-power’, ‘constant-voltage’ and ‘constant-impedance’ – are represented respectively by $\alpha=0, 1, 2$.

$$P(V) = P_0 \left(\frac{V}{V_0} \right)^\alpha \quad (2.2)$$

It has been noticed that the PowerFactory software for RMS simulations considers loads according to the ‘constant-impedance’ model, which means that their behavior is described by the Exponential Model equation, assuming $\alpha=2$. This is the proper cause of the power mismatching, since active loads in the analyzed LV network (the PV generation plants) are supposed to be ‘constant-power’ loads.

Therefore it has been necessary to change the logic of these loads, by adding a block able to change the load behaviors from ‘constant-impedance’ to ‘constant-power’. This block is a proper ‘correction block’ and implements the equation 2.3, where P_{ref} is the active power read from the text file and P_{mod} is the modified active power, which will effectively go to the load of the schematic:

$$P_{mod} = P_{ref} \left(\frac{1}{V}\right)^2 \quad (2.3)$$

Of course the same considerations could be valid with reference to the reactive power instead of the active power.

As seen in equation 2.3, the voltage V needs to be measured: together with the text file values, the voltage measurement is the input of the ‘correction block’. The new logic procedure is schematized in Figure 2.5, which is clearly valid for the active power, since for now it has been assumed that the reactive power absorbed-injected by the PVs is set into zero.

For this reason all the reactive power values in the text files – Q_{ref} – have been set into zero, and they could simply be furnished to the PV units without the necessity to be modified by the correction block.

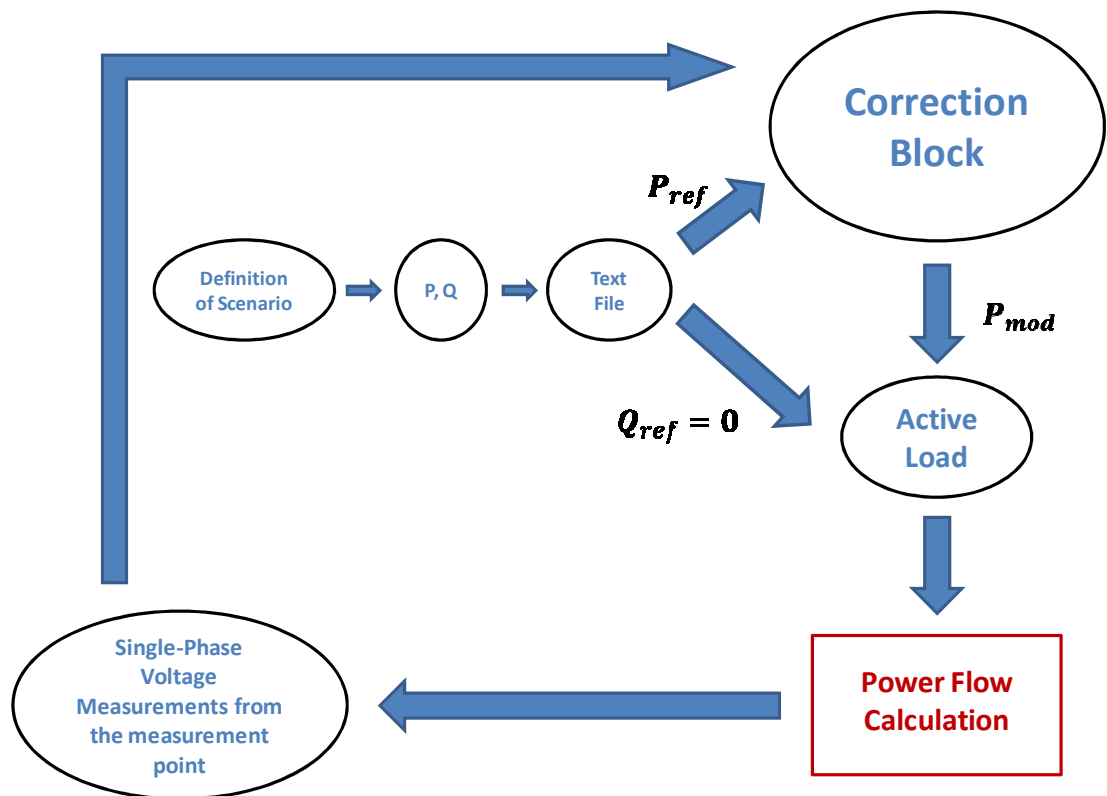


Figure 2.5. Active load logical model

At the end, thanks to this change it has been possible to have effectively 100% correspondence between the measured active power absorption and the input power data of the text-files for the PV plants.

For the second part of the simulations performed for the project, an additional logic model for the PV reactive power management has been needed to be created. Since the analysis will be described in detail in Chapter 3.3, the logical model of the active load including the reactive power calculator block is now depicted in Figure 2.6. It is clear that the reactive power values read from the text files are set into zero again, but thanks to the reactive power regulation algorithm the values furnished to the PV are different to zero and already ‘corrected’, since the block has P_{mod} instead of P_{ref} as one input.

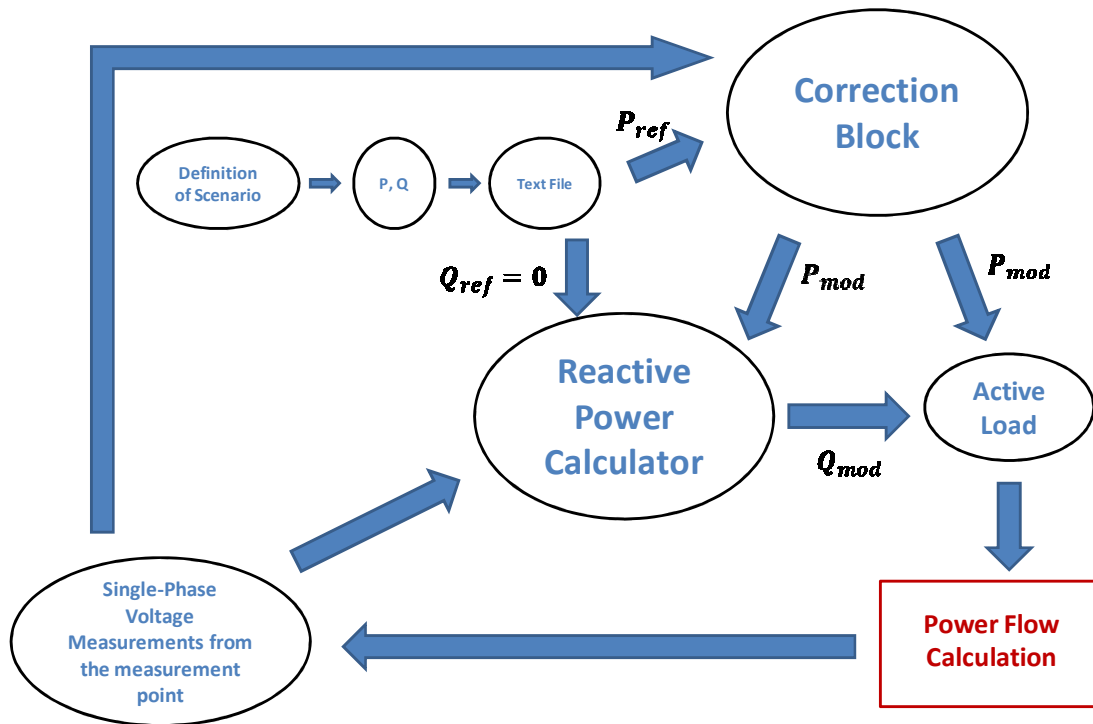


Figure 2.6. Active load with reactive power regulation logical model

So, summarizing, the first logic procedure without the correction block has been used for the passive loads, while the modified ones have been used for the PV plants. More detailed descriptions of the logic implementations in PowerFactory will be hereinafter furnished.

2.4. Transformer modeling

The On Load Tap Changer transformer has two main features according to the tap control logic which its operations are based on:

- **3-phase OLTC;**
- 3 single-phase OLTCs.

For simplicity, 3 single-phase OLTCs is named ‘**1-phase OLTC**’ afterwards.

The first technology performs 3-phase simultaneous tap changing actions according to phase-neutral voltage measurement from only one phase, while the 1-phase OLTC changes

the transformation ratio independently phase by phase, according to the three different phase-neutral voltages.

As described in Chapter 1.5, the OLTC changes the ratio of a transformer by adding or subtracting to and turns from either the primary or secondary winding. The transformer is therefore equipped with a regulating/tap winding which is connected to the OLTC.

Once the network model is built, the transformer needs to be represented as an admittance matrix connecting the PCC (LV busbar) to the MV network.

The classical approach used defining the transmission matrix of a generic single-phase transformer has been implemented to consider each phase's primitive matrix. Since for this work a control on the single phases has been needed in order to independently control the transformer ratios, the model has been built by three single-phase transformers, each secondary side connected between an earthed neutral point and a different phase of the LV grid, whereas at the primary side (MV busbar) the connection has been made between two phases, as for the Delta connection, resulting in a three-phase Delta-Wye transformer model, as shown in Figure 2.7.

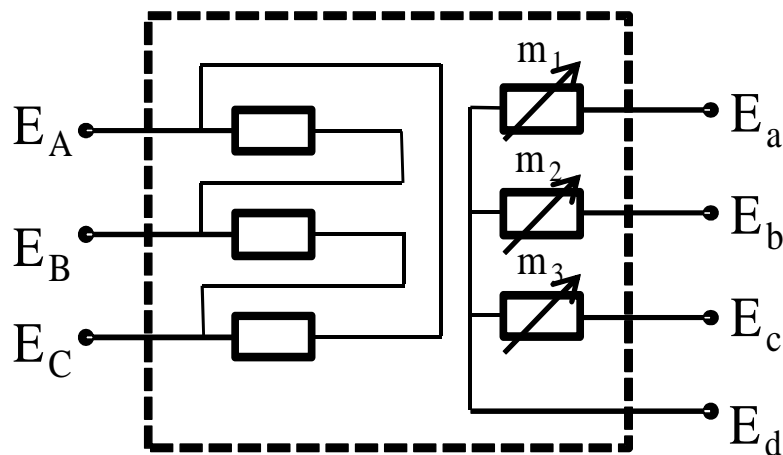


Figure 2.7 Three-phase Delta-Wye transformer model

From the schematic representation of the transformer model it can be noticed that, since the MV side works with isolated neutral, the fourth port is open, while at the secondary side the neutral point is connected to the relative conductor in the four-wire system.

As it can be seen in Figure 2.8, the terminals of the three single-phase transformers modeled in PowerFactory are so connected that there could be perfect correspondence to the real transformer type is D/yn.

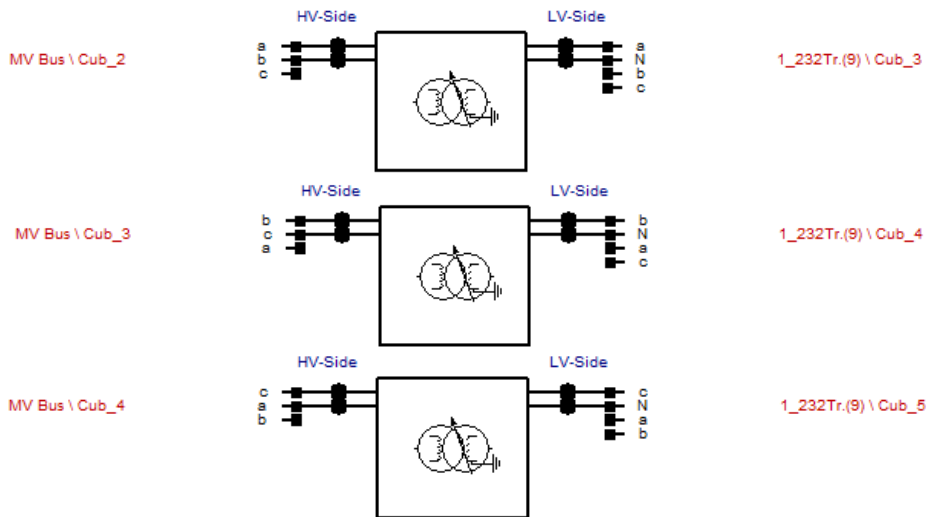


Figure 2.8. Single-phase transformers connection specification

As shown in the type edit window in Figure 2.9, each single-phase transformer has been set with:

- Rated power P_n : 210 kVA;
- Short-circuit voltage related to the positive sequence impedance $V_{cc\%}$: 4% (compared to the nominal one);
- Ratio of positive sequence impedance and resistance $\frac{X}{R}$: 10;
- Off-load current $i_{0\%}$: 0%;
- Off-load power P_0 : 0 kW.

The decision of setting into zero the inner iron losses is justified by the fact that the results analysis will not present any influence in terms of comparisons of different scenarios, since all of them will be characterized by the same amount of off-load inner losses. At any rate, considering for each single-phase transformer values of $i_{0\%}$ and P_0 respectively of 1.4% and 0.42 kW, the daily amount of off-load has been 30 kWh.

Figure 2.9. Single-phase transformer type edit window

In order to define the tap position controller of the single-phase transformers, a different approach – compared to the one of loads – has been needed to be used. In fact in this case (unlike loads modeling structure) there was no external data from text files as input data although direct measurements from the single line diagram needed to be performed.

Each single-phase transformer has been modeled basing on the same logic structure, which is depicted in Figure 2.10. Basically it is composed by phase-neutral voltage measurements from a certain point of the grid (the one at the end of the network), which are the input values of the ‘heart’ of the control system. Here, according to the measured voltage values and to the tapping logic law described in Chapter 2.4.1, tap selector position signals are provided as output signals and furnished to the single-phase transformer.

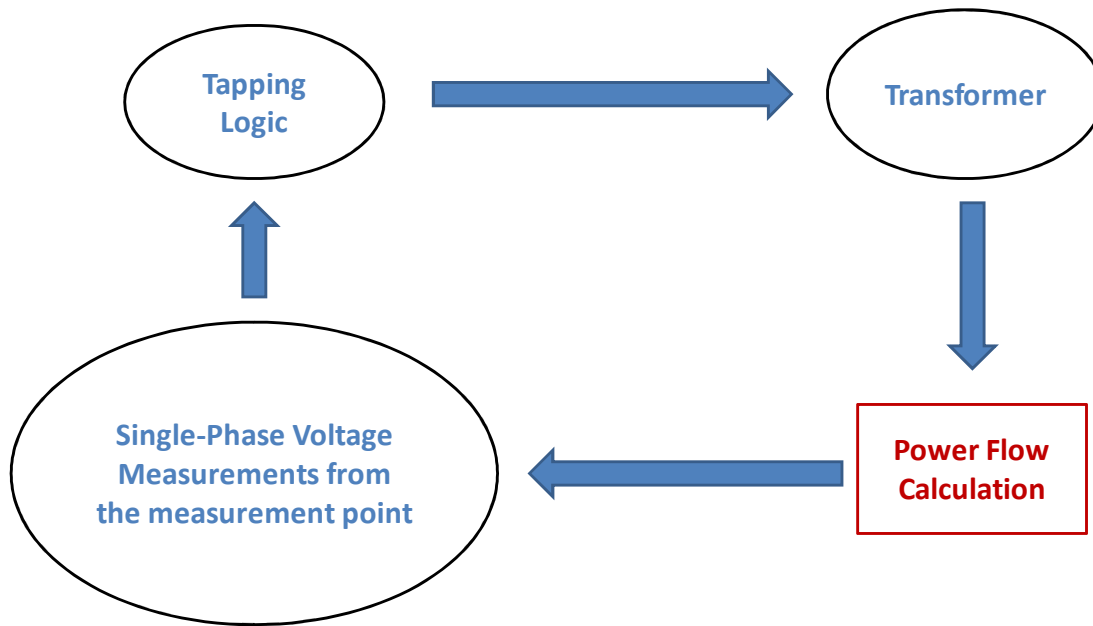


Figure 2.10. Transformer model logic

2.4.1. Tapping Logic

The logical method of controlling continuously the tap position has been very important in order to achieve a certain precision in following the unbalancing conditions: the more accurate the tap changing system, the more efficient the operation. Therefore the tapping logic which the decoupled phase OLTC unit operations are based on needs to be defined in detail.

Basically two different approaches could be used: an iterative method and a proportional method.

The operating principle of the iterative method is the following.

Voltage measurements at the measurement bus are performed: within a certain range in the neighborhood of the reference voltage V_{ref} (here set as the nominal voltage), the tap changer does not operate, laying on the zero-position. This range is also known as the Dead Band – DB or ‘non-action zone’. In order to achieve a tap position changing, the measured voltage needs to exceed the dead band. The tap position changes step by step (tap by tap), and the voltage increases or decreases by +1 or -1 step of a certain prefixed ΔV , which is nothing but a percentage of V_n .

After a cycle the comparison operation is repeated and the tap position is changed time by time till when the measured voltage value falls into the dead band.

In Figure 2.11 an operating scheme of the iterative method is presented.

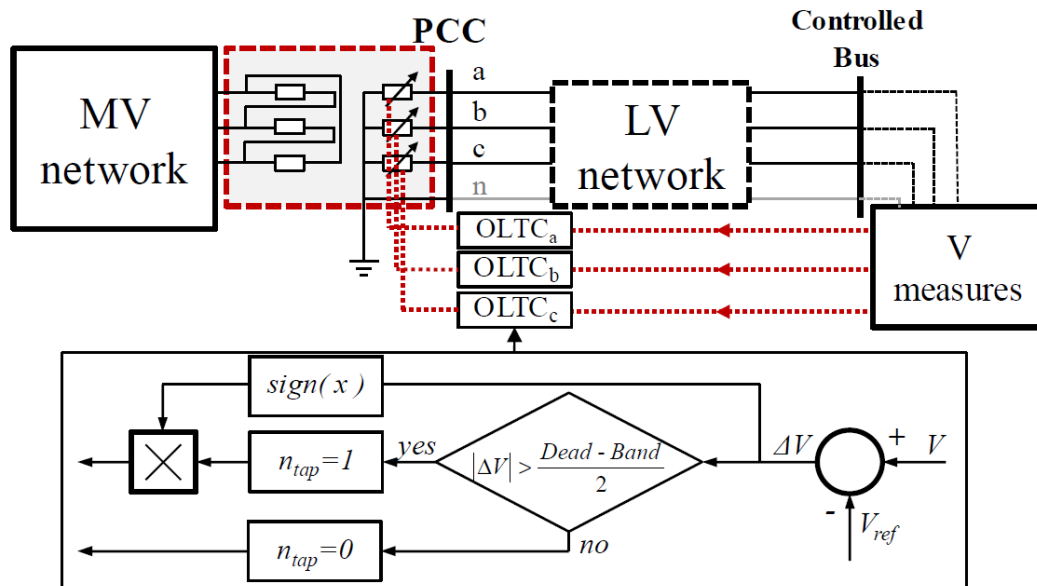


Figure 2.11. Setup of the iterative control strategy

On the other hand the proportional method focuses on changing directly the tap position according to voltage measurements at the measurement bus. To do this a tapping logic law needs to be set as input for the logic; theoretically both a discrete and a continuous mode regulation are possible. The discrete mode is based on a step law, where certain voltage values correspond to specific tap positions, which differs quite a lot one from the other.

Anyway the best way to control the tap position is using a continuous mode regulation, which means using a high number of very small steps with correspondent very small voltage variation. Such a high number of steps pursues continuative tap changings, performing a more accurate voltage regulation at the measurement busbar.

For the project, it has been decided to use the proportional method, whose logic control is basically easier than the iterative method. In order to achieve a more accurate voltage regulation the continuous mode logic has been chosen instead of the discrete one.

At the beginning two cases have been analyzed for each study case and each scenario. They were characterized by extreme tap positions of ± 1 or ± 2 , which means a maximum voltage deviation respectively of $\pm 2.5\%$ and $\pm 5\%$. That is because, as type setting of the single-phase transformers, it has been set that the additional voltage per tap is 2.5%.

In fact for both the cases the same tap sensitivity but different tap ranges have been used.

The first index (tap sensitivity) represents the voltage sensitivity of the tapping control method. Its value has been set at 0.001 p.u., which means that the OLTC operates according to the voltage measurements with a 0.001 p.u. precision.

The second index (tap range) represents the range of voltage within the tap position changes between the two extreme values. Its value has been set at 0.05 for '-1+1' case, and at 0.1 for '-2+2' case. Out of this range, the extreme tap position values are reached.

The two different tap control methods are represented in the following graph (Figure 2.12), where the values adopted for the simulation are plotted.

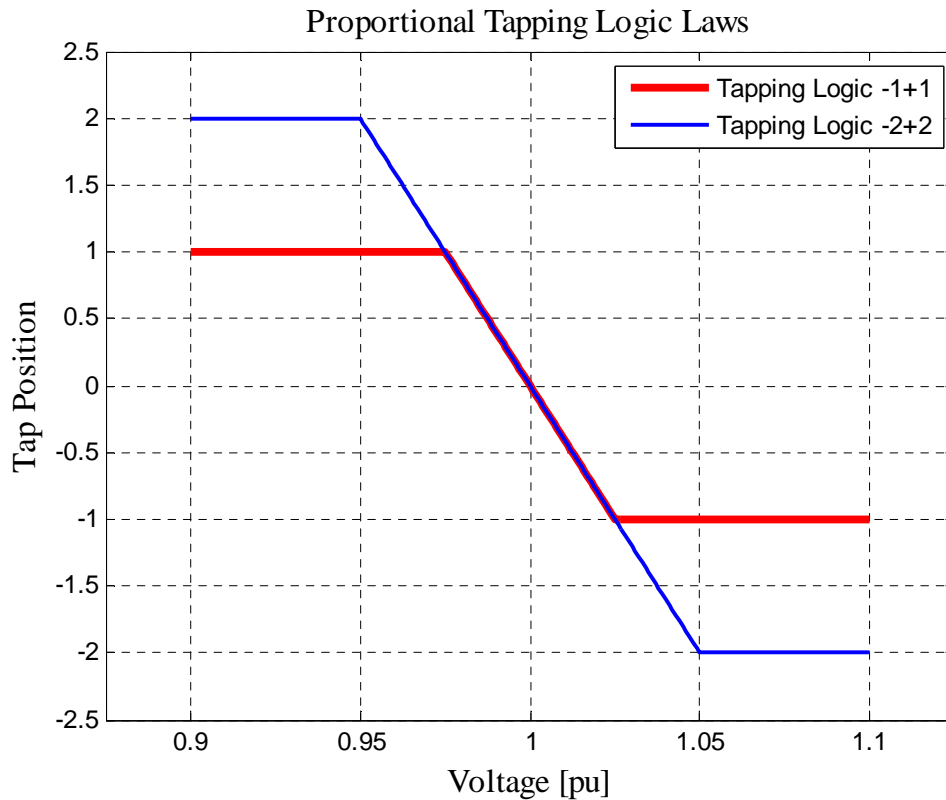


Figure 2.12. Tapping logic laws of the proportional method

Since the real transformer which will be adopted for real tests in the experimental facility SYSLAB-PowerLab.DK of the DTU Risø Campus will be able to offer a maximum voltage deviation of $\pm 5\%$, it has been decided to concentrate to simulations based on the ‘-2+2’ tapping logic.

The tap position values are furnished to the PowerFactory software as input data from a LookUp table, which represents perfectly the continuous tapping logic law of Figure 2.12.

2.5. Dynamics analysis – RMS Simulation in DIgSILENT PowerFactory

The dynamics simulation functions available in DIgSILENT PowerFactory are able to analyze the dynamic behavior of small systems and large power systems in the time domain. These functions therefore make it possible to model complex systems such as industrial networks and large transmission grids in detail, taking into account electrical and mechanical parameters [23].

The study of power system stability involves the analysis of the behavior of power systems under conditions before and after sudden changes in load or generation, during faults and outages. The robustness of a system is defined by the ability of the system to maintain stable operation under normal and perturbed conditions. It is therefore necessary to design and operate a power system so that transient events (i.e. probable contingencies), can be withstood without the loss of load or loss of synchronism in the power system. Transients in electrical power systems can be classified according to three possible timeframes:

- Short-term, or electromagnetic transients;
- Mid-term, or electromechanical transients;
- Long-term transients.

The multilevel modelling of power system elements and the use of advanced algorithms means that the functions in PowerFactory can analyze the complete range of transient phenomena in electrical power systems. Consequently, there are three different simulation functions available:

- A basic function which uses a symmetrical steady-state (RMS) network model for mid-term and long-term transients under balanced network conditions;
- A three-phase function which uses a steady-state (RMS) network model for mid-term and long-term transients under balanced and unbalanced network conditions, i.e. for analyzing dynamic behavior after unsymmetrical faults;
- An electromagnetic transient (EMT) simulation function using a dynamic network model for electromagnetic and electromechanical transients under balanced and

unbalanced network conditions. This function is particularly suited to the analysis of short-term transients.

Of course for this project the second type of simulation has been used (RMS values – unbalanced three phase case).

The three-phase RMS simulation function uses a steady-state, three-phase representation of the passive electrical network and can therefore compute unbalanced network conditions, either due to unbalanced network elements or due to asymmetrical faults. Dynamics in electromechanical, control and thermal devices are represented in the same way as in the basic RMS simulation function.

Asymmetrical electromechanical devices can be modelled and single-phase and two-phase networks can also be analyzed using this analysis function.

In addition to the balanced RMS simulation events, unbalanced fault events can be simulated, such as: single-phase and two-phase (to ground) short-circuits; phase to phase short-circuits; inter-circuit faults between different lines; single- and double-phase line interruptions.

All of these events can be modelled to occur simultaneously or separately, hence any combination of symmetrical and asymmetrical faults can be modelled.

Time-domain simulations in PowerFactory are initialized by a valid load flow, and PowerFactory functions determine the initial conditions for all power system elements including all controller units and mechanical components. These initial conditions represent the steady-state operating point at the beginning of the simulation, fulfilling the requirements that the derivatives of all state variables of loads, machines, controllers, etc., are zero.

Before the start of the simulation process, it is also determined what type of network representation must be used for further analysis, what step sizes to use, which events to handle and where to store the results.

In the Initial Conditions command (*ComInc*) dialogue (see Figure 2.13) all simulation settings can be defined, such as the simulation type (i.e. RMS or EMT, balanced or unbalanced) and simulation step size settings.

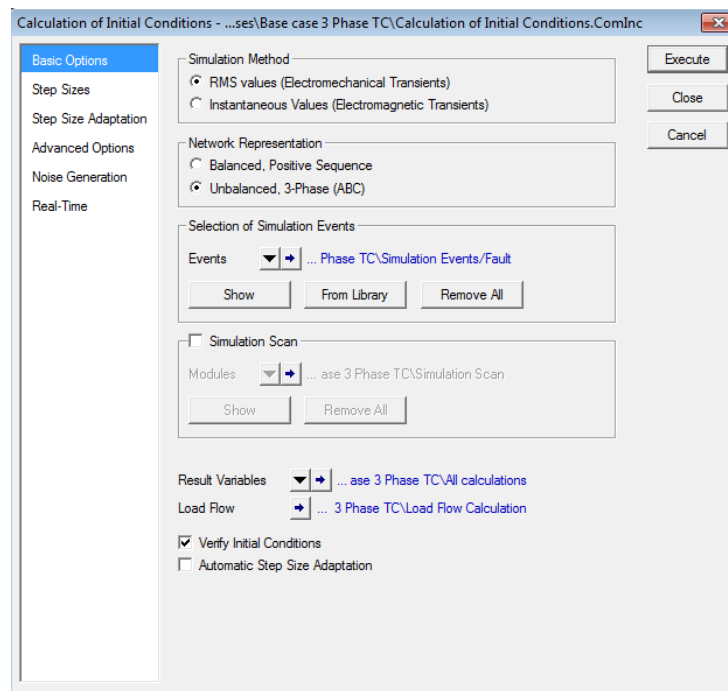


Figure 2.13. Initial conditions command dialogue window

The process of performing a transient simulation typically involves the following steps:

- Calculation of initial values, including a load flow calculation;
- Definition of result variables and/or simulation events;
- Optional definition of result graphs and/or other virtual instruments;
- Execution of simulation;
- Creating additional result graphs or virtual instruments, or editing existing ones;
- Changing settings, repeating calculations;
- Printing results.

During an EMT or RMS simulation, a large number of signal variables are changing over time. To reduce the available data and to narrow down the number of variables to those necessary for the analysis of each particular case, a selection of these signals for later use has to be defined. In this way it is necessary to define for each grid element which variables should be calculated, choosing from different category lists, such as Calculation Parameter,

Element Parameter, Type Parameter, Reference Parameter, Bus Results, Signals and Currents, Voltages and Powers.

As example in Figure 2.14 a variables selection window is shown.

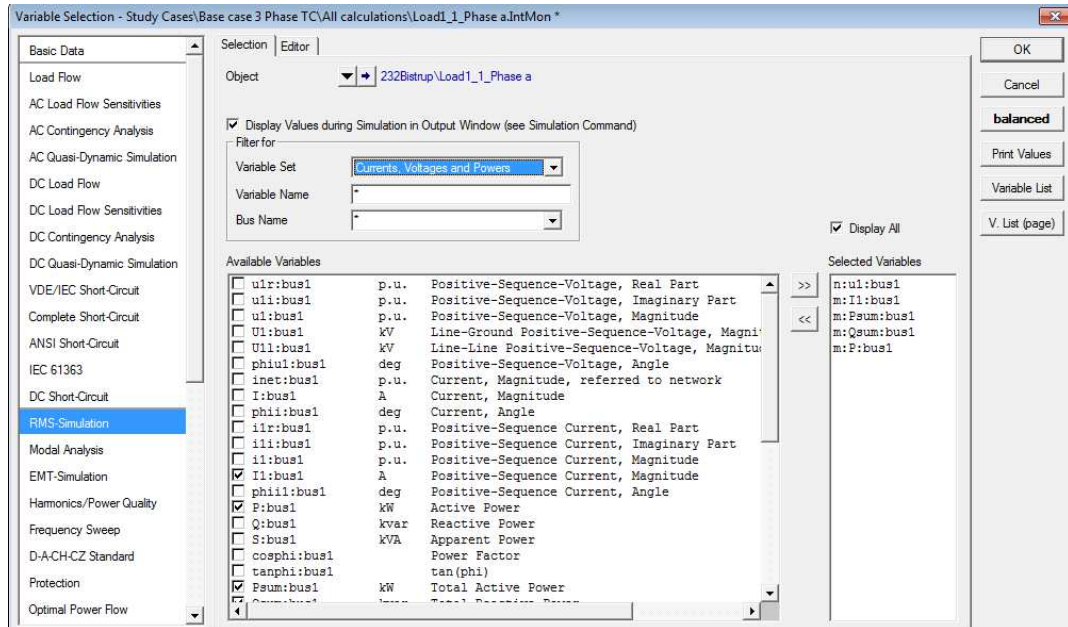


Figure 2.14. Variable selection window

Therefore, one or more result objects containing the result variables can be configured. The simulation function needs the reference to a result object to store the results.

Stability analysis calculations are typically based on predefined system models. In the majority of cases the standard IEEE definitions for controllers, prime movers and other associated devices and functions are used. Anyway it is otherwise possible to improve the system model not using the IEEE standard models, but instead building a new block diagram of the individual controller/mechanical system to represent the device. This facilitates highly accurate system modelling.

The PowerFactory modelling philosophy is targeted towards a strictly hierarchical system modelling approach, which combines both graphical and script-based modelling methods.

All the data, which represents power system Elements, Single Line Diagrams, Study Cases, system Operation Scenarios, calculation commands, program Settings etc., are stored as

objects inside a hierarchical set of folders. The folders are arranged in order to facilitate the definition of the studies and optimize the use of the tools provided by the program.

The objects are grouped according to the kind of element that they represent. These groups are known as ‘Classes’ within the PowerFactory environment.

The basis for the modelling approach is formed by the basic hierarchical levels of time-domain modelling:

- The **DSL block definitions**, based on the "DIGSILENT Simulation Language" (DSL), form the basic building blocks to represent transfer functions and differential equations for the more complex transient models.
- The **built-in models** and **common models**. The built-in models or elements are the transient PowerFactory models for standard power system equipment, i.e. for generators, motors, static VAR compensators, etc. The common models are based on the DSL block definitions and are the front-end of the user-defined transient models.
- The **composite models** are based on **composite frames** and are used to combine and interconnect several elements (built-in models) and/or common models. The composite frames enable the reuse of the basic structure of the composite model.

The following part explains the relationships between the Composite Model (which is using a Frame as type) and the Common Model (based on a block diagram as type) in detail.

The Composite Model (*ElmComp*) references the definition of a composite frame. This composite frame is basically a schematic diagram containing various empty slots, in which controller or elements can be assigned. These slots are then interconnected according to the diagram. The slots in the composite frame are pre-configured for specific transient models.

A window containing the list of Composite Models looks like Figure 2.15.

| Name | Gnd | Frame BlkDef | Out of Service | Slots BlkSlot | Net Elements Elm*Sta*.intRef |
|--------------------------------|-----------|------------------|-------------------------------------|------------------|-------------------------------|
| Composite - Trafo Phase a | 232Bstsup | Trafo controller | <input checked="" type="checkbox"/> | Vmeas An | Voltage Measurement Bus 6_3_a |
| Composite - Trafo Phase b | 232Bstsup | Trafo controller | <input checked="" type="checkbox"/> | Vmeas An | Voltage Measurement Bus 6_3_a |
| Composite - Trafo Phase c | 232Bstsup | Trafo controller | <input checked="" type="checkbox"/> | Vmeas An | Voltage Measurement Bus 6_3_a |
| Composite Model1_1_Phase a | 232Bstsup | ComLoad | <input type="checkbox"/> | Measurement Slot | Measurement File |
| Composite Model1_1_Phase b | 232Bstsup | ComLoad | <input type="checkbox"/> | Measurement Slot | Measurement File |
| Composite Model1_1_Phase c | 232Bstsup | ComLoad | <input type="checkbox"/> | Measurement Slot | Measurement File |
| Composite Model1_2_Phase a | 232Bstsup | ComLoad | <input type="checkbox"/> | Measurement Slot | Measurement File |
| Composite Model1_2_Phase b | 232Bstsup | ComLoad | <input type="checkbox"/> | Measurement Slot | Measurement File |
| Composite Model1_2_Phase b old | 232Bstsup | ComLoad | <input checked="" type="checkbox"/> | Measurement Slot | Measurement File |
| Composite Model1_2_Phase c | 232Bstsup | ComLoad | <input type="checkbox"/> | Measurement Slot | Measurement File |
| Composite Model1_2_Phase c old | 232Bstsup | ComLoad | <input checked="" type="checkbox"/> | Measurement Slot | Measurement File |
| Composite Model2_Phase a | 232Bstsup | ComLoad | <input type="checkbox"/> | Measurement Slot | Measurement File |
| Composite Model2_Phase b | 232Bstsup | ComLoad | <input type="checkbox"/> | Measurement Slot | Measurement File |
| Composite Model2_Phase c | 232Bstsup | ComLoad | <input type="checkbox"/> | Measurement Slot | Measurement File |
| Composite Model3_Phase a | 232Bstsup | ComLoad | <input type="checkbox"/> | Measurement Slot | Measurement File |
| Composite Model3_Phase b | 232Bstsup | ComLoad | <input type="checkbox"/> | Measurement Slot | Measurement File |
| Composite Model3_Phase c | 232Bstsup | ComLoad | <input type="checkbox"/> | Measurement Slot | Measurement File |
| Composite Model3_Phase a | 232Bstsup | ComLoad | <input type="checkbox"/> | Measurement Slot | Measurement File |
| Composite Model4_1_Phase b | 232Bstsup | ComLoad | <input type="checkbox"/> | Measurement Slot | Measurement File |
| Composite Model4_1_Phase c | 232Bstsup | ComLoad | <input type="checkbox"/> | Measurement Slot | Measurement File |
| Composite Model4_2_Phase a | 232Bstsup | ComLoad | <input type="checkbox"/> | Measurement Slot | Measurement File |
| Composite Model4_2_Phase b | 232Bstsup | ComLoad | <input type="checkbox"/> | Measurement Slot | Measurement File |
| Composite Model4_2_Phase c | 232Bstsup | ComLoad | <input type="checkbox"/> | Measurement Slot | Measurement File |
| Composite Model4_3_Phase a | 232Bstsup | ComLoad | <input type="checkbox"/> | Measurement Slot | Measurement File |
| Composite Model4_3_Phase b | 232Bstsup | ComLoad | <input type="checkbox"/> | Measurement Slot | Measurement File |
| Composite Model4_3_Phase c | 232Bstsup | ComLoad | <input type="checkbox"/> | Measurement Slot | Measurement File |
| Composite Model5_Phase a | 232Bstsup | ComLoad | <input type="checkbox"/> | Measurement Slot | Measurement File |
| Composite Model5_Phase b | 232Bstsup | ComLoad | <input type="checkbox"/> | Measurement Slot | Measurement File |
| Composite Model5_Phase c | 232Bstsup | ComLoad | <input type="checkbox"/> | Measurement Slot | Measurement File |
| Composite Model5_1_Phase a | 232Bstsup | ComLoad | <input type="checkbox"/> | Measurement Slot | Measurement File |
| Composite Model5_1_Phase b | 232Bstsup | ComLoad | <input type="checkbox"/> | Measurement Slot | Measurement File |
| Composite Model5_1_Phase c | 232Bstsup | ComLoad | <input type="checkbox"/> | Measurement Slot | Measurement File |
| Composite Model5_2_Phase a | 232Bstsup | ComLoad | <input type="checkbox"/> | Measurement Slot | Measurement File |
| Composite Model5_2_Phase b | 232Bstsup | ComLoad | <input type="checkbox"/> | Measurement Slot | Measurement File |
| Composite Model5_2_Phase c | 232Bstsup | ComLoad | <input type="checkbox"/> | Measurement Slot | Measurement File |
| Composite Model5_3_Phase a | 232Bstsup | ComLoad | <input type="checkbox"/> | Measurement Slot | Measurement File |
| Composite Model5_3_Phase b | 232Bstsup | ComLoad | <input type="checkbox"/> | Measurement Slot | Measurement File |
| Composite Model5_3_Phase c | 232Bstsup | ComLoad | <input type="checkbox"/> | Measurement Slot | Measurement File |
| Composite FV1_Phase a | 232Bstsup | ComLoadMod | <input type="checkbox"/> | Measurement Slot | Measurement File |
| Composite FV1_Phase b | 232Bstsup | ComLoadMod | <input type="checkbox"/> | Measurement Slot | Measurement File |
| Composite FV1_Phase c | 232Bstsup | ComLoadMod | <input type="checkbox"/> | Measurement Slot | Measurement File |
| Composite FV2_Phase a | 232Bstsup | ComLoadMod | <input type="checkbox"/> | Measurement Slot | Measurement File |
| Composite FV2_Phase b | 232Bstsup | ComLoadMod | <input type="checkbox"/> | Measurement Slot | Measurement File |
| Composite FV2_Phase c | 232Bstsup | ComLoadMod | <input type="checkbox"/> | Measurement Slot | Measurement File |
| Composite FV3_Phase a | 232Bstsup | ComLoadMod | <input type="checkbox"/> | Measurement Slot | Measurement File |
| Composite FV3_Phase b | 232Bstsup | ComLoadMod | <input type="checkbox"/> | Measurement Slot | Measurement File |
| Composite FV3_Phase c | 232Bstsup | ComLoadMod | <input type="checkbox"/> | Measurement Slot | Measurement File |
| Composite FV4_Phase a | 232Bstsup | ComLoadMod | <input type="checkbox"/> | Measurement Slot | Measurement File |
| Composite FV4_Phase b | 232Bstsup | ComLoadMod | <input type="checkbox"/> | Measurement Slot | Measurement File |
| Composite FV4_Phase c | 232Bstsup | ComLoadMod | <input type="checkbox"/> | Measurement Slot | Measurement File |
| Composite FV5_Phase a | 232Bstsup | ComLoadMod | <input type="checkbox"/> | Measurement Slot | Measurement File |
| Composite FV5_Phase b | 232Bstsup | ComLoadMod | <input type="checkbox"/> | Measurement Slot | Measurement File |
| Composite FV5_Phase c | 232Bstsup | ComLoadMod | <input type="checkbox"/> | Measurement Slot | Measurement File |
| Composite FV6_Phase a | 232Bstsup | ComLoadMod | <input type="checkbox"/> | Measurement Slot | Measurement File |
| Composite FV6_Phase b | 232Bstsup | ComLoadMod | <input type="checkbox"/> | Measurement Slot | Measurement File |
| Composite FV6_Phase c | 232Bstsup | ComLoadMod | <input type="checkbox"/> | Measurement Slot | Measurement File |

Figure 2.15. Composite models list window

The Composite Frame (*BlkDef*) has different slots which are interconnected according to the diagram. The composite model, which uses this composite frame, shows a list of the available slots and the name of the slot, as can be seen in Figure 2.16.

| Slots BlkSlot | Net Elements Elm*Sta*.intRef |
|---------------------|--------------------------------------|
| 1 MeasurementSlot | Measurement File |
| 2 Vmeas An | Voltage Measurement Bus1_Load1_1_a |
| 3 Vmeas Bn | Voltage Measurement Bus1_Load1_1_b |
| 4 Vmeas Cn | Voltage Measurement Bus1_Load1_1_c |
| 5 LoadSlot | Load1_1_Phase a |
| 6 Voltage Corrector | Voltage Corrector - Load_1_1_Phase a |

Figure 2.16. Composite model slots list window

The Built-In Models are pre-configured elements which do not need a specific model definition. Any kind of element which is able to provide input or output variables, e.g. converters, busbars, etc, can be inserted into the slots.

The Common Models (*ElmDsl*) combines a model definition with specific parameter settings. There are predefined definitions as well, so that the user can create his own model definitions.

A window containing the list of Common Models looks like Figure 2.17.

| Name | In Folder | Grid | Events | Model Definition BlkDef* | Out of Service | A-table integratio... | Parameter | Characteristics | Two Dimensional... | Net Element Elm*Slu*InRef | Signal Name |
|--------------------------------------|----------------------------|-----------|--------------------|-----------------------------|--------------------------|--------------------------|-----------|-----------------|--------------------|------------------------------|-------------|
| Actuator - Trafo Phase a | Composite - Trafo Phase a | 232Batrup | Actuator | Actuator | <input type="checkbox"/> | <input type="checkbox"/> | 0.5 | ... | ... | ... | ... |
| Actuator - Trafo Phase b | Composite - Trafo Phase b | 232Batrup | Actuator | Actuator | <input type="checkbox"/> | <input type="checkbox"/> | 0.5 | ... | 0... | ... | ... |
| Actuator - Trafo Phase c | Composite - Trafo Phase c | 232Batrup | Actuator | Actuator | <input type="checkbox"/> | <input type="checkbox"/> | 0.5 | ... | 0... | ... | ... |
| Tapping Controller - Trafo Phase a | Composite - Trafo Phase a | 232Batrup | Tapping controller | Tapping controller | <input type="checkbox"/> | <input type="checkbox"/> | 1... | 103 | ... | ... | ... |
| Tapping Controller - Trafo Phase b | Composite - Trafo Phase b | 232Batrup | Tapping controller | Tapping controller | <input type="checkbox"/> | <input type="checkbox"/> | 1... | 103 | ... | ... | ... |
| Tapping Controller - Trafo Phase c | Composite - Trafo Phase c | 232Batrup | Tapping controller | Tapping controller | <input type="checkbox"/> | <input type="checkbox"/> | 1... | 103 | ... | ... | ... |
| Voltage Corrector - Load_1_1_Phase a | Composite Model1_1_Phase a | 232Batrup | Voltage Corrector | Voltage Corrector | <input type="checkbox"/> | <input type="checkbox"/> | 1... | ... | ... | ... | ... |
| Voltage Corrector - Load_1_1_Phase b | Composite Model1_1_Phase b | 232Batrup | Voltage Corrector | Voltage Corrector | <input type="checkbox"/> | <input type="checkbox"/> | 0... | 0... | 0... | ... | ... |
| Voltage Corrector - Load_1_1_Phase c | Composite Model1_1_Phase c | 232Batrup | Voltage Corrector | Voltage Corrector | <input type="checkbox"/> | <input type="checkbox"/> | 0... | 0... | 0... | ... | ... |
| Voltage Corrector - Load_1_2_Phase a | Composite Model1_2_Phase a | 232Batrup | Voltage Corrector | Voltage Corrector | <input type="checkbox"/> | <input type="checkbox"/> | 1... | 0... | 0... | ... | ... |
| Voltage Corrector - Load_1_2_Phase b | Composite Model1_2_Phase b | 232Batrup | Voltage Corrector | Voltage Corrector | <input type="checkbox"/> | <input type="checkbox"/> | 0... | 0... | 0... | ... | ... |
| Voltage Corrector - Load_1_2_Phase c | Composite Model1_2_Phase c | 232Batrup | Voltage Corrector | Voltage Corrector | <input type="checkbox"/> | <input type="checkbox"/> | 0... | 0... | 0... | ... | ... |
| Voltage Corrector - Load_2_Phase a | Composite Model2_Phase a | 232Batrup | Voltage Corrector | Voltage Corrector | <input type="checkbox"/> | <input type="checkbox"/> | 1... | 0... | 0... | ... | ... |
| Voltage Corrector - Load_2_Phase b | Composite Model2_Phase b | 232Batrup | Voltage Corrector | Voltage Corrector | <input type="checkbox"/> | <input type="checkbox"/> | 0... | 0... | 0... | ... | ... |
| Voltage Corrector - Load_2_Phase c | Composite Model2_Phase c | 232Batrup | Voltage Corrector | Voltage Corrector | <input type="checkbox"/> | <input type="checkbox"/> | 0... | 0... | 0... | ... | ... |
| Voltage Corrector - Load_3_Phase a | Composite Model3_Phase a | 232Batrup | Voltage Corrector | Voltage Corrector | <input type="checkbox"/> | <input type="checkbox"/> | 1... | 0... | 0... | ... | ... |
| Voltage Corrector - Load_3_Phase b | Composite Model3_Phase b | 232Batrup | Voltage Corrector | Voltage Corrector | <input type="checkbox"/> | <input type="checkbox"/> | 0... | 0... | 0... | ... | ... |
| Voltage Corrector - Load_3_Phase c | Composite Model3_Phase c | 232Batrup | Voltage Corrector | Voltage Corrector | <input type="checkbox"/> | <input type="checkbox"/> | 0... | 0... | 0... | ... | ... |
| Voltage Corrector - Load_4_1_Phase a | Composite Model4_1_Phase a | 232Batrup | Voltage Corrector | Voltage Corrector | <input type="checkbox"/> | <input type="checkbox"/> | 1... | 0... | 0... | ... | ... |
| Voltage Corrector - Load_4_1_Phase b | Composite Model4_1_Phase b | 232Batrup | Voltage Corrector | Voltage Corrector | <input type="checkbox"/> | <input type="checkbox"/> | 0... | 0... | 0... | ... | ... |
| Voltage Corrector - Load_4_1_Phase c | Composite Model4_1_Phase c | 232Batrup | Voltage Corrector | Voltage Corrector | <input type="checkbox"/> | <input type="checkbox"/> | 0... | 0... | 0... | ... | ... |
| Voltage Corrector - Load_4_2_Phase a | Composite Model4_2_Phase a | 232Batrup | Voltage Corrector | Voltage Corrector | <input type="checkbox"/> | <input type="checkbox"/> | 1... | 0... | 0... | ... | ... |
| Voltage Corrector - Load_4_2_Phase b | Composite Model4_2_Phase b | 232Batrup | Voltage Corrector | Voltage Corrector | <input type="checkbox"/> | <input type="checkbox"/> | 0... | 0... | 0... | ... | ... |
| Voltage Corrector - Load_4_2_Phase c | Composite Model4_2_Phase c | 232Batrup | Voltage Corrector | Voltage Corrector | <input type="checkbox"/> | <input type="checkbox"/> | 0... | 0... | 0... | ... | ... |
| Voltage Corrector - Load_4_3_Phase a | Composite Model4_3_Phase a | 232Batrup | Voltage Corrector | Voltage Corrector | <input type="checkbox"/> | <input type="checkbox"/> | 1... | 0... | 0... | ... | ... |
| Voltage Corrector - Load_4_3_Phase b | Composite Model4_3_Phase b | 232Batrup | Voltage Corrector | Voltage Corrector | <input type="checkbox"/> | <input type="checkbox"/> | 0... | 0... | 0... | ... | ... |
| Voltage Corrector - Load_4_3_Phase c | Composite Model4_3_Phase c | 232Batrup | Voltage Corrector | Voltage Corrector | <input type="checkbox"/> | <input type="checkbox"/> | 0... | 0... | 0... | ... | ... |
| Voltage Corrector - Load_5_Phase a | Composite Model5_Phase a | 232Batrup | Voltage Corrector | Voltage Corrector | <input type="checkbox"/> | <input type="checkbox"/> | 1... | 0... | 0... | ... | ... |
| Voltage Corrector - Load_5_Phase b | Composite Model5_Phase b | 232Batrup | Voltage Corrector | Voltage Corrector | <input type="checkbox"/> | <input type="checkbox"/> | 0... | 0... | 0... | ... | ... |
| Voltage Corrector - Load_5_Phase c | Composite Model5_Phase c | 232Batrup | Voltage Corrector | Voltage Corrector | <input type="checkbox"/> | <input type="checkbox"/> | 0... | 0... | 0... | ... | ... |
| Voltage Corrector - Load_6_1_Phase a | Composite Model6_1_Phase a | 232Batrup | Voltage Corrector | Voltage Corrector | <input type="checkbox"/> | <input type="checkbox"/> | 1... | 0... | 0... | ... | ... |
| Voltage Corrector - Load_6_1_Phase b | Composite Model6_1_Phase b | 232Batrup | Voltage Corrector | Voltage Corrector | <input type="checkbox"/> | <input type="checkbox"/> | 0... | 0... | 0... | ... | ... |
| Voltage Corrector - Load_6_1_Phase c | Composite Model6_1_Phase c | 232Batrup | Voltage Corrector | Voltage Corrector | <input type="checkbox"/> | <input type="checkbox"/> | 0... | 0... | 0... | ... | ... |
| Voltage Corrector - Load_6_2_Phase a | Composite Model6_2_Phase a | 232Batrup | Voltage Corrector | Voltage Corrector | <input type="checkbox"/> | <input type="checkbox"/> | 1... | 0... | 0... | ... | ... |
| Voltage Corrector - Load_6_2_Phase b | Composite Model6_2_Phase b | 232Batrup | Voltage Corrector | Voltage Corrector | <input type="checkbox"/> | <input type="checkbox"/> | 0... | 0... | 0... | ... | ... |
| Voltage Corrector - Load_6_2_Phase c | Composite Model6_2_Phase c | 232Batrup | Voltage Corrector | Voltage Corrector | <input type="checkbox"/> | <input type="checkbox"/> | 0... | 0... | 0... | ... | ... |
| Voltage Corrector - Load_6_3_Phase a | Composite Model6_3_Phase a | 232Batrup | Voltage Corrector | Voltage Corrector | <input type="checkbox"/> | <input type="checkbox"/> | 1... | 0... | 0... | ... | ... |
| Voltage Corrector - Load_6_3_Phase b | Composite Model6_3_Phase b | 232Batrup | Voltage Corrector | Voltage Corrector | <input type="checkbox"/> | <input type="checkbox"/> | 0... | 0... | 0... | ... | ... |
| Voltage Corrector - Load_6_3_Phase c | Composite Model6_3_Phase c | 232Batrup | Voltage Corrector | Voltage Corrector | <input type="checkbox"/> | <input type="checkbox"/> | 0... | 0... | 0... | ... | ... |
| Voltage Corrector - PV1_Phase a | Composite PV1_Phase a | 232Batrup | Voltage Corrector | Voltage Corrector | <input type="checkbox"/> | <input type="checkbox"/> | 1... | 0... | 0... | ... | ... |
| Voltage Corrector - PV1_Phase b | Composite PV1_Phase b | 232Batrup | Voltage Corrector | Voltage Corrector | <input type="checkbox"/> | <input type="checkbox"/> | 0... | 0... | 0... | ... | ... |
| Voltage Corrector - PV1_Phase c | Composite PV1_Phase c | 232Batrup | Voltage Corrector | Voltage Corrector | <input type="checkbox"/> | <input type="checkbox"/> | 0... | 0... | 0... | ... | ... |
| Voltage Corrector - PV2_Phase a | Composite PV2_Phase a | 232Batrup | Voltage Corrector | Voltage Corrector | <input type="checkbox"/> | <input type="checkbox"/> | 1... | 0... | 0... | ... | ... |
| Voltage Corrector - PV2_Phase b | Composite PV2_Phase b | 232Batrup | Voltage Corrector | Voltage Corrector | <input type="checkbox"/> | <input type="checkbox"/> | 0... | 0... | 0... | ... | ... |
| Voltage Corrector - PV2_Phase c | Composite PV2_Phase c | 232Batrup | Voltage Corrector | Voltage Corrector | <input type="checkbox"/> | <input type="checkbox"/> | 0... | 0... | 0... | ... | ... |
| Voltage Corrector - PV3_Phase a | Composite PV3_Phase a | 232Batrup | Voltage Corrector | Voltage Corrector | <input type="checkbox"/> | <input type="checkbox"/> | 1... | 0... | 0... | ... | ... |
| Voltage Corrector - PV3_Phase b | Composite PV3_Phase b | 232Batrup | Voltage Corrector | Voltage Corrector | <input type="checkbox"/> | <input type="checkbox"/> | 0... | 0... | 0... | ... | ... |
| Voltage Corrector - PV3_Phase c | Composite PV3_Phase c | 232Batrup | Voltage Corrector | Voltage Corrector | <input type="checkbox"/> | <input type="checkbox"/> | 0... | 0... | 0... | ... | ... |
| Voltage Corrector - PV4_Phase a | Composite PV4_Phase a | 232Batrup | Voltage Corrector | Voltage Corrector | <input type="checkbox"/> | <input type="checkbox"/> | 1... | 0... | 0... | ... | ... |
| Voltage Corrector - PV4_Phase b | Composite PV4_Phase b | 232Batrup | Voltage Corrector | Voltage Corrector | <input type="checkbox"/> | <input type="checkbox"/> | 0... | 0... | 0... | ... | ... |
| Voltage Corrector - PV4_Phase c | Composite PV4_Phase c | 232Batrup | Voltage Corrector | Voltage Corrector | <input type="checkbox"/> | <input type="checkbox"/> | 0... | 0... | 0... | ... | ... |
| Voltage Corrector - PV5_Phase a | Composite PV5_Phase a | 232Batrup | Voltage Corrector | Voltage Corrector | <input type="checkbox"/> | <input type="checkbox"/> | 1... | 0... | 0... | ... | ... |
| Voltage Corrector - PV5_Phase b | Composite PV5_Phase b | 232Batrup | Voltage Corrector | Voltage Corrector | <input type="checkbox"/> | <input type="checkbox"/> | 0... | 0... | 0... | ... | ... |
| Voltage Corrector - PV5_Phase c | Composite PV5_Phase c | 232Batrup | Voltage Corrector | Voltage Corrector | <input type="checkbox"/> | <input type="checkbox"/> | 0... | 0... | 0... | ... | ... |
| Voltage Corrector - PV6_Phase a | Composite PV6_Phase a | 232Batrup | Voltage Corrector | Voltage Corrector | <input type="checkbox"/> | <input type="checkbox"/> | 1... | 0... | 0... | ... | ... |
| Voltage Corrector - PV6_Phase b | Composite PV6_Phase b | 232Batrup | Voltage Corrector | Voltage Corrector | <input type="checkbox"/> | <input type="checkbox"/> | 0... | 0... | 0... | ... | ... |
| Voltage Corrector - PV6_Phase c | Composite PV6_Phase c | 232Batrup | Voltage Corrector | Voltage Corrector | <input type="checkbox"/> | <input type="checkbox"/> | 0... | 0... | 0... | ... | ... |

Figure 2.17. Composite models list window

The common model has a reference to the Model Definition (*BlkDef*), which looks similar to the composite frame. Here different blocks are defined and connected together according to the diagram. The input and output variables have to fit with the slot definition of the slot that the model is defined for.

Usually not all slots of the composite model must necessarily be used: there can also be empty slots. In such cases, the input of this slot is unused and the output is assumed to be constant over the entire simulation.

2.6. Grid elements modeling in PowerFactory

After having described quite specifically the way which has been chosen for the characterizations of transformer, loads and PVs (Chapter 2.3 and Chapter 2.4) and after having furnished several information regarding the operational structure of the PowerFactory software (Chapter 2.5), in the following subparagraphs slot connections of the Composite Frames related to network elements are presented.

2.6.1. Transformer Controller

Each single-phase transformer has been related to the same frame-block, which as can be seen in Figure 2.18 is composed by three measurement slots, the '*Tapping log. ElmTap**' slot, the '*Actuator- ElmE^s**' slot and finally the '*Transformer ElmTr2**' slot.

Because of the different test requirements of the project (no tap action, three-phase coordinated continuous tap action and single phase continuous tap action) three measurement blocks instead of just one have been used. In this way the same frame-block could be adapted to any scenario by managing the three 'input blocks'. The measured voltages have been phase-n voltages and the measurement point has been the last bus-bar at the end of the line, as described in the Chapter 3.1.

The only one voltage that time to time has been measured (uA, uB or uC) was the input of the second block (namely '*Tapping log.*' slot), the 'heart' of the control system: its operations were based on a continuous tapping logic which according to the x-values (i.e. voltage values) provided corresponding tap selector positions (y-values). The tap position values have been manually furnished to the PowerFactory software as input data from a 'look-up' table, which represents perfectly the continuous tapping logic law of Figure 2.12. If for instance a measured voltage value has assumed an intermediate value of the ones reported in the 'look-up' table, thanks to the command '*lapprox*' a linear approximation for the corresponding tap position value has been provided.

The output signal goes into the ‘*Actuator- ElmE^s**’ slot which is a delay-integrator block, whose output signal goes into the last block, that applies the new tap position to single-phase transformers. For the three common models of the single-phase transformers it has been decided to consider a delay of 0.5 s.

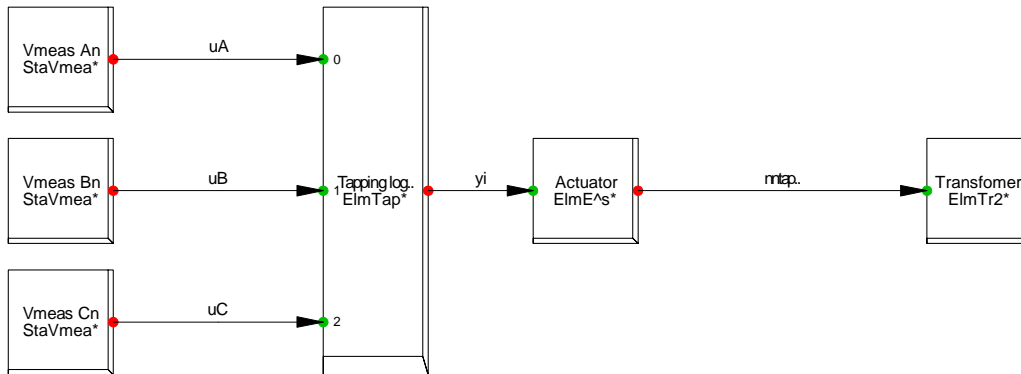


Figure 2.18. Transformers frame block

The script which the ‘*Tapping log.*’ slot refers to are the following:

```

inc(nntap) = 0;
inc(uA) = 1;
inc(uB) = 1;
inc(uC) = 1;
!uA = flagA*sqrt(sqrt(ur_A)+sqrt(ui_A));
!uB = flagB*sqrt(sqrt(ur_B)+sqrt(ui_B));
!uC = flagC*sqrt(sqrt(ur_C)+sqrt(ui_C));
u = flagA*uA+flagB*uB+flagC*uC;
!note: the flag is needed because we are reading all 3 phase meas.
! we want to select just one input at the time
!inc(u)=1;
nntap = lapprox(u,array_V);
!vardef(Vref) = 'p.u.';Reference voltage'
!vardef(Vdeadband) = 'p.u.';Dead band'
  
```

The equations which the delay slot – ‘*Actuator block*’ – refers to are the following:

```

limits(T)=[0,]
inc(yo)=yi
yo=delay(yi,T)
  
```

2.6.2. Passive Loads

As already said, real measurement data have been used to calculate the absorbed active and reactive power amounts, which were located in several text files and have been used to characterize every single load.

Each load had the same frame-block named ‘*ComLoad*’ which, as can be seen in Figure 2.19, was composed by the Measurement ‘*ElmFile**’ slot and the ‘*LoadSlot ElmLod**’. The first one opened the text files, read the active and reactive power values and gave them out as two outputs. These values (P_{ext} and Q_{ext}) were the input data of the second block, which made the load characterized by the real time-depending absorbed quantities.

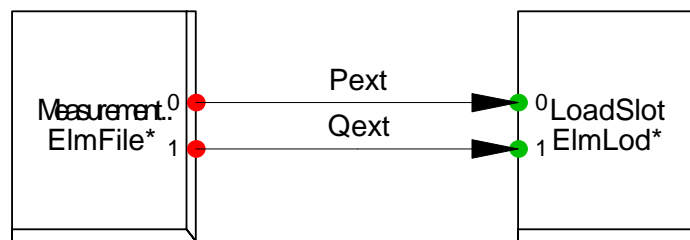


Figure 2.19. Passive loads frame block

2.6.3. Active Loads

As already said, because the PV should be represented as ‘constant-power’ active loads, an additional block able to change the load behaviors from ‘constant-impedance’ to ‘constant-power’ has been needed.

This slot, called ‘*Voltage Correctort ElmCom**’, is a proper ‘correction block’, which implements the equation 2.3, where P_{ref} is the active power read from the text file and P_{mod} is the modified active power, which will effectively go into the ‘*LoadSlot*’ slot:

As for the transformer controller, three measurement blocks (instead of just one) have been used. By managing these three blocks (enabling one at a time), the same frame-block could be used to refer the operations to the elements connected to different phases.

The modified frame-block is reported in Figure 2.20.

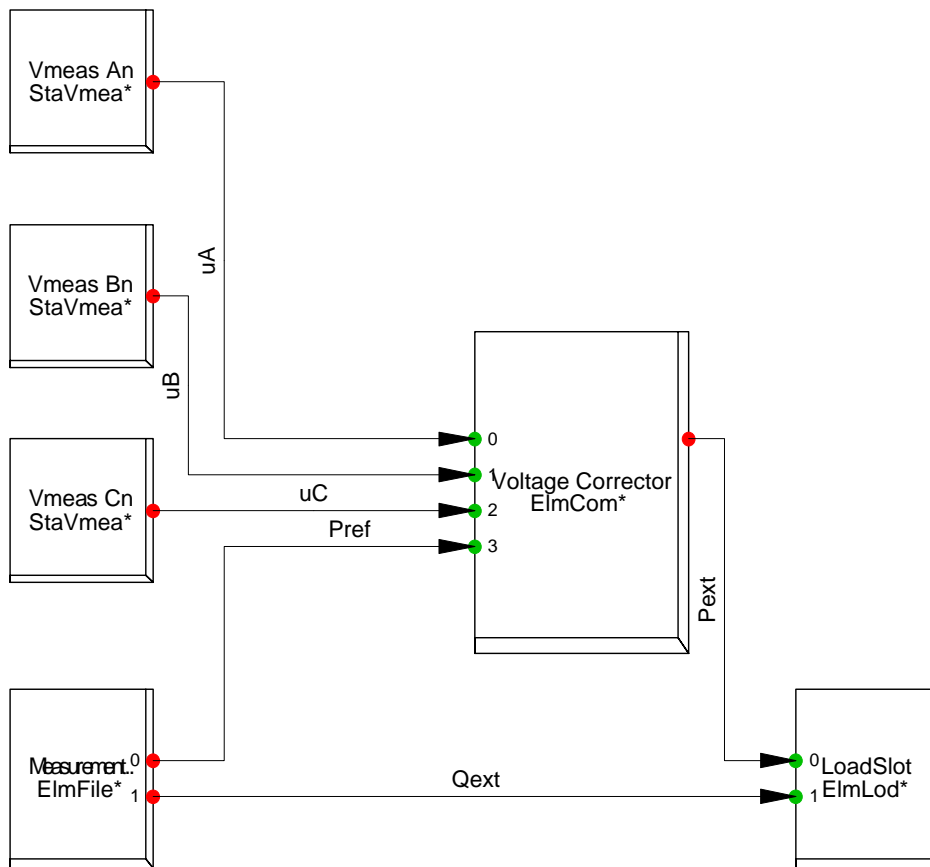


Figure 2.20. Active loads frame block

The script which the 'Voltage Corrector' slot refers to are the following:

```
inc(uA) = 1;
inc(uB) = 1;
inc(uC) = 1;
inc(Pmod) = 0;
!uA = flagA*sqrt(sqrt(ur_A)+sqrt(ui_A));
!uB = flagB*sqrt(sqrt(ur_B)+sqrt(ui_B));
!uC = flagC*sqrt(sqrt(ur_C)+sqrt(ui_C));
u = flagA*uA+flagB*uB+flagC*uC;
!note: the flag is needed because we are reading all 3 phase meas.
! we want to select just one input at the time
!inc(u)=1;
Pmod = Pref*sqrt(1/u);
```

2.6.4. Active Loads with Q regulation

As already said, for the second part of the simulations performed for the project, an additional logic model for the PV reactive power management has been needed to be created.

As will be in detail described in Chapter 3.3, a certain reactive power control method has been implemented: it provided reactive power values according both to phase-neutral voltage measurement and to active power instantaneous production.

As it can be seen in Figure 2.21, the slot which includes the reactive power management algorithm is '*Reactive Power Calculator*', which as input has the corrected active power value coming out from the '*Voltage Corrector*' slot and the phase-neutral voltage measured time by time coming from the '*Vmeas*' slot.

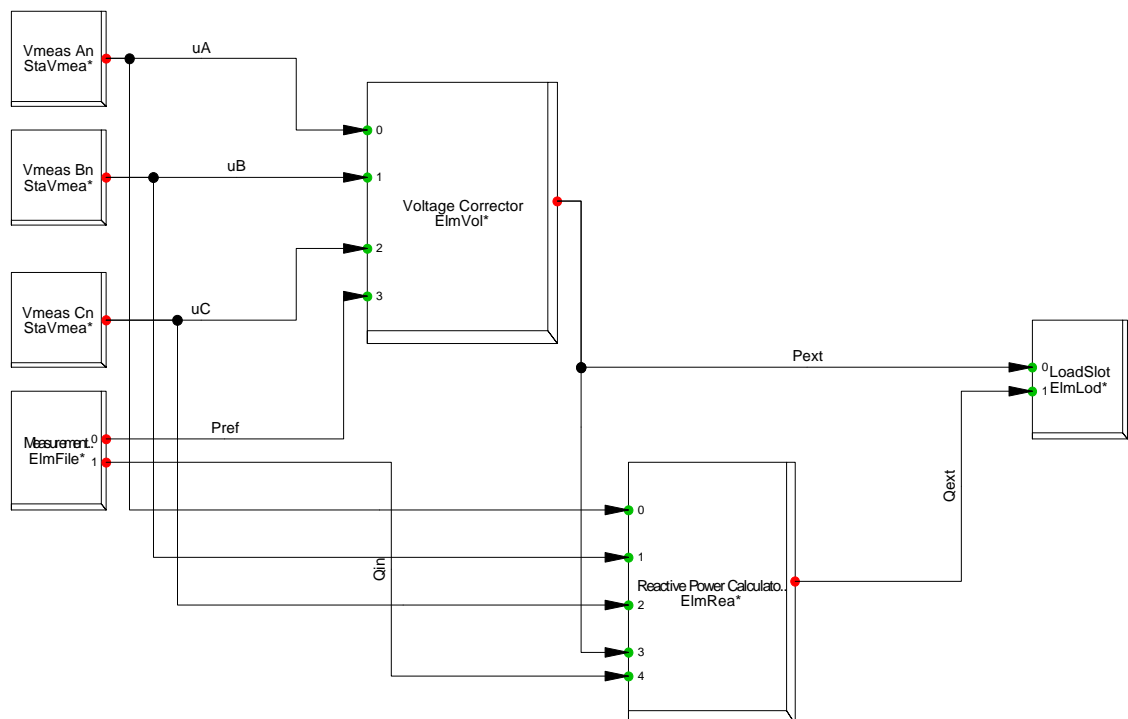


Figure 2.21. Active loads frame block

The output reactive power values have been calculated according to a ‘look-up’ table, which has been manually furnished into the Common Models specifications which time by time the ‘*Reactive Power Calculator*’ slot is related to. It represents perfectly the $Q=f(V,P)$ function chosen in Chapter 3.3, since it directly provides reactive power values in relationship to the two inputs it receives.

If for instance a measured voltage or an active power production value has assumed an intermediate value of the ones reported in the ‘look-up’ table, thanks to the command ‘*sapprox2*’ a spline approximation for the corresponding reactive power value has been provided. Finally it has been decided to consider a certain delay (2 s) in order to represent in a more realistic way the real behavior of the inverter.

The script which the ‘*Reactive Power Calculator*’ slot refers to are the following:

```
inc(uA) = 1;
inc(uB) = 1;
inc(uC) = 1;
inc(Ppu) = 0;
inc(Qpu) = 0;
u = flagA*uA+flagB*uB+flagC*uC;
!note: the flag is needed because we are reading all 3 phase meas.
! we want to select just one input at the time
!inc(u)=1;
Ppu=Pmod/Pn;
Qpu = (delay((sapprox2(Ppu,u,matrix_Q)),2))*OnOff;
Q= Qin + Qpu*Pn;
! OnOff is used to enable-disable the Q reg:
! OnOff=0 --> without Q reg
! OnOff=1 --> with Q reg
```


Chapter 3

Scenarios and Indexes Definition

Contents

| | | |
|---------------|---|-----------|
| 3.1. | Testing scenarios | 55 |
| 3.1.1. | <i>Phase-neutral voltages at each bus</i> | 57 |
| 3.1.2. | <i>Phase- ground voltages at the secondary side of the transformer</i> | 58 |
| 3.1.3. | <i>Neutral conductor potential at each bus</i> | 58 |
| 3.1.4. | <i>Voltage Unbalance Factor – VUF – at the bus in the worst phase-neutral voltages conditions</i> | 59 |
| 3.1.5. | <i>Absolute and relative line power losses for each phase and the total ones..</i> | 59 |
| 3.2. | PV cases..... | 60 |
| 3.3. | PV reactive power regulation..... | 64 |
| 3.4. | Italian and German technical standards | 66 |
| 3.4.1. | <i>Italian Technical Standard CEI 0-21 – Rules for passive and active users</i> | 66 |
| 3.4.2. | <i>German Technical Standard VDE-AR-N 4105 – Power generation systems connected to the LV distribution network</i> | 71 |
| 3.5. | VUF calculation..... | 75 |
| 3.6. | Power losses calculation..... | 77 |

3.1. Testing scenarios

In order to run a proper feasibility study, it has been necessary to consider the impact of the device in several grid configurations by comparing the results of different study cases. They,

as said in advance in Chapter 2.4, have been characterized by two different tapping logic control systems, whose influences have been compared to the case without any tapping action. Therefore the three control actions are:

- **‘Base Case’**: the transformer is not equipped with any tap changing device;
- **‘3-Phase Case’**: the OLTC is controlled synchronously on the three phases, taking as reference the phase-neutral voltage at phase a;
- **‘1-Phase Case’**: the control is set to independently commute the tap position on each phase winding.

The network layout and the passive loads profiles (both in terms of active and reactive power) has always been the same, since a real Danish passive low voltage network from Dong Eldistribution has been considered as reference.

Therefore, starting from this passive layout, other several different grid configurations have been studied. Basically they have been characterized by different penetration levels and different unbalanced connections to the grid of small distributed generation plants from renewable sources, precisely photovoltaic plants. All these cases could be considered divided into two main categories: first considering that PVs inject only active power without any reactive power contribution, and then considering certain reactive power control logic.

The assumption of the lack of Q injection-absorption in the first cases is justified by the fact that in Denmark there is no standardized grid code about the reactive power regulation by the PV plants connected to the low voltage network. Due to this, it has been decided to create a function according to some topics taken from both Italian and German Technical Standards – respectively CEI 0-21 and VDE-AR-N 4105 – (as described in detail in the Chapter 3.4).

For each study case and each PV penetration level, several parameters have been monitored and analyzed during the daily simulations:

- Phase-neutral voltages at each bus;
- Phase-ground voltages at primary and secondary side of the transformer;
- Neutral conductor potential at each bus;
- Voltage Unbalance Factor – VUF – at the bus in the worst phase-neutral voltages conditions;

- Absolute and relative line power losses for each phase and the total ones.

For each parameter monitored, in order to check the feasibility of the device in that specific grid layout, different limit values have been considered.

3.1.1. Phase-neutral voltages at each bus

The limit values of the phase-neutral voltages at each bus must stay within $\pm 10\%$ of the nominal value, i.e. between 0.9 and 1.1 p.u.. In order to find the bus characterized by the most unbalanced conditions it has been decided to analyze the phase-neutral voltages at each bus. According to the ‘worst bus’, voltage values analysis and VUF calculations have been performed.

As example hereby a 3D plot of the phase-neutral voltages at each bus is depicted in Figure 3.1. It refers to a random analyzed case: the one characterized by a single-phase tap changing regulation and by a PV penetration level of 30% (i.e. a PV power of 105 kW equally split into phases a and b) without any reactive power control. As it can be easily deduced, the bus characterized by the most unbalanced conditions is the one at the end of the line, i.e. bus 6.

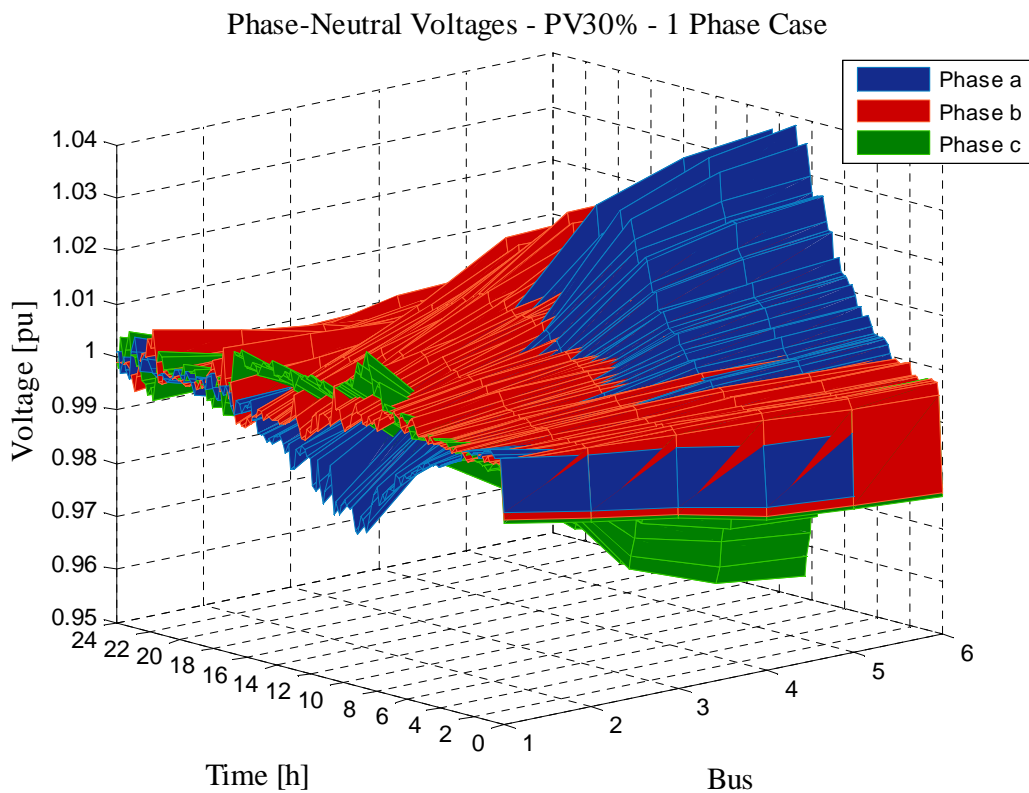


Figure 3.1. Phase-Neutral Voltages at each bus

Actually the final bus is the one at the end of Line 11-13, i.e. bus 6.3. For this reason all the analysis regarding the phase-neutral voltages as well as the calculations of the voltage unbalance factor VUF are performed referring to bus 6.3, which for simplicity, from this point forward is called bus 6.

3.1.2. Phase- ground voltages at the secondary side of the transformer

As described in Chapter 1.2, the maximum acceptable voltage drop from the primary transformation substation (i.e. from the HV/MV transformer) to the final user is $\pm 10\%$ of the nominal value. For this reason, assuming that the medium voltage distribution line is characterized by a voltage drop of around 5%, the maximum acceptable voltage drop along the low voltage feeder is supposed to be $\pm 5\%$. So finally can be said that the limit range of the phase-ground voltages at the secondary side of the transformer is between 0.95 and 1.05 p.u..

3.1.3. Neutral conductor potential at each bus

About the neutral conductor potential at each bus, since it is considered as a proper active conductor, there is not any specific standard which imposes any limit.

Nevertheless it is common to get the voltage drops monitored, because high values of neutral conductor voltage could be dangerous.

In addition, they have to be taken into account since they are caused by the neutral conductor current. It has double meaning: it provokes increasing of line power losses and it is an indicator of the unbalance of the grid, since it is a proper representation of the zero sequence of the three-phase voltage.

For these reasons has been decided that the neutral conductor potential at each bus should stay below 5% of the nominal value, i.e. below 12 V.

It has been noticed that in all the cases studied the neutral conductor potential always assumes highest values at bus 6: thus only comparisons between its shapes at bus 6 have been plotted.

3.1.4. Voltage Unbalance Factor – VUF – at the bus in the worst phase-neutral voltages conditions

In a three-phase system, voltage unbalance takes place when the magnitudes of phase or line voltages are different or the phase angles differ from the balanced conditions, or both.

As it will be said in Chapter 3.6, the Voltage Unbalance Factor definition chosen is the *True Definition*, which is defined as the ratio of the negative sequence voltage component to the positive sequence voltage component. The percentage voltage unbalance factor (% VUF), or the true definition, is given by equation 3.5.

According to the European Standard EN 50160 [1], the Voltage Unbalance Factor has the following limitation: under normal operating conditions, during each period of one week, 95% of the 10 min mean r.m.s. values of the negative phase sequence component (fundamental) of the supply voltage shall be within the range 0% to 2% of the positive phase sequence component (fundamental).

3.1.5. Absolute and relative line power losses for each phase and the total ones

It has been decided to monitor the power losses in the different cases and in the different test scenarios, in order to evaluate the impact of the OLTC device on line losses.

As it will be said in detail in Chapter 3.5, the approach used is based on active power measurements for each phase: values measured at the high voltage side of the transformer, at the load busses and at the PV busses. The idea is to calculate the power losses of lines by subtracting the total absorbed power (the amount of active power absorbed by all the loads and the power which flows from the LV to the MV side through the transformer, ' P_{OUT} ') from the total injected power (the amount of active power injected by the PV plants and the medium voltage network, ' P_{IN} '), as it is shown in equation 3.10.

3.2. PV cases

Maintaining always the same passive load grid configuration, a certain amount of distributed PV plants has been considered connected to the grid. As already said above, for each different total PV power connection case three different scenarios have been studied: the base case, 3-Phase case and 1-Phase case.

Certainly since several scenarios needed to be studied, not only a single and unique PV case has been defined. Thus it has been necessary to set installed power amounts and natures of the PV power plants which case by case have been connected to the network with different phase-connection configurations.

As first step some hypothesis and assumptions have been taken into account, such as:

- Theoretical reference daily PV production;
- PV penetration level definition;
- PV connections to the three phases;
- Reactive power regulation by PVs.

Regarding the input PV power, for every single PV plant ('customer') always the same reference day has been used.

As depicted in the graph in Figure 3.2, it has been decided to take as reference a typical May-day PV production of a 1 kWp PV plant in clear-sky condition and with different panel orientations: the panels are pointing South (blue line), or are scattered in various orientation and inclination, from East to West from 30° to 45° (red line). In this way two different output power cases are shown: with- and without optimized systems. For the simulations the 'optimized systems' active power values have been used.

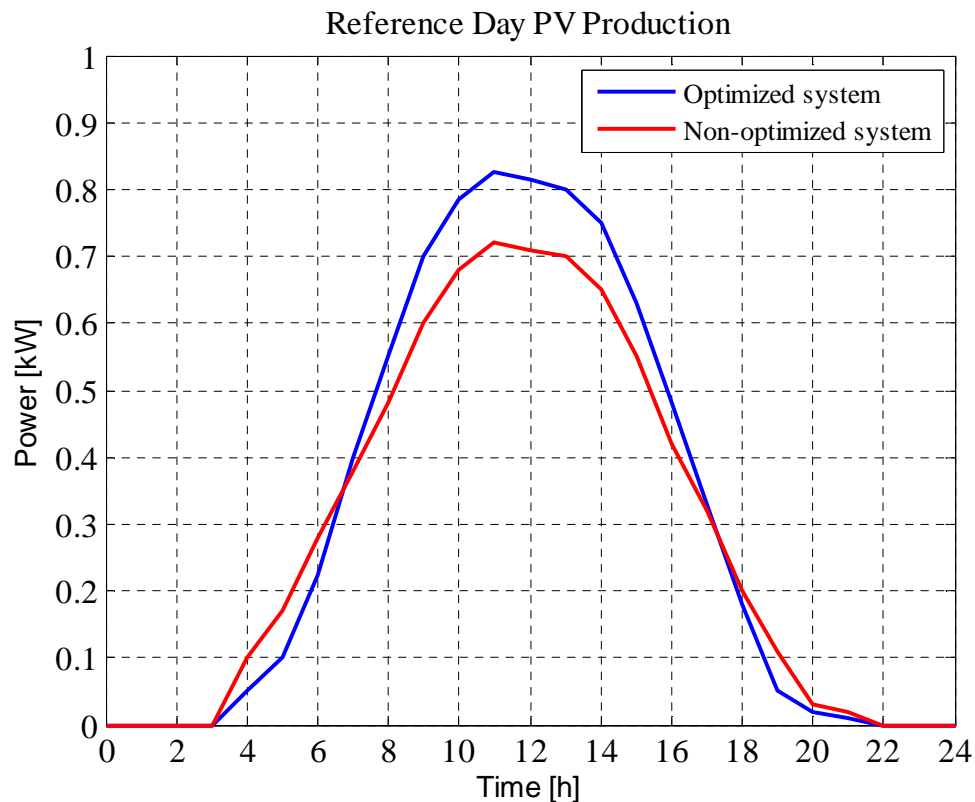


Figure 3.2. Reference daily production of a 1kWp PV plant under optimized and non-optimized conditions

These values have been considered to calculate, case by case, the different active power injection values from the six PV buses respectively into the three phases. In other words, basing on this reference graph, it has been possible to create all the input values for these active loads.

The input power values are saved in several text files, which will be open to characterize the PV behaviors during the 24 hours day-time, since these active loads, exactly as the passive ones, refer to the same frame-block.

The residential solar plants have been supposed to be characterized by an installed capacity of 5 kVA. In this way the PV penetration level defined in this study has been calculated as the number of the customers installing a 5 kWp solar plant divided by the total number of customers.

Generally the total installed PV peak power in a LV network is determined by the number of customers, the maximum rated power of one PV inverter (5 kVA) as well as the penetration.

According to the definition used in [24], PV penetration levels are defined as described below.

This method to estimate the amount of PV in the network has the advantage of giving the possibility of creating a uniform distribution across the entire feeder of PV power. Naturally practical cases may differ from this situation. The PV penetration level L_{PV} is expressed in percent and in combination with the number of customers $n_{customers}$ and the maximum rated power of one PV inverter S_r (5 kVA) it determines the total installed PV power in the respective feeder S_{PV} as in equation 3.1.

$$L_{PV}[\%] = \frac{n_{customers} \cdot S_r}{S_{TOT}} \cdot 100 = \frac{S_{PV}}{S_{TOT}} \cdot 100 \quad (3.1)$$

It has been considered that the total amount of the PV power plants is 70 ‘customers’, and all of them have an installed peak active power of 5 kWp. So it has been assumed that the total PV power considerable is 350 kW, which corresponds to the scenario of 100% PV penetration level.

For the simulations it has been necessary to define both the input values of the PV production levels during the day and the way of connection to the network, which depends on the different penetration levels and phase connections of the different cases.

As it can be seen in Table 3.1, different scenarios have been considered: depending on the PV penetration level [%], the total number of PV ‘customers’ (each one with a PV power of 5 kWp), and how the total PV power is split in the three phases [% for each phase].

| PV penetration level [%] | Total PV power for a LV network with 70 customers; one PV inverter 5 kVA | Phase connections (a, b, c with different penetration [%]) | Number of customers |
|---------------------------------|---|---|----------------------------|
| 0 | 0 | N.A | 0 |
| 10 | 35 | a (100) | 7 |
| 20 | 70 | a (100) | 14 |
| 30 | 105 | a, b (50,50) | 21 |
| 40 | 140 | a, b (50,50) | 28 |
| 50 | 175 | a, b (50,50) | 35 |
| 60 | 210 | a, b (50,50) | 42 |
| 70 | 245 | a, b, c (50,30,20) | 49 |
| 80 | 280 | a, b, c (50,30,20) | 56 |
| 90 | 315 | a, b, c (50,30,20) | 63 |
| 100 | 350 | a, b, c (50,30,20) | 70 |

Table 3.1. Different PV penetration level characterizations

These scenarios have been considered as reference for the real simulations which have been run.

Suddenly it has been noticed that the unbalancing connections of the 30 to 60% PV penetration cases (50% of the PV power installed at phase a and 50% at phase b) lead to not too realistic and acceptable results.

Hence further scenarios characterized by less unbalanced connections have been studied (Table 3.2):

| PV penetration level [%] | Total PV power for a LV network with 70 customers; one PV inverter 5 kVA | Phase connections (a, b, c with different penetration [%]) | Number of customers |
|---------------------------------|---|---|----------------------------|
| 40 | 140 | a, b, c (50,30,20) | 28 |
| 50 | 175 | a, b, c (50,30,20) | 35 |
| 60 | 210 | a, b, c (50,30,20) | 42 |

Table 3.2. Additional less unbalanced PV penetration level characterizations

Since the Danish grid code do not provide for any technical guidelines about the reactive power management by the small distributed generation plants connected to the LV network, as first approach it has been decided to run all the simulations without any reactive power regulation. After these cases it has been chosen to implement a function able to define the amount of reactive power injection/absorption by the PVs, so that it could be possible to compare the results and look for its influence; analysis and comparisons have been performed in the 1-Phase cases, which are actually the most important for the proper feasibility study. In this way it has been possible to analyze the effects of the reactive power regulation algorithm in the best cases and see if the situation could be further improved.

3.3. PV reactive power regulation

Considering the possibility of the PVs to inject and absorb inductive-capacitive reactive power, it could easily be possible that the PV hosting capacity of the network could be higher than the limits which have been found previously. Anyway it has been interesting to study all the effects – both positive and negatives – which this further regulation could lead to.

Different reactive power control methods are possible, based on fixed Q values or depending on other parameters, such as voltage at the PV connection bus or active power injected by the plant. Basically 5 main methods are potentially usable: *fixed cos ϕ* , *cos ϕ (P) characteristics*, *fixed Q*, *Q(U) droop function* and *remote set values method*.

As previously said, nowadays the Danish grid code do not provide for any technical guidelines about the reactive power management by the small distributed generation plants connected to the LV network. Anyway, since Denmark, Italy and Germany belong to the same synchronous region, it is reasonable to expect that future Danish requirements will experience harmonization with other European regulations.

For this reason it has been decided to start from the Italian and German technical standards in order to implement an algorithm which could be efficient and practically conform to the European guideline.

The function of the controller has been created according to technical rules for low voltage active users recommended by the Italian and German Technical Standards – respectively CEI 0-21 [25] and VDE-AR-N 4105 [26] (which will be better described in Chapter 3.4). These standards set different requirements on the reactive power production by the PV inverter greater than 3 kW and define several variations depending on the size of the plant together with specific DSO-users agreements.

Starting from these guidelines and with reference to [27], a new regulation function has been created: it has both voltage and active power dependence, as described in equation 3.2:

$$Q = f(V, P) \quad (3.2)$$

The implemented Reactive Power Control capability (RPC capability) from PVs is depicted in Figure 3.3.

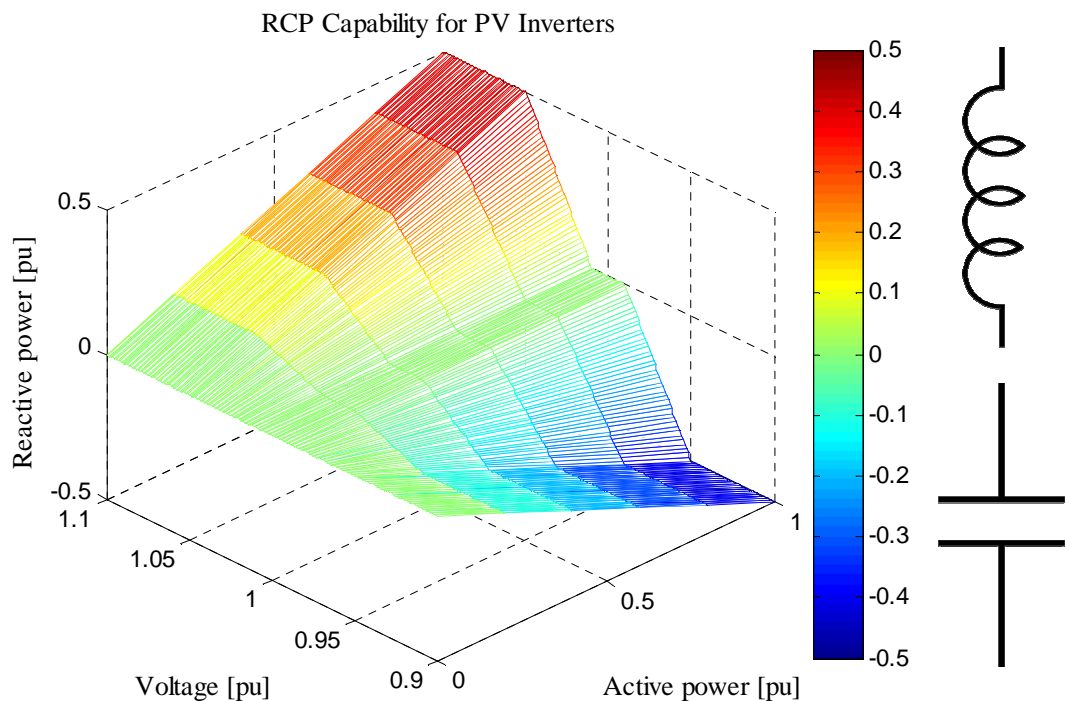


Figure 3.3. Reactive Power Control capability for PV inverter

An extremely important note is that in our project the PVs have always been considered as loads. Because of this, positive values of reactive power mean that it has an inductive nature and gets absorbed by the PV; on the other hand – if negative – it behaves like a capacitor and it is injected into the grid.

The main objective of this control is voltage lowering by reactive inductive power absorption whenever the PV is producing high amount of power. The voltage rises may be particularly sensible if the PV is localized in weak feeders or feeders with high density of other active sources.

According to the European Standard, voltage limits have been set to $\pm 10\%$ the nominal voltage U_n , i.e. $U_{\min}=0.9$ p.u. and $U_{\max}=1.1$ p.u. The green area between $0.99 U_n$ and $1.01 U_n$ can be interpreted as a dead band without any reactive power control regardless how the produced active power changes. The red area represents operation in overvoltage conditions when the inverter consumes reactive power up to 0.5 p.u. in order to lower the voltages. Likewise, the inverter injects up to 0.5 p.u. of reactive power when operation conditions are in the blue under-voltage area.

3.4. Italian and German technical standards

Both the Italian Technical Standard CEI 0-21 [25] and the German VDE-AR-N 4105 [26] set different requirements on the reactive power production by the PV inverter greater than 3 kW and define several variations depending on the size of the plant together with specific DSO-users agreements.

Hereby detailed descriptions of the two standards are presented.

3.4.1. Italian Technical Standard CEI 0-21 – Rules for passive and active users

All the DG plants characterized by nominal power greater than 3 kW and connected to the grid through one or more inverter devices must participate to the voltage control by reactive power absorption.

The absorption and emission of reactive power is oriented to the limitation of over- and under-voltages which take place due to the generator itself because of the active power injection.

In the Standard guideline there is a part including several rules along with the capability curves that must be respected by the active users. In particular, as showed in Figure 3.4, there are two curves (one binding called triangular capability and the other one optional called rectangular capability) about the voltage regulation by means of the reactive power control. The triangular capability obliges the inverter to change its power factor if the plant is producing active power and voltage out of the predetermined tolerance band. The rectangular capability requires changing the power factor even if the plant is not producing active power instead.

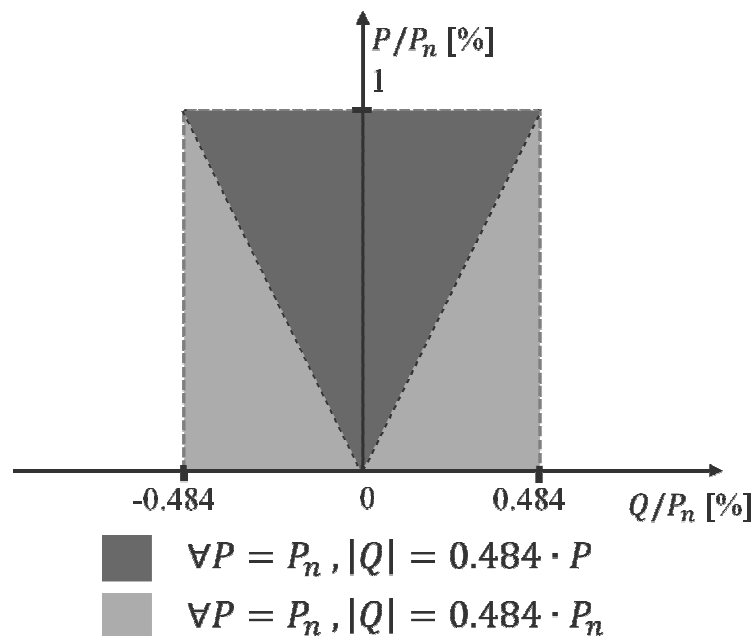


Figure 3.4. Rectangular and triangular capability curves, for inverters in power plants with total power > 6 kW

PV plants bigger than 3 kWp have to absorb-inject reactive power following a certain logic according one of the following ways:

- According to the 'a' curve $\cos \varphi (P)$ in Figure 3.5;

- According to a constant $\cos \varphi$ value (curve 'b' in Figure 3.5) which can be set till the maximum capability limit of 0.9 (0.95 if the plant is lower than 6 kW).

All the converters must be set the characteristic curve 'a', which is univocally defined as linear interpolation of three points:

- A: $P = 0.2P_n$; $\cos \varphi = 1$;
- B: $P = 0.5P_n$; $\cos \varphi = 1$;
- C: $P = P_n$; $\cos \varphi = \cos \varphi_{\min}$.

Where $\cos \varphi_{\min}$ is equal to 0.95 for plants with power till 6 kW or to 0.90 in case of converters bigger than 6 kW.

The standard characteristic curve 'b' Figure 3.5 is defined by two points:

- D: $P = P_n$; $\cos \varphi = \cos \varphi_{\min}$;
- E: $P = 0.05P_n$; $\cos \varphi = \cos \varphi_{\min}$.

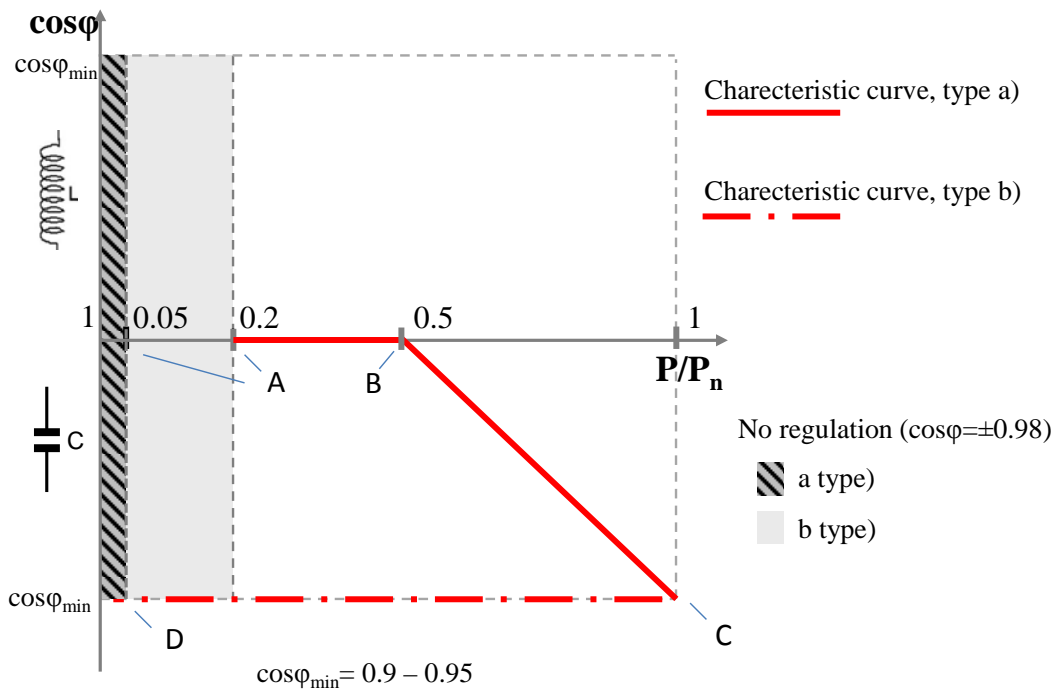


Figure 3.5. Standard characteristic curves $\cos \varphi = f(P)$

PV plants bigger than 6 kWp needs a inverters able to absorb-inject reactive power following a certain logic based on V values, following a function $Q=f(V)$.

This type of regulation could need to exceed the triangular capability curve, therefore in these cases the rectangular one could be set as limit.

According to the two plots in the picture below, the convention utilized is the following:

- Positive reactive power: the generator absorbs reactive power injecting current which is delayed compared to the voltage;
- Negative reactive power: the generator injects reactive power injecting current which is advanced compared to the voltage.

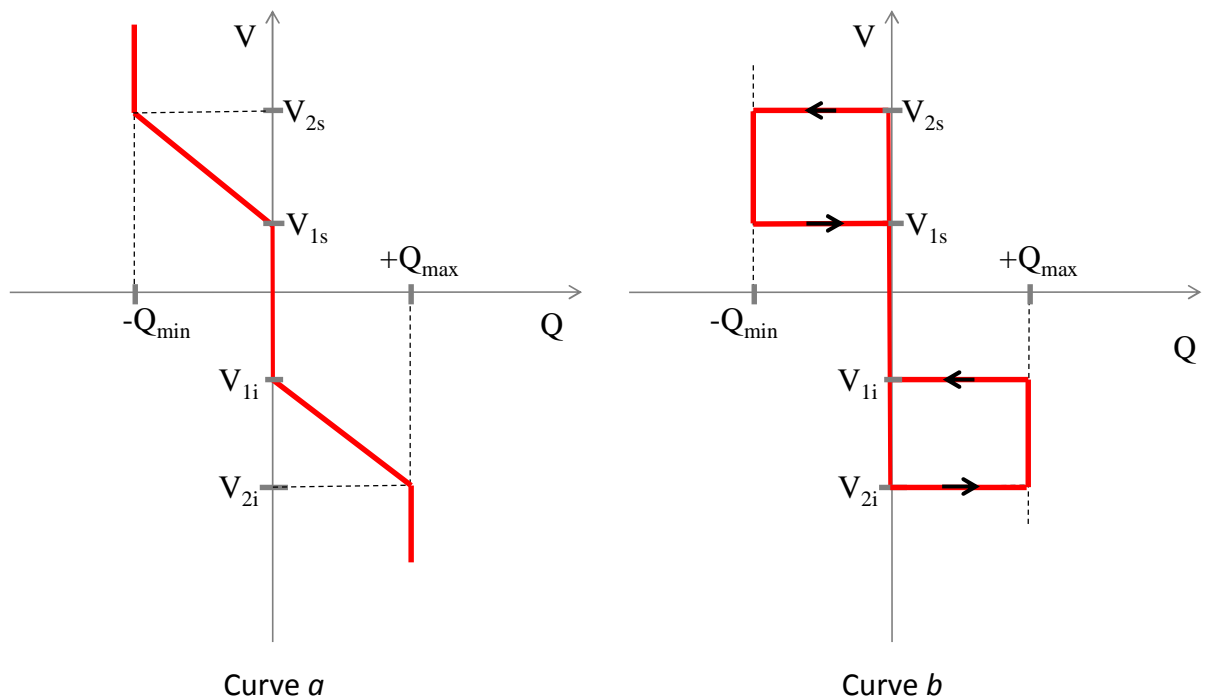


Figure 3.6. Standard characteristic curves $Q=f(V)$

Since the reactive power regulation based on voltage measurements $Q=f(V)$ is conventionally seen as finalized to perform a ‘grid service’ asked by the distributor, this modality is activated only at the instance of the distributor.

The characteristic curve $Q=f(V)$ is univocally defined by the following parameters:

- V_1 and V_2 are defined by the DSO, but it must be:
- $V_n < V_{1s} ; V_{2s} < V_{\max} ; V_n > V_{1i} ; V_{2i} < V_{\min}$;
- $V_{\min} \geq 0.9 V_n$;
- $V_{\max} \leq 1.1 V_n$;
- $-Q_{\min}$ and $+Q_{\max}$ correspond to the limits of the triangular capability of Figure 3.4;
- The provision for the reactive power regulation is furnished by the DSO to the active user together with the connection authorization;
- According to the network topology, the load and the feed-in power, the DSO can provide different characteristic curves, but they must be related to the one in Figure 3.6, but with different limit values (within the limits above).

The operation mode with automatic reactive power regulation according to the laws $Q=f(V)$ of Figure 3.6, is enabled when the feed-in power exceeds the lock-in value, which is $0.20 P_n$ by default, but can be changed between $0.10 P_n$ and P_n with $0.10 P_n$ steps.

The feed-in stops when the active power reduces below the lock-out value, by default equal to $0.05 P_n$.

Operating mode of automatic reactive power regulation according to the standard characteristic $Q=f(V)$:

- Referring to Figure 3.6-a: for $V > V_{1s}$ or $V < V_{1i}$ the inverter shall check if the injected active power is bigger than the lock-in value;
- Referring to Figure 3.6-b: for $V > V_{2s}$ or $V < V_{2i}$ the inverter shall check if the injected active power is bigger than the lock-in value;
- If the check is positive, the reactive power regulation is activated according to the profiles in Figure 3.6 within 10 seconds, otherwise the machine keeps on injecting power with $\cos \varphi$ equal to one till when P is lower than lock-in value;
- The operation condition gets deactivated ONLY if the active power injected is below the lock-out value, or the voltage measured is within the range $V_{1s} - V_{1i}$.

3.4.2. *German Technical Standard VDE-AR-N 4105 – Power generation systems connected to the LV distribution network*

Power generator systems shall allow for operation under normal stationary operating conditions in the voltage tolerance band $\pm 10\%$ U_n and their permissible operation points starting with an active power output of more than 20% of the rated active power with the following displacement factors $\cos \varphi$:

- $S_{\max} \leq 3.68 \text{ kVA}$

$0.95_{\text{under-excited}} \leq \cos \varphi \leq 0.95_{\text{over-excited}}$ in accordance with DIN EN 50438;

- $3.68 \text{ kVA} < S_{\max} \leq 13.8 \text{ kVA}$

Characteristic curve provided by the network operator within $0.95_{\text{under-excited}} \leq \cos \varphi \leq 0.95_{\text{over-excited}}$;

- $S_{\max} > 13.8 \text{ kVA}$

Characteristic curve provided by the network operator within $0.90_{\text{under-excited}} \leq \cos \varphi \leq 0.90_{\text{over-excited}}$.

In the load-reference arrow system, this means the operation in Quadrant II (under-excited) or III (over-excited).

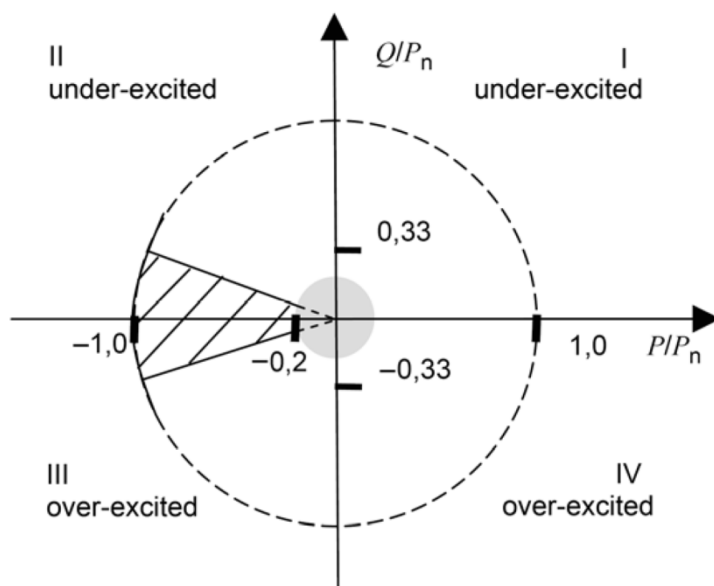


Figure 3.7. Limit power range for the reactive power of a power generation system within the range of $3.68 \text{ kVA} < S_{max} \leq 13.8 \text{ kVA}$ (load-reference arrow system)

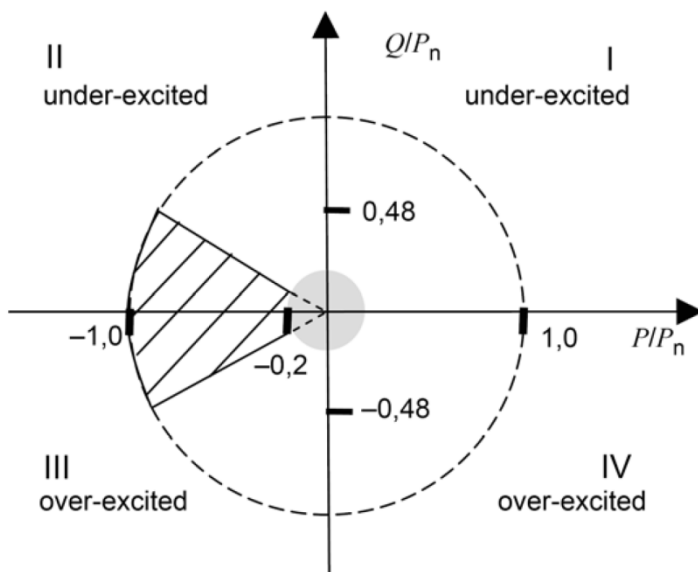


Figure 3.8. Limit power range for the reactive power of a power generation system within the range of $S_{max} > 13.8 \text{ kVA}$ (load-reference arrow system)

Within the hatched triangles for the reactive power limit shown in Figure 3.7 and Figure 3.8 the reactive power of the power generation system shall be freely adjustable.

Upon a change in the active power, the reactive power shall be able to adjust itself automatically in correspondence to the predefined $\cos \varphi$.

Type and set points of the reactive power setting will be determined by the respective network conditions and can therefore be provided individually by the network operator within the limit triangles.

For power generation systems, whose power generation units feed over inverters or synchronous generators capable to generate reactive power, it is permitted to provide as default either

- A displacement factor/active power characteristic $\cos \varphi (P)$; or
- A fixed displacement factor $\cos \varphi$.

If the network operator provides a characteristic curve, then any set point resulting from that curve shall be set automatically on the power generation unit within 10 seconds.

As a rule, characteristic curve based regulation shall not be applied for power generation systems with generators directly coupled to the network which, due their very operational principle, cannot control the reactive power and, therefore, use constant capacities. In that case, the network operator provides a fixed displacement factor $\cos \varphi$.

The characteristic curve $\cos \varphi (P)$ is suitable for power generation systems with fluctuating power feed-in, such as PV systems.

As can be observed in Figure 3.9, the PV inverters are required to inject reactive power (inductive) starting at 50% power generation and at 100% the power factor reaches 0.9 (lagging) per units with rated power above 13.8 kVA and 0.95 (lagging) per units below this level.

One property of this type of control is that the inverters will inject reactive power independently of the location in the feeder in comparison with $Q(U)$ algorithm in which the farthest inverter would inject always more reactive power than the ones closer to the transformer. Thus, overall better control of the voltage is assumed, since all inverters in the network are taking part. The disadvantage is that the inverters might inject reactive power into the network even though it may not be required (no overvoltage situation).

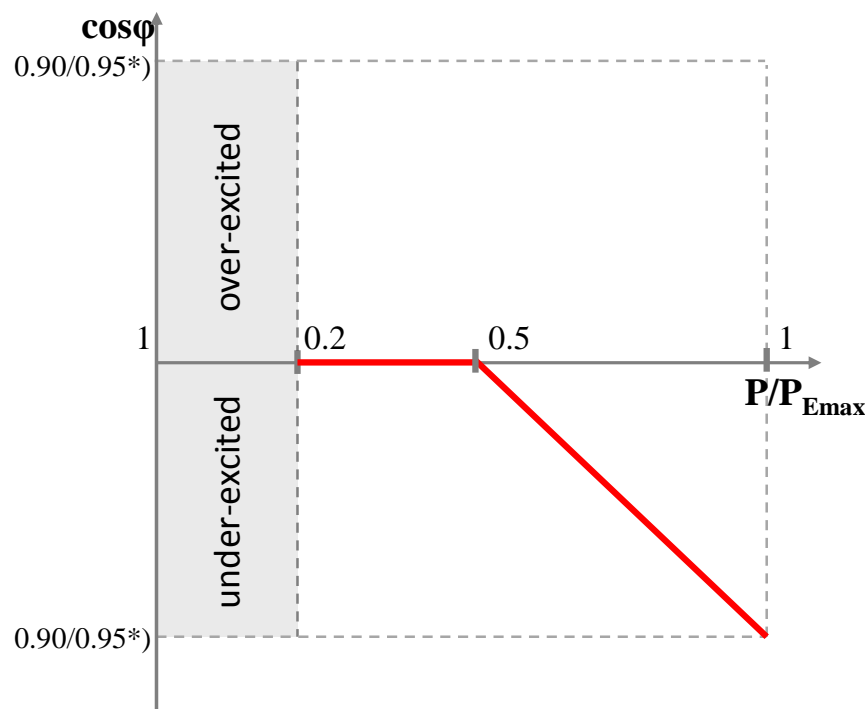


Figure 3.9. Standard characteristic curve for $\cos \varphi (P) ; *$ depending on $\Sigma S_{E_{max}}$

Depending on network topology, network load and feed-in power, the network operator can also require a characteristic curve differing from the standard characteristic curve for $\cos \varphi (P)$.

For excess feeding the use of an ‘intelligent’ reactive current compensation system is required, which, depending on the overall behavior of the customer system for extraction or feed-in, regulates the displacement factor respectively required for the entire customer system at the network connection point. As long as the required reactive current compensation systems are not commercially available, it is advisable to use a differentiated approach when specifying the displacement factor $\cos \varphi$ of the power generation system.

In cases where the feed-in power is less than one third of the maximum extraction power agreed, a specific default for the displacement factor is normally not required, nevertheless for minimization of the losses in the entire system, a set value of 1 shall be aimed for.

If a reactive energy clearing is applied that is influenced by the power generation system, than both the network operator and the system operator should always coordinate their procedures for a reactive power compensation of the costumer system and for the default displacement factor for the power generation system.

3.5. VUF calculation

As previously said, a very important parameter to calculate and monitor has been an index able to quantify the amount of the Voltage Unbalance.

In a three-phase system, voltage unbalance takes place when the magnitudes of phase or line voltages are different or the phase angles differ from the balanced conditions, or both.

The three possible definitions of Voltage Unbalance are stated and analyzed below.

- *NEMA (National Equipment Manufacturer's Association) Definition:* the voltage unbalance, also known as the *Line Voltage Unbalance Rate (LVUR)*, is given by equation 3.3:

$$\%LVUR = \frac{\text{max voltage deviation from the avg line voltage}}{\text{avg line voltage}} * 100 \quad (3.3)$$

It assumes that the average voltage is always equal to the rated value and since it works only with magnitudes, phase angels are not included.

- *IEEE Definition:* the voltage unbalance, also known as the *Phase Voltage Unbalance Rate (PVUR)*, is given by equation 3.4:

$$\%PVUR = \frac{\text{max voltage deviation from the avg phase voltage}}{\text{avg phase voltage}} * 100 \quad (3.4)$$

The IEEE uses the same definition of voltage unbalance as NEMA, the only difference being that the IEEE uses phase voltages rather than line-to-line voltages. Here again, phase angle information is lost since only magnitudes are considered.

- *True Definition:* the true definition of voltage unbalance is defined as the ratio of the negative sequence voltage component to the positive sequence voltage component. The percentage *Voltage Unbalance Factor (% VUF)*, or the true definition, is given by equation 3.5:

$$\%VUF = \frac{\text{negative sequence voltage component}}{\text{positive sequence voltage component}} * 100 \quad (3.5)$$

The positive and negative sequence voltage components are obtained by resolving three-phase unbalanced line voltages V_{ab} , V_{bc} , and V_{ca} (or phase voltages) into two symmetrical components V_{pos} and V_{neg} (of the line or phase voltages). The two balanced components are given by equations 3.6 and 3.7:

$$V_{pos} = \frac{V_{ab} + a * V_{bc} + a^2 * V_{ca}}{3} \quad (3.6)$$

$$V_{neg} = \frac{V_{ab} + a^2 * V_{bc} + a * V_{ca}}{3} \quad (3.7)$$

Where a and a^2 are two complex operators whose definition is shown respectively in equations 3.8 and 3.9:

$$a = e^{j\frac{2}{3}\pi} = -\frac{1}{2} + j\frac{\sqrt{3}}{2} \quad (3.8)$$

$$\alpha^2 = e^{-j\frac{2}{3}\pi} = -\frac{1}{2} - j\frac{\sqrt{3}}{2} \quad (3.9)$$

It has been decided to use the last unbalance factor definition, i.e. the True Definition.

The VUF calculations have been performed by using the software Matlab. All the values of the positive and negative sequence voltage components have been obtained directly from PowerFactory as text files and used as input matrix for Matlab operations.

3.6. Power losses calculation

In order to evaluate the technical feasibility, an accurate power loss calculation (even phase by phase sometimes) has been needed to be performed.

Certainly always the same algorithm has been used for the different study cases and scenarios.

Basically the software Power System offers the chance to estimate the line losses directly by using the correspondence tool: it calculates the line losses branch by branch and phase by phase so it would have been possible to find out the total power loss of lines for each network configuration case simply by adding them.

From a theoretical point of view this method is sufficient but not from a practical one: in fact in the reality it would be impossible to know a priori the amount of power loss of each branch. For this reason a different calculation method has been used.

The approach which has been used is based on active power measurements for each phase: values measured at the high voltage side of the transformer, at the load busses and at the PV busses. The idea is to calculate the power losses of lines by subtracting the total absorbed power (the amount of active power absorbed by all the loads ' P_{OUT} ') from the total injected power (the amount of active power injected by the PV plants and the medium voltage network ' P_{IN} '), as shown in equation 3.10.

$$P_{LOSS} = P_{IN} - P_{OUT} \quad (3.10)$$

Because the PV plants have been modeled in the software as active loads – but still loads – the active power measured at their busses resulted to be negative: for this reason their absolute values needed to be considered. Moreover has to be noticed that, because of the power injection of the PVs, the phase power measured at the HV side of the transformer was not always positive, but it could result negative. This is due to the fact that sometimes the medium voltage network absorbed power from the low voltage side instead of supplying it. For this reason the phase active power measured at the transformer has been needed to be considered with its effectively sign and not to use the absolute values, so that if positive it had to be added to the PV power while if negative it had to be added to the load power.

As described, the power loss calculation equation (3.11) is the following:

$$P_{LOSS} = P_{IN} - P_{OUT} = |P_{PV}| + P_{TR} - P_{LOADS} \quad (3.11)$$

This formula has been used individually for the three phases, as well as globally for a total power loss calculation.

Since the locations of PV plants and loads in the grid have not been taken into account, what have not been calculated are the single losses branch by branch. In fact with this approach the calculation goal was to find the total power losses of the whole low voltage network, including the transformer inner losses. This can be deduced by the following picture (Figure 3.10), which as example refers to part of the analyzed low voltage network and only to the phase a.

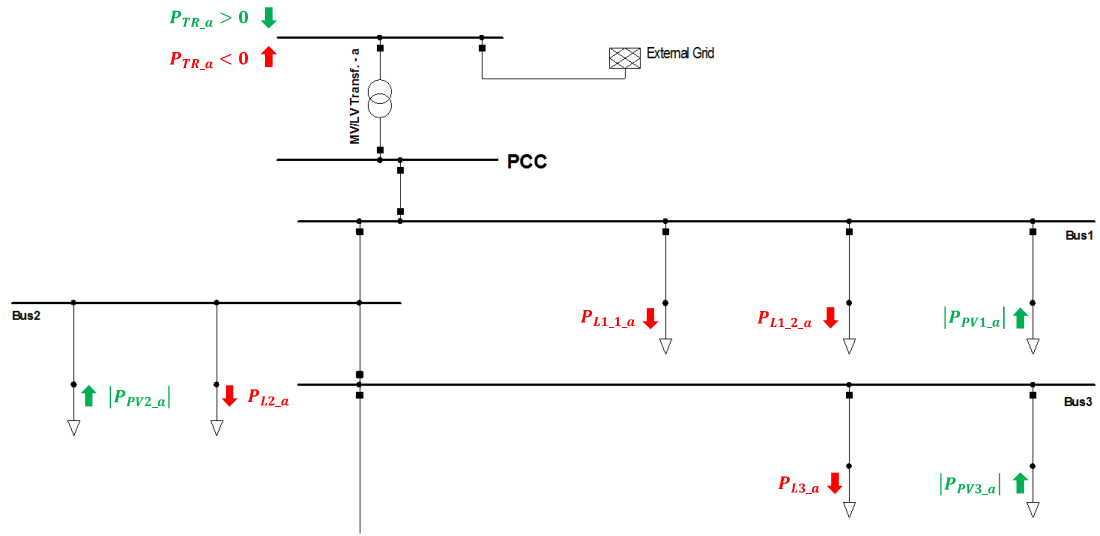


Figure 3.10. Power flow conventions for the power losses calculation

It can be seen that the rows are red colored when power gets out of the grid (P_{OUT} : loads absorptions or negative power through the transformer), while they are green when it gets in (P_{IN} : PV power injections or positive power through the transformer).

Another important calculation which has been performed is the comparison of the calculated power loss amounts to the total injected power, which means the calculation of the 'Power Loss Ratio' by using the following principle (3.12):

$$\%PLR = \frac{P_{LOSS}}{P_{IN}} * 100 = \frac{P_{IN} - P_{OUT}}{P_{IN}} * 100 \quad (3.12)$$

As said, the P_{IN} definition changes during the day time because of the different sign that the power at the transformer could have. In this way it has been assumed that it should be considered as part of P_{IN} if it has positive value, otherwise it should not be included.

Basing on this consideration, the following formulas (3.13 and 3.14) can be written:

- if $P_{TR} > 0$ the Power Loss ratio is:

$$\%PLR = \frac{P_{LOSS}}{P_{IN}} * 100 = \frac{P_{IN} - P_{OUT}}{P_{IN}} * 100 = \frac{|P_{PV}| + P_{TR} - P_{LOADS}}{|P_{PV}| + P_{TR}} * 100 \quad (3.13)$$

- if $P_{TR} < 0$ it is:

$$\%PLR = \frac{P_{LOSS}}{P_{IN}} * 100 = \frac{P_{IN} - P_{OUT}}{P_{IN}} * 100 = \frac{|P_{PV}| + P_{TR} - P_{LOADS}}{|P_{PV}|} * 100 \quad (3.14)$$

This formula has been used individually for the three phases, as well as globally for a total power loss calculation.

All these calculations have been performed by using the software Matlab.

All the active power values have been obtained from Power Factory as exported text files and used as input matrix for Matlab calculations.

For each case of different PV penetration level, the same script file has been used. Each one contains the code for the 3 different cases (base case, 3-Phase case and 1-Phase case).

Chapter 4

Simulation Results

Contents

| | | |
|-------------|--|------------|
| 4.1. | Without Q regulation cases: plots and numerical results..... | 82 |
| 4.1.1. | <i>PV10% – 35 kW – phase a.....</i> | <i>83</i> |
| 4.1.2. | <i>PV30% – 105 kW – phases a and b.....</i> | <i>89</i> |
| 4.1.3. | <i>PV40% – 140 kW – phases a and b.....</i> | <i>96</i> |
| 4.1.4. | <i>PV50% – 175 kW – phases a and b.....</i> | <i>102</i> |
| 4.1.5. | <i>PV40% – 140 kW – phases a, b and c.....</i> | <i>109</i> |
| 4.1.6. | <i>PV50% – 175 kW – phases a, b and c.....</i> | <i>115</i> |
| 4.1.7. | <i>PV60% – 210 kW – phases a, b and c.....</i> | <i>122</i> |
| 4.1.8. | <i>PV70% – 245 kW – phases a, b and c.....</i> | <i>128</i> |
| 4.1.9. | <i>PV80% – 280 kW – phases a, b and c.....</i> | <i>135</i> |
| 4.2. | Without Q regulation cases: results comments and analysis | 142 |
| 4.3. | With Q regulation cases: plots and numerical results | 155 |
| 4.3.1. | <i>PV40% – 140 kW – phases a and b.....</i> | <i>156</i> |
| 4.3.2. | <i>PV50% – 175 kW – phases a and b.....</i> | <i>160</i> |
| 4.3.3. | <i>PV70% – 245 kW – phases a, b and c.....</i> | <i>165</i> |
| 4.3.4. | <i>PV80% – 280 kW – phases a, b and c.....</i> | <i>169</i> |
| 4.4. | With Q regulation cases: results comments and analysis..... | 176 |

4.1. Without Q regulation cases: plots and numerical results

All the following scenarios will be based on comparisons between the base case and the 3-phase case as well as between the base case and the 1-phase case.

The plots and the numerical results reported will be:

- Phase-neutral voltages at the worst bus;
- Phase-ground voltages at the transformer level, both at the MV and the LV sides;
- Neutral-ground voltage at the worst bus;
- The VUF at the worst bus;
- Total power losses of lines;
- Total power loss ratio;
- A table containing numerical values of energy amounts entering/exiting into/from the system.

4.1.1. PV10% – 35 kW – phase a

Out of the phase-neutral voltage profiles at the worst bus (bus 6) from base case to the 3-phase case, only the voltage at phase a gets closer to 1 p.u., since the tap control is based on phase a measurement. Phase-neutral voltages and tap positions are depicted in Figure 4.1 and in Figure 4.2.

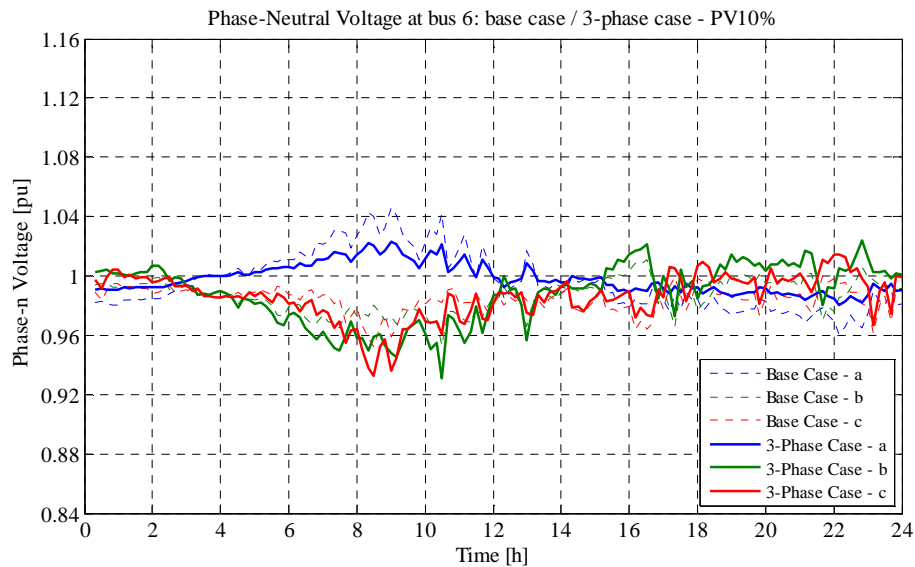


Figure 4.1. Phase-Neutral Voltage at bus 6 – 3-Phase/Base Case comparison in the scenario with 35 kW of PV connected to phase a

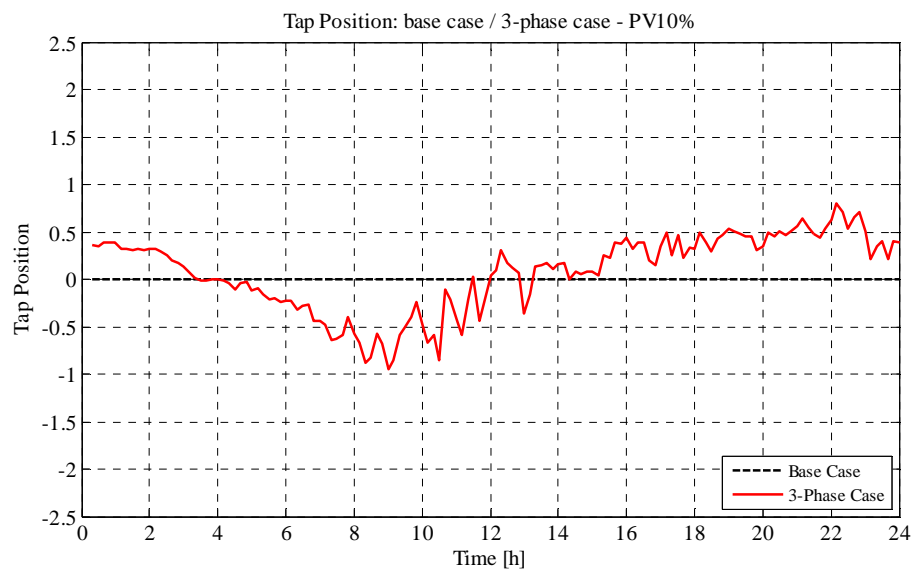


Figure 4.2. Tap Position – 3-Phase/Base Case comparison in the scenario with 35 kW of PV connected to phase a

On the other hand in the 1-phase case the tap control is based on all the three phases values, so that all the three phase-neutral voltages are closer to 1 p.u.. Phase-neutral voltages and tap positions are depicted respectively in Figure 4.3 and in Figure 4.4.

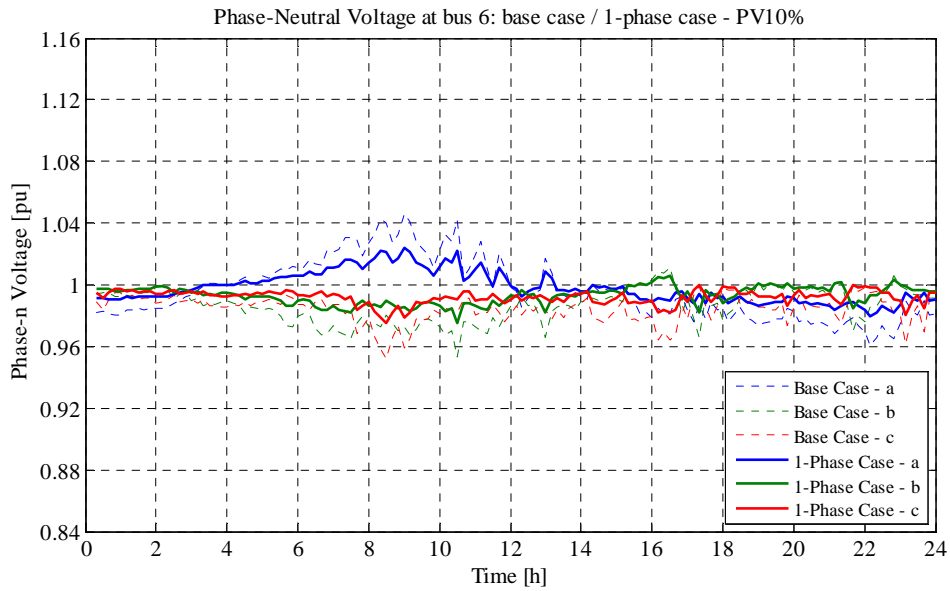


Figure 4.3. Phase-Neutral Voltage at bus 6 – 1-Phase/Base Case comparison in the scenario with 35 kW of PV connected to phase a

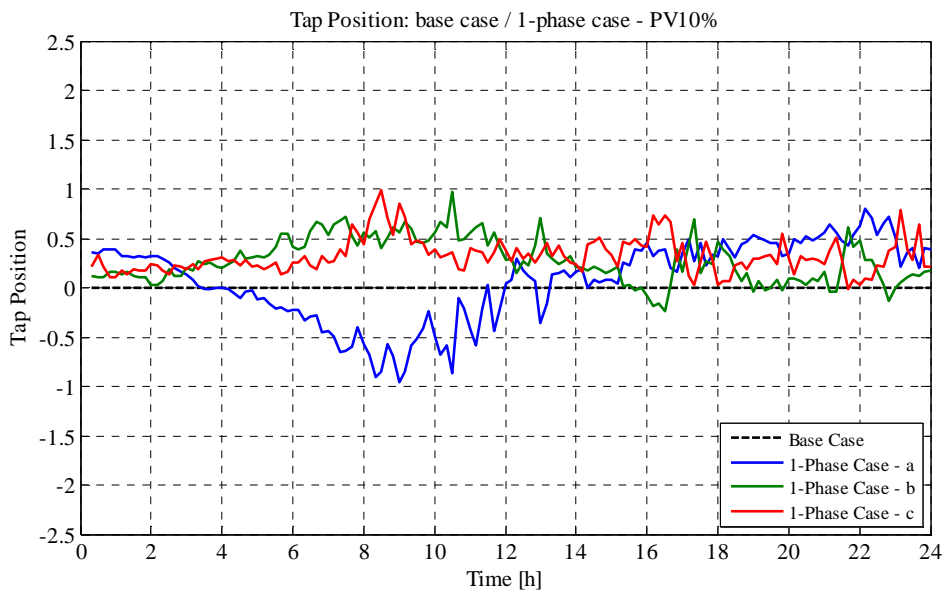


Figure 4.4. Tap Position – 1-Phase/Base Case comparison in the scenario with 35 kW of PV connected to phase a

As it can be seen in Figure 4.5 the phase-ground voltages at the primary side of the transformer do not change in the 3-phase case compared to the base case. On the other hand (Figure 4.6), at the LV side they change because of the 3-phase tapping, staying within the range $-3\%/+1.5\%$.

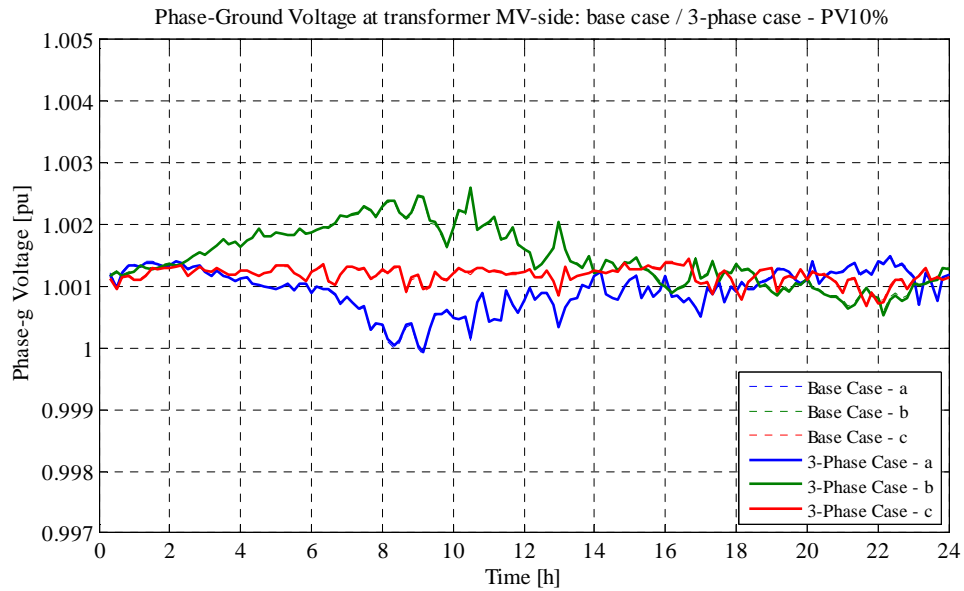


Figure 4.5. Phase-Ground Voltage at transformer MV-side – 3-Phase/Base Case comparison in the scenario with 35 kW of PV connected to phase a

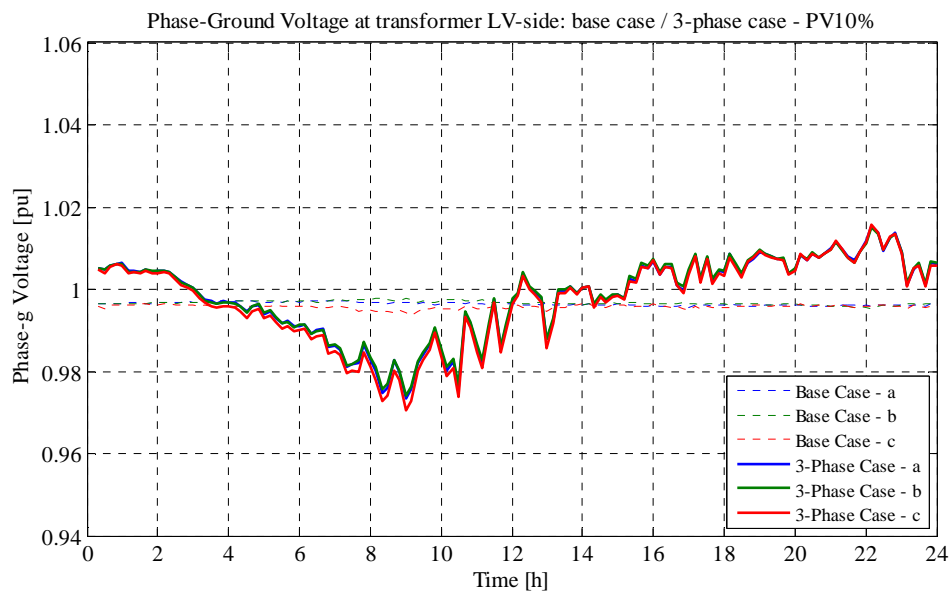


Figure 4.6. Phase-Ground Voltage at transformer LV-side – 3-Phase/Base Case comparison in the scenario with 35 kW of PV connected to phase a

The same situation is valid at the MV-side in the 1-phase case, as it can be seen in Figure 4.7. At the LV side they change independently because of the 1-phase tapping, staying within the range -3%/+2% (Figure 4.8).

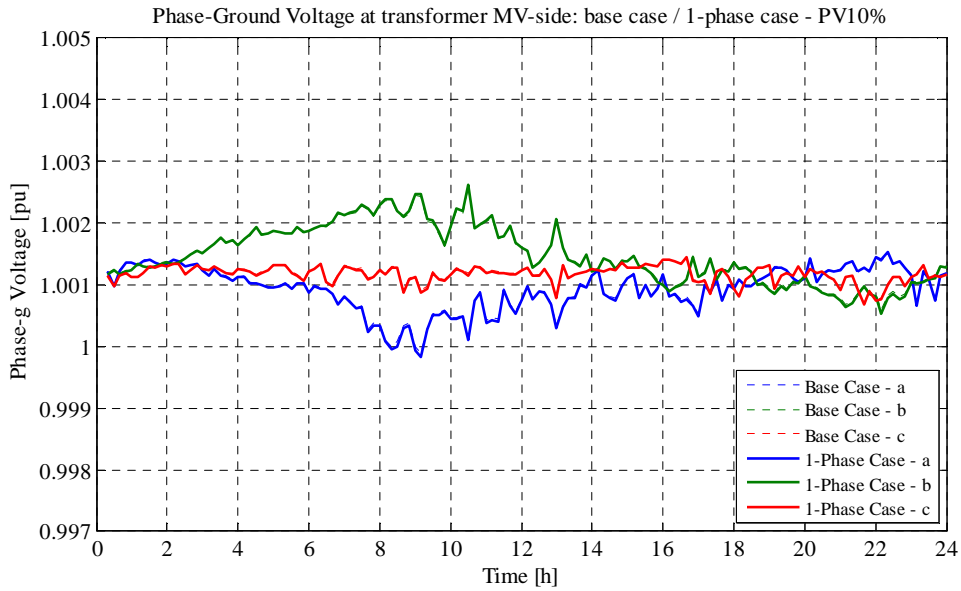


Figure 4.7. Phase-Ground Voltage at transformer MV-side – 1-Phase/Base Case comparison in the scenario with 35 kW of PV connected to phase a

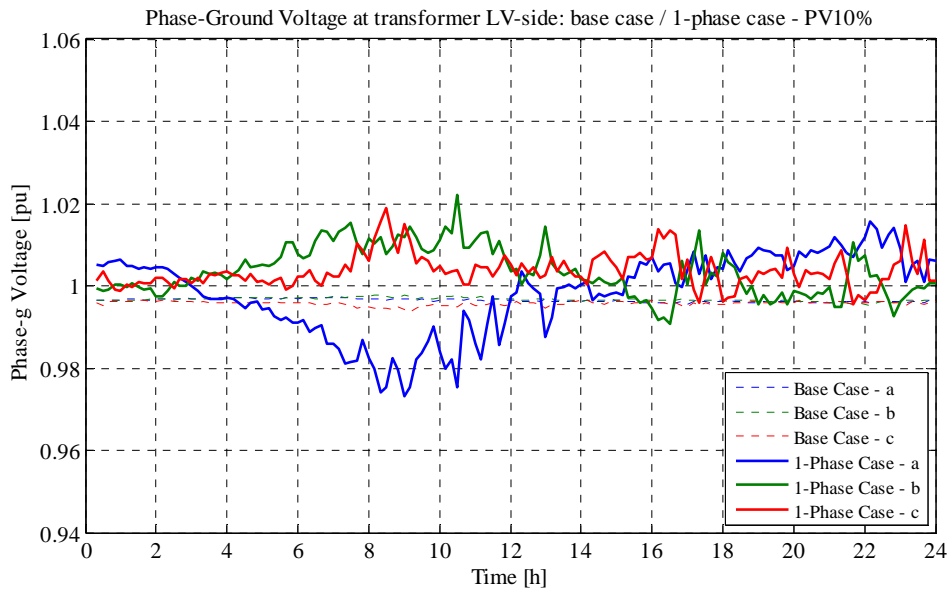


Figure 4.8. Phase-Ground Voltage at transformer LV-side – 1-Phase/Base Case comparison in the scenario with 35 kW of PV connected to phase a

As shown in Figure 4.9, the neutral-ground voltage at bus 6 does not change after tapping, so its peaks stay below 2.3%.

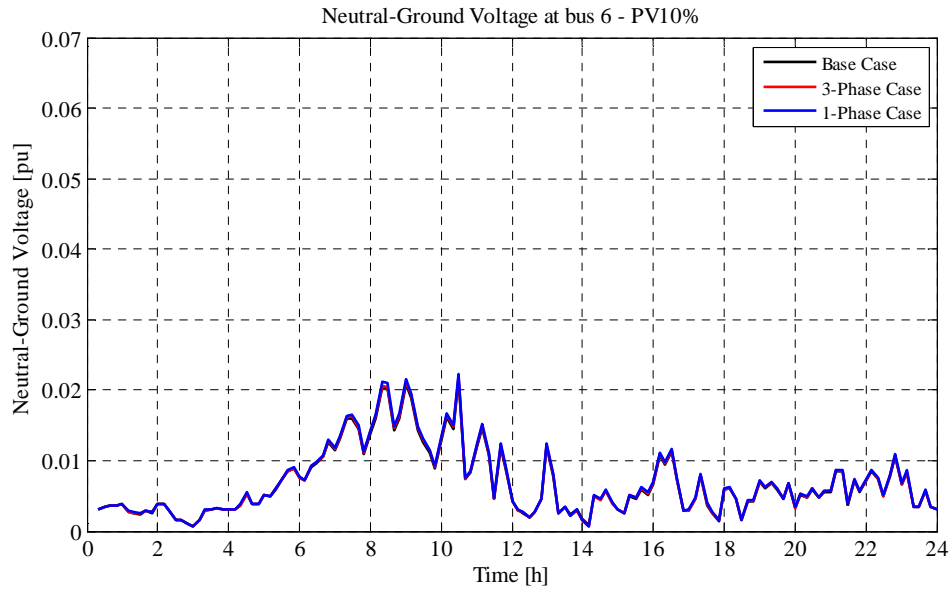


Figure 4.9. Neutral-Ground Voltage at bus 6 – 3-Phase/1-Phase/Base Case comparison in the scenario with 35 kW of PV connected to phase a

The VUF at bus 6 does not increase after tapping, in fact as shown in Figure 4.10 its peak values lay below 1.25%.

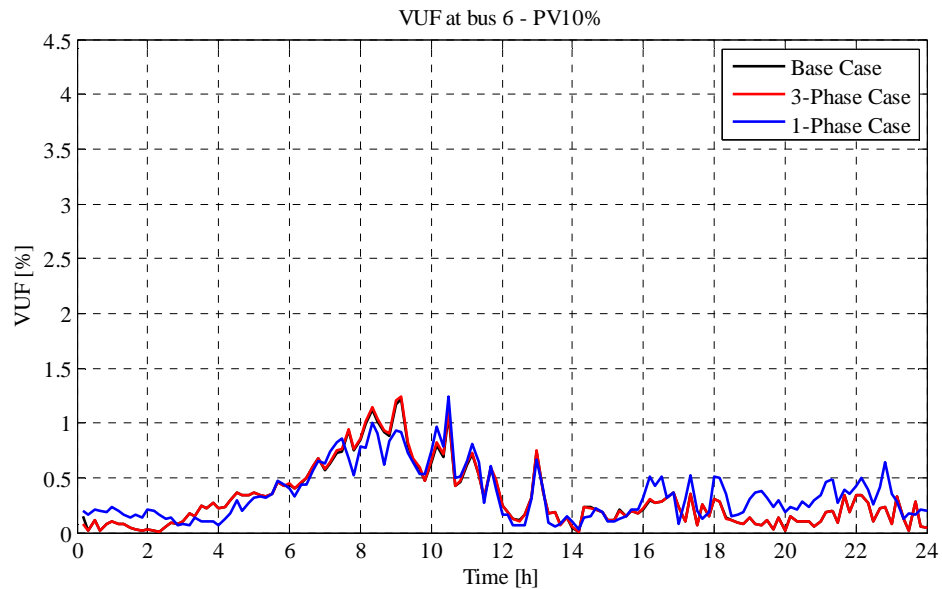


Figure 4.10. VUF at bus 6 – 3-Phase/1-Phase/Base Case comparison in the scenario with 35 kW of PV connected to phase a

As it can be seen in Figure 4.11 and Figure 4.12, the total power losses of lines and the total power loss ratio as well do not increase after tapping in both the cases.

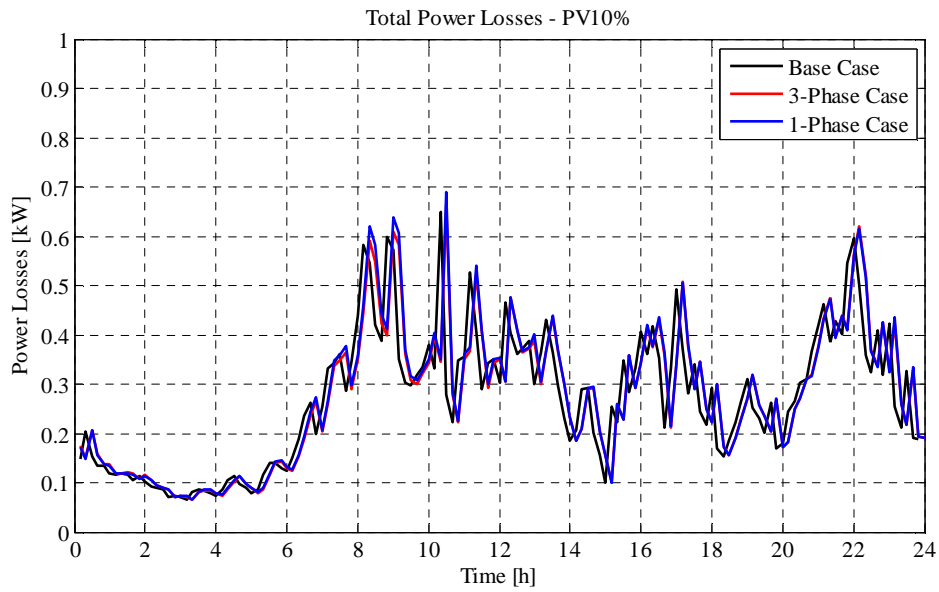


Figure 4.11. Total Power Losses – 3-Phase/1-Phase/Base Case comparison in the scenario with 35 kW of PV connected to phase a

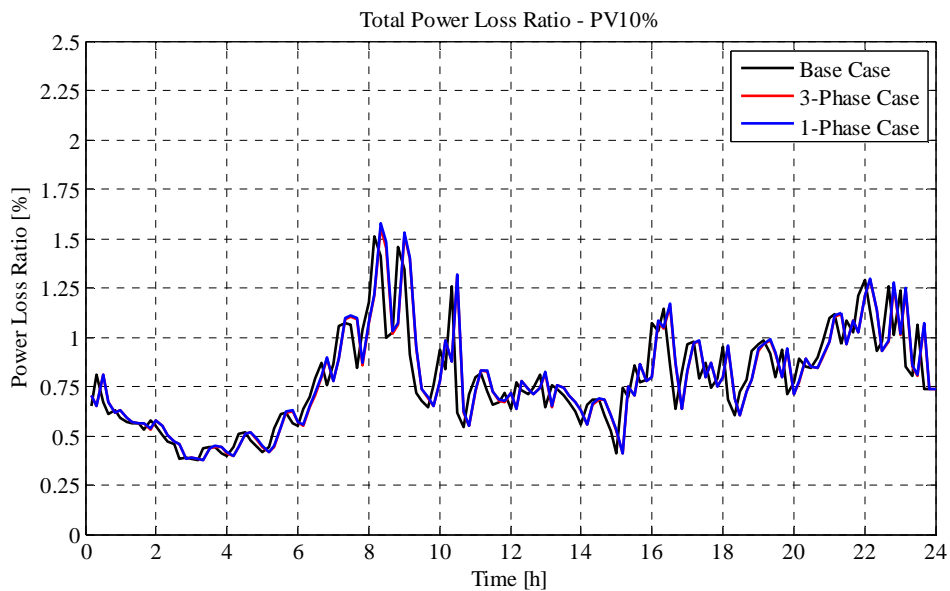


Figure 4.12. Total Power Loss Ratio – 3-Phase/1-Phase/Base Case comparison in the scenario with 35 kW of PV connected to phase a

In Table 4.1 the total energy amounts absorbed by loads, injected by PVs and the amount through the transformer are reported together with the absolute energy loss, the energy loss ratio and the energy deviations from the base case.

| Case | Total Energy absorbed by loads [kWh] | Total Energy injected by PV [kWh] | Energy through the transformer [kWh] | Energy Loss [kWh] | Energy Loss Ratio [%] | Energy Loss Deviation [%, compared to base case] |
|-----------|--------------------------------------|-----------------------------------|--------------------------------------|-------------------|-----------------------|--|
| Base Case | 749.43 | 244.53 | 511.35 | 6.45 | 0.85% | +0.00% |
| 3-Phase | 756.92 | 244.49 | 519.02 | 6.59 | 0.86% | +2.18% |
| 1-Phase | 761.75 | 244.48 | 523.93 | 6.66 | 0.87% | +3.33% |

Table 4.1. PV10% scenario – energy analysis

4.1.2. PV30% – 105 kW – phases a and b

Out of the three phase-neutral voltages at the worst bus (bus 6) from base case to the 3-phase case only the voltage at phase a gets closer to 1 p.u., since the tap control is based on phase a measurement. Its peak decreases from 1.08 to 1.04 p.u., while the one at phase c decreases below the limit of 0.90 p.u.. Phase-neutral voltages and tap positions are depicted in Figure 4.13 and in Figure 4.14.

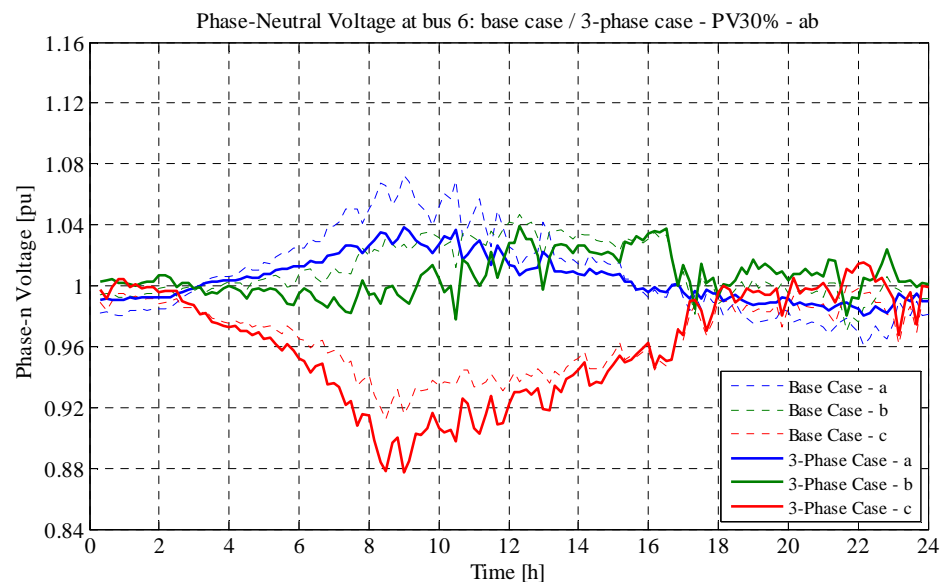


Figure 4.13. Phase-Neutral Voltage at bus 6 – 3-Phase/Base Case comparison in the scenario with 105 kW of PV connected to phase a and b

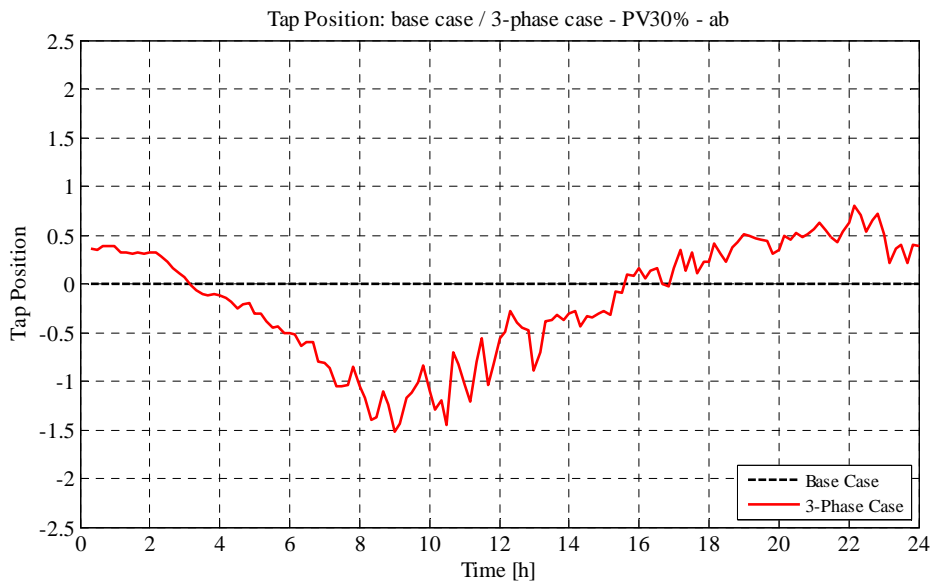


Figure 4.14. Tap Position – 3-Phase/Base Case comparison in the scenario with 105 kW of PV connected to phase a and b

On the other hand in the 1-phase case the tap control is based on all the three phases values, so that all the three phase-neutral voltages are closer to 1 p.u.: voltages at phases a and b decrease, while the one at phase c gets higher. Phase-neutral voltages and tap positions are depicted respectively in Figure 4.15 and Figure 4.16.

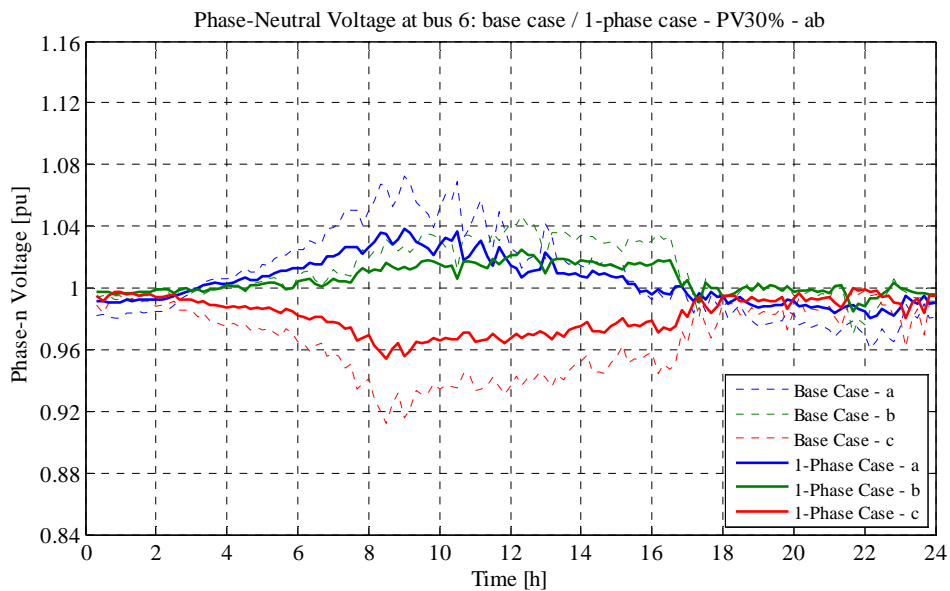


Figure 4.15. Phase-Neutral Voltage at bus 6 – 1-Phase/Base Case comparison in the scenario with 105 kW of PV connected to phase a and b

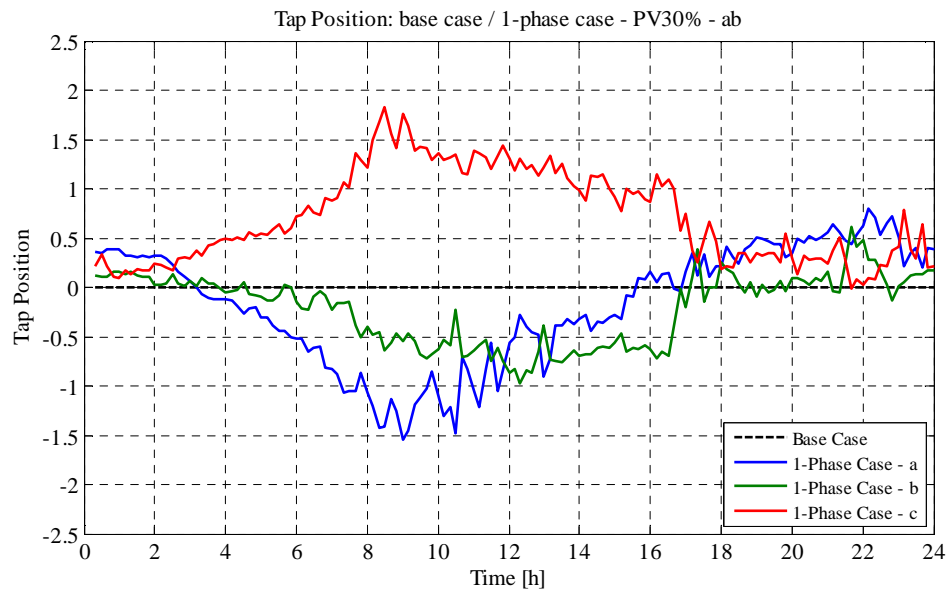


Figure 4.16. Tap Position – 1-Phase/Base Case comparison in the scenario with 105 kW of PV connected to phase a and b

As it can be seen in Figure 4.17, the phase-ground voltages at the primary side of the transformer do not change in the 3-phase case compared to the base case. On the other hand (Figure 4.18), at the LV side they change because of the 3-phase tapping, staying within the range $-4\%/+1.5\%$.

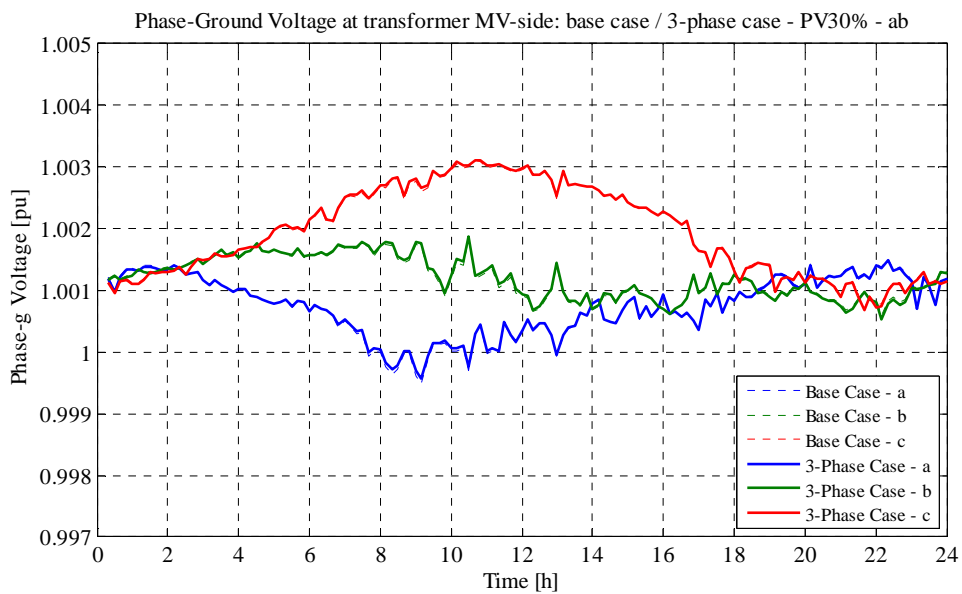


Figure 4.17. Phase-Ground Voltage at transformer MV-side – 3-Phase/Base Case comparison in the scenario with 105 kW of PV connected to phase a and b

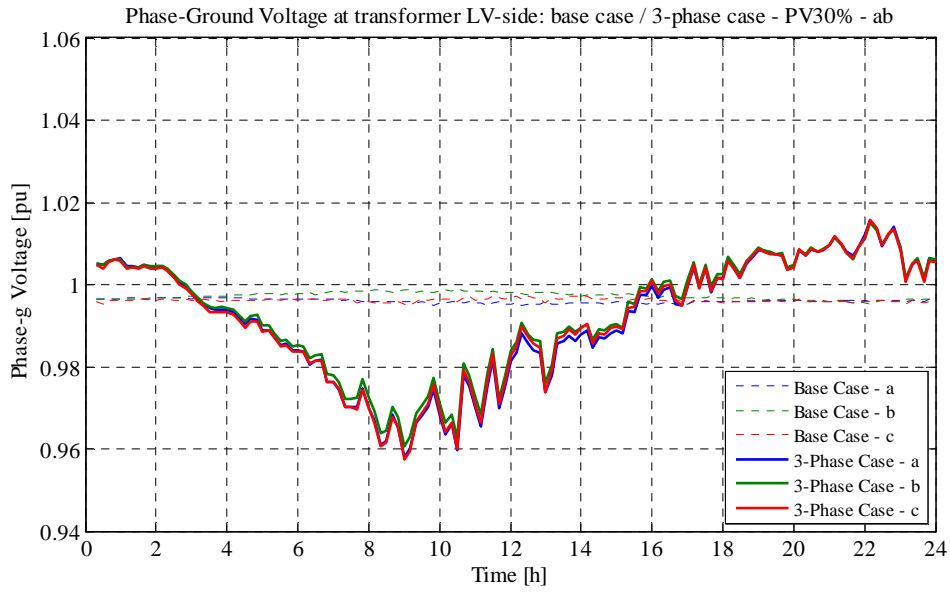


Figure 4.18. Phase-Ground Voltage at transformer LV-side – 3-Phase/Base Case comparison in the scenario with 105 kW of PV connected to phase a and b

The same situation is valid at the MV-side in the 1-phase case, as it can be seen in Figure 4.19. At the LV side they change independently because of the 1-phase tapping, staying within the range -4%/+4% (Figure 4.20).

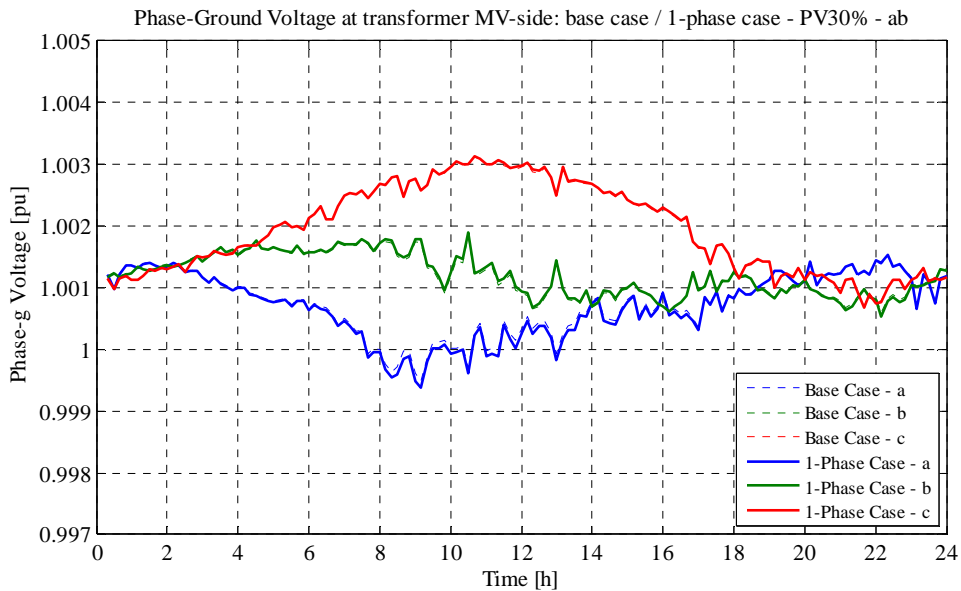


Figure 4.19. Phase-Ground Voltage at transformer MV-side – 1-Phase/Base Case comparison in the scenario with 105 kW of PV connected to phase a and b

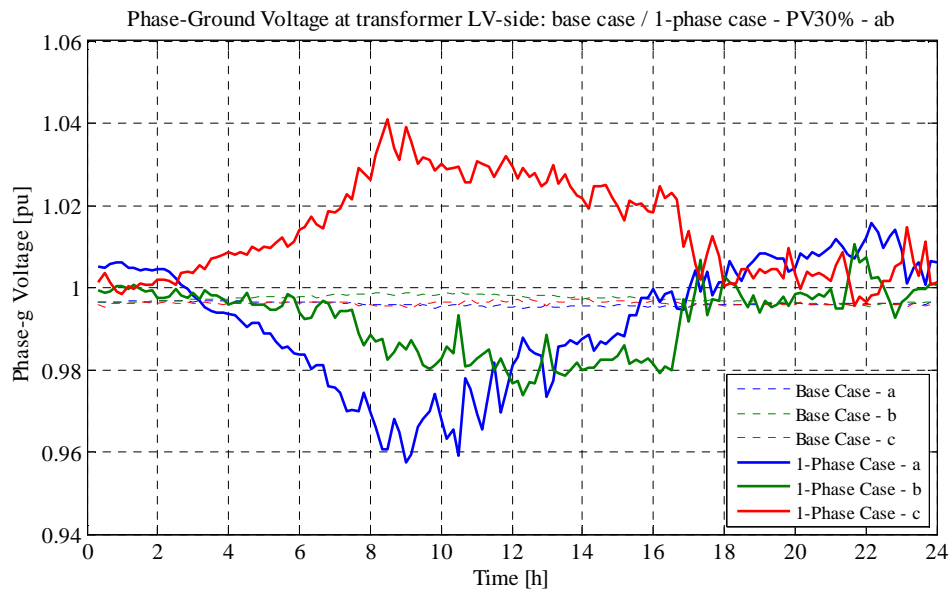


Figure 4.20. Phase-Ground Voltage at transformer LV-side – 1-Phase/Base Case comparison in the scenario with 105 kW of PV connected to phase a and b

As shown in Figure 4.21, the neutral-ground voltage at bus 6 does not change after tapping, so its peaks stay below 4%.

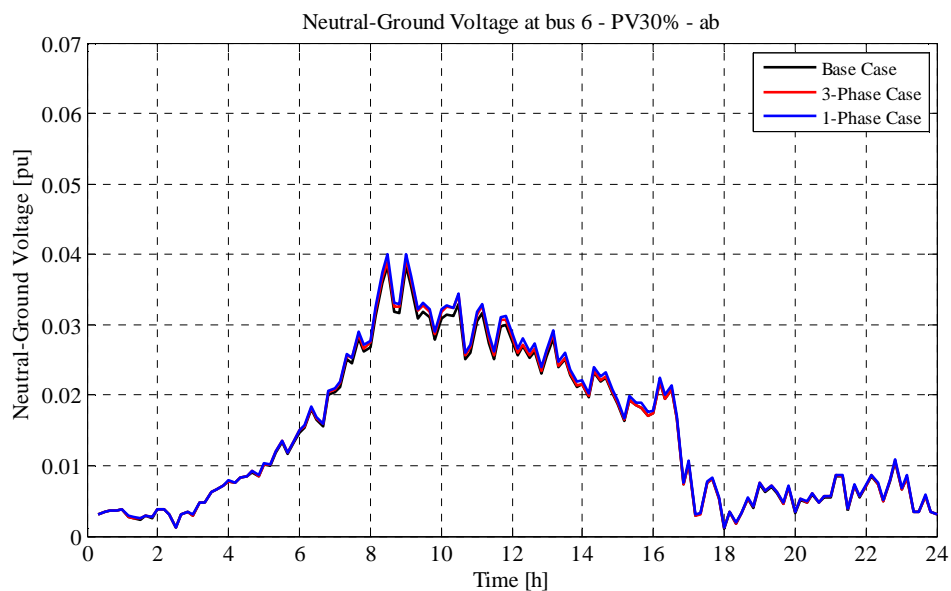


Figure 4.21. Neutral-Ground Voltage at bus 6 – 3-Phase/1-Phase/Base Case comparison in the scenario with 105 kW of PV connected to phase a and b

The VUF at bus 6 (Figure 4.22) does not increase in the 3-phase case, while it grows in the 1-phase case: peaks grows from 1.4 % till 1.9%.

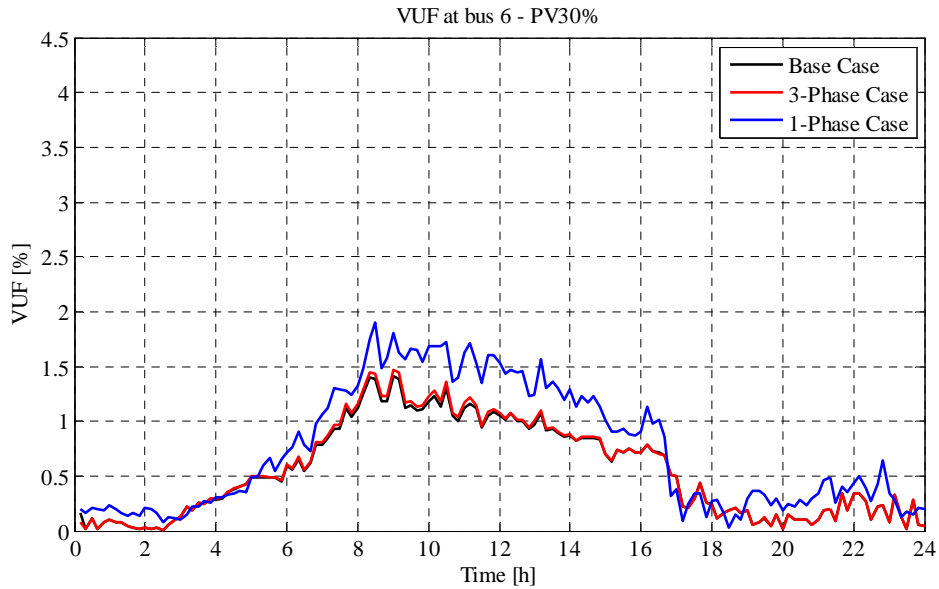


Figure 4.22. VUF at bus 6 – 3-Phase/1-Phase/Base Case comparison in the scenario with 105 kW of PV connected to phase a and b

As it can be seen in Figure 4.23 and Figure 4.24, the total power losses of lines and the total power loss ratio as well do not present a so relevant increase after tapping in both the cases.

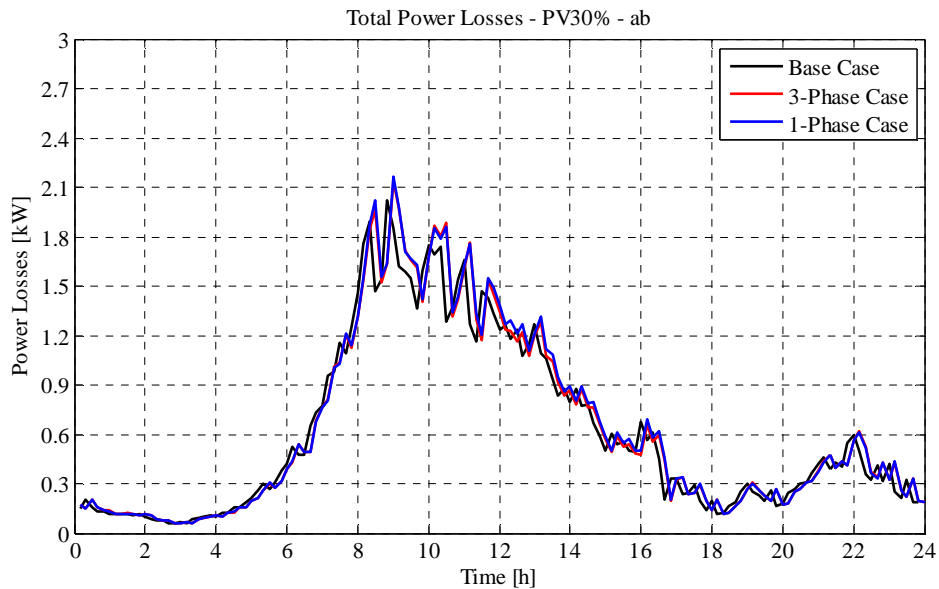


Figure 4.23. Total Power Losses – 3-Phase/1-Phase/Base Case comparison in the scenario with 105 kW of PV connected to phase a and b

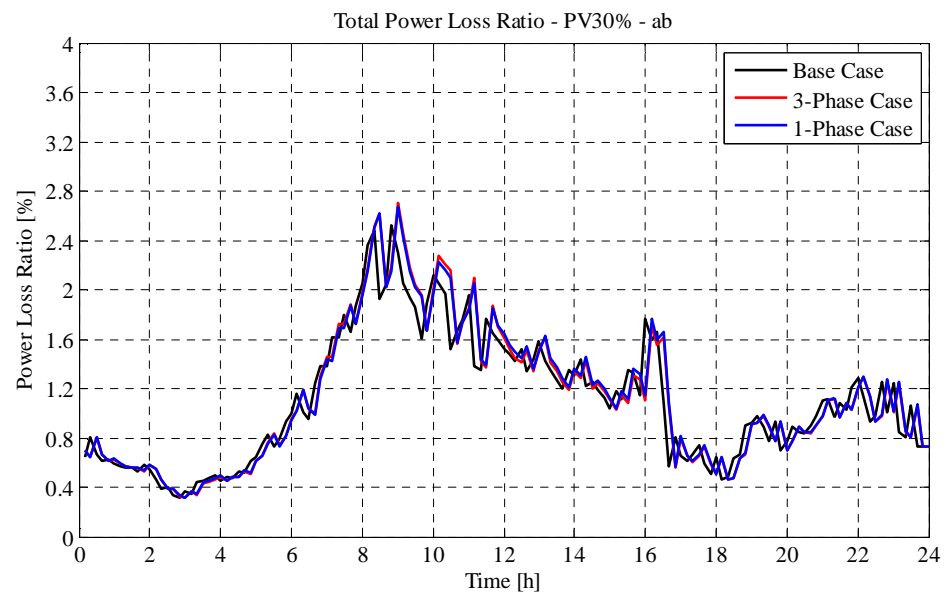


Figure 4.24. Total Power Loss Ratio – 3-Phase/1-Phase/Base Case comparison in the scenario with 105 kW of PV connected to phase a and b

In Table 4.2 the total energy amounts absorbed by loads, injected by PVs and the amount through the transformer are reported together with the absolute energy loss, the energy loss ratio and the energy deviations from the base case.

| Case | Total Energy absorbed by loads [kWh] | Total Energy injected by PV [kWh] | Energy through the transformer [kWh] | Energy Loss [kWh] | Energy Loss Ratio [%] | Energy Loss Deviation [%, compared to base case] |
|-----------|--------------------------------------|-----------------------------------|--------------------------------------|-------------------|-----------------------|--|
| Base Case | 756.30 | 731.21 | 39.74 | 14.65 | 1.90% | +0.00% |
| 3-Phase | 753.48 | 730.71 | 37.82 | 15.05 | 1.96% | +2.73% |
| 1-Phase | 763.29 | 730.60 | 47.93 | 15.24 | 1.96% | +4.01% |

Table 4.2. PV30% ab scenario – energy analysis

4.1.3. *PV40% – 140 kW – phases a and b*

Out of the three phase-neutral voltages at the worst bus (bus 6) from base case to the 3-phase case only the voltage at phase a gets closer to 1 p.u., since the tap control is based on phase a measurement. Its peak decreases from 1.10 to 1.05 p.u., while the one at phase c decreases below the limit of 0.84 p.u.. Phase-neutral voltages and tap positions are depicted respectively in Figure 4.25 and in Figure 4.26.

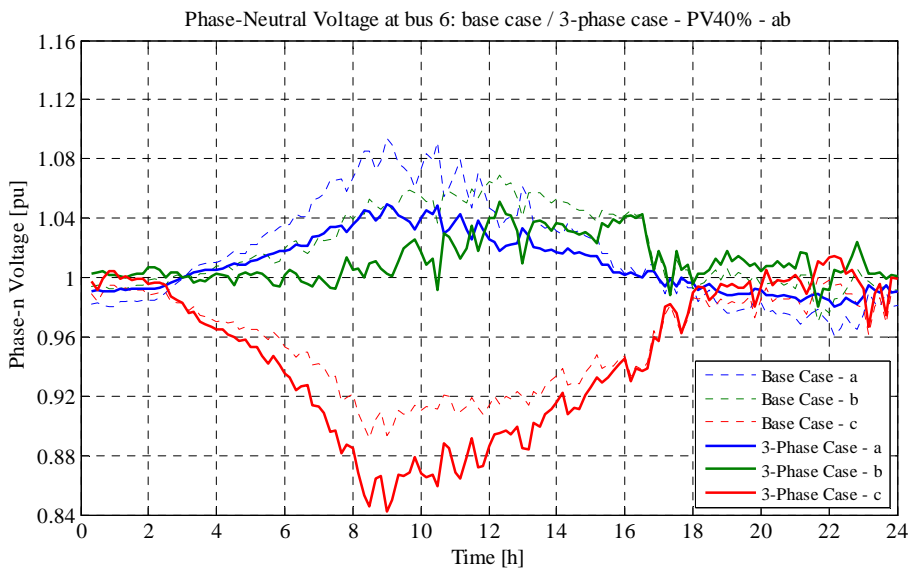


Figure 4.25. Phase-Neutral Voltage at bus 6 – 3-Phase/Base Case comparison in the scenario with 140 kW of PV connected to phase a and b

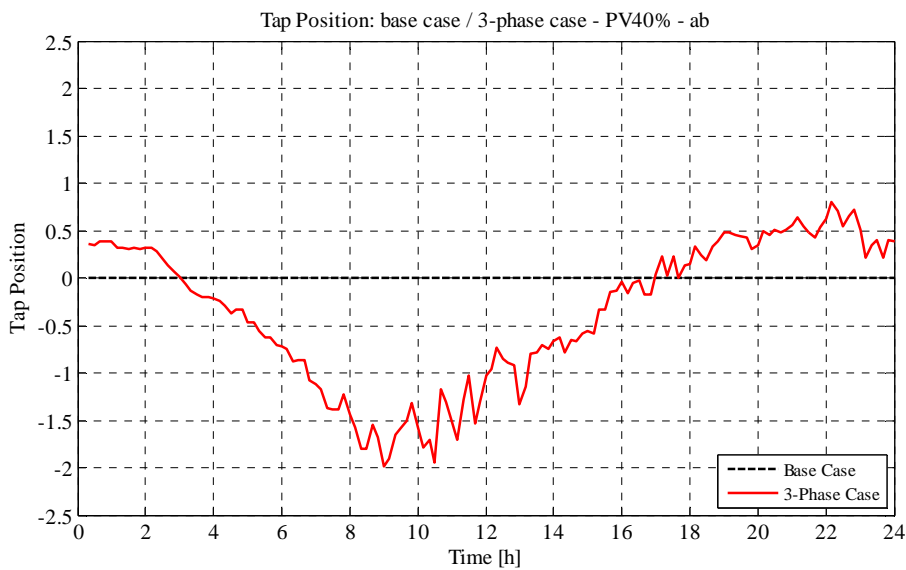


Figure 4.26. Tap Position – 3-Phase/Base Case comparison in the scenario with 140 kW of PV connected to phase a and b

On the other hand in the 1-phase case the tap control is based on all the three phases values, so that all the three phase-neutral voltages are closer to 1 p.u.: voltages at phases a and b decrease, while the one at phase c gets higher. Phase-neutral voltages and tap positions are depicted respectively in Figure 4.27 and in Figure 4.28.

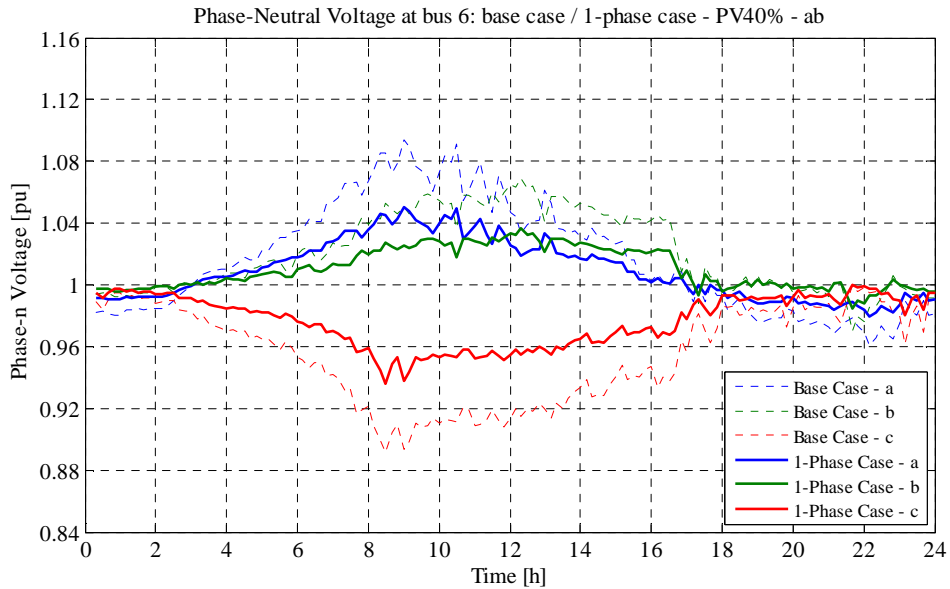


Figure 4.27. Phase-Neutral Voltage at bus 6 – 1-Phase/Base Case comparison in the scenario with 140 kW of PV connected to phase a and b

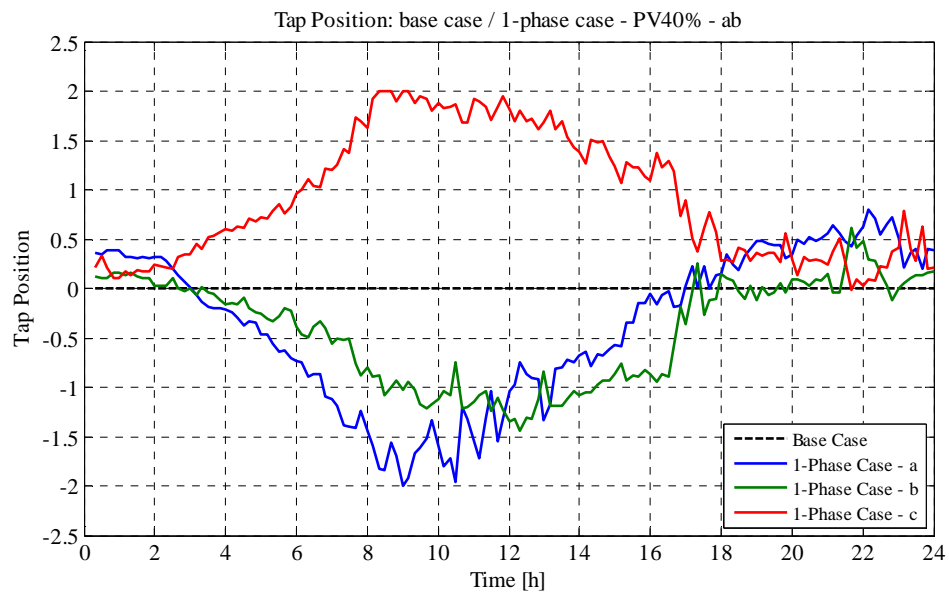


Figure 4.28. Tap Position – 1-Phase/Base Case comparison in the scenario with 140 kW of PV connected to phase a and b

As it can be seen in Figure 4.29, the phase-ground voltages at the primary side of the transformer do not change in the 3-phase case compared to the base case. On the other hand (Figure 4.30), at the LV side they change because of the 3-phase tapping, staying within the range -5%/+2%.

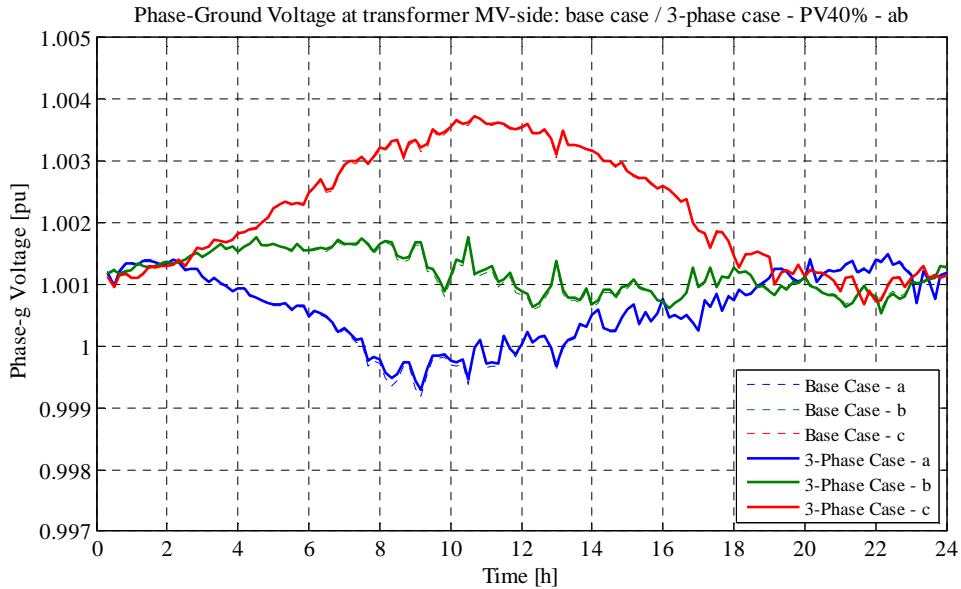


Figure 4.29. Phase-Ground Voltage at transformer MV-side – 3-Phase/Base Case comparison in the scenario with 140 kW of PV connected to phase a and b

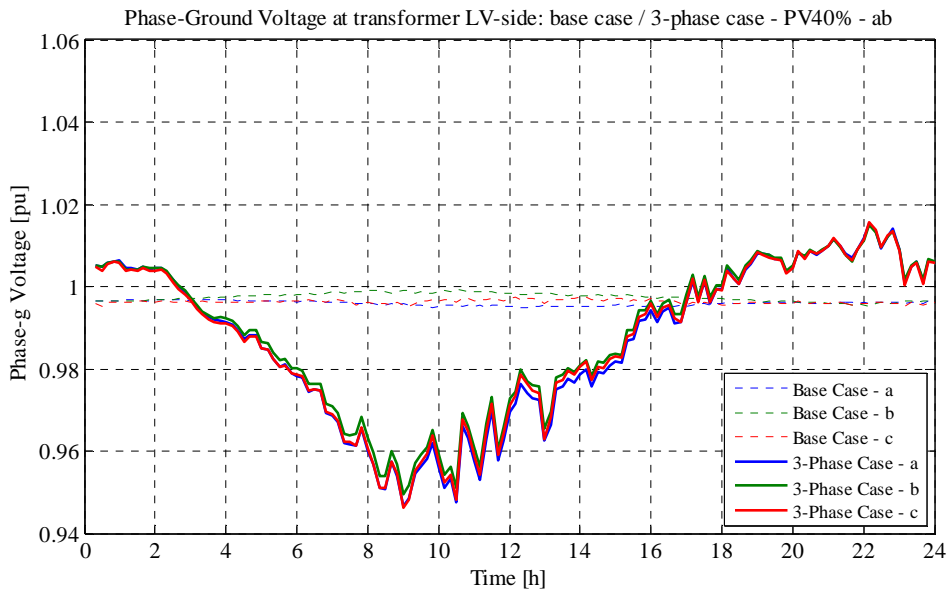


Figure 4.30. Phase-Ground Voltage at transformer LV-side – 3-Phase/Base Case comparison in the scenario with 140 kW of PV connected to phase a and b

The same situation is valid at the MV-side in the 1-phase case, as it can be seen in Figure 4.31. At the LV side they change independently because of the 1-phase tapping, staying within the range -5%/+5% (Figure 4.32).

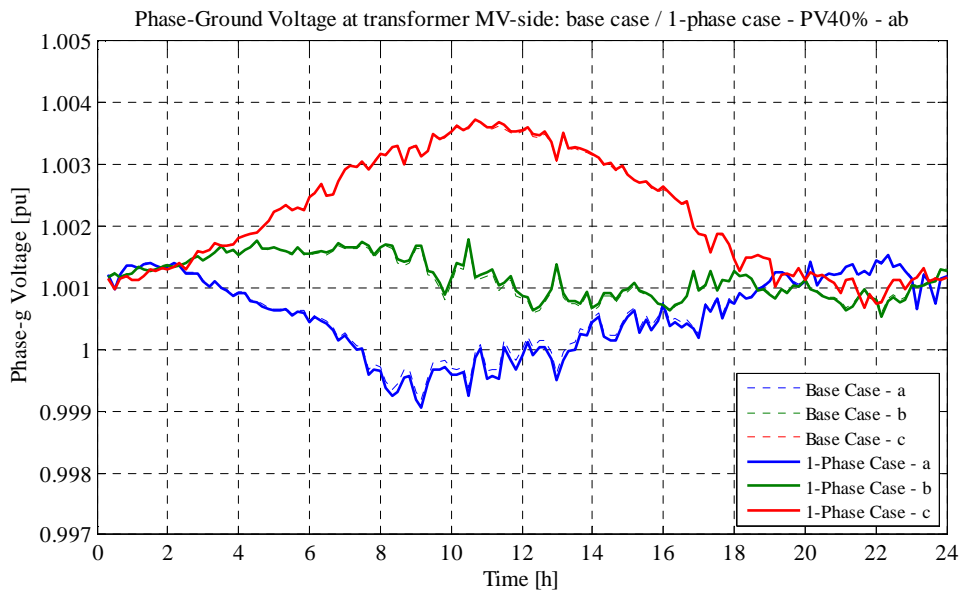


Figure 4.31. Phase-Ground Voltage at transformer MV-side – 1-Phase/Base Case comparison in the scenario with 140 kW of PV connected to phase a and b

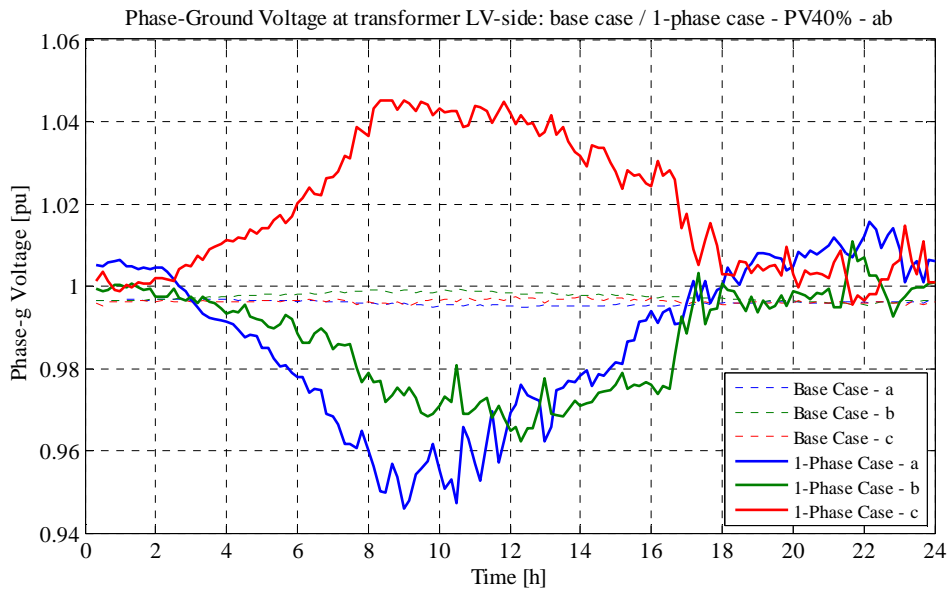


Figure 4.32. Phase-Ground Voltage at transformer LV-side – 1-Phase/Base Case comparison in the scenario with 140 kW of PV connected to phase a and b

As shown in Figure 4.33, the neutral-ground voltage at bus 6 does not change after tapping, so its peaks stay below 5.5%.

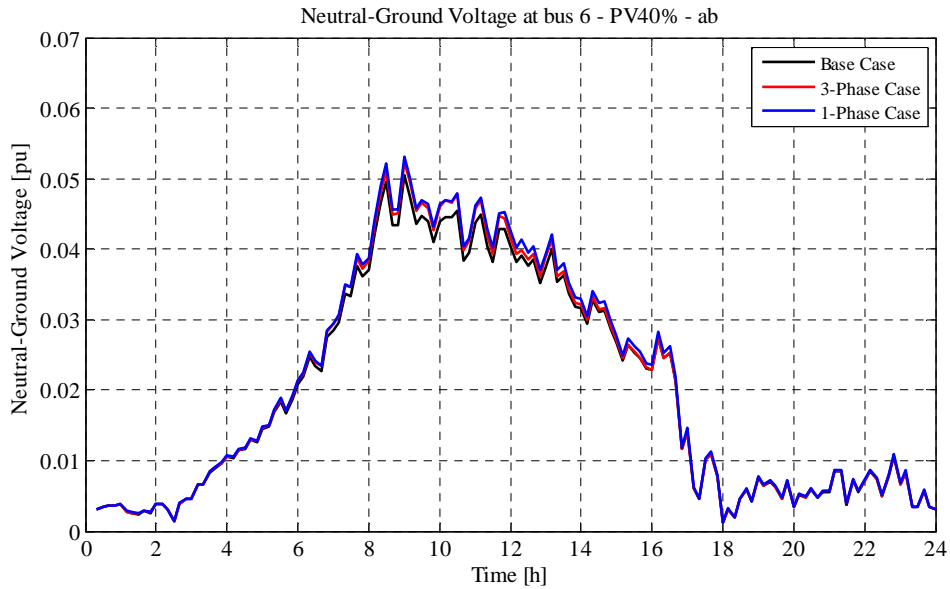


Figure 4.33. Neutral-Ground Voltage at bus 6 – 3-Phase/1-Phase/Base Case comparison in the scenario with 140 kW of PV connected to phase a and b

The VUF at bus 6 (Figure 4.34) does not increase in the 3-phase case, while it grows in the 1-phase case: peaks grows from 1.7 % till 2.5%.

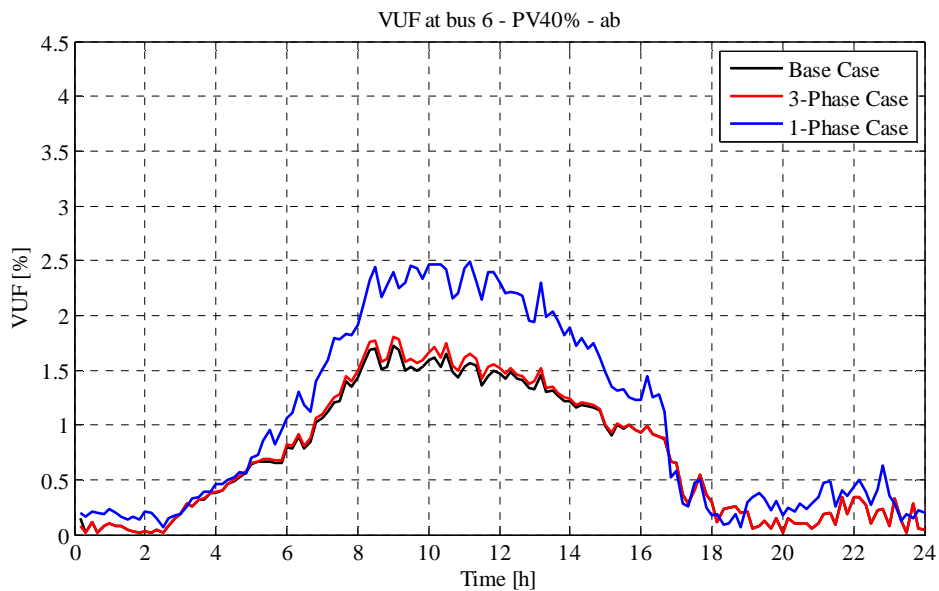


Figure 4.34. VUF at bus 6 – 3-Phase/1-Phase/Base Case comparison in the scenario with 140 kW of PV connected to phase a and b

As it can be seen in Figure 4.35 and Figure 4.36, the total power losses of lines and the total power loss ratio as well do not present a so relevant increase after tapping in both the cases.

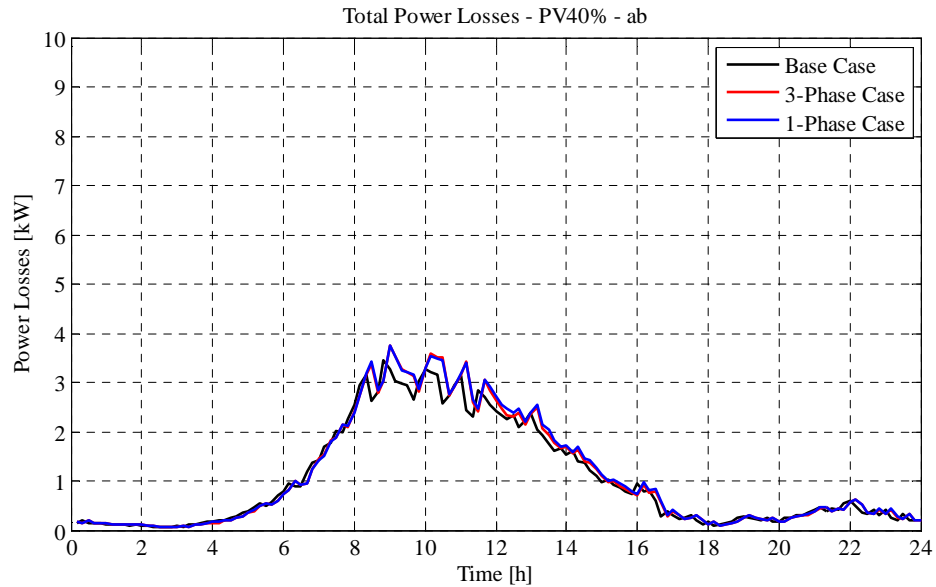


Figure 4.35. Total Power Losses – 3-Phase/1-Phase/Base Case comparison in the scenario with 140 kW of PV connected to phase a and b

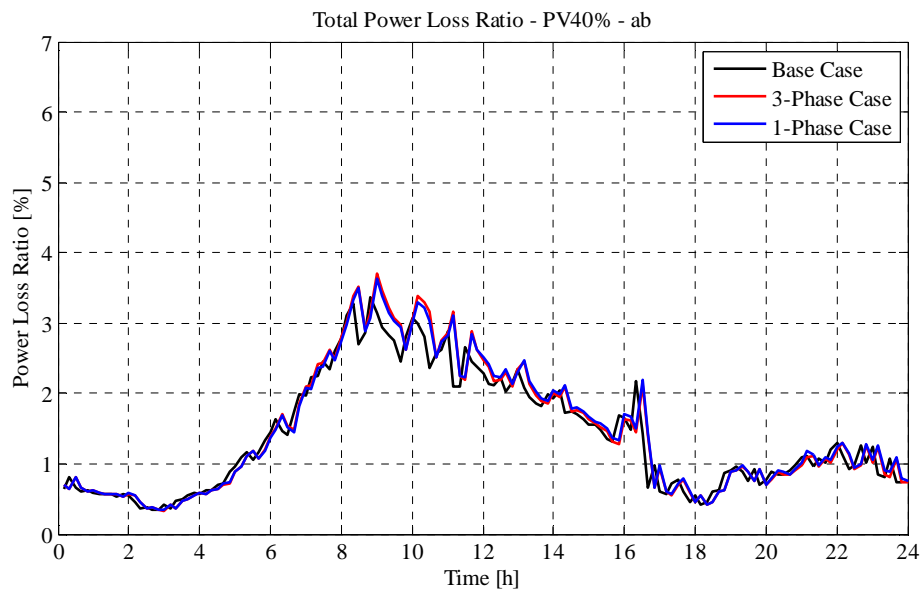


Figure 4.36. Total Power Loss Ratio – 3-Phase/1-Phase/Base Case comparison in the scenario with 140 kW of PV connected to phase a and b

In Table 4.3 the total energy amounts absorbed by loads, injected by PVs and the amount through the transformer are reported together with the absolute energy loss, the energy loss ratio and the energy deviations from the base case.

| Case | Total Energy absorbed by loads [kWh] | Total Energy injected by PV [kWh] | Energy through the transformer [kWh] | Energy Loss [kWh] | Energy Loss Ratio [%] | Energy Loss Deviation [%, compared to base case] |
|-----------|--------------------------------------|-----------------------------------|--------------------------------------|-------------------|-----------------------|--|
| Base Case | 760.44 | 971.93 | -186.77 | 24.72 | 2.54% | +0.00% |
| 3-Phase | 749.57 | 971.02 | -195.24 | 26.21 | 2.70% | +6.01% |
| 1-Phase | 763.71 | 970.58 | -180.62 | 26.25 | 2.70% | +6.18% |

Table 4.3. PV40% ab scenario – energy analysis

4.1.4. PV50% – 175 kW – phases a and b

Out of the three phase-neutral voltages at the worst bus (bus 6) from base case to the 3-phase case only the voltage at phase a gets closer to 1 p.u., since the tap control is based on phase a measurement. Its peak decreases from 1.13 to 1.08 p.u., while the one at phase c decreases below the limit: till 0.82 p.u.. Phase-neutral voltages and tap positions are depicted respectively in Figure 4.37 and in Figure 4.38.

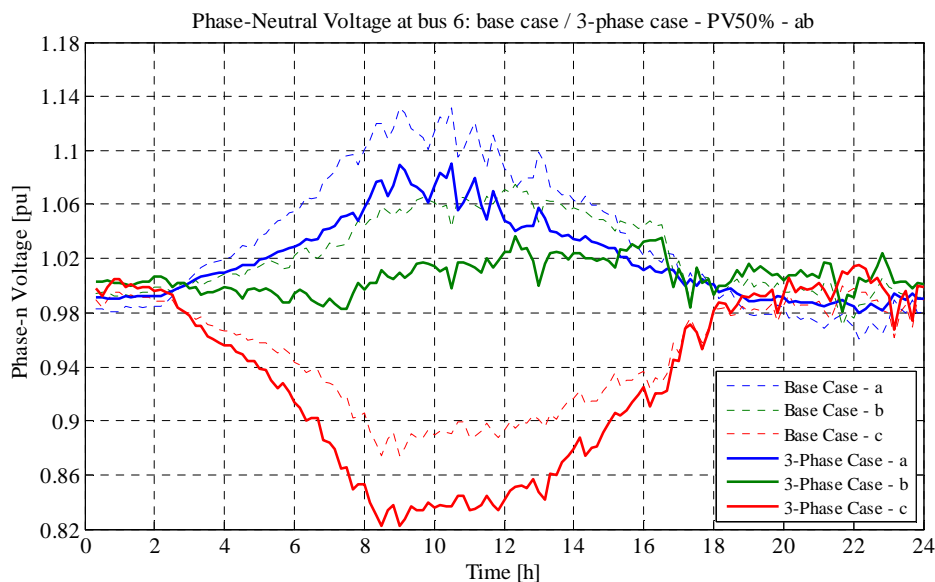


Figure 4.37. Phase-Neutral Voltage at bus 6 – 3-Phase/Base Case comparison in the scenario with 175 kW of PV connected to phase a and b

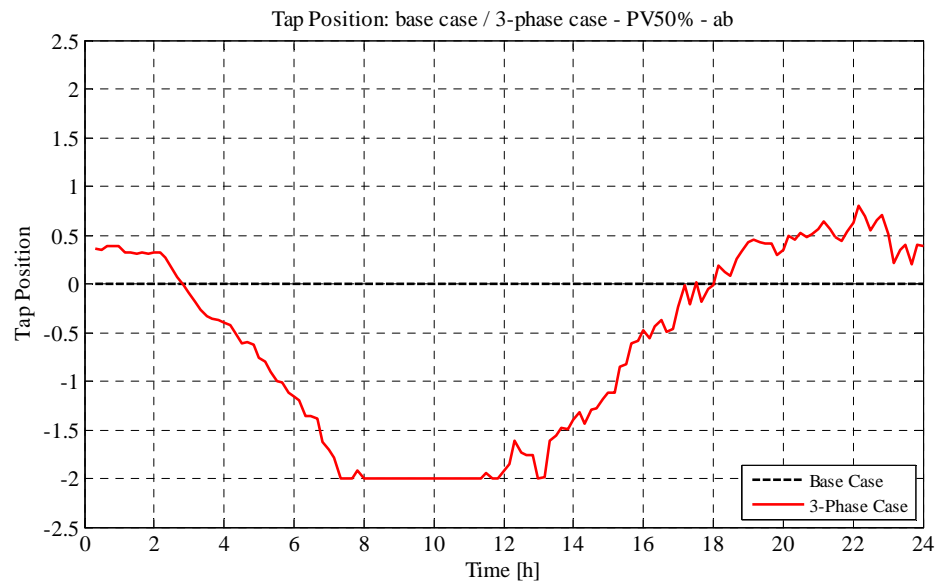


Figure 4.38. Tap Position – 3-Phase/Base Case comparison in the scenario with 175 kW of PV connected to phase a and b

On the other hand in the 1-phase case the tap control is based on all the three phases values, so that all the three phase-neutral voltages are closer to 1 p.u.: voltages at phases a and b decrease, while the one at phase c gets higher. Phase-neutral voltages and tap positions are depicted respectively in Figure 4.39 and in Figure 4.40.

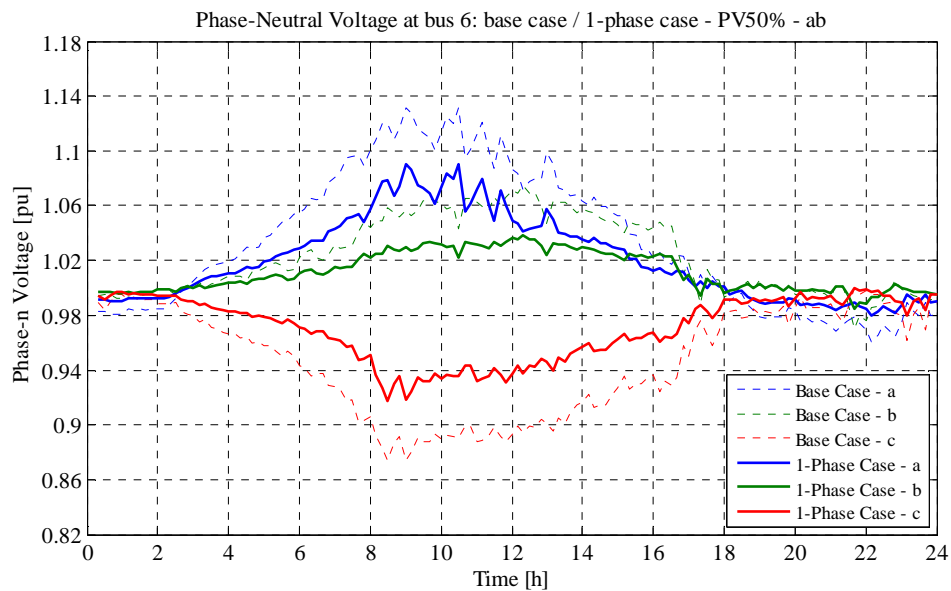


Figure 4.39. Phase-Neutral Voltage at bus 6 – 1-Phase/Base Case comparison in the scenario with 175 kW of PV connected to phase a and b

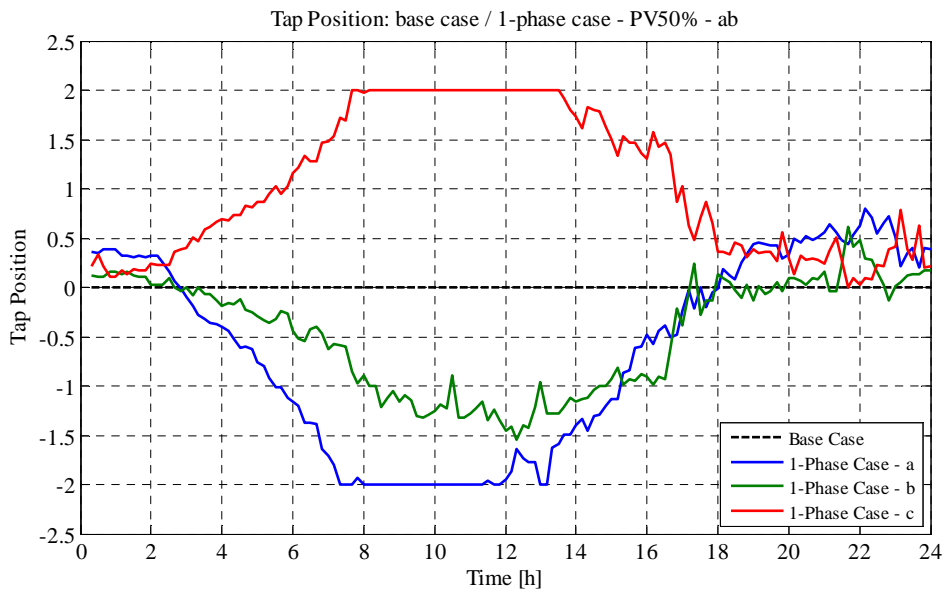


Figure 4.40. Tap Position – 1-Phase/Base Case comparison in the scenario with 175 kW of PV connected to phase a and b

As it can be seen in Figure 4.41, the phase-ground voltages at the primary side of the transformer do not change in the 3-phase case compared to the base case. On the other hand (Figure 4.42), at the LV side they change because of the 3-phase tapping, staying within the range -5%/+2%.

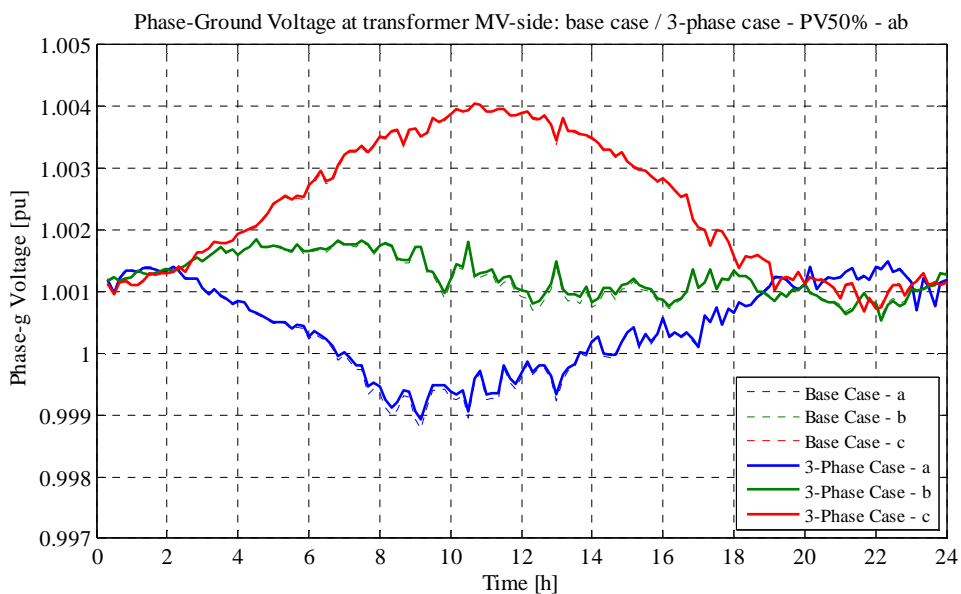


Figure 4.41. Phase-Ground Voltage at transformer MV-side – 3-Phase/Base Case comparison in the scenario with 175 kW of PV connected to phase a and b

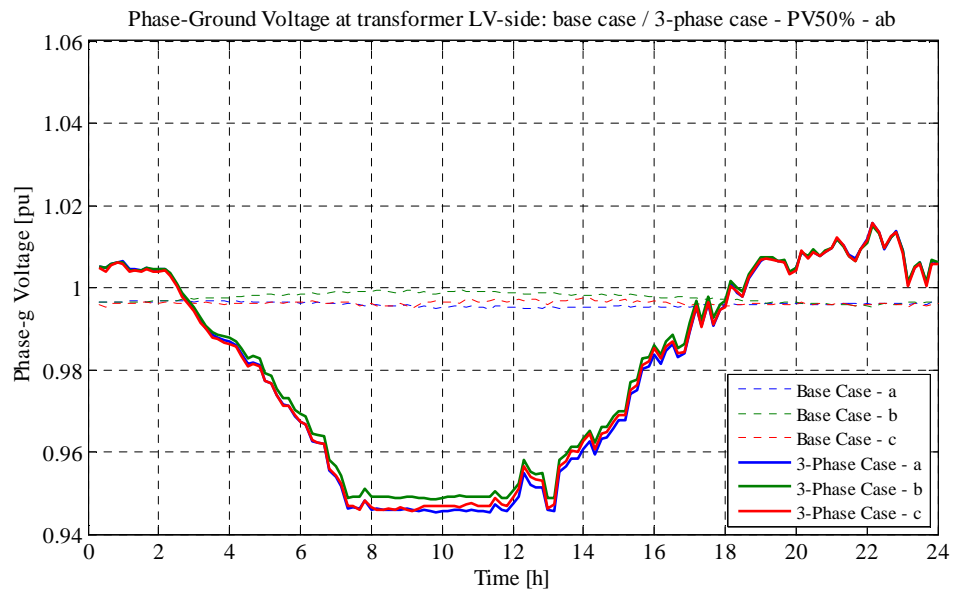


Figure 4.42. Phase-Ground Voltage at transformer LV-side – 3-Phase/Base Case comparison in the scenario with 175 kW of PV connected to phase a and b

The same situation is valid at the MV-side in the 1-phase case, as can be seen in Figure 4.43. At the LV side they change independently because of the 1-phase tapping, staying within the range -5%/+5% (Figure 4.44).

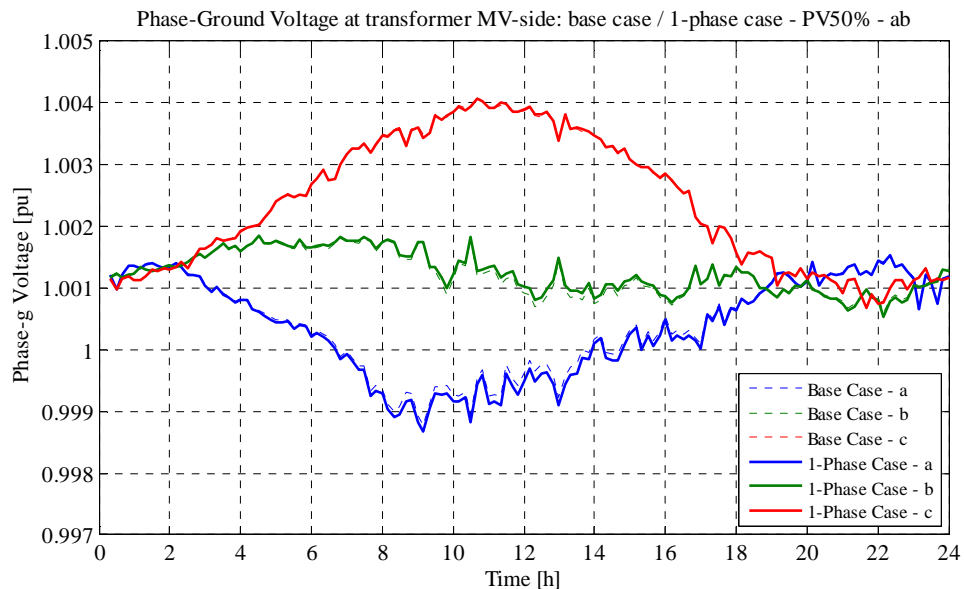


Figure 4.43. Phase-Ground Voltage at transformer MV-side – 1-Phase/Base Case comparison in the scenario with 175 kW of PV connected to phase a and b

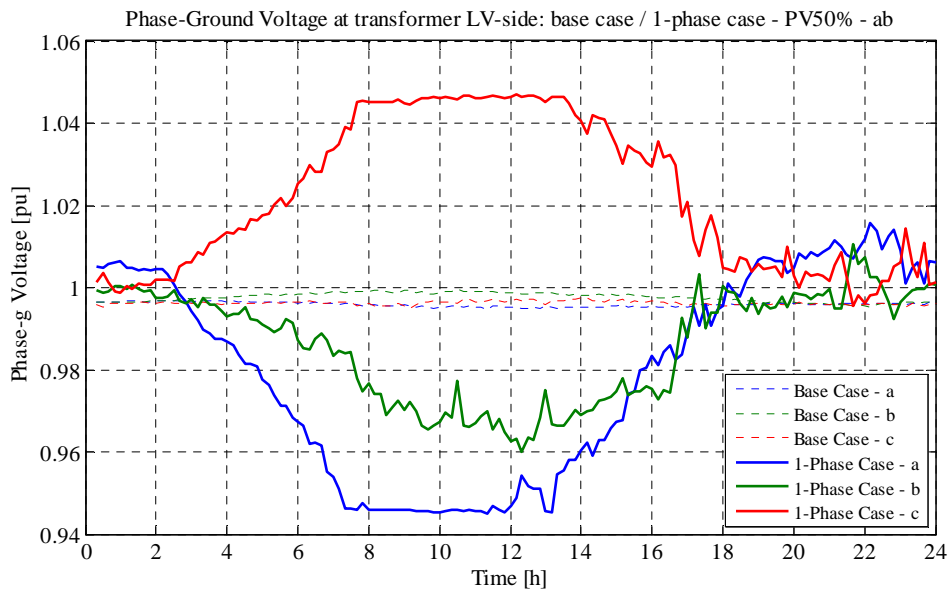


Figure 4.44. Phase-Ground Voltage at transformer LV-side – 1-Phase/Base Case comparison in the scenario with 175 kW of PV connected to phase a and b

As shown in Figure 4.45, the neutral-ground voltage at bus 6 does not change after tapping, so its peaks stay below 7%.

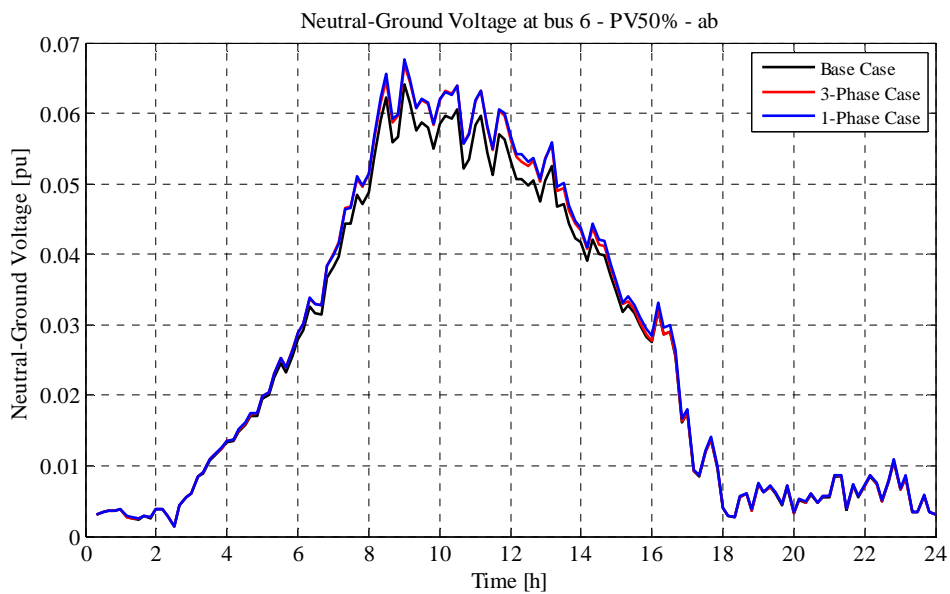


Figure 4.45. Neutral-Ground Voltage at bus 6 – 3-Phase/1-Phase/Base Case comparison in the scenario with 175 kW of PV connected to phase a and b

The VUF at bus 6 (Figure 4.46) does not increase in the 3-phase case, while it grows in the 1-phase case: peaks grows from 2.1 % till 2.9%.

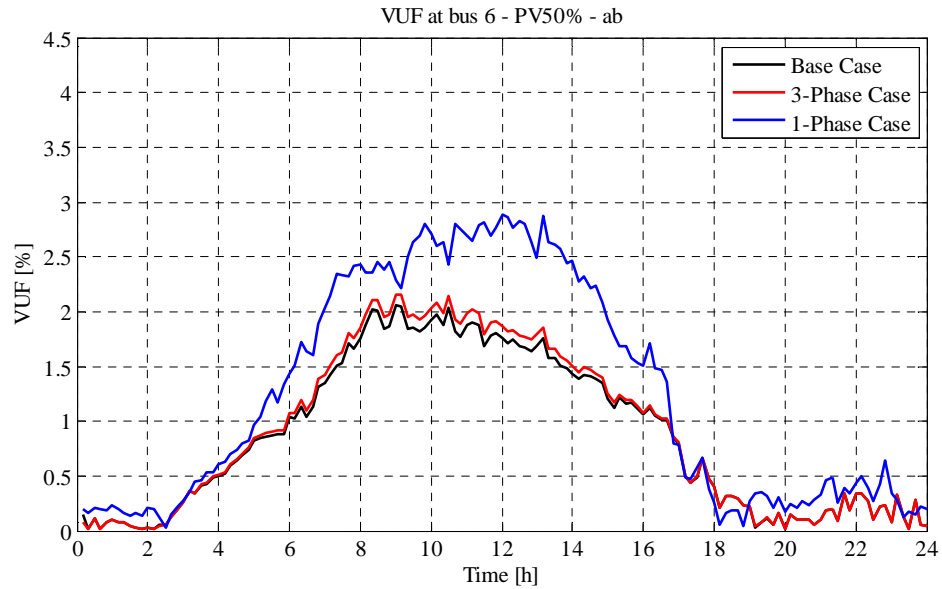


Figure 4.46. VUF at bus 6 – 3-Phase/1-Phase/Base Case comparison in the scenario with 175 kW of PV connected to phase a and b

As it can be seen in Figure 4.47 and Figure 4.48, the total power losses of lines and the total power loss ratio as well do not present a so relevant increase after tapping in both the cases.

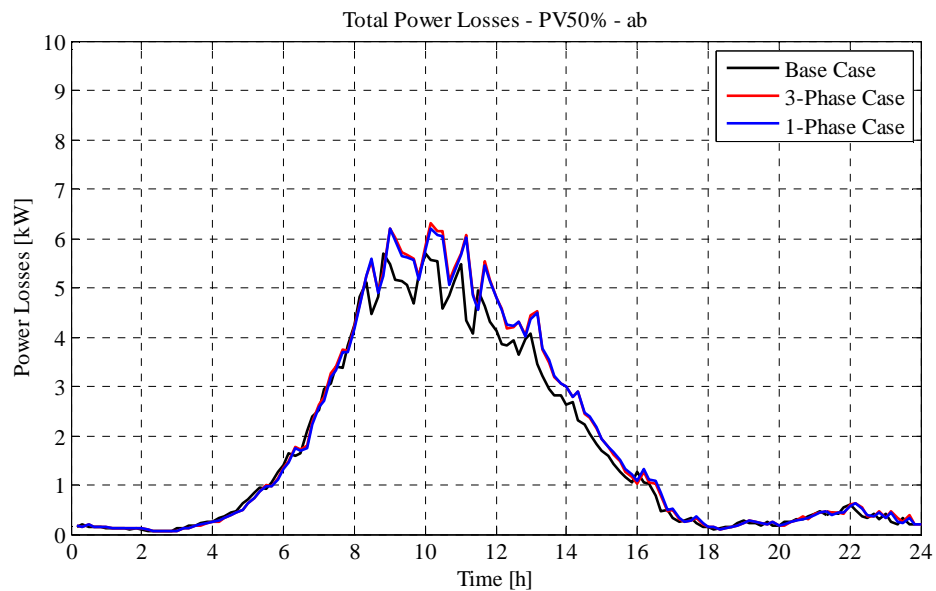


Figure 4.47. Total Power Losses – 3-Phase/1-Phase/Base Case comparison in the scenario with 175 kW of PV connected to phase a and b

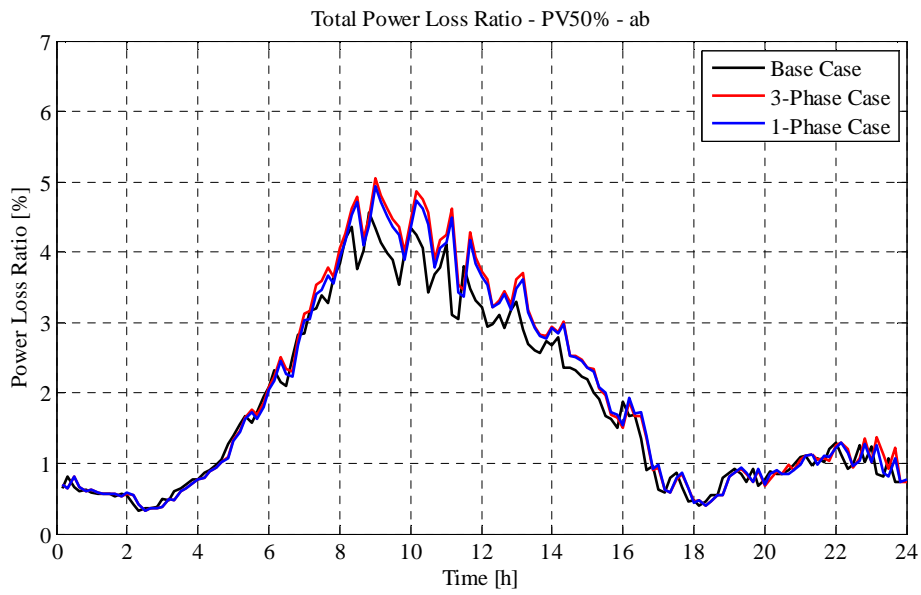


Figure 4.48. Total Power Loss Ratio – 3-Phase/1-Phase/Base Case comparison in the scenario with 175 kW of PV connected to phase a and b

In Table 4.4 the total energy amounts absorbed by loads, injected by PVs and the amount through the transformer are reported together with the absolute energy loss, the energy loss ratio and the energy deviations from the base case.

| Case | Total Energy absorbed by loads [kWh] | Total Energy injected by PV [kWh] | Energy through the trafo [kWh] | Energy Loss [kWh] | Energy Loss Ratio [%] | Energy Loss Deviation [%, compared to base case] |
|-----------|--------------------------------------|-----------------------------------|--------------------------------|-------------------|-----------------------|--|
| Base Case | 767.25 | 1209.34 | -401.80 | 40.30 | 3.33% | +0.00% |
| 3-Phase | 744.07 | 1207.03 | -418.98 | 43.98 | 3.64% | +9.13% |
| 1-Phase | 765.04 | 1207.02 | -398.23 | 43.75 | 3.62% | +8.56% |

Table 4.4. PV50% ab scenario – energy analysis

4.1.5. PV40% – 140 kW – phases a, b and c

Out of the three phase-neutral voltages at the worst bus (bus 6) from base case to the 3-phase case only the voltage at phase a gets closer to 1 p.u., since the tap control is based on phase a measurement. Its peak decreases from 1.06 to 1.03 p.u., while the one at phase c decreases till 0.93 p.u.. Phase-neutral voltages and tap positions are depicted respectively in Figure 4.49 and in Figure 4.50.

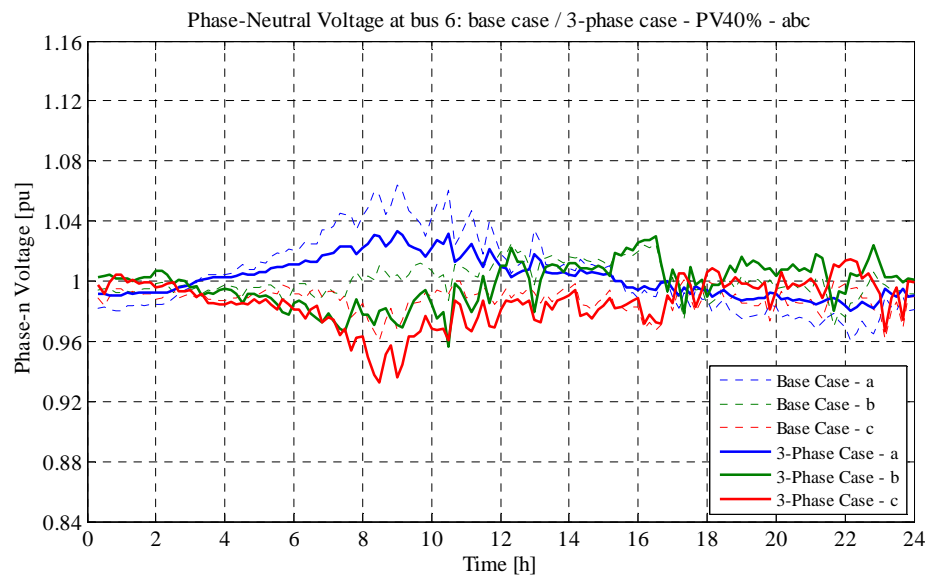


Figure 4.49. Phase-Neutral Voltage at bus 6 – 3-Phase/Base Case comparison in the scenario with 140 kW of PV connected to phase a, b and c

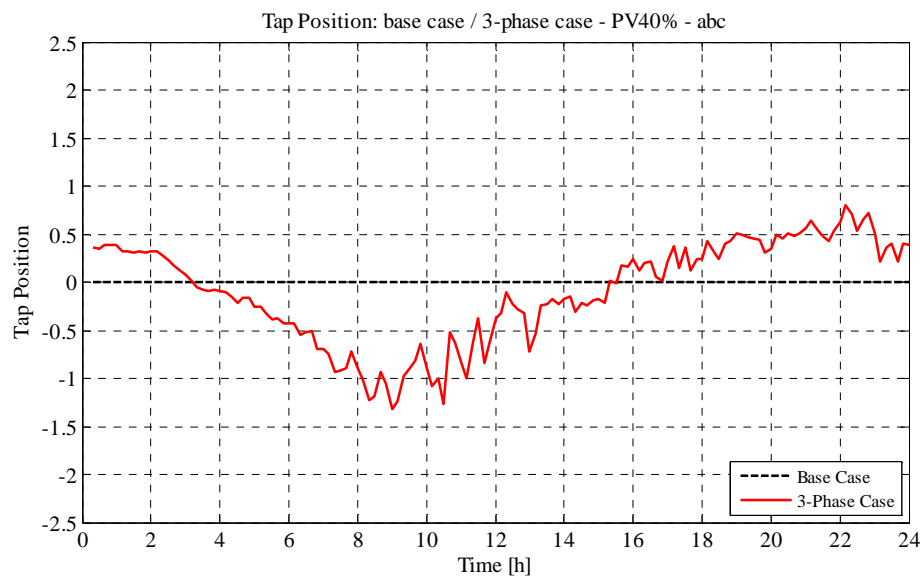


Figure 4.50. Tap Position – 3-Phase/Base Case comparison in the scenario with 140 kW of PV connected to phase a, b and c

On the other hand in the 1-phase case the tap control is based on all the three phases values, so that all the three phase-neutral voltages are closer to 1 p.u.: voltages at phases a and b decrease, while the one at phase c gets higher: till 0.98. Phase-neutral voltages and tap positions are depicted respectively in Figure 4.51 and in Figure 4.52.

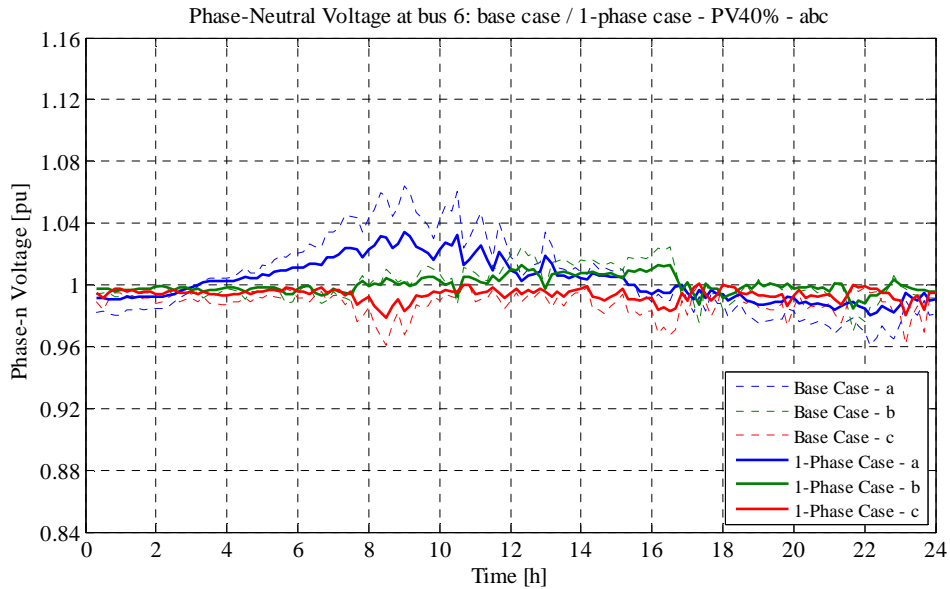


Figure 4.51. Phase-Neutral Voltage at bus 6 – 1-Phase/Base Case comparison in the scenario with 140 kW of PV connected to phase a, b and c

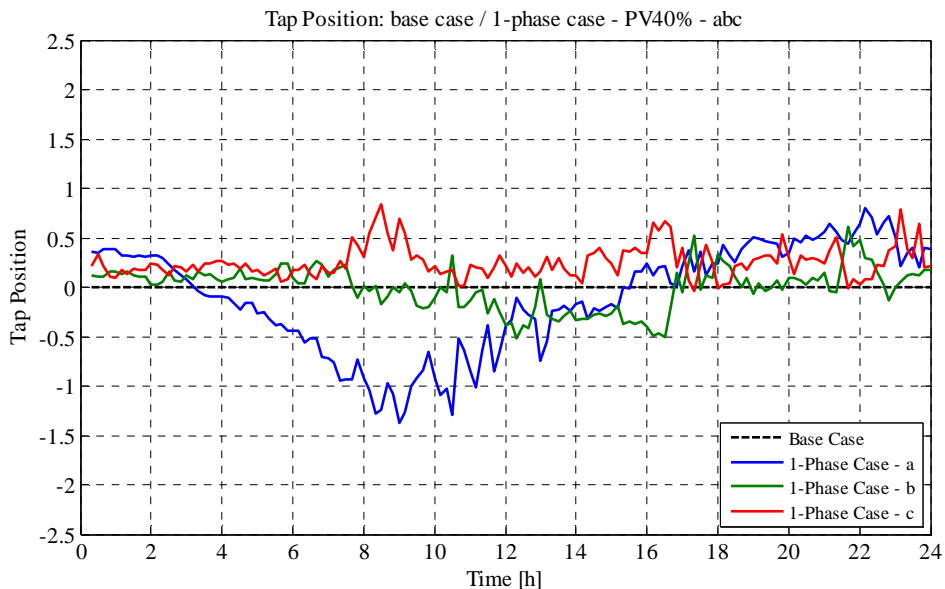


Figure 4.52. Tap Position – 1-Phase/Base Case comparison in the scenario with 140 kW of PV connected to phase a, b and c

As always the phase-ground voltages at the primary side of the transformer do not change in the 3-phase case compared to the base case (Figure 4.53). On the other hand (Figure 4.54), at the LV side they change because of the 3-phase tapping, staying within the range $-4\%/+2\%$.

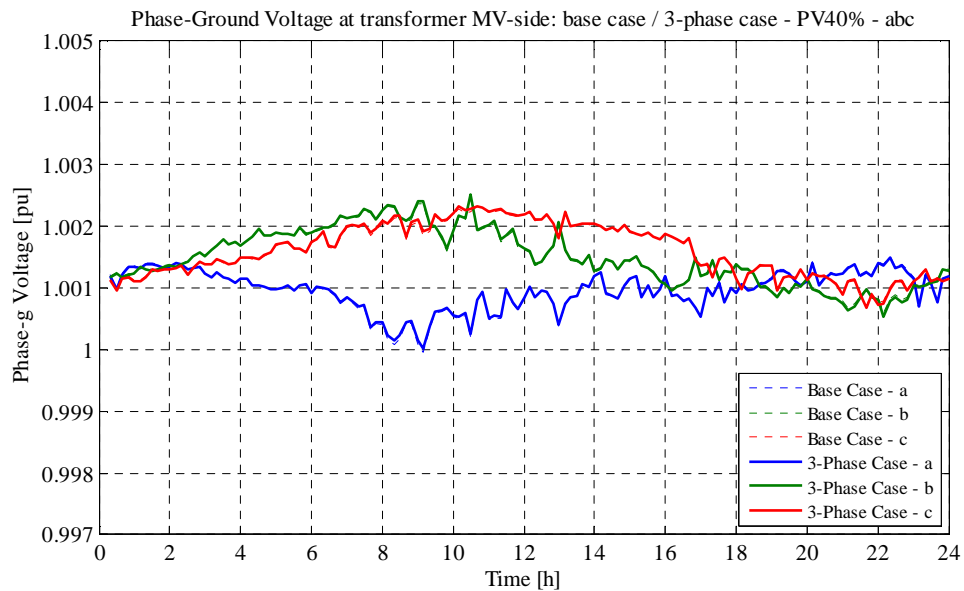


Figure 4.53. Phase-Ground Voltage at transformer MV-side – 3-Phase/Base Case comparison in the scenario with 140 kW of PV connected to phase a, b and c

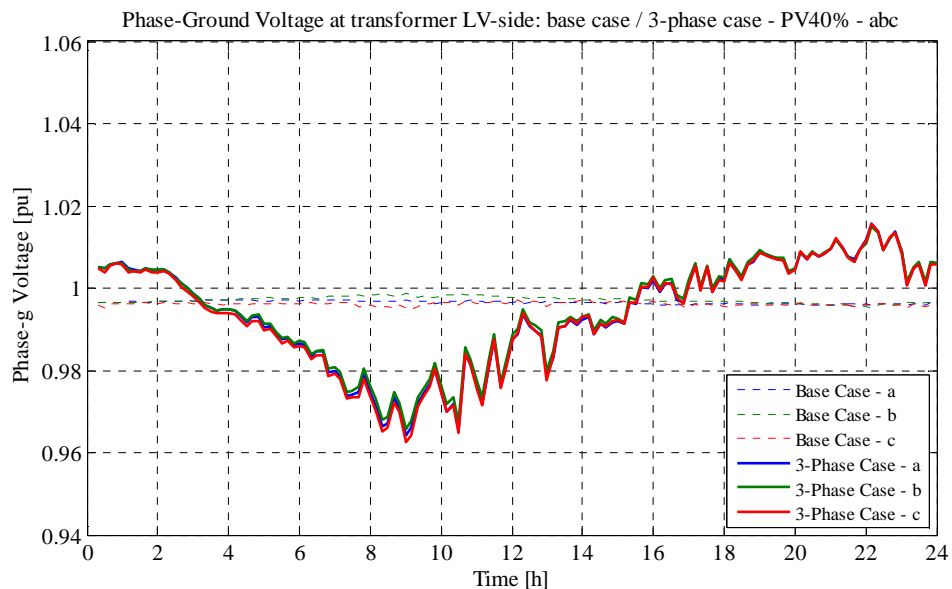


Figure 4.54. Phase-Ground Voltage at transformer LV-side – 3-Phase/Base Case comparison in the scenario with 140 kW of PV connected to phase a, b and c

As always, the same situation is valid at the MV-side in the 1-phase case, as it can be seen in Figure 4.55. At the LV side they change independently because of the 1-phase tapping, staying within the range -4%/+2% (Figure 4.56).

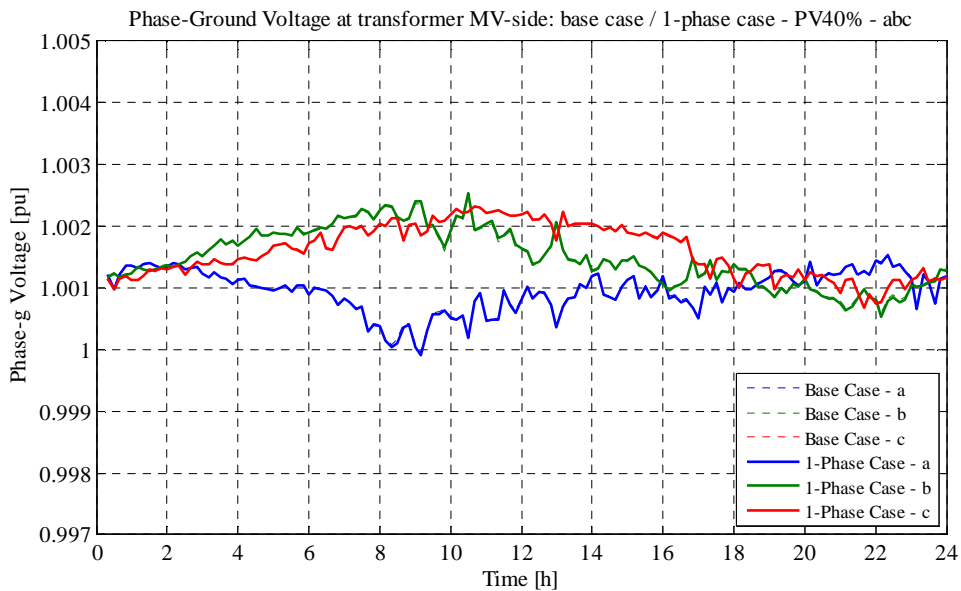


Figure 4.55. Phase-Ground Voltage at transformer MV-side – 1-Phase/Base Case comparison in the scenario with 140 kW of PV connected to phase a, b and c

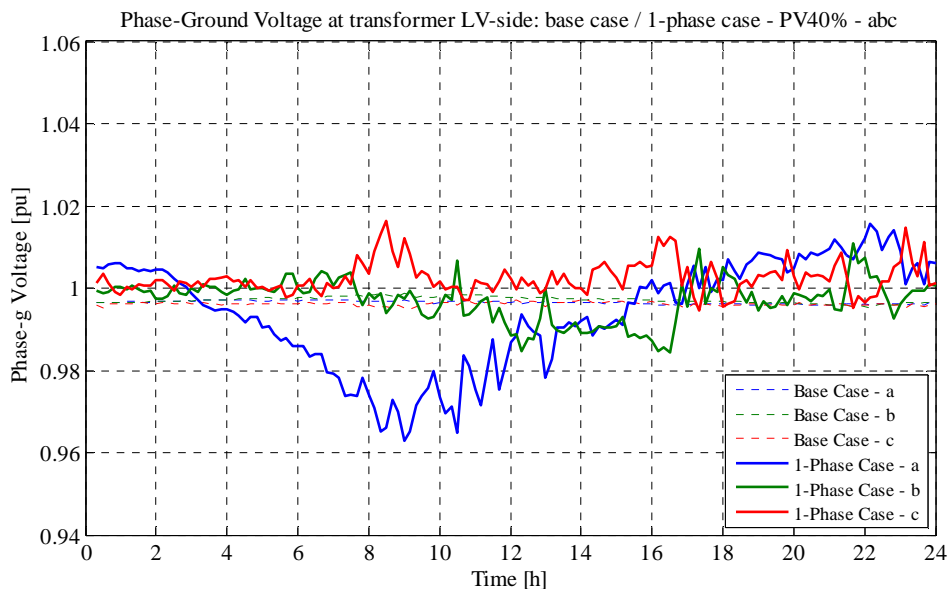


Figure 4.56. Phase-Ground Voltage at transformer LV-side – 1-Phase/Base Case comparison in the scenario with 140 kW of PV connected to phase a, b and c

As shown in Figure 4.57, the neutral-ground voltage at bus 6 does not change after tapping, so its peaks stay below 2.5%.

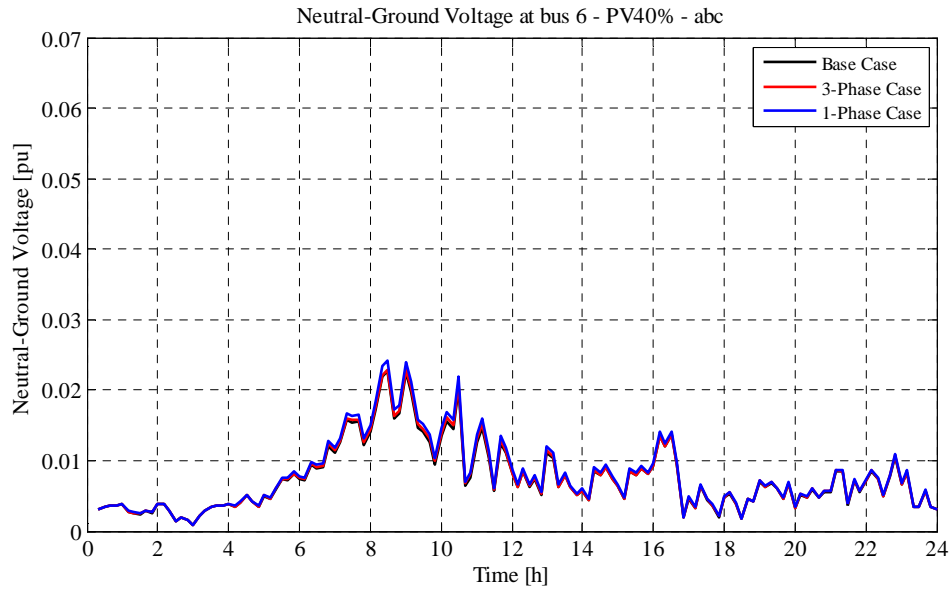


Figure 4.57. Neutral-Ground Voltage at bus 6 – 3-Phase/1-Phase/Base Case comparison in the scenario with 140 kW of PV connected to phase a, b and c

The VUF at bus 6 (Figure 4.58) does not increase in the two tapping cases: its peaks stay below 1.25%.

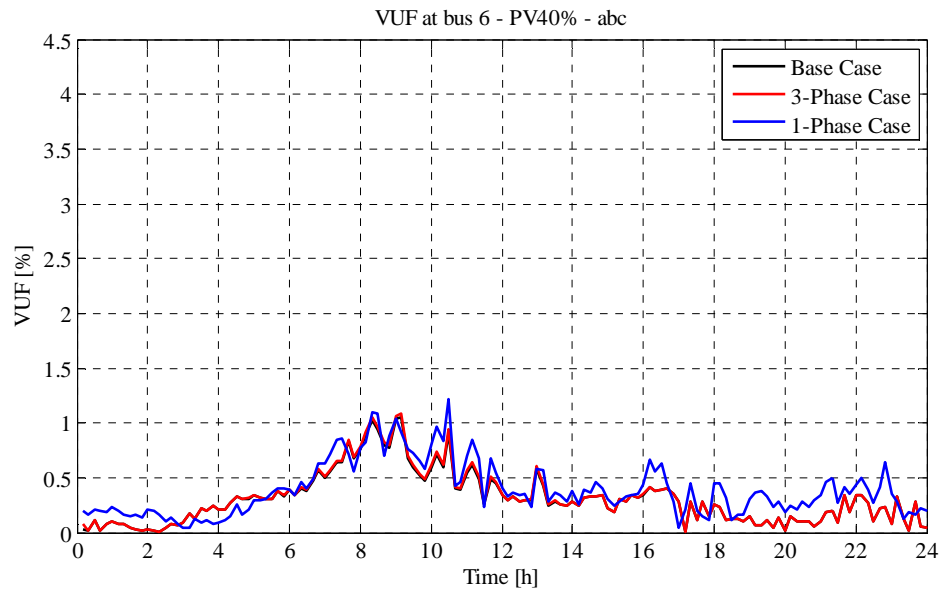


Figure 4.58. VUF at bus 6 – 3-Phase/1-Phase/Base Case comparison in the scenario with 140 kW of PV connected to phase a, b and c

As it can be seen in Figure 4.59 and Figure 4.60, the total power losses of lines and the total power loss ratio as well do not present a so relevant increase after tapping in both the cases.

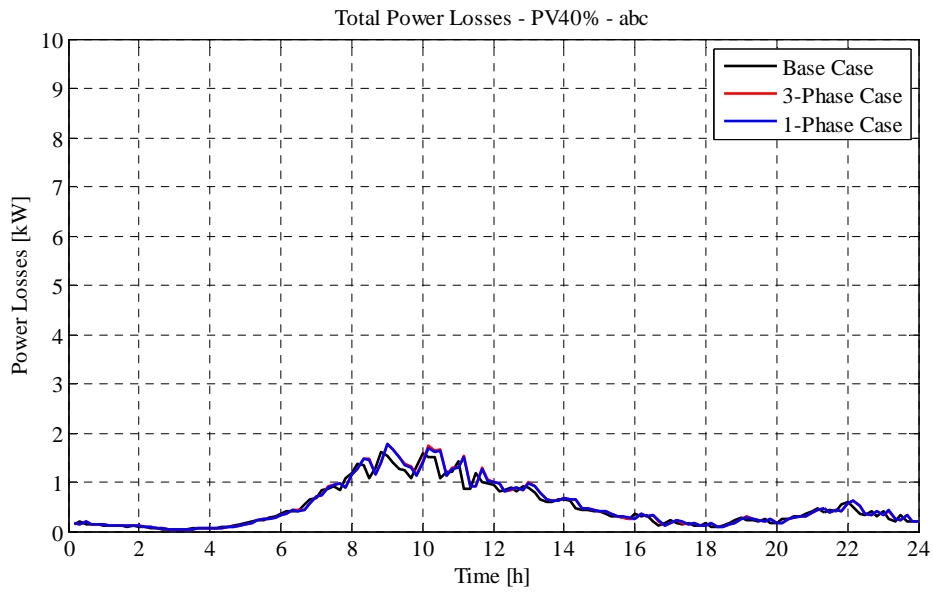


Figure 4.59. Total Power Losses – 3-Phase/1-Phase/Base Case comparison in the scenario with 140 kW of PV connected to phase a, b and c

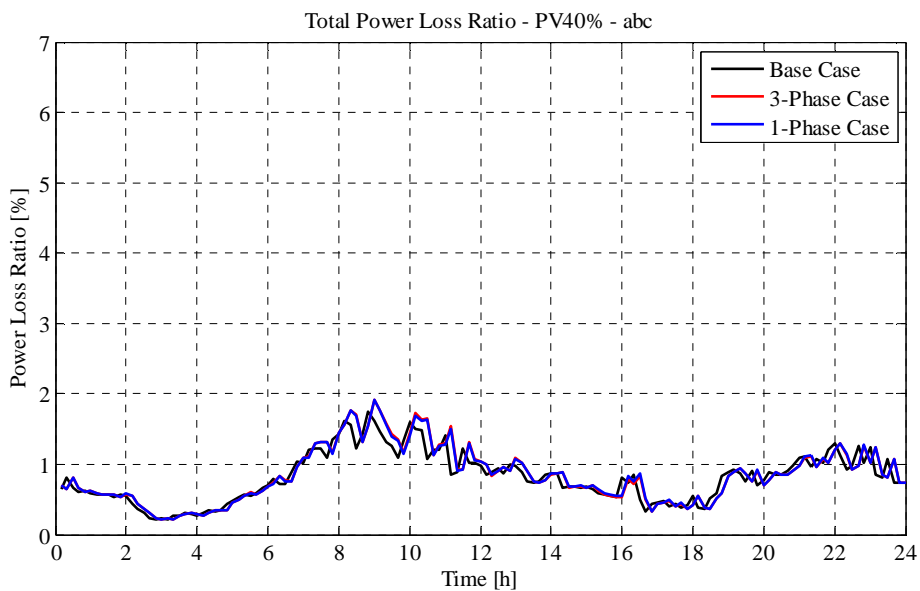


Figure 4.60. Total Power Loss Ratio – 3-Phase/1-Phase/Base Case comparison in the scenario with 140 kW of PV connected to phase a, b and c

In Table 4.5 the total energy amounts absorbed by loads, injected by PVs and the amount through the transformer are reported together with the absolute energy loss, the energy loss ratio and the energy deviations from the base case.

| Case | Total Energy absorbed by loads [kWh] | Total Energy injected by PV [kWh] | Energy through the trafo [kWh] | Energy Loss [kWh] | Energy Loss Ratio [%] | Energy Loss Deviation [%, compared to base case] |
|-----------|--------------------------------------|-----------------------------------|--------------------------------|-------------------|-----------------------|--|
| Base Case | 759.78 | 981.99 | -210.60 | 11.61 | 1.18% | +0.00% |
| 3-Phase | 760.07 | 981.97 | -209.68 | 12.22 | 1.24% | +5.29% |
| 1-Phase | 764.90 | 981.84 | -204.78 | 12.16 | 1.24% | +4.77% |

Table 4.5. PV40% abc scenario – energy analysis

4.1.6. PV50% – 175 kW – phases a, b and c

Out of the three phase-neutral voltages at the worst bus (bus 6) from base case to the 3-phase case only the voltage at phase a gets closer to 1 p.u., since the tap control is based on phase a measurement. Its peak decreases from 1.11 to 1.06 p.u., while the one at phase c decreases till 0.895 p.u.. Phase-neutral voltages and tap positions are depicted respectively in Figure 4.61 and in Figure 4.62.

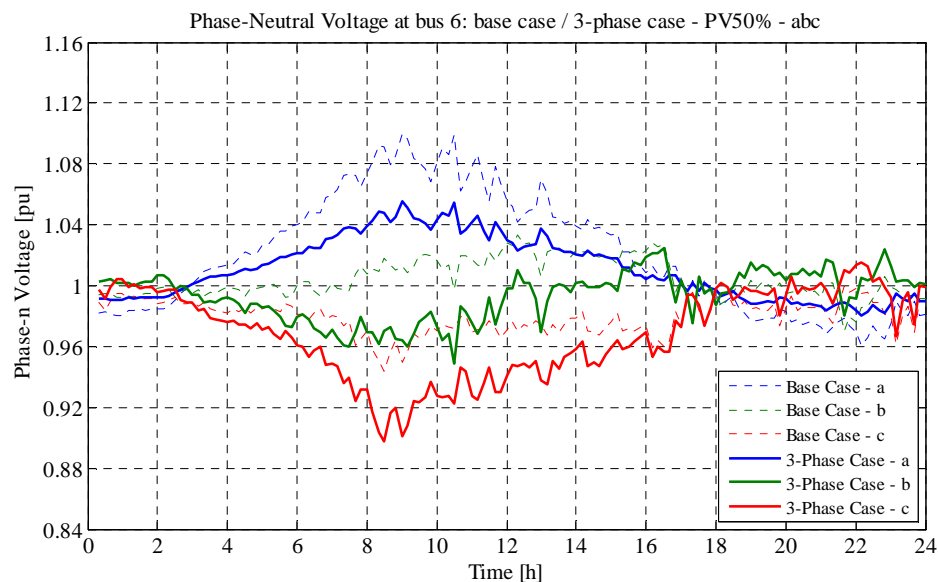


Figure 4.61. Phase-Neutral Voltage at bus 6 – 3-Phase/Base Case comparison in the scenario with 175 kW of PV connected to phase a, b and c

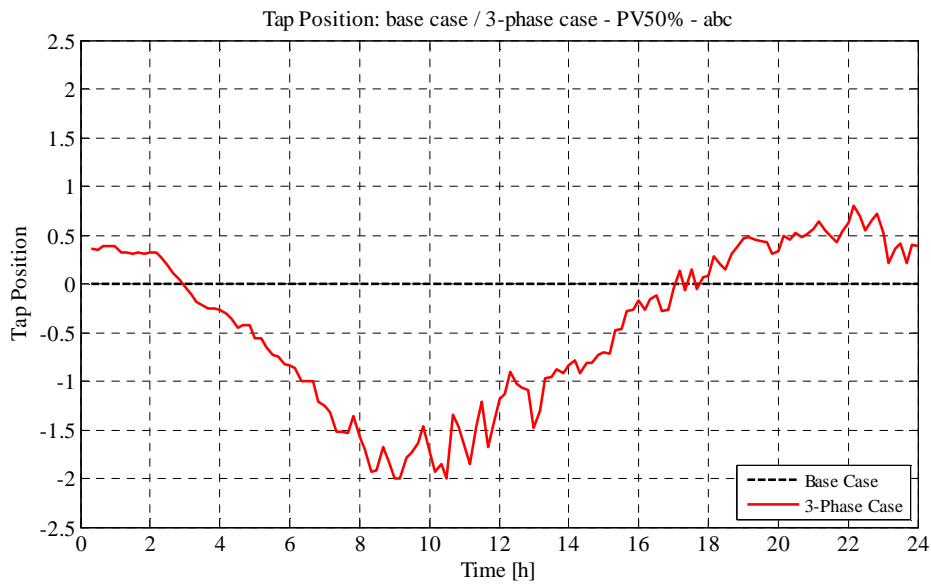


Figure 4.62. Tap Position – 3-Phase/Base Case comparison in the scenario with 175 kW of PV connected to phase a, b and c

On the other hand in the 1-phase case the tap control is based on all the three phases values, so that all the three phase-neutral voltages are closer to 1 p.u.: voltages at phases a and b decrease, while the one at phase c gets higher: till 0.97. Phase-neutral voltages and tap positions are depicted respectively in Figure 4.63 and in Figure 4.64.

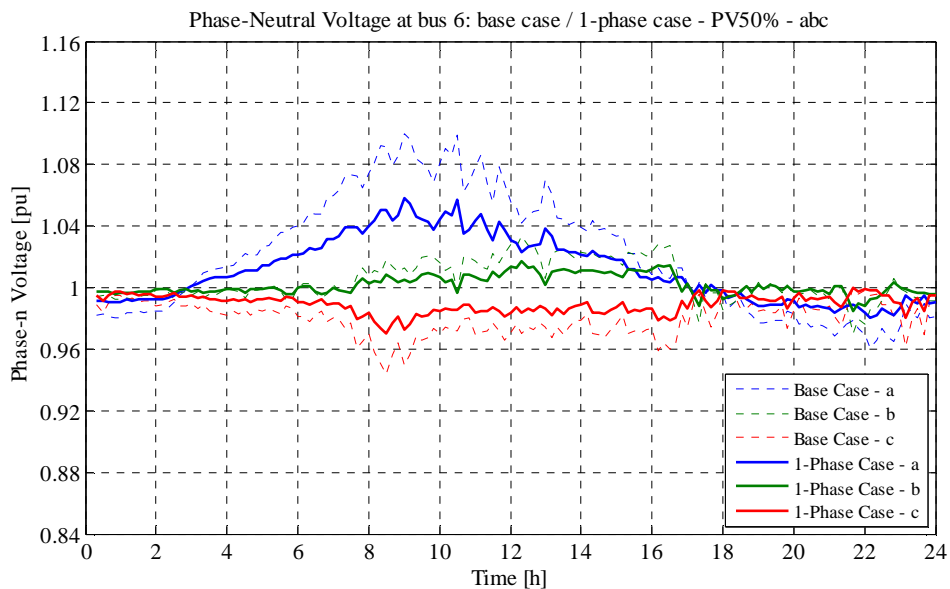


Figure 4.63. Phase-Neutral Voltage at bus 6 – 1-Phase/Base Case comparison in the scenario with 175 kW of PV connected to phase a, b and c

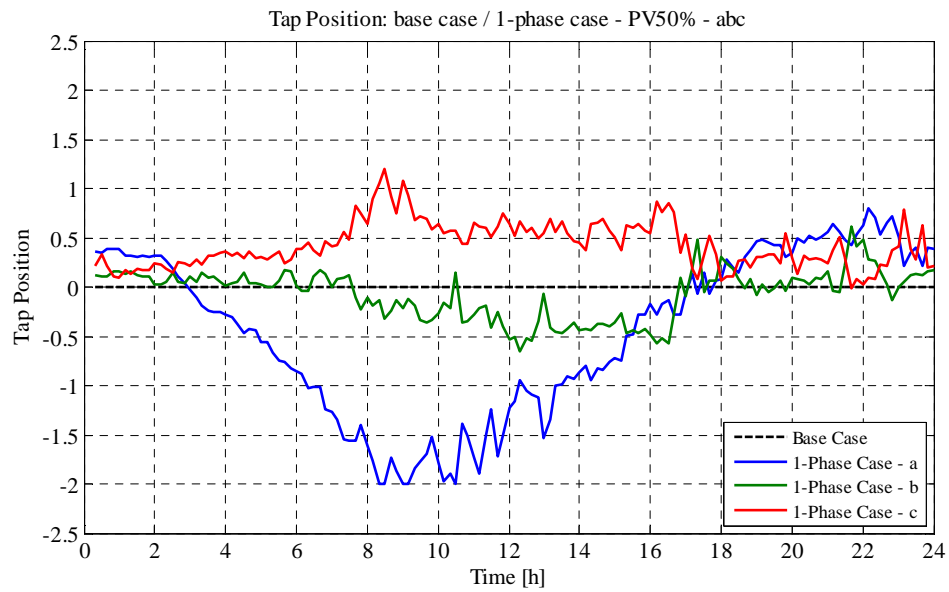


Figure 4.64. Tap Position – 1-Phase/Base Case comparison in the scenario with 175 kW of PV connected to phase a, b and c

As always, the phase-ground voltages at the MV side of the transformer do not change in the 3-phase case compared to the base case (Figure 4.65). On the other hand (Figure 4.66), at the LV side they change because of the 3-phase tapping, staying within the range $-5\%/+2\%$.

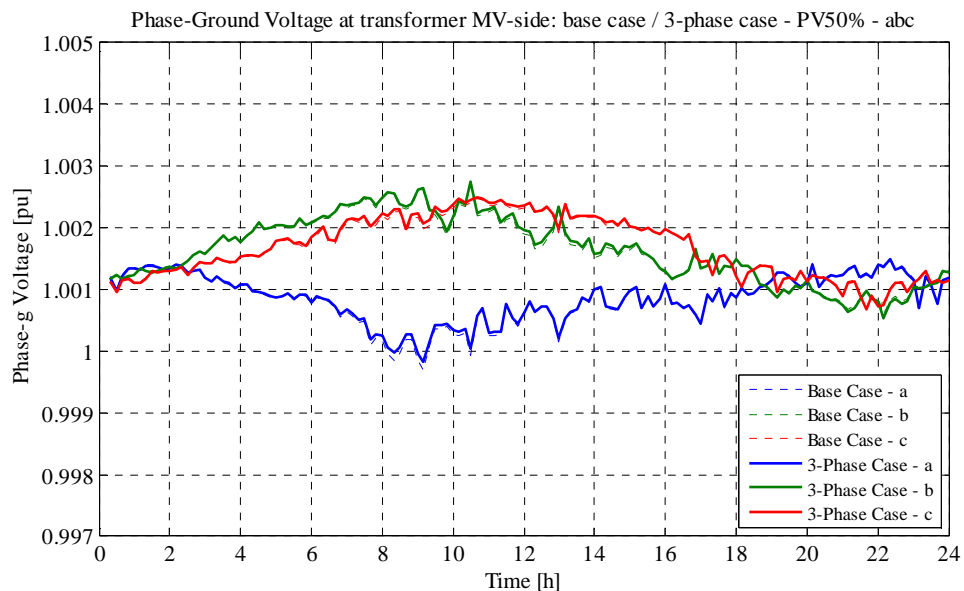


Figure 4.65. Phase-Ground Voltage at transformer MV-side – 3-Phase/Base Case comparison in the scenario with 175 kW of PV connected to phase a, b and c

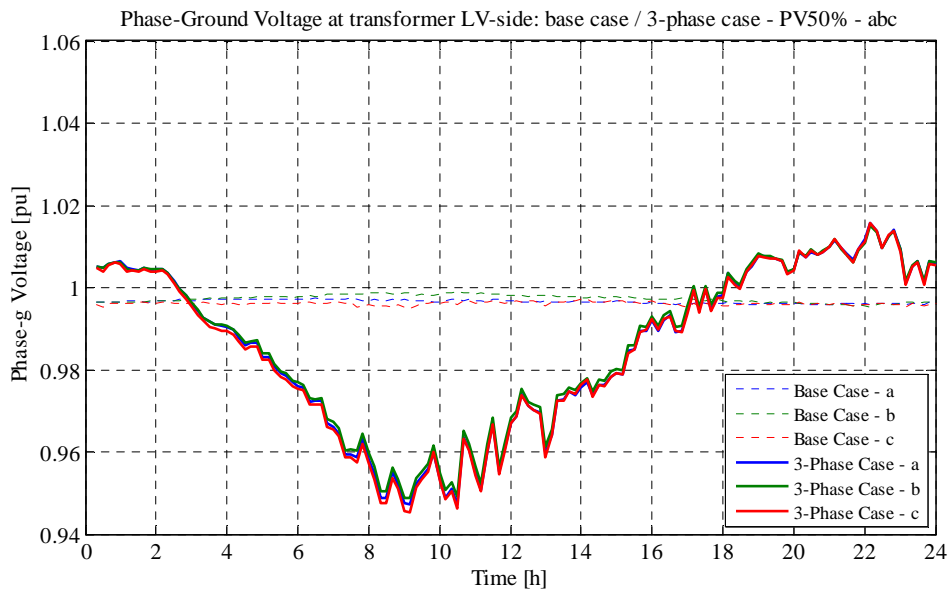


Figure 4.66. Phase-Ground Voltage at transformer LV-side – 3-Phase/Base Case comparison in the scenario with 175 kW of PV connected to phase a, b and c

As always, the same situation is valid at the MV-side in the 1-phase case, as it can be seen in Figure 4.67. At the LV side they change independently because of the 1-phase tapping, staying within the range -5%/+2.5% (Figure 4.68).

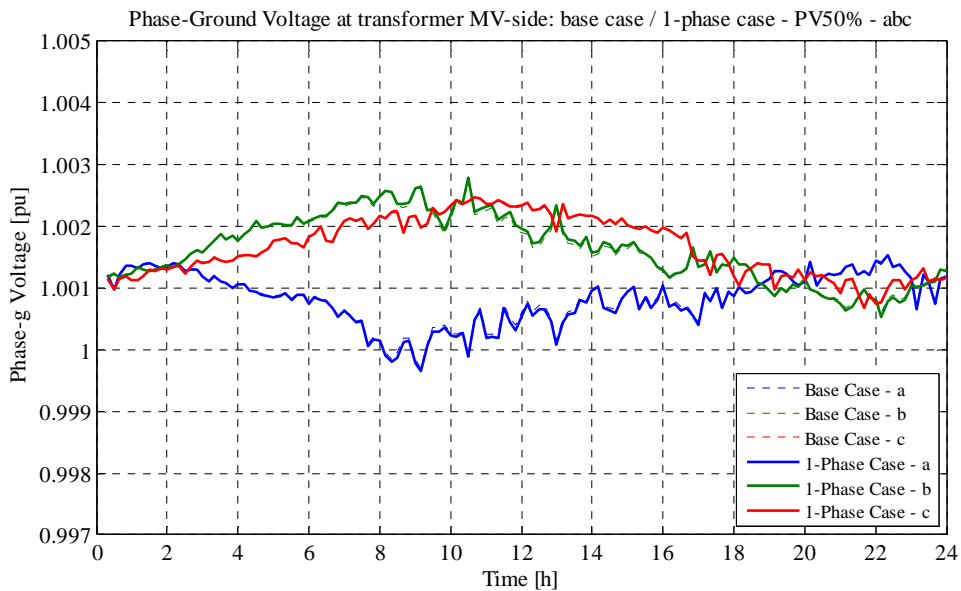


Figure 4.67. Phase-Ground Voltage at transformer MV-side – 1-Phase/Base Case comparison in the scenario with 175 kW of PV connected to phase a, b and c

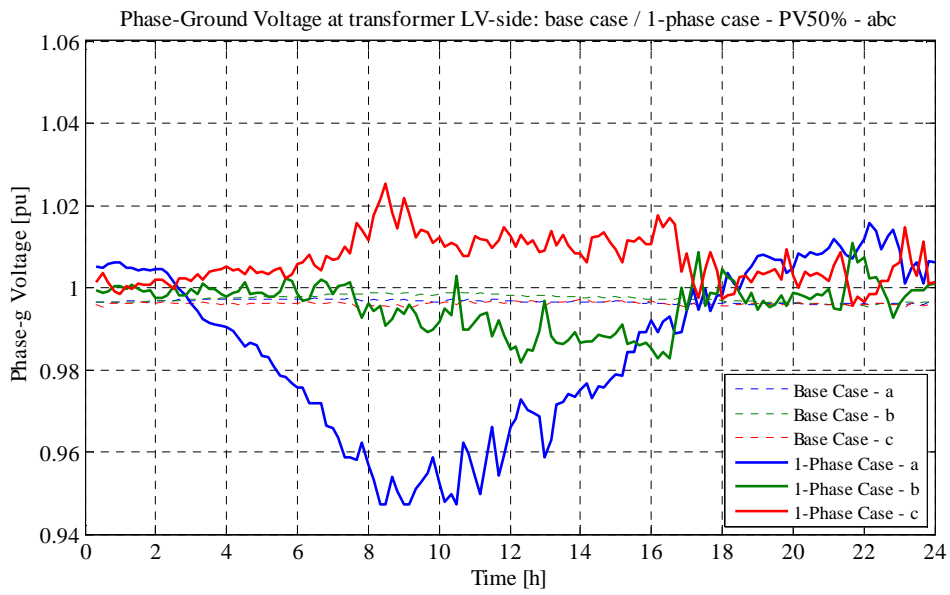


Figure 4.68. Phase-Ground Voltage at transformer LV-side – 1-Phase/Base Case comparison in the scenario with 175 kW of PV connected to phase a, b and c

As shown in Figure 4.69, the neutral-ground voltage at bus 6 does not change after tapping, so its peaks stay below 4%.

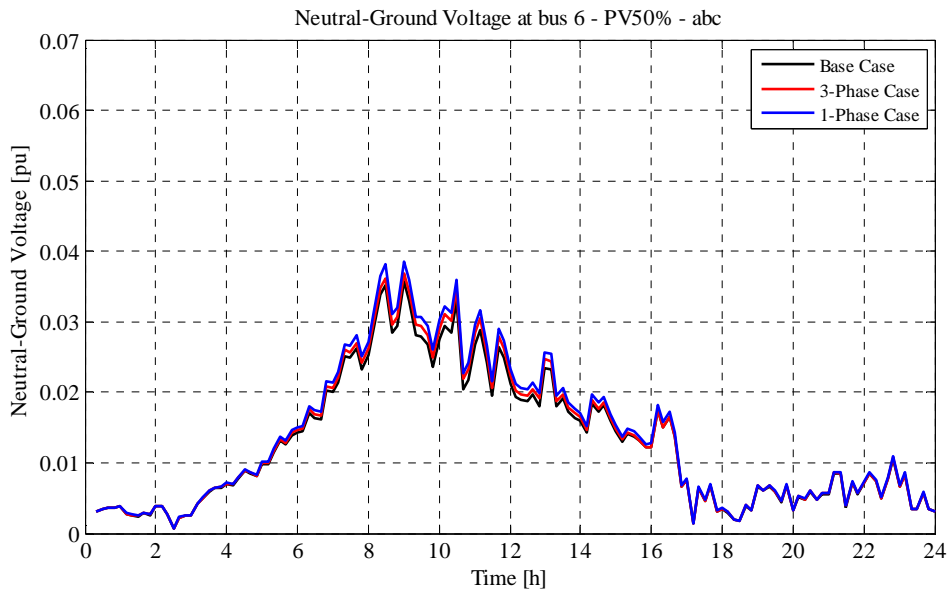


Figure 4.69. Neutral-Ground Voltage at bus 6 – 3-Phase/1-Phase/Base Case comparison in the scenario with 175 kW of PV connected to phase a, b and c

The VUF at bus 6 (Figure 4.70) does not increase in the 3-phase case, while it grows in the 1-phase case: peaks grows from 1.4 % till 1.8%.

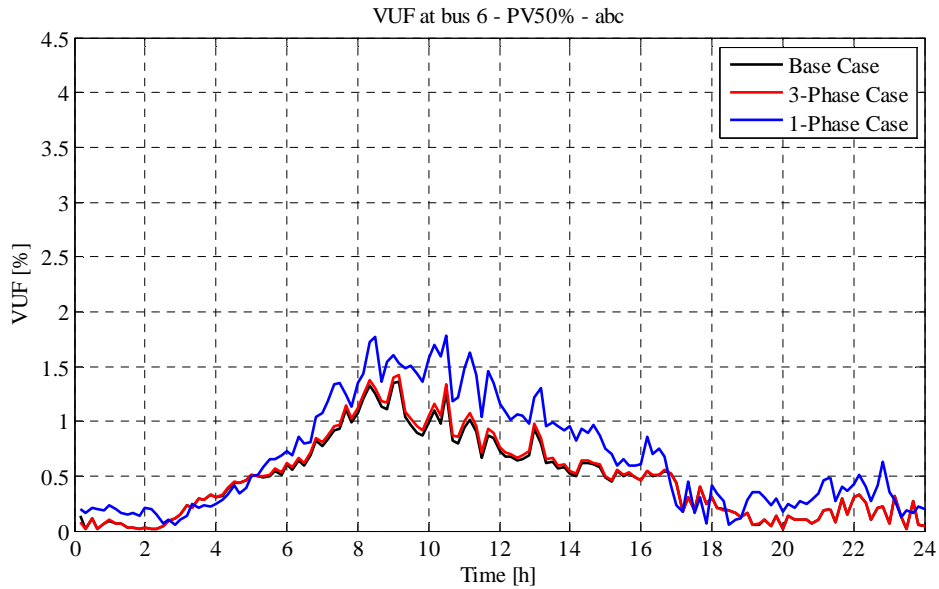


Figure 4.70. VUF at bus 6 – 3-Phase/1-Phase/Base Case comparison in the scenario with 175 kW of PV connected to phase a, b and c

As it can be seen in Figure 4.71 and Figure 4.72, the total power losses of lines and the total power loss ratio as well do present a small increase after tapping in both the cases.

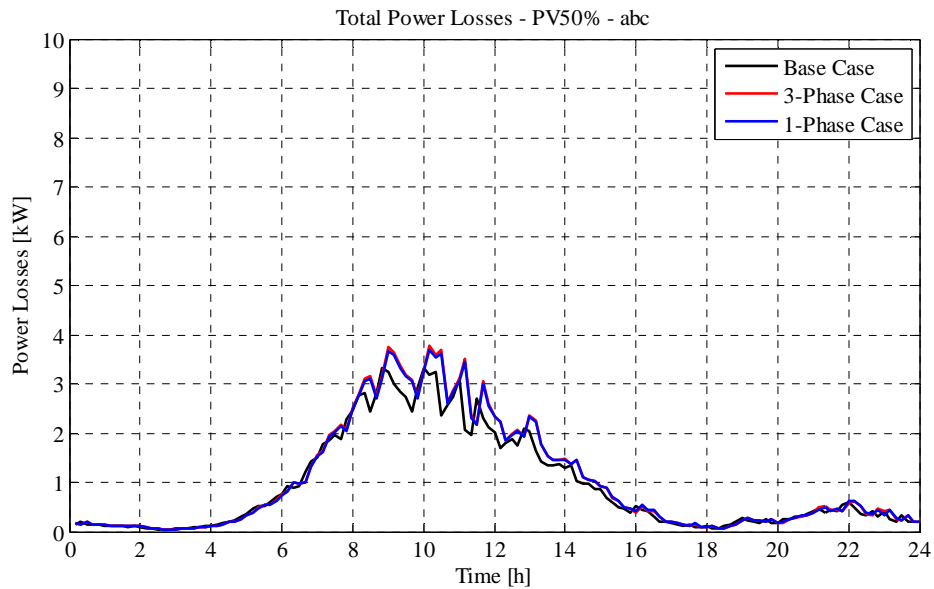


Figure 4.71. Total Power Losses – 3-Phase/1-Phase/Base Case comparison in the scenario with 175 kW of PV connected to phase a, b and c

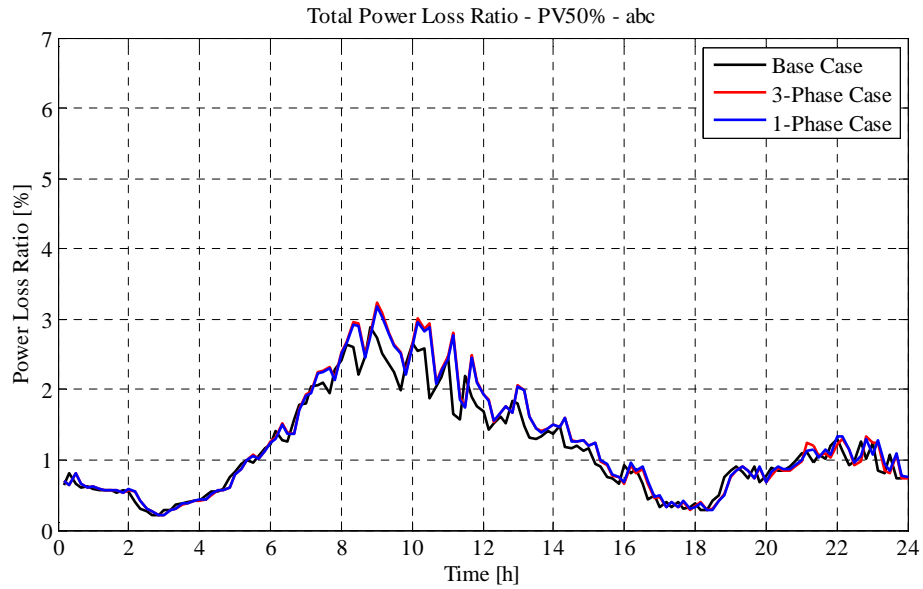


Figure 4.72. Total Power Loss Ratio – 3-Phase/1-Phase/Base Case comparison in the scenario with 175 kW of PV connected to phase a, b and c

In Table 4.6 the total energy amounts absorbed by loads, injected by PVs and the amount through the transformer are reported together with the absolute energy loss, the energy loss ratio and the energy deviations from the base case.

| Case | Total Energy absorbed by loads [kWh] | Total Energy injected by PV [kWh] | Energy through the trafo [kWh] | Energy Loss [kWh] | Energy Loss Ratio [%] | Energy Loss Deviation [%, compared to base case] |
|-----------|--------------------------------------|-----------------------------------|--------------------------------|-------------------|-----------------------|--|
| Base Case | 766.62 | 1224.70 | -436.63 | 21.45 | 1.75% | +0.00% |
| 3-Phase | 752.51 | 1224.48 | -448.38 | 23.59 | 1.93% | +9.98% |
| 1-Phase | 765.86 | 1224.08 | -434.89 | 23.33 | 1.91% | +8.76% |

Table 4.6. PV50% abc scenario – energy analysis

4.1.7. PV60% – 210 kW – phases a, b and c

Out of the three phase-neutral voltages at the worst bus (bus 6) from base case to the 3-phase case only the voltage at phase a gets closer to 1 p.u., since the tap control is based on phase a measurement. Its peak decreases from 1.11 to 1.06 p.u., while the one at phase c decreases till 0.89 p.u.. Phase-neutral voltages and tap positions are depicted respectively in Figure 4.73 and in Figure 4.74.

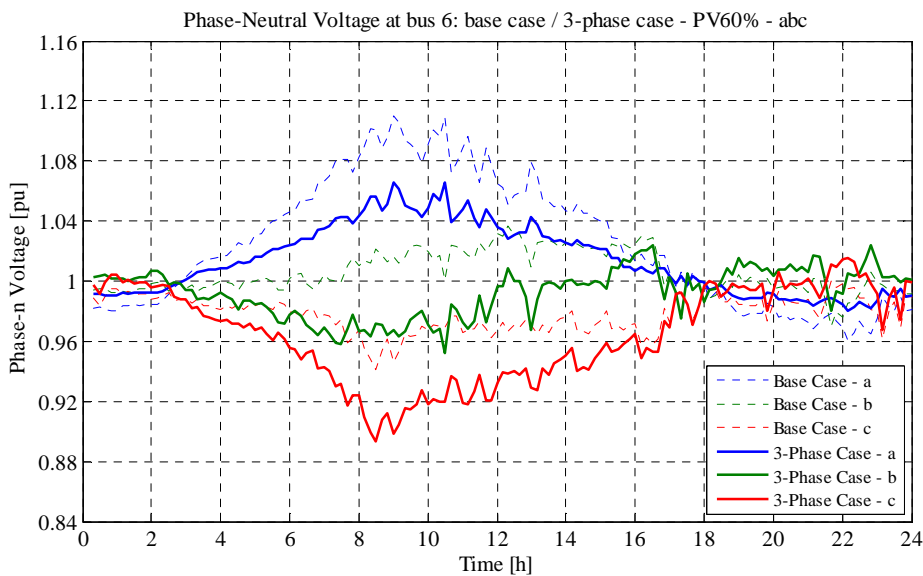


Figure 4.73. Phase-Neutral Voltage at bus 6 – 3-Phase/Base Case comparison in the scenario with 210 kW of PV connected to phase a, b and c

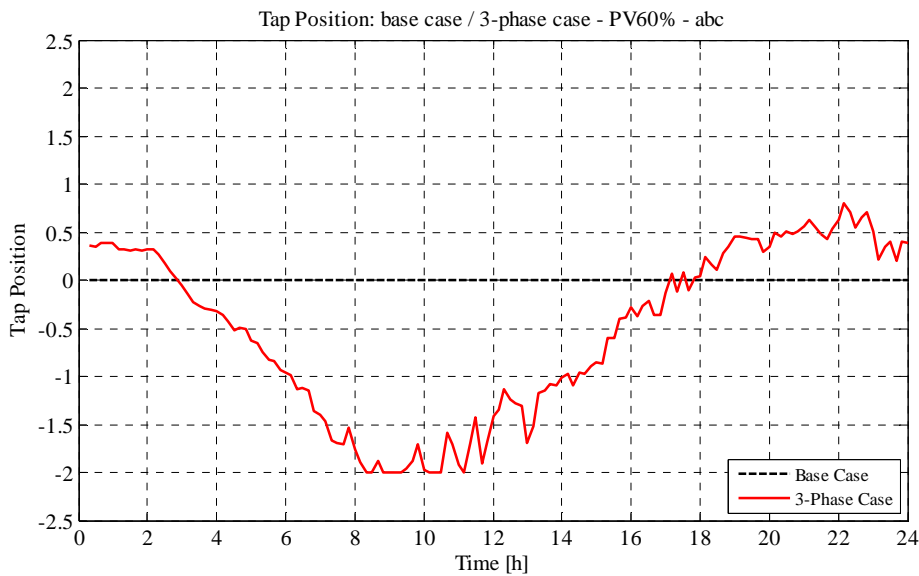


Figure 4.74. Tap Position – 3-Phase/Base Case comparison in the scenario with 210 kW of PV connected to phase a, b and c

On the other hand in the 1-phase case the tap control is based on all the three phases values, so that all the three phase-neutral voltages are closer to 1 p.u.: voltages at phases a and b decrease, while the one at phase c gets higher: till 0.97. Phase-neutral voltages and tap positions are depicted respectively in Figure 4.75 and in Figure 4.76.

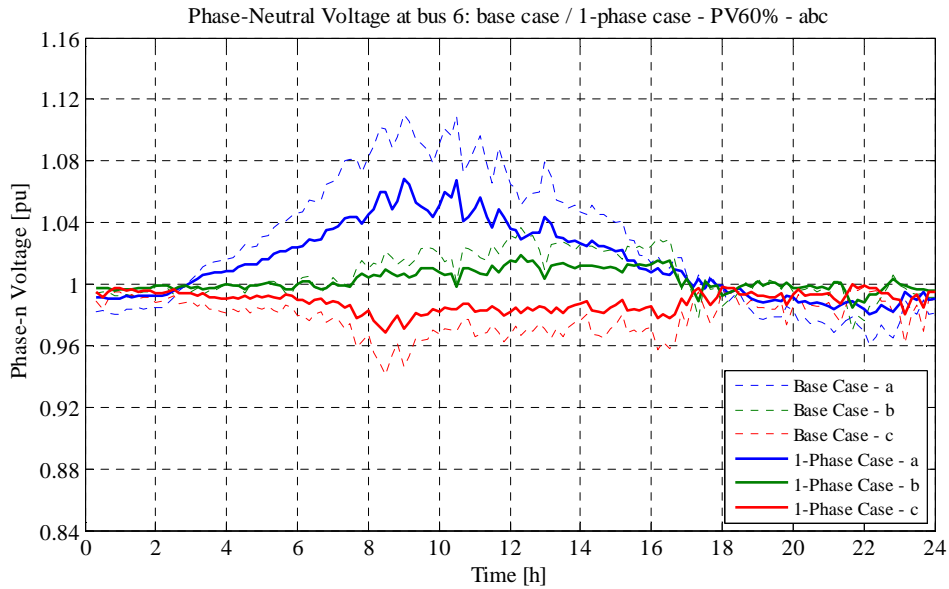


Figure 4.75. Phase-Neutral Voltage at bus 6 – 1-Phase/Base Case comparison in the scenario with 210 kW of PV connected to phase a, b and c

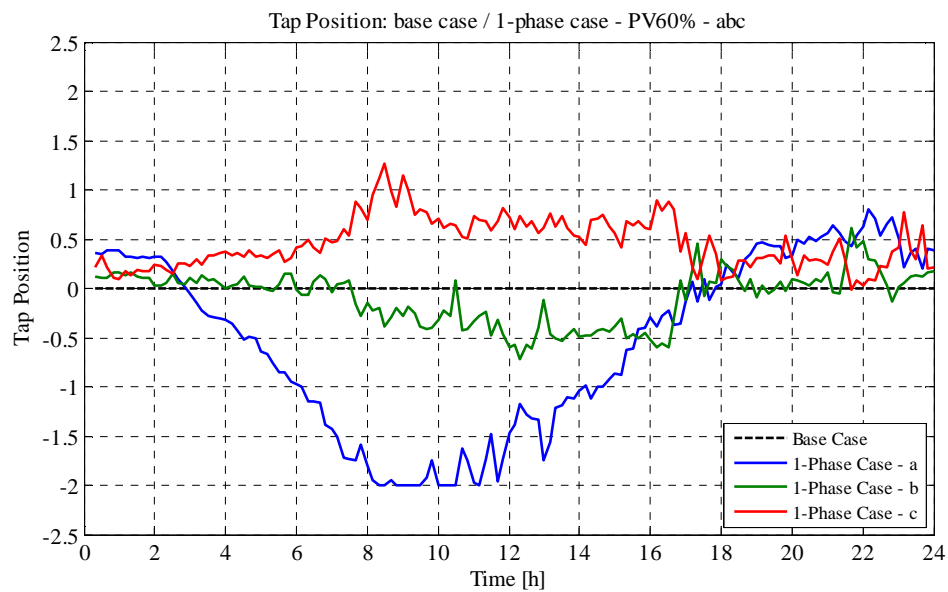


Figure 4.76. Tap Position – 1-Phase/Base Case comparison in the scenario with 210 kW of PV connected to phase a, b and c

As always, the phase-ground voltages at the MV side of the transformer do not change in the 3-phase case compared to the base case (Figure 4.77). On the other hand (Figure 4.78), at the LV side they change because of the 3-phase tapping, staying within the range -5%/+2%.

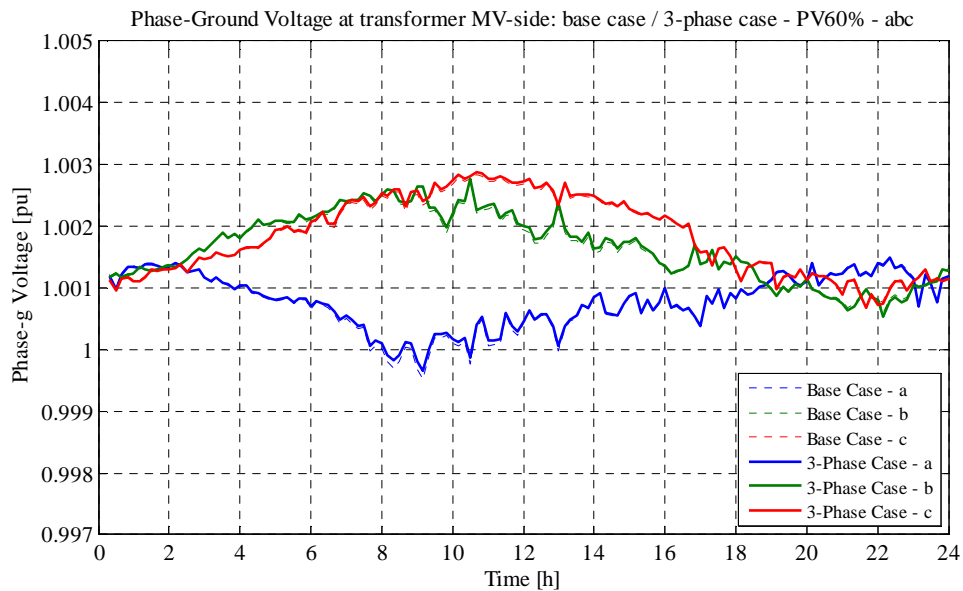


Figure 4.77. Phase-Ground Voltage at transformer MV-side – 3-Phase/Base Case comparison in the scenario with 210 kW of PV connected to phase a, b and c

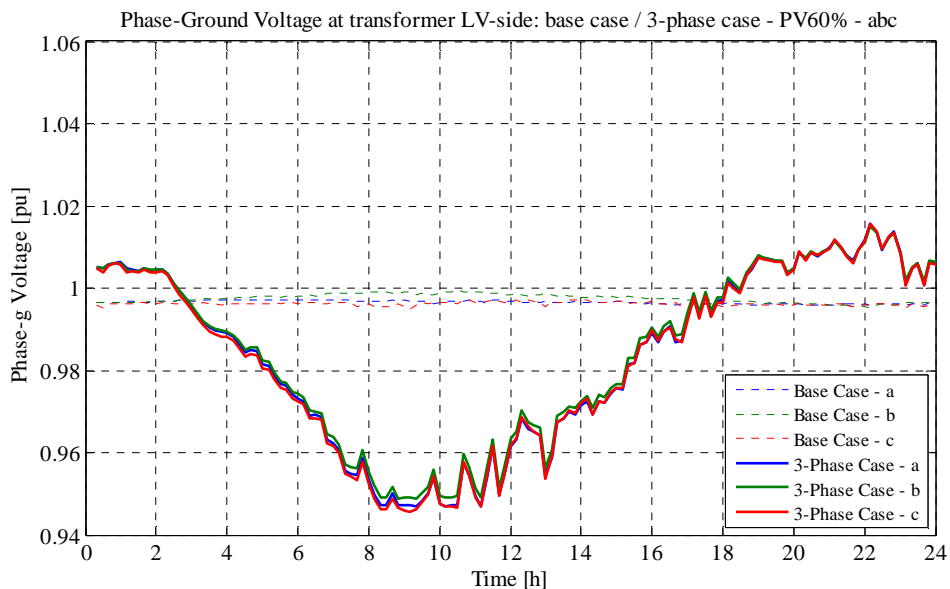


Figure 4.78. Phase-Ground Voltage at transformer LV-side – 3-Phase/Base Case comparison in the scenario with 210 kW of PV connected to phase a, b and c

As always, the same situation is valid at the MV-side in the 1-phase case, as it can be seen in Figure 4.79. At the LV side they change independently because of the 1-phase tapping, staying within the range -5%/+2.8% (Figure 4.80).

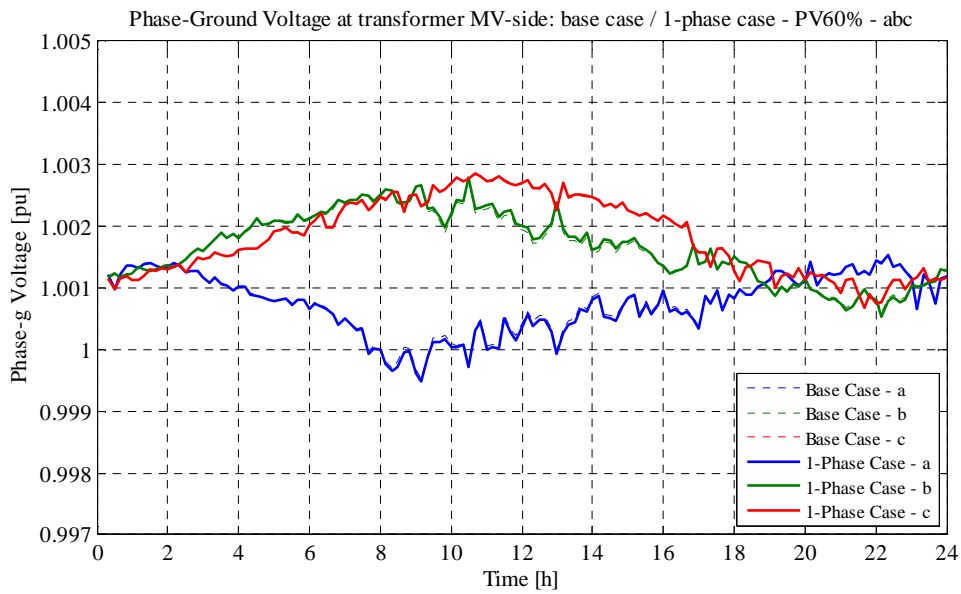


Figure 4.79. Phase-Ground Voltage at transformer MV-side – 1-Phase/Base Case comparison in the scenario with 210 kW of PV connected to phase a, b and c

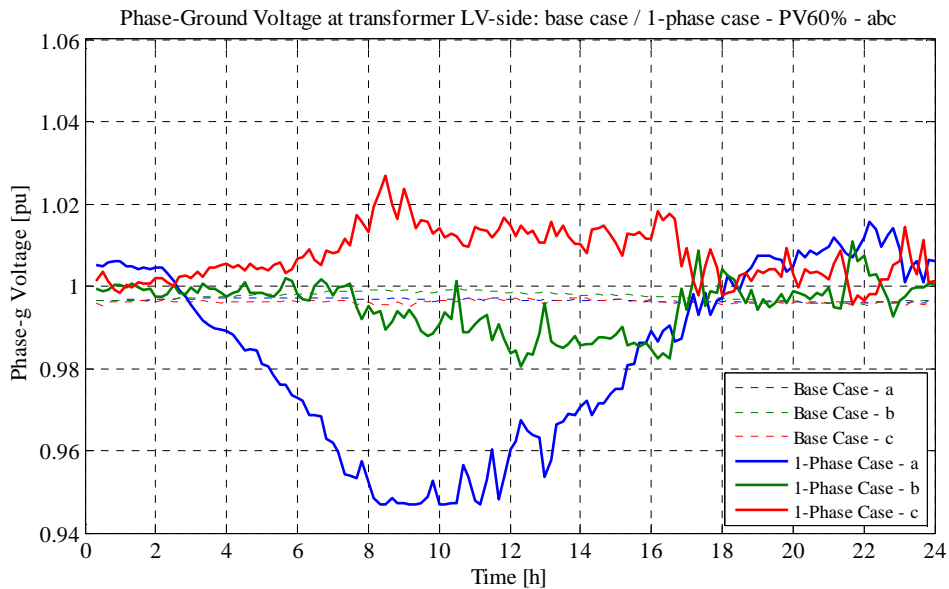


Figure 4.80. Phase-Ground Voltage at transformer LV-side – 1-Phase/Base Case comparison in the scenario with 210 kW of PV connected to phase a, b and c

As shown in Figure 4.81, the neutral-ground voltage at bus 6 does not change after tapping, so its peaks stay below 2.5%.

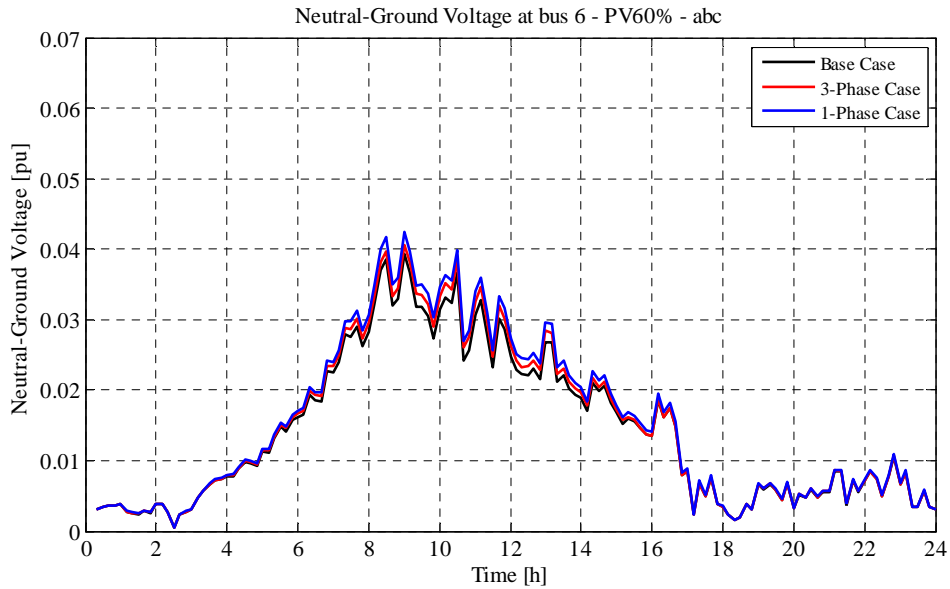


Figure 4.81. Neutral-Ground Voltage at bus 6 – 3-Phase/1-Phase/Base Case comparison in the scenario with 210 kW of PV connected to phase a, b and c

The VUF at bus 6 (Figure 4.82) does not increase in the 3-phase case, while it grows in the 1-phase case: peaks grows from 1.5 % till 1.8%.

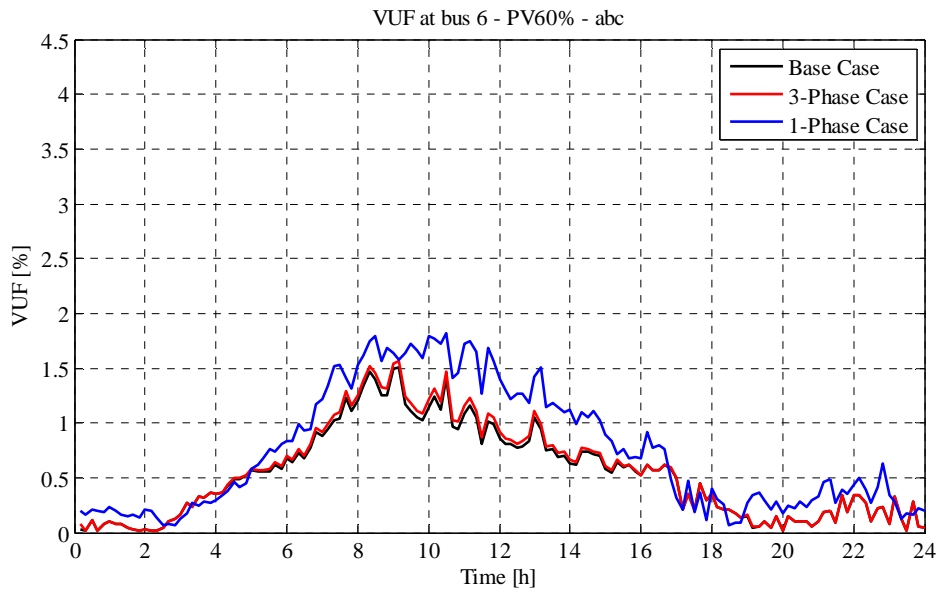


Figure 4.82. VUF at bus 6 – 3-Phase/1-Phase/Base Case comparison in the scenario with 210 kW of PV connected to phase a, b and c

As it can be seen in Figure 4.83 and Figure 4.84, the total power losses of lines and the total power loss ratio as well do present a certain increase after tapping in both the cases.

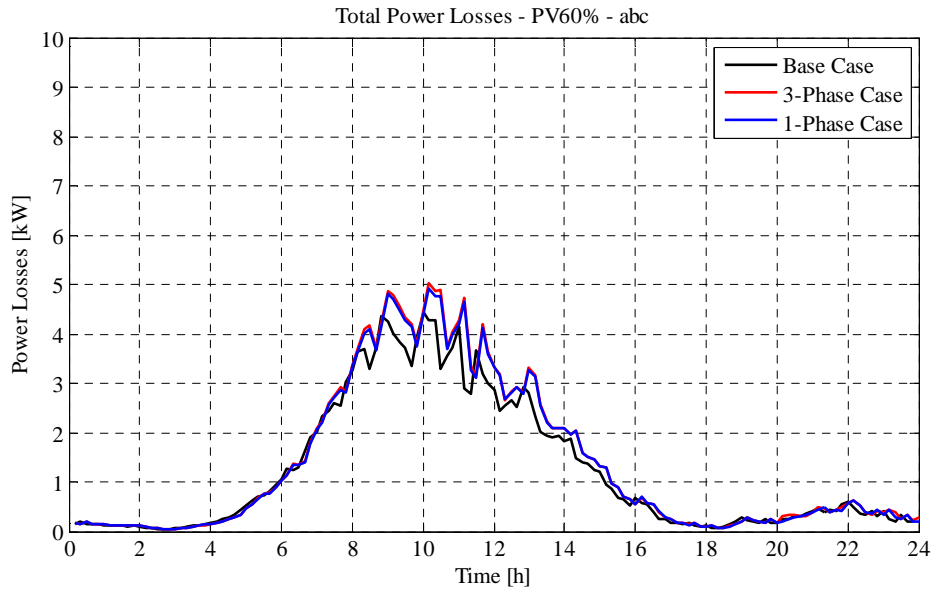


Figure 4.83. Total Power Losses – 3-Phase/1-Phase/Base Case comparison in the scenario with 210 kW of PV connected to phase a, b and c

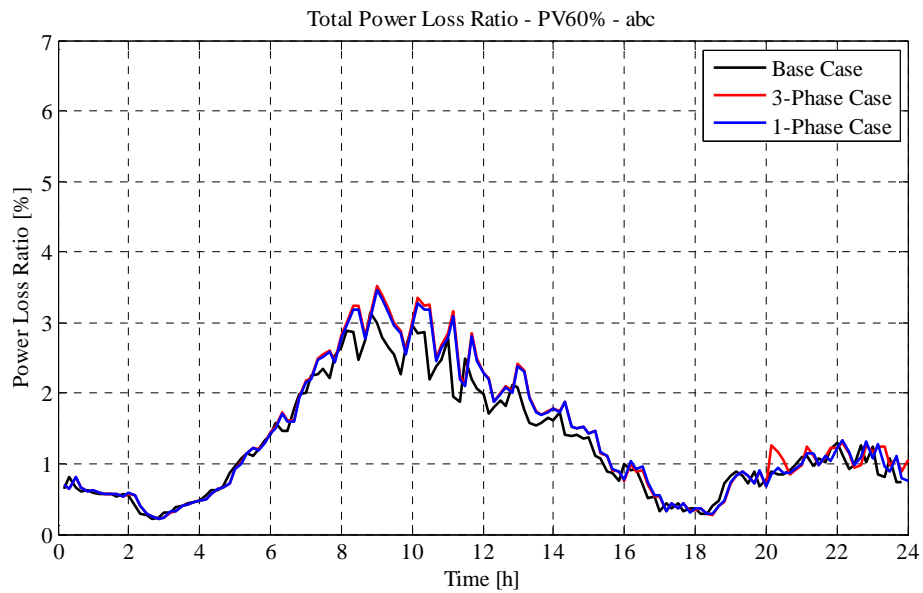


Figure 4.84. Total Power Loss Ratio – 3-Phase/1-Phase/Base Case comparison in the scenario with 210 kW of PV connected to phase a, b and c

In Table 4.7 the total energy amounts absorbed by loads, injected by PVs and the amount through the transformer are reported together with the absolute energy loss, the energy loss ratio and the energy deviations from the base case.

| Case | Total Energy absorbed by loads [kWh] | Total Energy injected by PV [kWh] | Energy through the trafo [kWh] | Energy Loss [kWh] | Energy Loss Ratio [%] | Energy Loss Deviation [%, compared to base case] |
|-----------|--------------------------------------|-----------------------------------|--------------------------------|-------------------|-----------------------|--|
| Base Case | 769.70 | 1468.77 | -670.66 | 28.41 | 1.93% | +0.00% |
| 3-Phase | 751.97 | 1468.50 | -684.89 | 31.64 | 2.15% | +11.37% |
| 1-Phase | 767.24 | 1467.91 | -669.63 | 31.04 | 2.11% | +9.26% |

Table 4.7. PV60% abc scenario – energy analysis

4.1.8. PV70% – 245 kW – phases a, b and c

Out of the three phase-neutral voltages at the worst bus (bus 6) from base case to the 3-phase case only the voltage at phase a gets closer to 1 p.u., since the tap control is based on phase a measurement. Its peak decreases from 1.13 to 1.088 p.u., while the one at phase c decreases till 0.899 p.u.. Phase-neutral voltages and tap positions are depicted respectively in Figure 4.85 and in Figure 4.86.

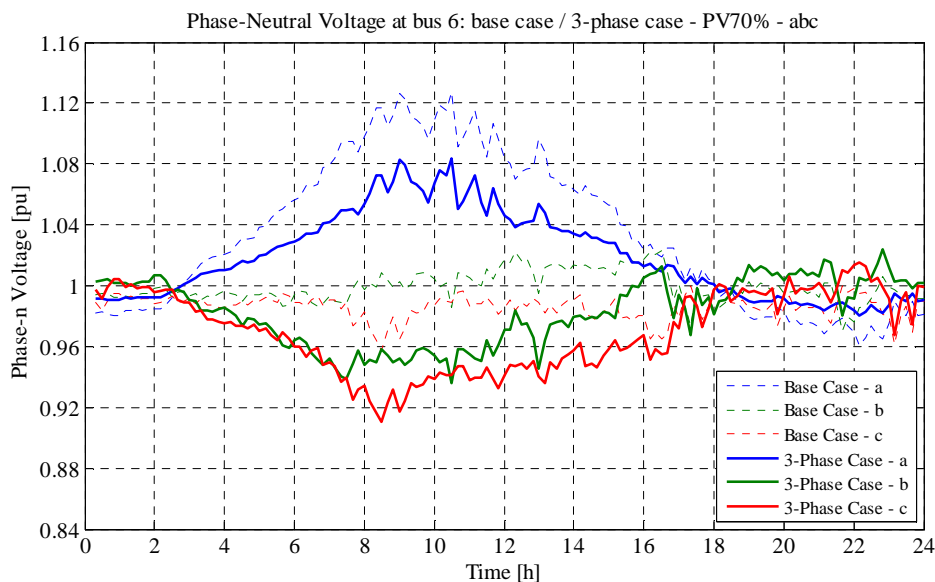


Figure 4.85. Phase-Neutral Voltage at bus 6 – 3-Phase/Base Case comparison in the scenario with 245 kW of PV connected to phase a, b and c

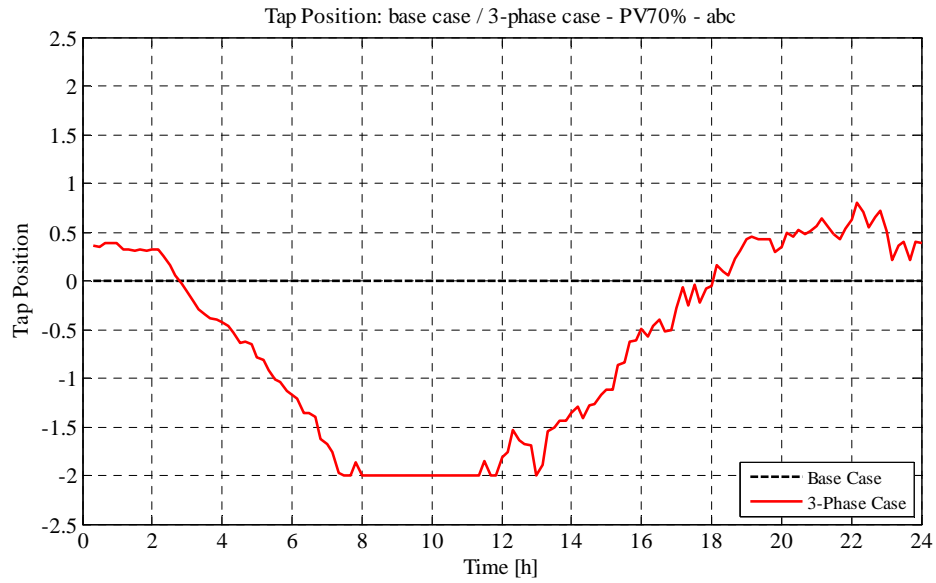


Figure 4.86. Tap Position – 3-Phase/Base Case comparison in the scenario with 245 kW of PV connected to phase a, b and c

On the other hand in the 1-phase case the tap control is based on all the three phases values, so that all the three phase-neutral voltages are closer to 1 p.u.: voltages at phases a and b decrease, while the one at phase c gets higher and within the limit: till 0.98. Phase-neutral voltages and tap positions are depicted respectively in Figure 4.87 and in Figure 4.88.

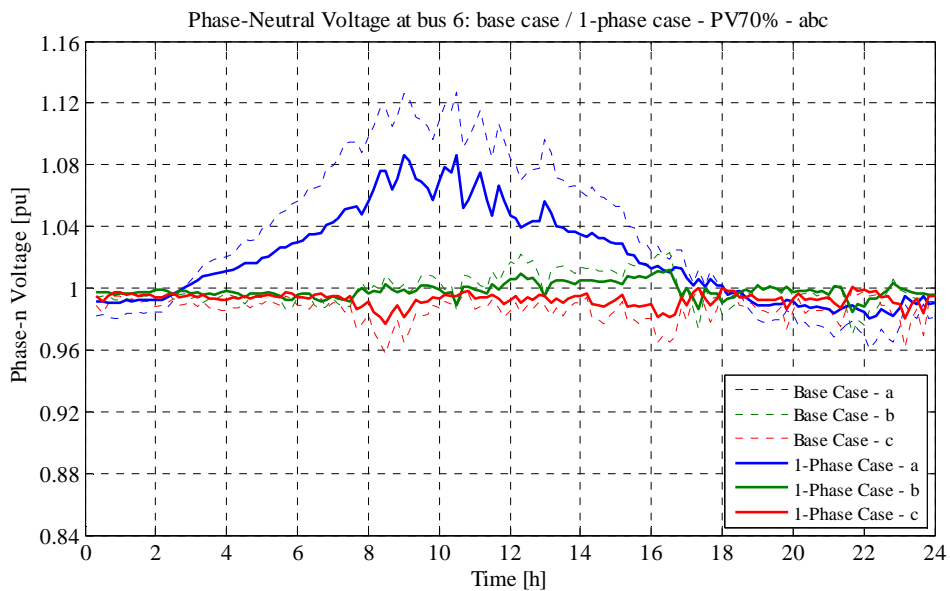


Figure 4.87. Phase-Neutral Voltage at bus 6 – 1-Phase/Base Case comparison in the scenario with 245 kW of PV connected to phase a, b and c

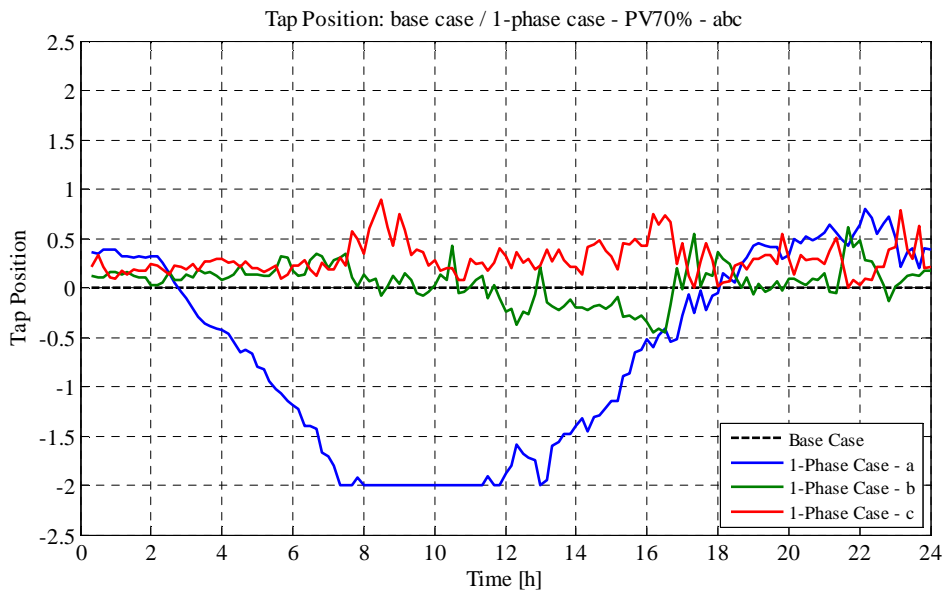


Figure 4.88. Tap Position – 1-Phase/Base Case comparison in the scenario with 245 kW of PV connected to phase a, b and c

As always, the phase-ground voltages at the MV side of the transformer do not change in the 3-phase case compared to the base case (Figure 4.89). On the other hand (Figure 4.90), at the LV side they change because of the 3-phase tapping, staying within the range -5%/+2%.

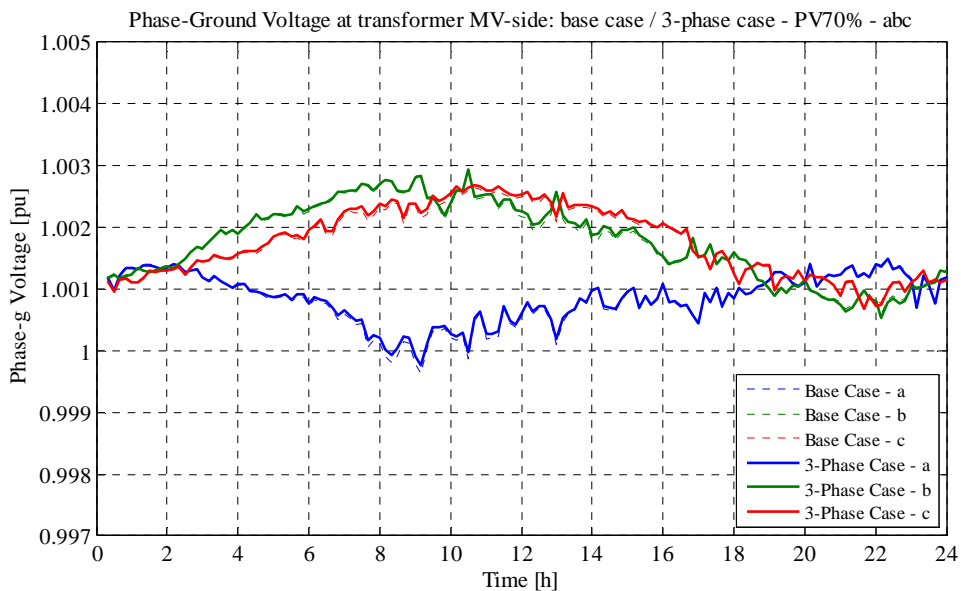


Figure 4.89. Phase-Ground Voltage at transformer MV-side – 3-Phase/Base Case comparison in the scenario with 245 kW of PV connected to phase a, b and c

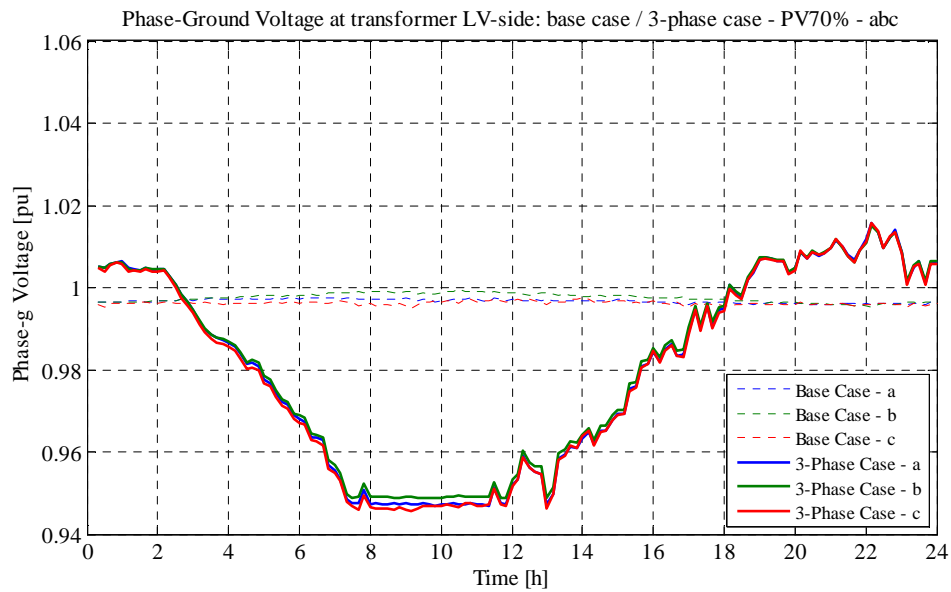


Figure 4.90. Phase-Ground Voltage at transformer LV-side – 3-Phase/Base Case comparison in the scenario with 245 kW of PV connected to phase a, b and c

As always, the same situation is valid at the MV-side in the 1-phase case, as it can be seen in Figure 4.91. At the LV side they change independently because of the 1-phase tapping, staying within the range -5%/+2% (Figure 4.92).

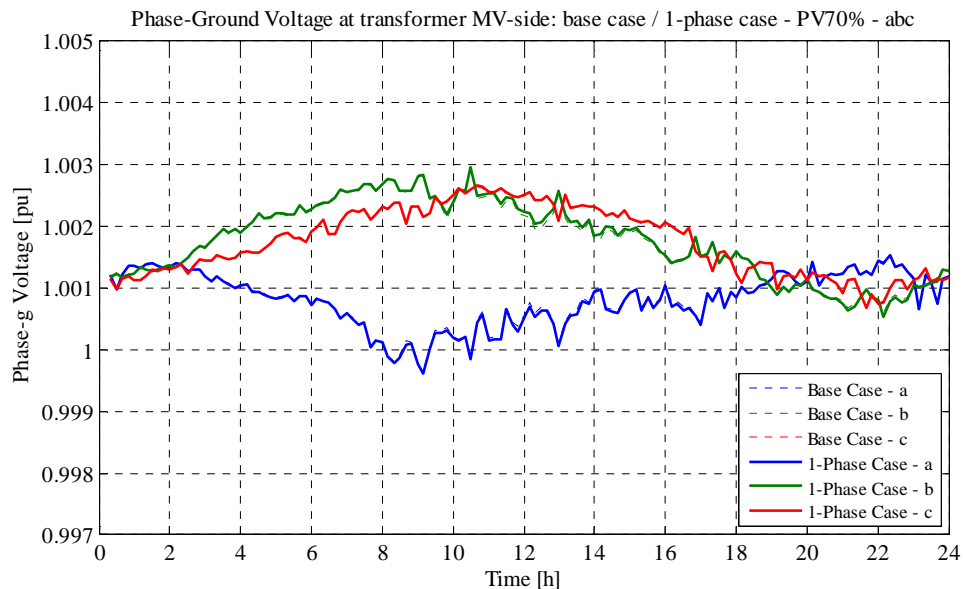


Figure 4.91. Phase-Ground Voltage at transformer MV-side – 1-Phase/Base Case comparison in the scenario with 245 kW of PV connected to phase a, b and c

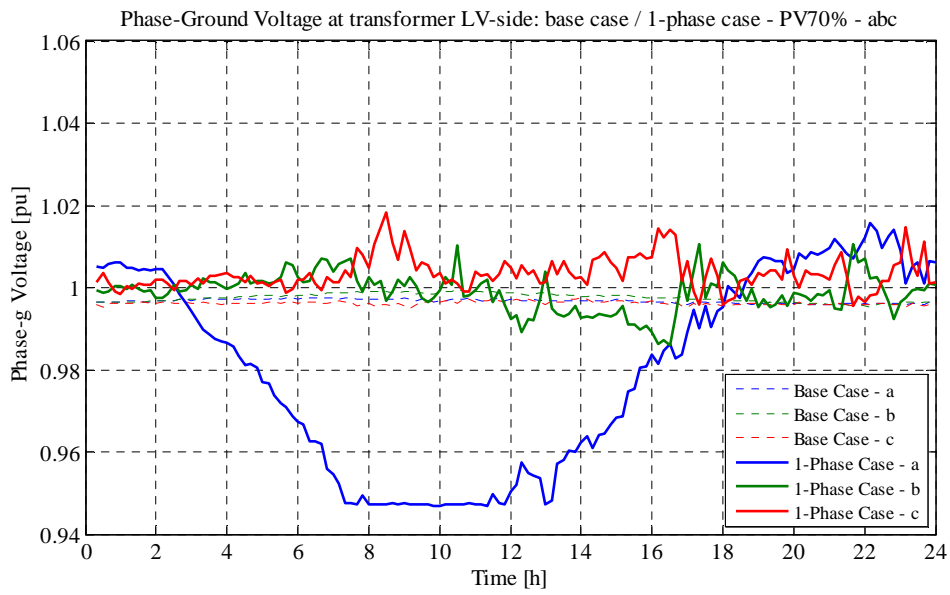


Figure 4.92. Phase-Ground Voltage at transformer LV-side – 1-Phase/Base Case comparison in the scenario with 245 kW of PV connected to phase a, b and c

As shown in Figure 4.93, the neutral-ground voltage at bus 6 does not change after tapping, so its peaks stay below 4.5%.

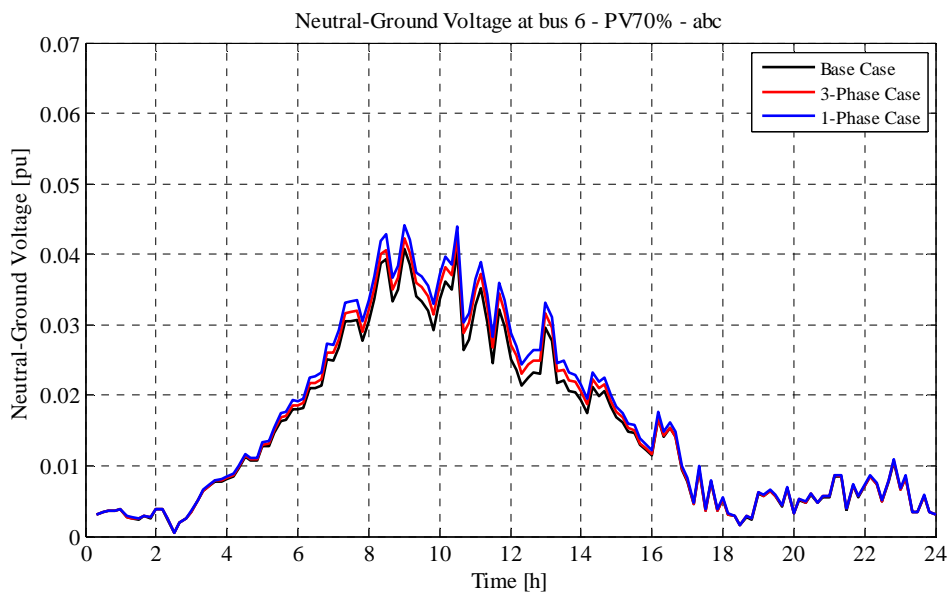


Figure 4.93. Neutral-Ground Voltage at bus 6 – 3-Phase/1-Phase/Base Case comparison in the scenario with 245 kW of PV connected to phase a, b and c

The VUF at bus 6 (Figure 4.94) does not increase in the 3-phase case, while it grows in the 1-phase case: peaks grows from 1.7 % till 2.05%.

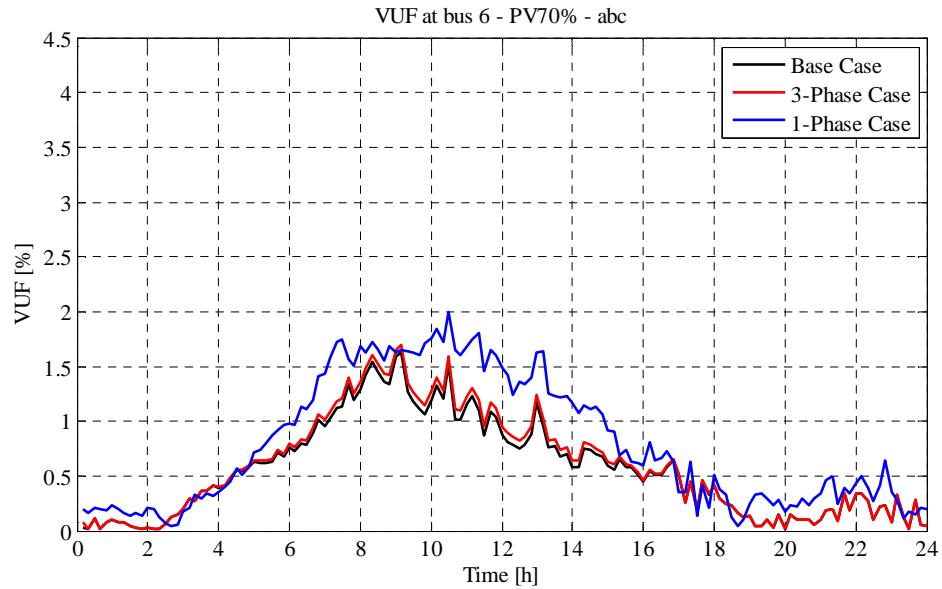


Figure 4.94. VUF at bus 6 – 3-Phase/1-Phase/Base Case comparison in the scenario with 245 kW of PV connected to phase a, b and c

As it can be seen in Figure 4.95 and Figure 4.96, the total power losses of lines and the total power loss ratio as well do present a certain increase after tapping in both the cases.

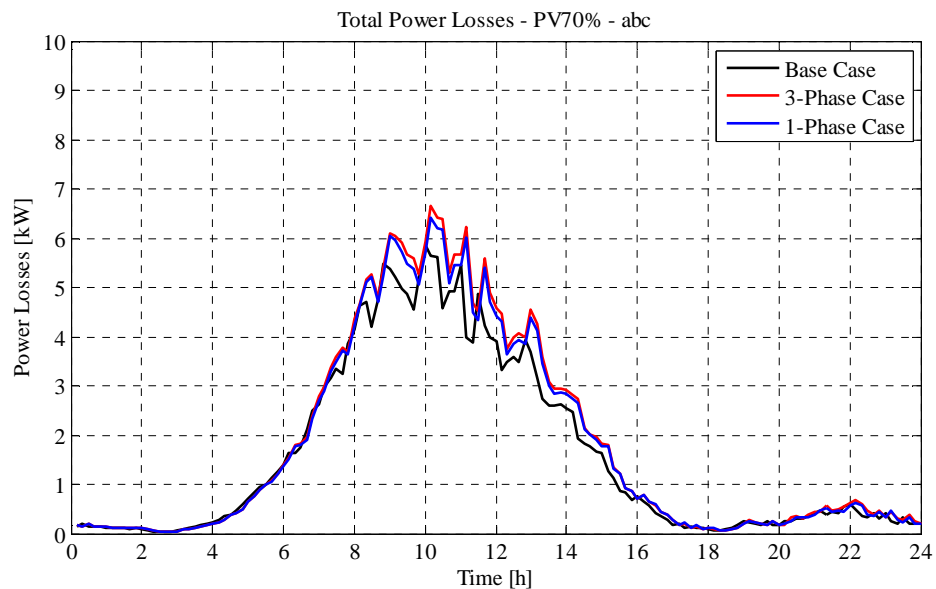


Figure 4.95. Total Power Losses – 3-Phase/1-Phase/Base Case comparison in the scenario with 245 kW of PV connected to phase a, b and c

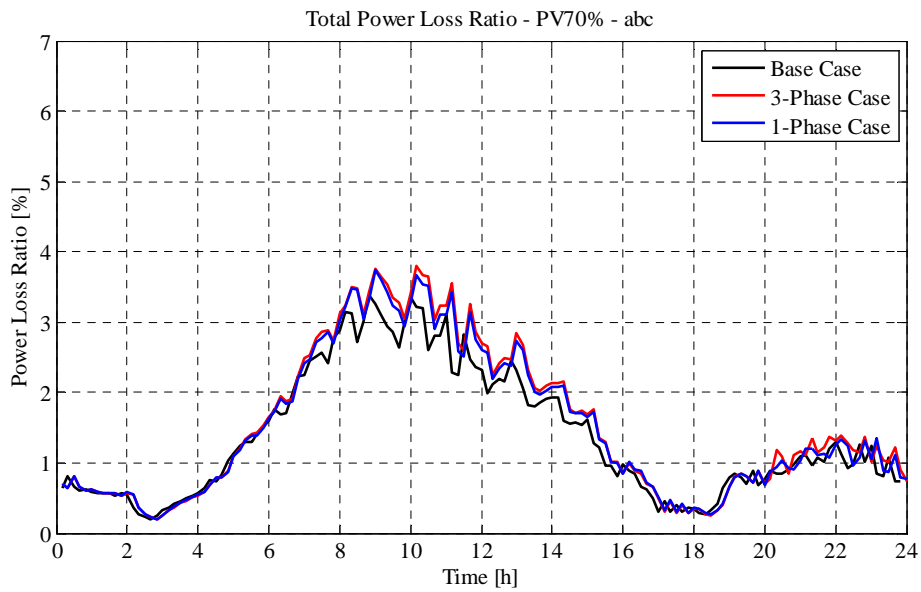


Figure 4.96. Total Power Loss Ratio – 3-Phase/1-Phase/Base Case comparison in the scenario with 245 kW of PV connected to phase a, b and c

In Table 4.8 the total energy amounts absorbed by loads, injected by PVs and the amount through the transformer are reported together with the absolute energy loss, the energy loss ratio and the energy deviations from the base case.

| Case | Total Energy absorbed by loads [kWh] | Total Energy injected by PV [kWh] | Energy through the trafo [kWh] | Energy Loss [kWh] | Energy Loss Ratio [%] | Energy Loss Deviation [%, compared to base case] |
|-----------|--------------------------------------|-----------------------------------|--------------------------------|-------------------|-----------------------|--|
| Base Case | 774.76 | 1714.48 | -901.62 | 38.10 | 2.22% | +0.00% |
| 3-Phase | 751.56 | 1714.29 | -919.65 | 43.08 | 2.51% | +13.07% |
| 1-Phase | 769.12 | 1713.54 | -902.70 | 41.72 | 2.43% | +9.50% |

Table 4.8. PV70% abc scenario – energy analysis

4.1.9. PV80% – 280 kW – phases a, b and c

Out of the three phase-neutral voltages at the worst bus (bus 6) from base case to the 3-phase case only the voltage at phase a gets closer to 1 p.u., since the tap control is based on phase a measurement. Its peak decreases from 1.16 to 1.12 p.u., while the one at phase c decreases till 0.89 p.u.. Phase-neutral voltages and tap positions are depicted respectively in Figure 4.97 and in Figure 4.98.

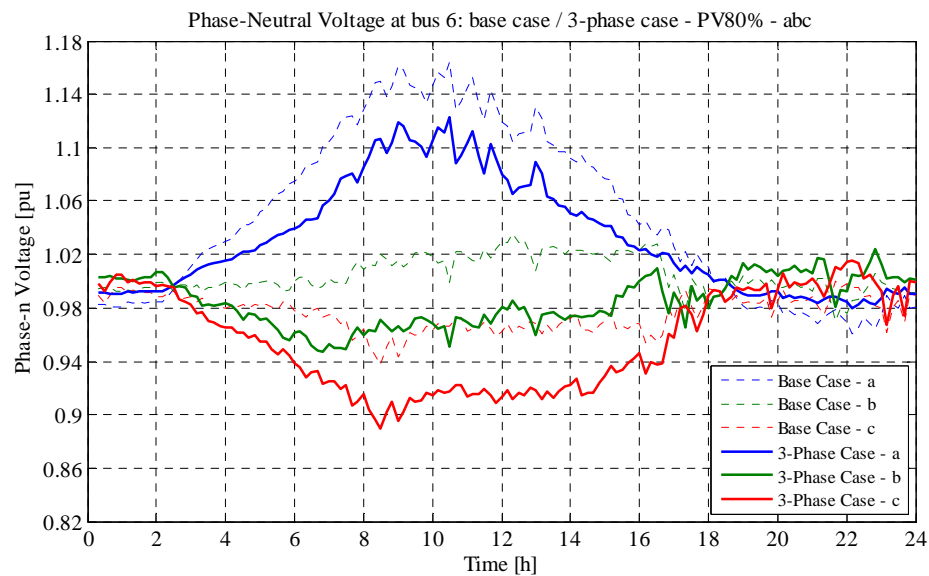


Figure 4.97. Phase-Neutral Voltage at bus 6 – 3-Phase/Base Case comparison in the scenario with 280 kW of PV connected to phase a, b and c

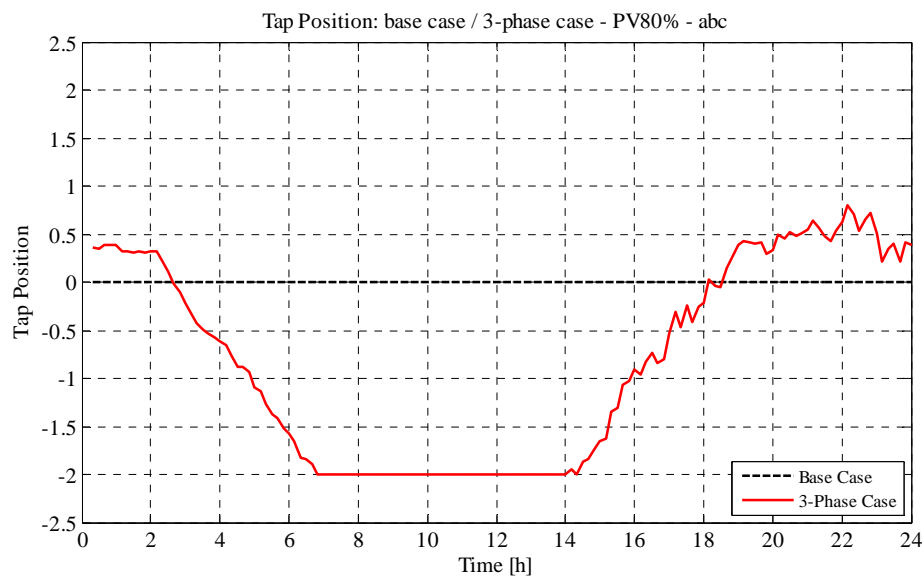


Figure 4.98. Tap Position – 3-Phase/Base Case comparison in the scenario with 280 kW of PV connected to phase a, b and c

On the other hand in the 1-phase case the tap control is based on all the three phases values, so that all the three phase-neutral voltages are closer to 1 p.u.: voltages at phases a and b decrease, while the one at phase c gets higher and within the limit: till 0.97. Phase-neutral voltages and tap positions are depicted respectively in Figure 4.99 and in Figure 4.100.

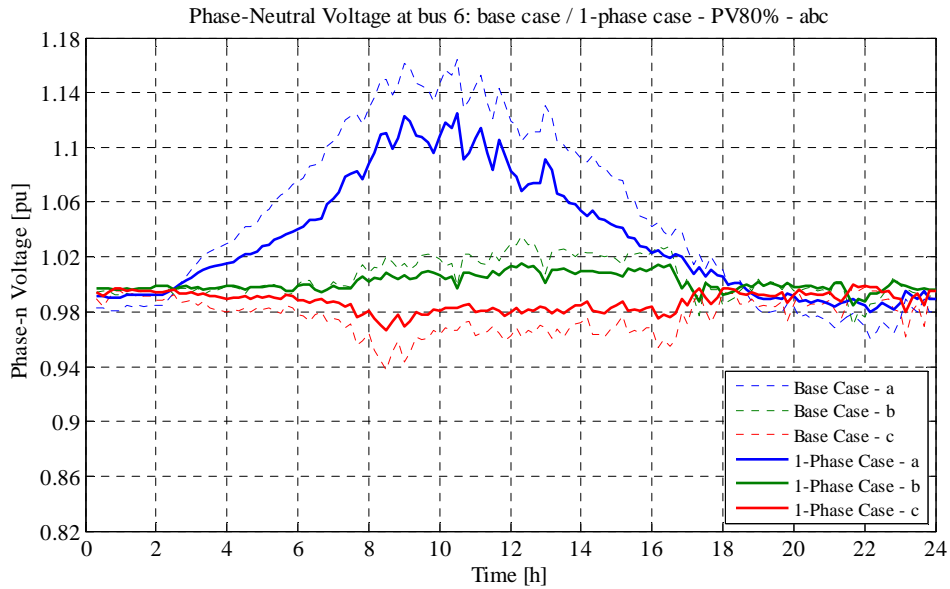


Figure 4.99. Phase-Neutral Voltage at bus 6 – 1-Phase/Base Case comparison in the scenario with 280 kW of PV connected to phase a, b and c

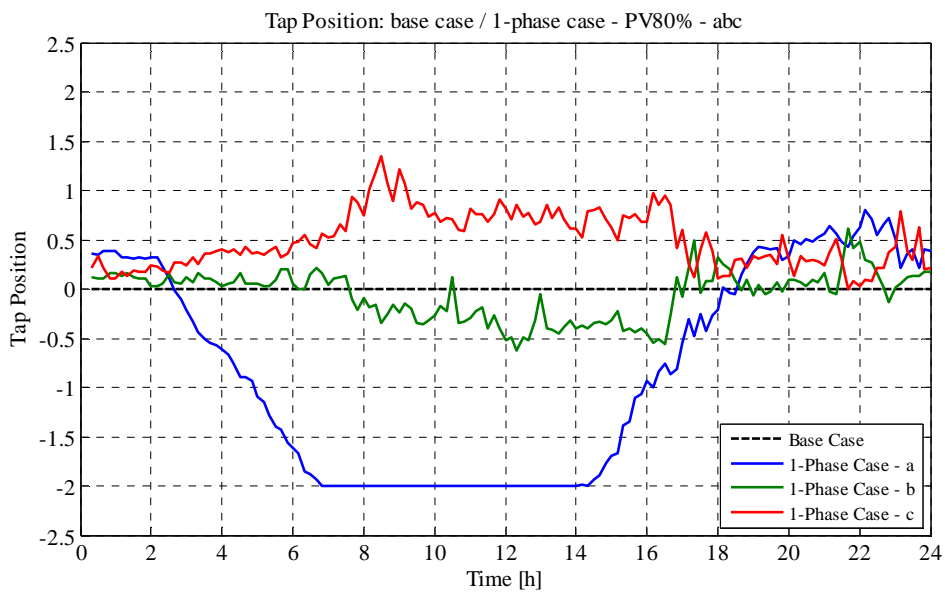


Figure 4.100. Tap Position – 1-Phase/Base Case comparison in the scenario with 280 kW of PV connected to phase a, b and c

As always the phase-ground voltages at the MV side of the transformer do not change in the 3-phase case compared to the base case (Figure 4.101). On the other hand (Figure 4.102), at the LV side they change because of the 3-phase tapping, staying within the range -5%/+2%.

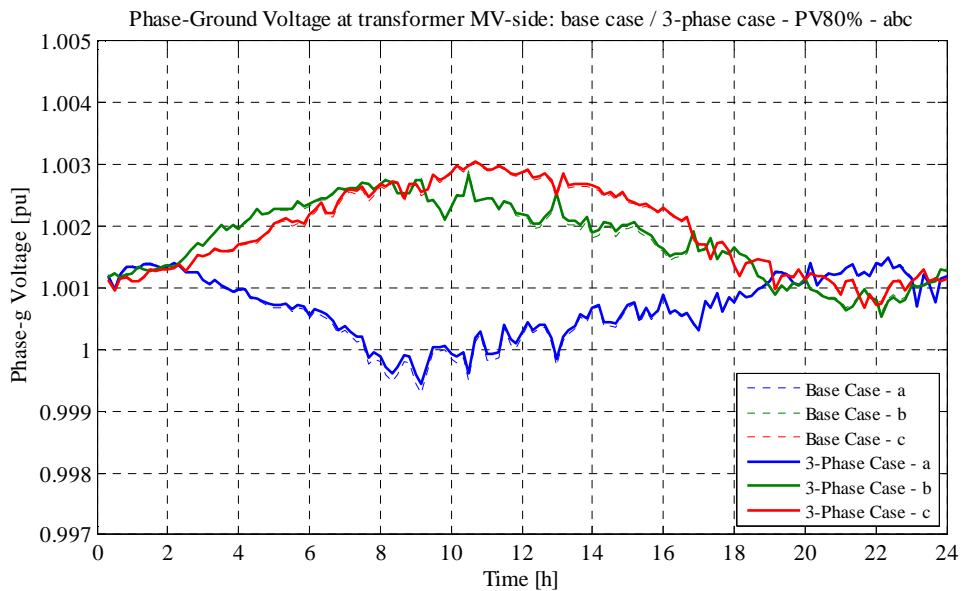


Figure 4.101. Phase-Ground Voltage at transformer MV-side – 3-Phase/Base Case comparison in the scenario with 280 kW of PV connected to phase a, b and c

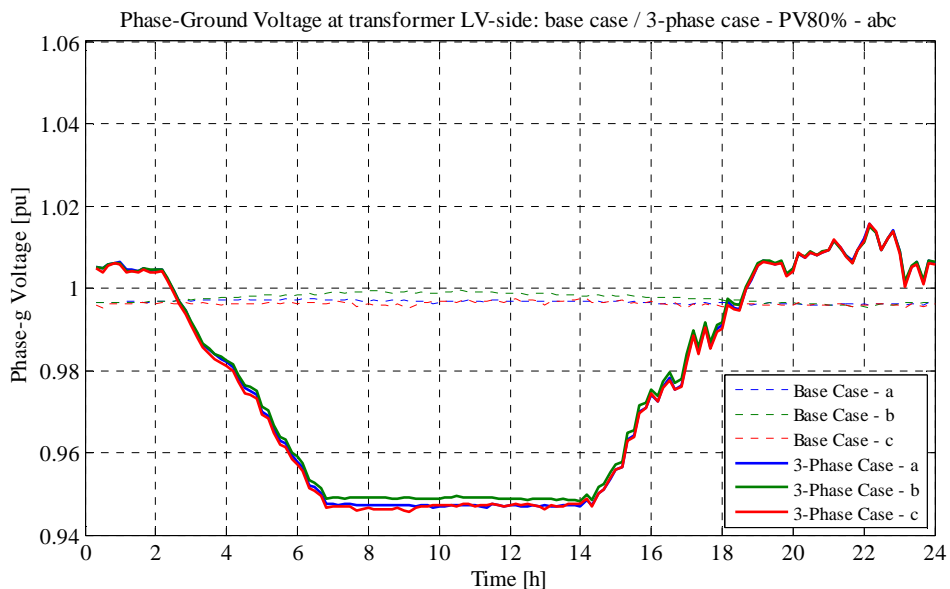


Figure 4.102. Phase-Ground Voltage at transformer LV-side – 3-Phase/Base Case comparison in the scenario with 280 kW of PV connected to phase a, b and c

As always, the same situation is valid at the MV-side in the 1-phase case, as can be seen in Figure 4.103. At the LV side they change independently because of the 1-phase tapping, staying within the range -5%/+3% (Figure 4.104).

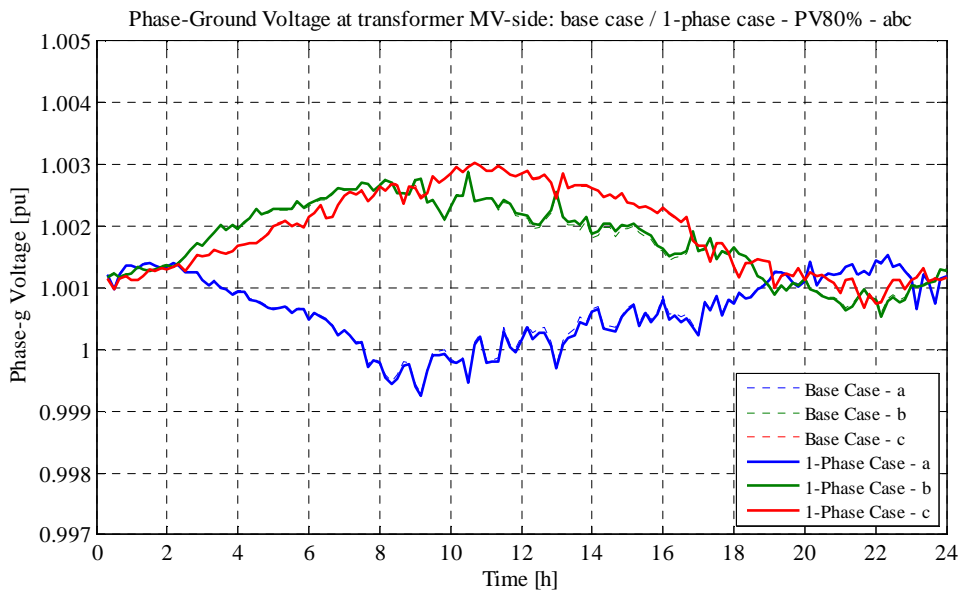


Figure 4.103. Phase-Ground Voltage at transformer MV-side – 1-Phase/Base Case comparison in the scenario with 280 kW of PV connected to phase a, b and c

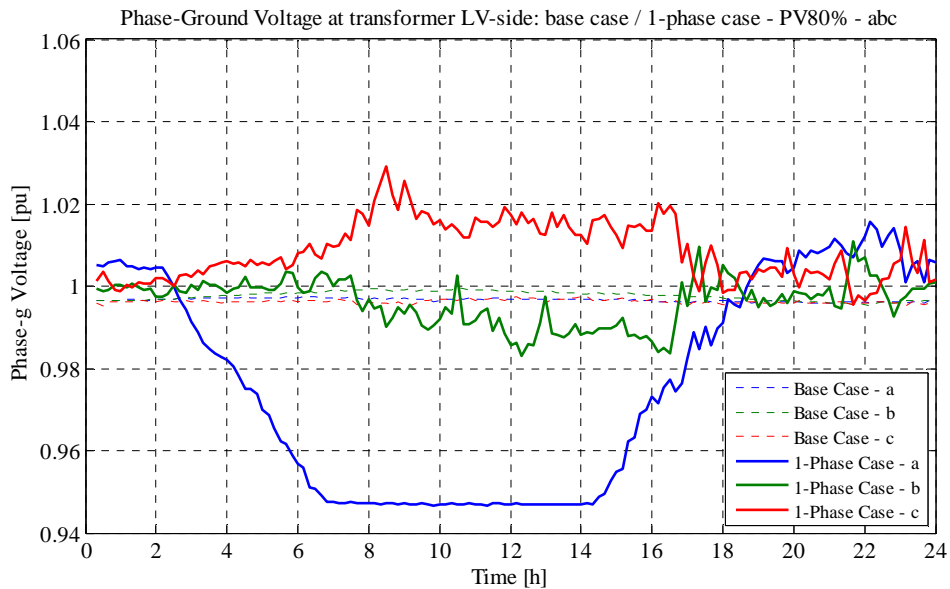


Figure 4.104. Phase-Ground Voltage at transformer LV-side – 1-Phase/Base Case comparison in the scenario with 280 kW of PV connected to phase a, b and c

As shown in Figure 4.105, the neutral-ground voltage at bus 6 does not change after tapping, so its peaks stay below 6%.

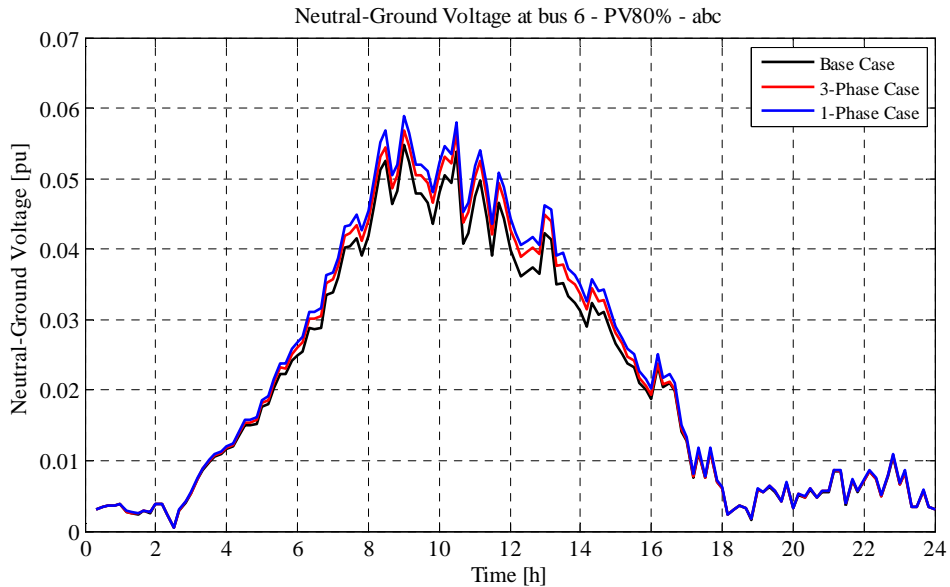


Figure 4.105. Neutral-Ground Voltage at bus 6 – 3-Phase/1-Phase/Base Case comparison in the scenario with 280 kW of PV connected to phase a, b and c

The VUF at bus 6 (Figure 4.106) does not increase in the 3-phase case, while it grows in the 1-phase case: peaks grows from 1.8 % till 2.05%.

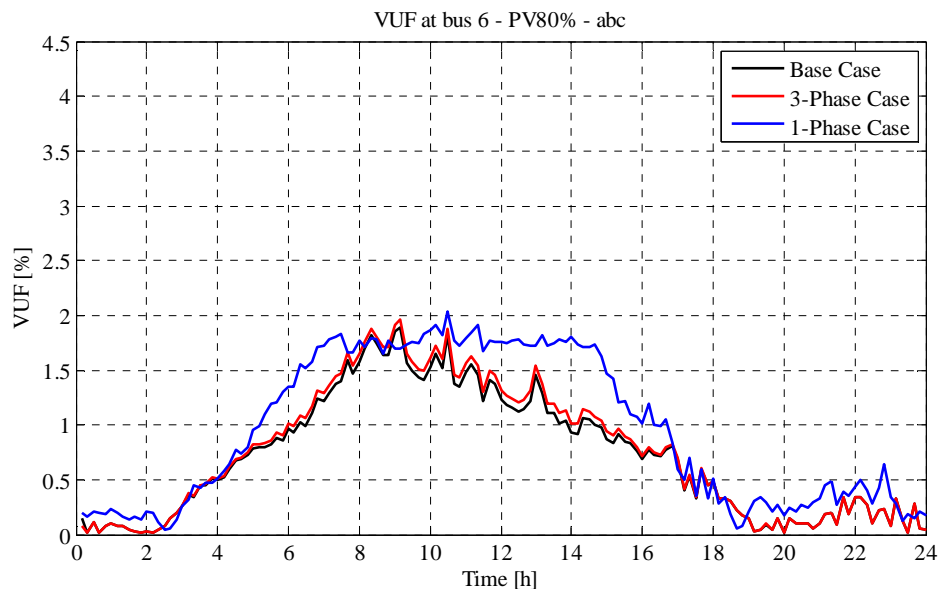


Figure 4.106. VUF at bus 6 – 3-Phase/1-Phase/Base Case comparison in the scenario with 280 kW of PV connected to phase a, b and c

As it can be seen in Figure 4.107 and Figure 4.108, the total power losses of lines and the total power loss ratio as well do present a certain increase after tapping in both the cases.

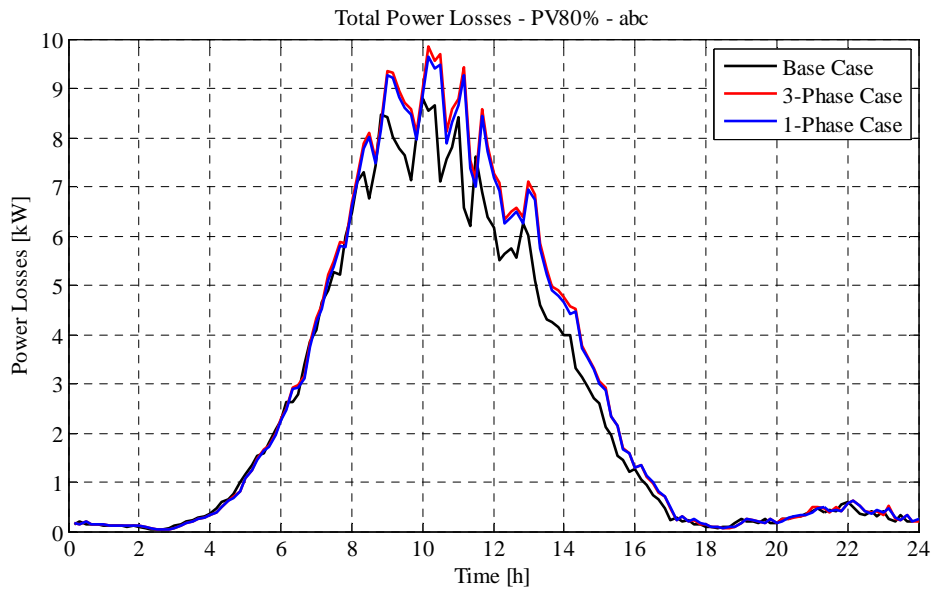


Figure 4.107. Total Power Losses – 3-Phase/1-Phase/Base Case comparison in the scenario with 280 kW of PV connected to phase a, b and c

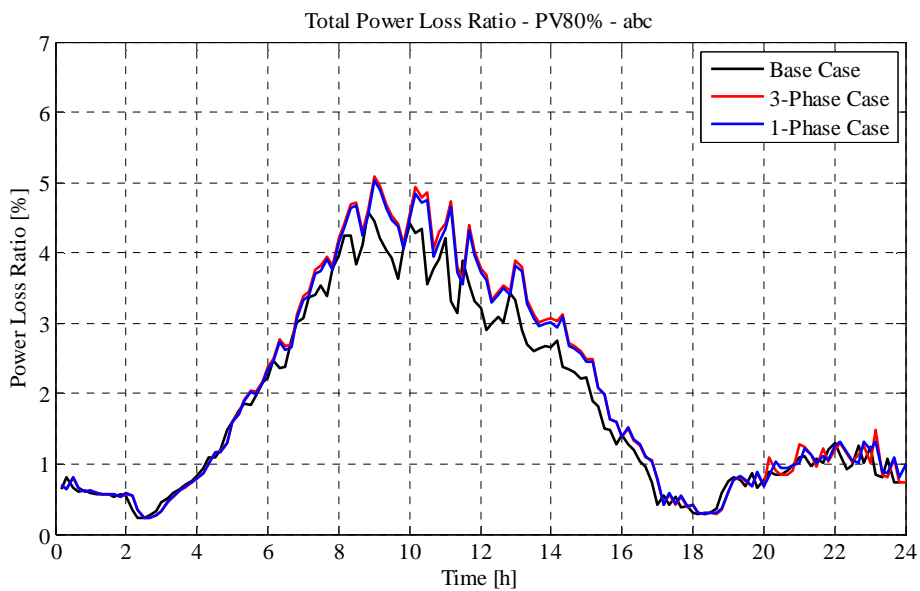


Figure 4.108. Total Power Loss Ratio – 3-Phase/1-Phase/Base Case comparison in the scenario with 280 kW of PV connected to phase a, b and c

In Table 4.9 the total energy amounts absorbed by loads, injected by PVs and the transformer and the corresponding absolute energy loss amount, energy loss ratio and energy deviations from the base case re reported.

| Case | Total Energy absorbed by loads [kWh] | Total Energy injected by PV [kWh] | Energy through the trafo [kWh] | Energy Loss [kWh] | Energy Loss Ratio [%] | Energy Loss Deviation [%, compared to base case] |
|-----------|--------------------------------------|-----------------------------------|--------------------------------|-------------------|-----------------------|--|
| Base Case | 781.33 | 1953.92 | -1114.50 | 58.09 | 2.97% | +0.00% |
| 3-Phase | 752.19 | 1953.00 | -1135.35 | 65.46 | 3.35% | +12.69% |
| 1-Phase | 774.00 | 1952.04 | -1114.35 | 63.69 | 3.26% | +9.64% |

Table 4.9. PV80% abc scenario – energy analysis

4.2. Without Q regulation cases: results comments and analysis

Summarizing the simulation results reported till now, it has been possible to find out the positive-negative effects of the tapping actions in the different PV penetration level scenarios, always referring to the same unbalanced passive loads profiles and without considering any reactive power control system by the PV plants.

After testing all the above mentioned scenarios, the results highlighted a PV hosting capacity of 105 kW (30% case) considering the very unbalanced situation of PV power injection only into phases a and b, i.e. 52.5 kW connected to phase a and the same amount to b.

10% Case

About the 10% case, which refers to the situation of 35 kW of PV connected only to phase a, it can be seen that even in the base case the situation could be acceptable:

- phase-neutral voltages at the final bus within the range -5%/+5%;
- phase-ground voltages at the transformer level practically at the nominal values;
- neutral-ground voltage peaks at the final bus at around 2.3% of the phase-ground nominal value (230 V);
- VUF below 1.2%;
- amount of energy losses of about 6.45 kWh;
- maximum power loss ratio of about 1.5%.

The situation is practically the same in the 3-phase case, in which the phase-neutral voltages at the final bus stay within the range -7%/+3%. The VUF is practically not changing because the voltage at phase a gets lower, as phases b and c. What has changed is the amount of the total energy loss, which is now around 6.59 kWh, i.e. around +2.18% compared to the base case.

In the 1-phase case the situation about phase-neutral voltages and VUF at the worst bus is better, while the energy losses rises a bit:

- phase-neutral voltages at the final bus within the range $-2.5\%/+2.5\%$;
- phase-ground voltages at the transformer level within the range $-3\%/+2.5\%$;
- neutral-ground voltage peaks at the final bus at around 2% of the nominal value;
- VUF below 1.25%;
- amount of energy losses of about 6.66 kWh, i.e. around +3.33% compared to the base case;
- maximum power loss ratio of about 1.6%.

In Table 4.10 the total energy amounts absorbed by loads, injected by PVs and the transformer and the corresponding absolute energy loss amount, energy loss ratio and energy deviations from the base case are reported.

| Case | Total Energy absorbed by loads [kWh] | Total Energy injected by PV [kWh] | Energy through the transformer [kWh] | Energy Loss [kWh] | Energy Loss Ratio [%] | Energy Loss Deviation [%, compared to base case] |
|-----------|--------------------------------------|-----------------------------------|--------------------------------------|-------------------|-----------------------|--|
| Base Case | 749.43 | 244.53 | 511.35 | 6.45 | 0.85% | +0.00% |
| 3-Phase | 756.92 | 244.49 | 519.02 | 6.59 | 0.86% | +2.18% |
| 1-Phase | 761.75 | 244.48 | 523.93 | 6.66 | 0.87% | +3.33% |

Table 4.10. PV10% scenario – energy analysis

30% Case

About the 30% case, which refers to the situation of 105 kW of PV equally connected to phases a and b, it can be noticed that in the 3-phase case it is not possible to have phase-neutral voltages at the final bus which are within the acceptable range $\pm 10\%$ of the nominal value, because the voltage at phase c gets lower the -10% limit, since the tapping is based on voltage measurements at phase a, which is higher than 1 p.u., causing down-shifting of the three phases. For this reason it can be said that this scenario with this PV penetration level cannot be considered feasible in this case with this tapping logic (which refers to just one phase voltage measurement). So it can be deduced that the maximum PV hosting capacity of the network with the 3-phase tapping logic is 10%, (i.e. the unbalanced connection of 35 kW

to phase a, without power injection into phases b and c) in this particular unbalanced load condition.

Different is the situation in the base case or in the 1-phase case: it is possible to obtain acceptable voltages, VUF and losses.

Base Case results:

- phase-neutral voltages at the final bus within the range -8.5%/+7%;
- phase-ground voltages at the transformer level practically at the nominal values;
- neutral-ground voltage peaks at the final bus at around 4% of the nominal value;
- VUF below 1.4%;
- amount of energy losses of about 14.65 kWh;
- maximum power loss ratio of about 2.6%.

1-Phase Case results:

- phase-neutral voltages at the final bus within the range -5%/+4%;
- phase-ground voltages at the transformer level within the range -4%/+4%;
- neutral-ground voltage peaks at the final bus below 4% of the nominal value;
- VUF below 1.9%;
- amount of energy losses of about 15.24 kWh, i.e. around +4.01% compared to the base case;
- maximum power loss ratio of about 2.7%.

In Table 4.11 the total energy amounts absorbed by loads, injected by PVs and the transformer and the corresponding absolute energy loss amount, energy loss ratio and energy deviations from the base case re reported.

| Case | Total Energy absorbed by loads [kWh] | Total Energy injected by PV [kWh] | Energy through the transformer [kWh] | Energy Loss [kWh] | Energy Loss Ratio [%] | Energy Loss Deviation [%, compared to base case] |
|-----------|--------------------------------------|-----------------------------------|--------------------------------------|-------------------|-----------------------|--|
| Base Case | 756.30 | 731.21 | 39.74 | 14.65 | 1.90% | +0.00% |
| 3-Phase | 753.48 | 730.71 | 37.82 | 15.05 | 1.96% | +2.73% |
| 1-Phase | 763.29 | 730.60 | 47.93 | 15.24 | 1.96% | +4.01% |

Table 4.11. PV30% ab scenario – energy analysis

40% and 50% Cases

About the 40% and 50% cases, which refer respectively to the situation of 140 kW and 175 kW of PV equally connected to phases a and b, it can be noticed that both in the base case and in the 3-phase case it is not possible to have phase-neutral voltages at the final bus which are within the acceptable range $\pm 10\%$ of the nominal value (as it was in the 30% scenario in the 3-phase case). For this reason it can be said that 40% and 50% of PV penetration level cases cannot be considered feasible without a phase-wise control.

A phase-wise control can further improve the phase-neutral voltage values at the final bus with acceptable losses. This improvement has been seen to affect negatively the VUF value: maximum values are around at 2.5% and 2.9% respectively for 40% and 50% cases.

This effect is due to the unbalanced production of the PVs, which is very high because only connections to phases a and b are performed; in addition it should be considered that the total energy injected by the PV plants (respectively 970 and 1207 kWh) is very high compared to the energy absorbed by the loads (around 760 kWh).

So, even if the phase-wise tapping control allows the three phase-neutral voltages to get close to the nominal value, negative effects on the unbalance level are caused to the voltage sequences. In fact, referring to the phase-neutral voltages sequences, the VUF increase is due to the reduction of the positive sequence magnitude, while the negative sequence magnitude increases during the PV production period. This can be seen in the graphs in Figure 4.109 – which refer to the 40% case – where the solid lines represent the base case, while the dashed one the 1-phase case.

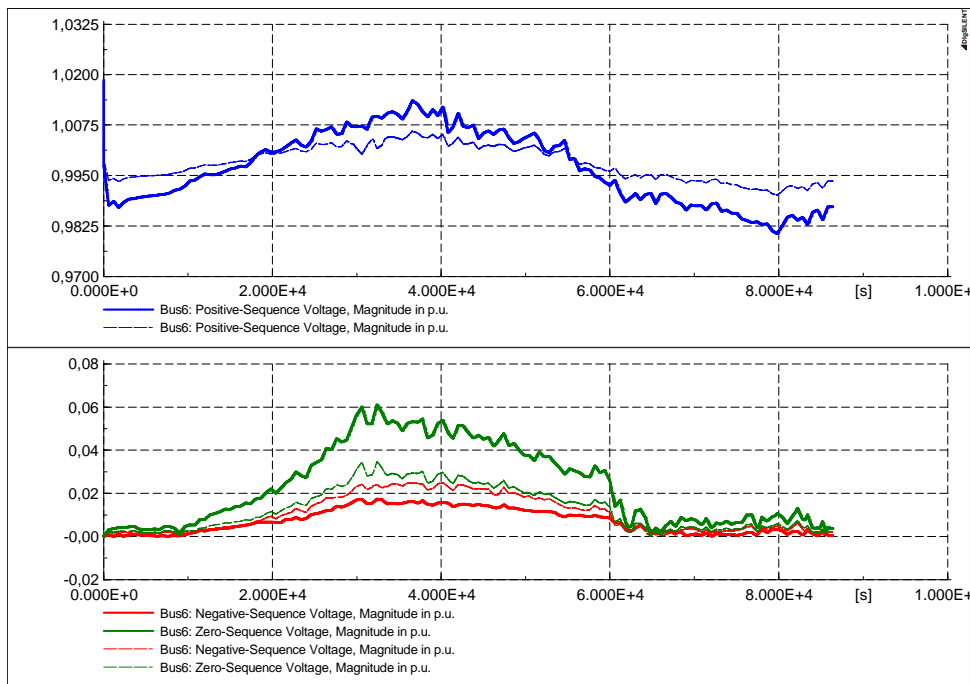


Figure 4.109. Phase-neutral voltage sequences analysis at bus 6

According to the voltage sequences shown above, it has been decided to analyze the currents flowing in the final part of line (i.e. 'line 10-11'): amplitudes, angles and sequences.

A comparison between the base case and the 1-phase case has been performed (respectively reported in Figure 4.110 and Figure 4.111).

As previously said, PV units have been modeled as constant power units while loads as constant impedances. For this reason, since in the PV production period the injected power is much higher than the loads absorption, the phase current is inversely proportional to the voltage; on the other hand when PVs are not producing, current and voltage are directly proportional, because now the constant-impedance behavior is predominant.

Basically not any relevant difference can be noticed between the two cases, because the voltage variations in percentage (few percentage points) cause the discussed current variations.

Anyway high values of both the inverse and the zero sequences compared to the positive one can be seen because the PV power injection has been chosen to be extremely unbalanced.

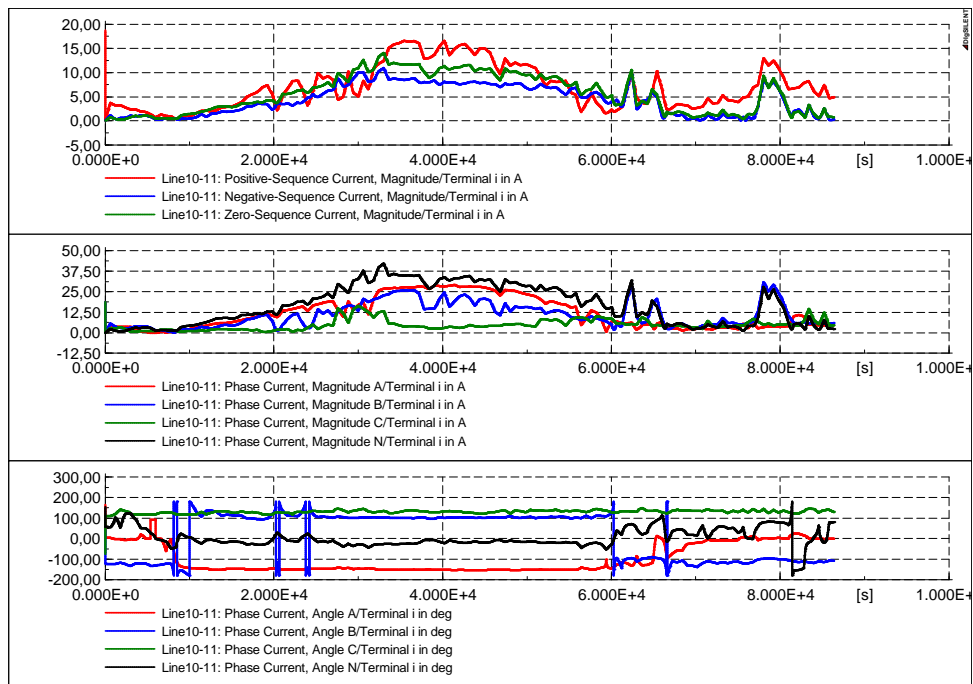


Figure 4.110. Phase current magnitude, angle and sequences analysis at line 10-11 in the Base Case

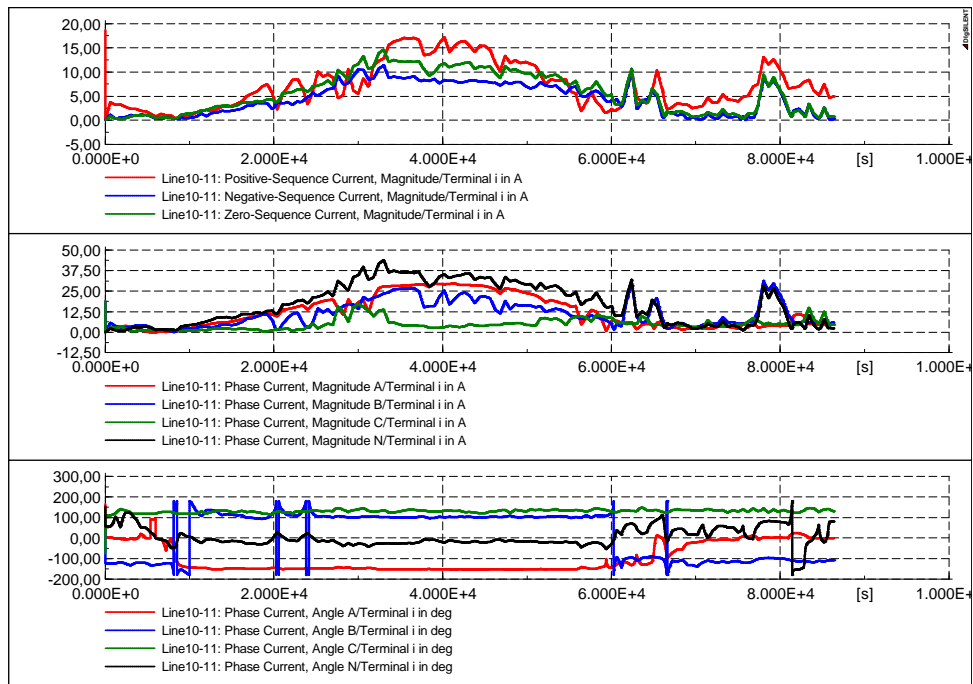


Figure 4.111. Phase current magnitude, angle and sequences analysis at line 10-11 in the 1-Phase Case

In Table 4.12 and Table 4.13 the total energy amounts absorbed by loads, injected by PVs and the transformer and the corresponding absolute energy loss amount, energy loss ratio and energy deviations from the base case re reported referring respectively to the 40% ab and the 50% ab scenario.

| Case | Total Energy absorbed by loads [kWh] | Total Energy injected by PV [kWh] | Energy through the transformer [kWh] | Energy Loss [kWh] | Energy Loss Ratio [%] | Energy Loss Deviation [%, compared to base case] |
|-----------|--------------------------------------|-----------------------------------|--------------------------------------|-------------------|-----------------------|--|
| Base Case | 760.44 | 971.93 | -186.77 | 24.72 | 2.54% | +0.00% |
| 3-Phase | 749.57 | 971.02 | -195.24 | 26.21 | 2.70% | +6.01% |
| 1-Phase | 763.71 | 970.58 | -180.62 | 26.25 | 2.70% | +6.18% |

Table 4.12. PV40% ab scenario – energy analysis

| Case | Total Energy absorbed by loads [kWh] | Total Energy injected by PV [kWh] | Energy through the trafo [kWh] | Energy Loss [kWh] | Energy Loss Ratio [%] | Energy Loss Deviation [%, compared to base case] |
|-----------|--------------------------------------|-----------------------------------|--------------------------------|-------------------|-----------------------|--|
| Base Case | 767.25 | 1209.34 | -401.80 | 40.30 | 3.33% | +0.00% |
| 3-Phase | 744.07 | 1207.03 | -418.98 | 43.98 | 3.64% | +9.13% |
| 1-Phase | 765.04 | 1207.02 | -398.23 | 43.75 | 3.62% | +8.56% |

Table 4.13. PV50% ab scenario – energy analysis

Summarizing, it can finally be deduced that the maximum PV hosting capacity of the network (considering the unbalanced connection to phases a and b, without power injection into phase c) in this determinate unbalanced load condition, is the one corresponding to the 30% case, i.e. the situation of 105 kW of PV equally connected to phases a and b.

Anyway it is highly possible that the PV hosting capacity could be higher than 105 kW if the PV connections are distributed (probably not compulsorily equally) on the three phases instead of only into two, according to a more realistic degree of unbalance. In these conditions other acceptable cases with higher PV penetration levels could probably be found, in which both the phase-neutral voltage and the VUF can lay within the limits.

In order to evaluate the PV hosting capacity of the network under more realistic situations, further simulations characterized by unbalanced three-phase PV connections have been performed.

The following unbalanced distribution has been considered to split the PV power: 50% of the total PV power connected to phase a, 30% to phase b and 20% to phase c.

With this not too heavy unbalanced configuration the worst bus remained the same: bus 6. Due to this, the phase-neutral voltages as well as the VUF have been considered referring again to bus 6, the one at the end of the network.

It has been decided to repeat the 40% and 50% cases – 140 and 157 kW – changing the power distribution as described above and to consider further cases with progressive increasing PV installed power.

40% Case with abc connections

About the 40% case with connections to the three phases, it can be noticed that both in the base case and in the ones with the tapping actions the phase-neutral voltages at the worst bus (bus 6) are within the acceptable range $\pm 10\%$ of the nominal value. Losses and VUF are acceptable as well.

For this reason it can be said that this scenario with this PV penetration level can be considered feasible.

Base case results:

- phase-neutral voltages at the final bus within the range $-4\%/+6\%$;
- phase-ground voltages at the transformer level practically at the nominal values;
- neutral-ground voltage peaks at around 2.5% of the nominal value;
- VUF below 1.1%;
- amount of energy losses of about 11.61 kWh;
- maximum power loss ratio of about 1.7%.

1-Phase case results:

- phase-neutral voltages at the final bus within the range $-2\%/+3.5\%$;
- phase-ground voltages at the transformer level within the range $-4\%/+2\%$;
- neutral-ground voltage peaks below 2.5% of the nominal value;

- VUF below 1.25%;
- amount of energy losses of about 12.22 kWh, i.e. around +5.29% compared to the base case;
- maximum power loss ratio of about 1.8%.

In Table 4.14 the total energy amounts absorbed by loads, injected by PVs and the transformer and the corresponding absolute energy loss amount, energy loss ratio and energy deviations from the base case re reported.

| Case | Total Energy absorbed by loads [kWh] | Total Energy injected by PV [kWh] | Energy through the trafo [kWh] | Energy Loss [kWh] | Energy Loss Ratio [%] | Energy Loss Deviation [%, compared to base case] |
|-----------|--------------------------------------|-----------------------------------|--------------------------------|-------------------|-----------------------|--|
| Base Case | 759.78 | 981.99 | -210.60 | 11.61 | 1.18% | +0.00% |
| 3-Phase | 760.07 | 981.97 | -209.68 | 12.22 | 1.24% | +5.29% |
| 1-Phase | 764.90 | 981.84 | -204.78 | 12.16 | 1.24% | +4.77% |

Table 4.14. PV40% abc scenario – energy analysis

50-60-70% Cases with abc connections

The 50%, 60% and 70% cases, which refer respectively to PV power connections of 175, 210 and 245 kW – show that the PV hosting capacity could be higher than 140 kW only if phase-wise tap actions are performed. In fact both in the base case and in the 3-phase case the phase-neutral voltages could not stay within the acceptable limit range.

Anyway, an higher PV power penetration could not be considered acceptable although phase-wise tapping actions: this is because the 70% case leads to VUF peak value which is higher than 2%.

The results of the 70% scenario in the 1-phase case are so summarized:

- phase-neutral voltages at the final bus within the range -2%/+8.8%;
- phase-ground voltages at the transformer level within the range -5%/+2%;
- neutral-ground voltage peaks below 4.5% of the nominal value;
- VUF peak around 2.05%;

- amount of energy losses of about 41.72 kWh, i.e. around +9.50% compared to the base case (38.10 kWh);
- maximum power loss ratio of about 3.8%.

In Table 4.15, Table 4.16 and Table 4.17 the total energy amounts absorbed by loads, injected by PVs and the transformer and the corresponding absolute energy loss amount, energy loss ratio and energy deviations from the base case re reported referring respectively to the 50%, 60% and 70% scenarios.

| Case | Total Energy absorbed by loads [kWh] | Total Energy injected by PV [kWh] | Energy through the trafo [kWh] | Energy Loss [kWh] | Energy Loss Ratio [%] | Energy Loss Deviation [%, compared to base case] |
|-----------|--------------------------------------|-----------------------------------|--------------------------------|-------------------|-----------------------|--|
| Base Case | 766.62 | 1224.70 | -436.63 | 21.45 | 1.75% | +0.00% |
| 3-Phase | 752.51 | 1224.48 | -448.38 | 23.59 | 1.93% | +9.98% |
| 1-Phase | 765.86 | 1224.08 | -434.89 | 23.33 | 1.91% | +8.76% |

Table 4.15. PV50% abc scenario – energy analysis

| Case | Total Energy absorbed by loads [kWh] | Total Energy injected by PV [kWh] | Energy through the trafo [kWh] | Energy Loss [kWh] | Energy Loss Ratio [%] | Energy Loss Deviation [%, compared to base case] |
|-----------|--------------------------------------|-----------------------------------|--------------------------------|-------------------|-----------------------|--|
| Base Case | 769.70 | 1468.77 | -670.66 | 28.41 | 1.93% | +0.00% |
| 3-Phase | 751.97 | 1468.50 | -684.89 | 31.64 | 2.15% | +11.37% |
| 1-Phase | 767.24 | 1467.91 | -669.63 | 31.04 | 2.11% | +9.26% |

Table 4.16. PV60% abc scenario – energy analysis

| Case | Total Energy absorbed by loads [kWh] | Total Energy injected by PV [kWh] | Energy through the trafo [kWh] | Energy Loss [kWh] | Energy Loss Ratio [%] | Energy Loss Deviation [%, compared to base case] |
|-----------|--------------------------------------|-----------------------------------|--------------------------------|-------------------|-----------------------|--|
| Base Case | 774.76 | 1714.48 | -901.62 | 38.10 | 2.22% | +0.00% |
| 3-Phase | 751.56 | 1714.29 | -919.65 | 43.08 | 2.51% | +13.07% |
| 1-Phase | 769.12 | 1713.54 | -902.70 | 41.72 | 2.43% | +9.50% |

Table 4.17. PV70% abc scenario – energy analysis

80% Case with abc connections

Whenever the peak value of 2.05% of the VUF is not considered a problem for the technical feasibility of the 70% study case, this case could be considered acceptable.

For this reason in order to find the extreme situation, a further case has been studied: the 80% case, which refers to PV power connection of 280 kW.

The situation regarding the VUF peak is now still not too worse than the one found in the 70% case, but on the other hand the phase-neutral voltages exceed the limit range. Due to this the 80% case could not be considered acceptable.

The results of the 80% scenario in the 1-phase case are so summarized:

- phase-neutral voltages at the final bus within the range -3%/+12%;
- phase-ground voltages at the transformer level within the range -5%/+3%;
- neutral-ground voltage peaks below 5.5% of the nominal value;
- VUF peak around 2.05%;
- amount of energy losses of about 63.69 kWh, i.e. around +9.64% compared to the base case (58.09 kWh);
- maximum power loss ratio of about 5%.

In Table 4.18 the total energy amounts absorbed by loads, injected by PVs and the transformer and the corresponding absolute energy loss amount, energy loss ratio and energy deviations from the base case are reported.

| Case | Total Energy absorbed by loads [kWh] | Total Energy injected by PV [kWh] | Energy through the trafo [kWh] | Energy Loss [kWh] | Energy Loss Ratio [%] | Energy Loss Deviation [%, compared to base case] |
|-----------|--------------------------------------|-----------------------------------|--------------------------------|-------------------|-----------------------|--|
| Base Case | 781.33 | 1953.92 | -1114.50 | 58.09 | 2.97% | +0.00% |
| 3-Phase | 752.19 | 1953.00 | -1135.35 | 65.46 | 3.35% | +12.69% |
| 1-Phase | 774.00 | 1952.04 | -1114.35 | 63.69 | 3.26% | +9.64% |

Table 4.18. PV80% abc scenario – energy analysis

At the end it can be concluded that, thanks to this new connection configuration, the 40% scenario is now acceptable both without and with tapping action, which means that with these connections the amount of PV power 140 kW is admissible.

The 50% and 60% cases – respectively 175 and 210 kW – showed that the PV hosting capacity could be higher than 140kW only if phase-wise tap actions are performed.

Similar considerations can be done regarding the 70% case – 245 kW – only if the VUF peak of 2.05% is not considered as a strictly limitation.

On the other hand, an higher PV power could not be considered acceptable although a phase-wise tapping.

So finally it can be concluded that in 3-phase case unbalanced PV power injection the hosting capacity has become much bigger compared to previous 2-phase connection cases if single phase tap actions are performed: it grows from 140 kW to 210 kW or even 245 kW if the 70% case is considered acceptable.

So the 245 kW case can be seen as the limit because, as it can be seen in the following table, the 80% case (280 kW) leads to phase-neutral voltages which exceed the limit range within they should stay: $\pm 10\%$ of the nominal value.

At the end it should also be remembered that until now simple conditions without any reactive power injection by the PV plants has been considered. It could easily be possible that the PV hosting capacity of the network could be higher than 105 kW (even if the connections are again to phases a and b), if the PVs could inject inductive-capacitive reactive power, following a voltage and active power dependence law: $Q=f(V,P)$. In fact, thanks to the reactive power injected by the PV plants, the VUF of the 40% and 50% with a and b connections cases could decrease under the 2% limit, or the phase-neutral voltages in the 80% case could get closer to 1 p.u. and stay within the limits.

All the analyzed scenarios and cases results are simply summarized in Table 4.19:

PV 10% Scenario: 35 kW PV connected to phase a

| Case | Voltages deviation (an, bn, cn) at bus 6 | Max VUF at bus 6 | Max neutral potential | Total losses [kWh] |
|-----------|--|------------------|-----------------------|--------------------|
| Base Case | -5%/+5% | 1.2% | 2.3% | 6.45 |
| 3-Phase | -7%/+3% | 1.25% | 2.3% | 6.59 |
| 1-Phase | -2.5%/+2.5% | 1.25% | 2.3% | 6.66 |

PV 30% Scenario: 105 kW PV connected to phases a and b

| Case | Voltages deviation (an, bn, cn) at bus 6 | Max VUF at bus 6 | Max neutral potential | Total losses [kWh] |
|-----------|--|------------------|-----------------------|--------------------|
| Base Case | -8.5%/+7% | 1.4% | 4% | 14.65 |
| 3-Phase | -12%/+4% | 1.5% | 4% | 15.05 |
| 1-Phase | -5%/+4% | 1.9% | 4% | 15.24 |

PV 40% Scenario: 140 kW PV connected to phases a and b

| Case | Voltages deviation (an, bn, cn) at bus 6 | Max VUF at bus 6 | Max neutral potential | Total losses [kWh] |
|-----------|--|------------------|-----------------------|--------------------|
| Base Case | -10.1%/+10% | 1.7% | 5.5% | 24.72 |
| 3-Phase | -16%/+5% | 1.8% | 5.5% | 26.21 |
| 1-Phase | -6.5%/+5% | 2.5% | 5.5% | 26.25 |

PV 50% Scenario: 175 kW PV connected to phases a and b

| Case | Voltages deviation (an, bn, cn) at bus 6 | Max VUF at bus 6 | Max neutral potential | Total losses [kWh] |
|-----------|--|------------------|-----------------------|--------------------|
| Base Case | -12%/+13% | 2.05% | 7% | 40.30 |
| 3-Phase | -18%/+8% | 2.2% | 7% | 43.98 |
| 1-Phase | -8%/+9% | 2.9% | 7% | 43.75 |

PV 40% Scenario: 140 kW PV connected to phases a, b and c

| Case | Voltages deviation (an, bn, cn) at bus 6 | Max VUF at bus 6 | Max neutral potential | Total losses [kWh] |
|-----------|--|------------------|-----------------------|--------------------|
| Base Case | -4%/+6% | 1% | 2.5% | 11.61 |
| 3 Phase | -6.5%/+3.5% | 1% | 2.5% | 12.22 |
| 1 Phase | -2%/+3.5% | 1.25% | 2.5% | 12.16 |

PV 50% Scenario: 175 kW PV connected to phases a, b and c

| Case | Voltages deviation (an, bn, cn) at bus 6 | Max VUF at bus 6 | Max neutral potential | Total losses [kWh] |
|-----------|--|------------------|-----------------------|--------------------|
| Base Case | -6%/+11% | 1.4% | 4% | 21.45 |
| 3 Phase | -10.5%/+6% | 1.4% | 4% | 23.59 |
| 1 Phase | -3%/+6% | 1.8% | 4% | 23.33 |

PV 60% Scenario: 210 kW PV connected to phases a, b and c

| Case | Voltages deviation (an, bn, cn) at bus 6 | Max VUF at bus 6 | Max neutral potential | Total losses [kWh] |
|-----------|--|------------------|-----------------------|--------------------|
| Base Case | -6%/+11% | 1.5% | 4% | 28.41 |
| 3 Phase | -11%/+7% | 1.5% | 4% | 31.64 |
| 1 Phase | -3%/+7% | 1.8% | 4% | 31.04 |

PV 70% Scenario: 245 kW PV connected to phases a, b and c

| Case | Voltages deviation (an, bn, cn) at bus 6 | Max VUF at bus 6 | Max neutral potential | Total losses [kWh] |
|-----------|--|------------------|-----------------------|--------------------|
| Base Case | -4%/+13% | 1.7% | 4.5% | 38.10 |
| 3 Phase | -10.1%/+8.8% | 1.7% | 4.5% | 43.08 |
| 1 Phase | -2%/+8.8% | 2.05% | 4.5% | 41.72 |

PV 80% Scenario: 280 kW PV connected to phases a, b and c

| Case | Voltages deviation (an, bn, cn) at bus 6 | Max VUF at bus 6 | Max neutral potential | Total losses [kWh] |
|-----------|--|------------------|-----------------------|--------------------|
| Base Case | -6%/+16% | 1.8% | 5.5% | 58.09 |
| 3 Phase | -11%/+12% | 1.9% | 5.5% | 65.46 |
| 1 Phase | -3%/+12% | 2.05% | 5.5% | 63.69 |

Table 4.19. Overall summary of all the scenarios and cases

4.3. With Q regulation cases: plots and numerical results

The next analyzed scenarios will be based on comparisons between the previous 1-phase cases without any reactive power simulations and the ones with it.

As before, the plots and the numerical values reported will be:

- Phase-neutral voltages at the worst bus;
- Phase-ground voltages at the transformer level, both at the MV and the LV sides;
- Neutral-ground voltage at the worst bus;
- The VUF at the worst bus;
- Total power losses of lines;
- Total power loss ratio;
- A table containing numerical values of energy amounts entering/exiting into/from the system.

4.3.1. PV40% – 140 kW – phases a and b

All the three phase-neutral voltages at the worst bus (bus 6) from 1-phase case without any reactive power regulation and the one with it get closer to 1 p.u. Phase-neutral voltages and tap positions are depicted respectively in Figure 4.112 and in Figure 4.113.

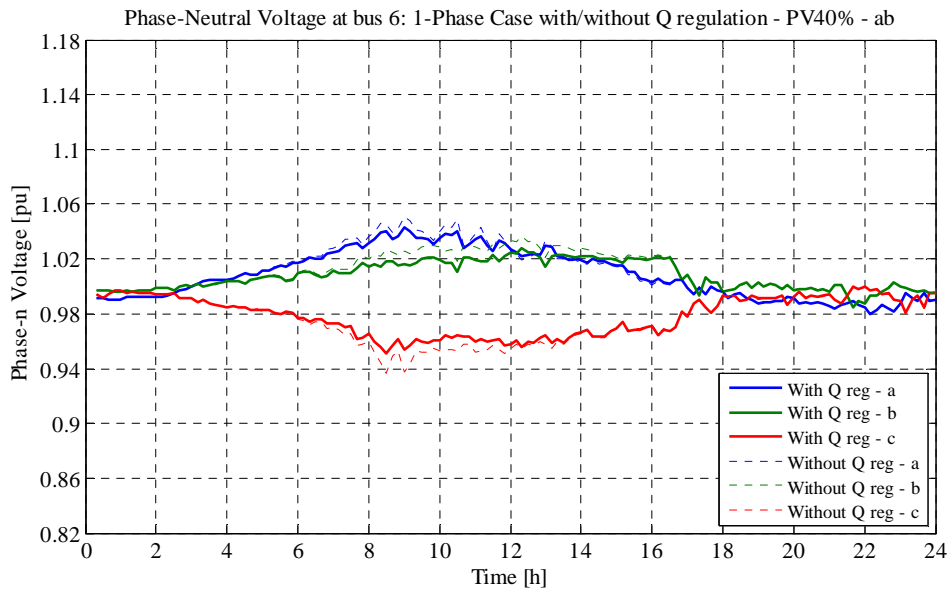


Figure 4.112. Phase-Neutral Voltage at bus 6 – 1-Phase Case – With/Without Q regulation comparison in the scenario with 140 kW of PV connected to phase a and b

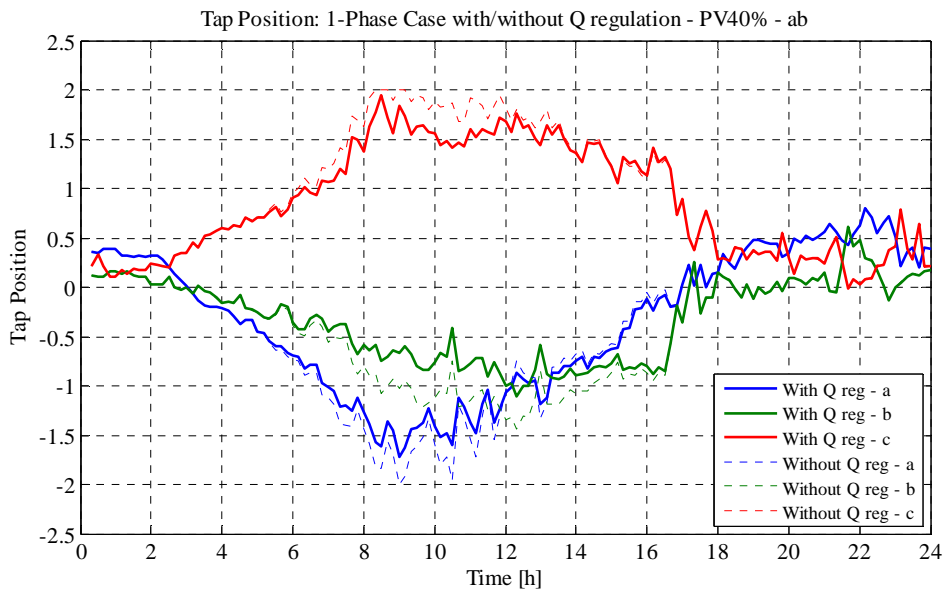


Figure 4.113. Tap Position – 1-Phase Case – With/Without Q regulation comparison in the scenario with 140 kW of PV connected to phase a and b

About the phase-ground voltages at the MV side of the transformer, it can be said that they all reduce because of the Q regulation (Figure 4.114). On the other hand, at the LV side only the one at phase c gets reduced, while the other two increase: it can be seen from Figure 4.115 that all the three voltages get closer to 1 p.u..

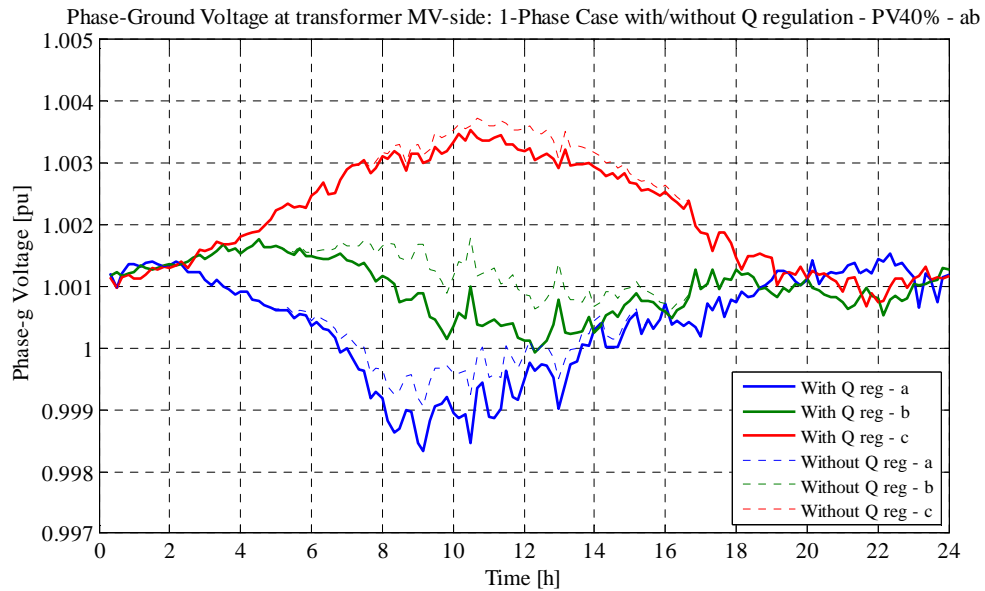


Figure 4.114. Phase-Ground Voltage at transformer MV-side – 1-Phase Case – With/Without Q regulation comparison in the scenario with 140 kW of PV connected to phase a and b

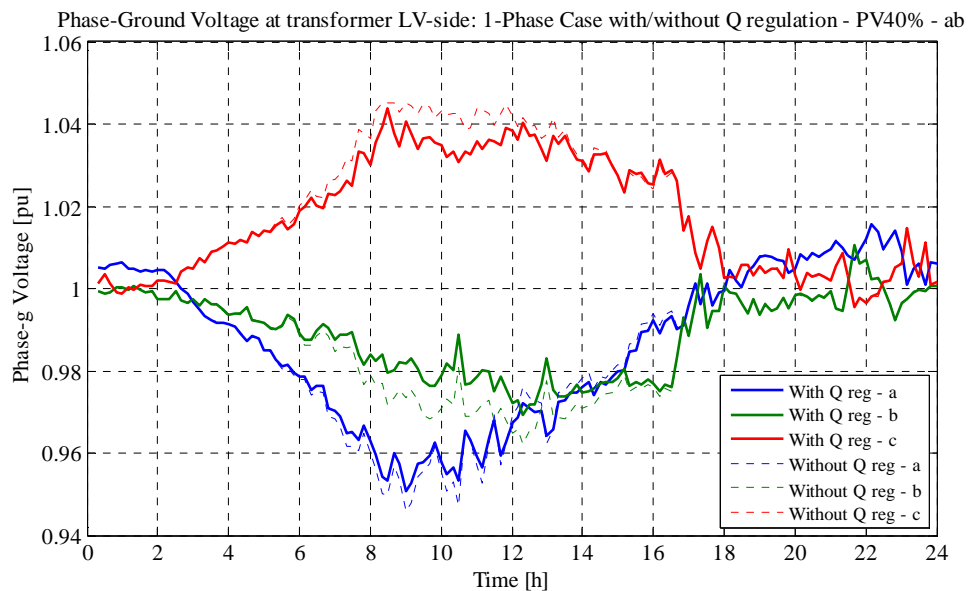


Figure 4.115. Phase-Ground Voltage at transformer LV-side – 1-Phase Case – With/Without Q regulation comparison in the scenario with 140 kW of PV connected to phase a and b

As depicted in Figure 4.116 the Q regulation makes the neutral-ground voltage at the worst bus gets closer: peaks decrease from 5.5% to 4.5%.

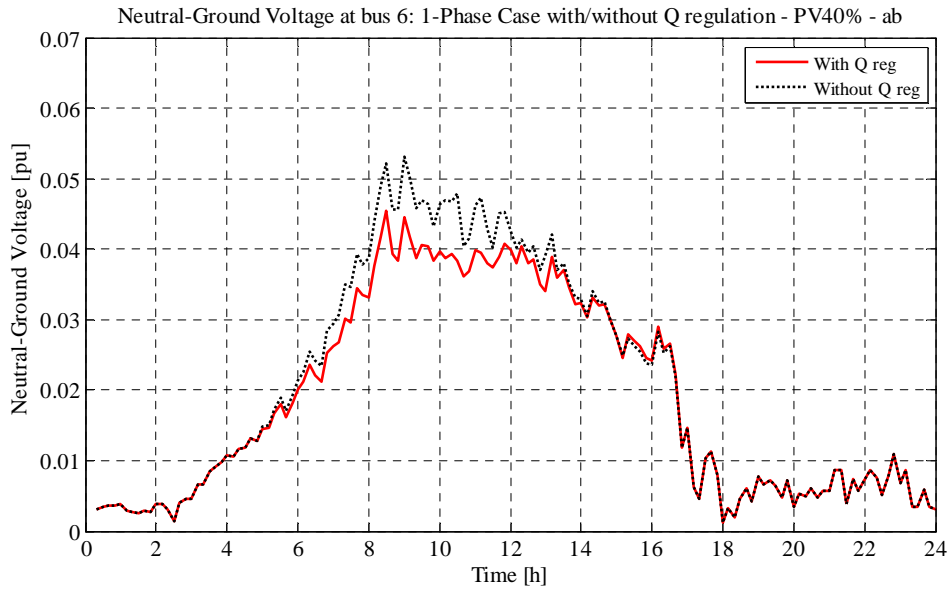


Figure 4.116. Neutral-Ground Voltage at bus 6 – 1-Phase Case – With/Without Q regulation comparison in the scenario with 140 kW of PV connected to phase a and b

From Figure 4.117 it can be deduced that the Q regulation is not able to reduce the VUF at bus 6: peaks are again around 2.5%.

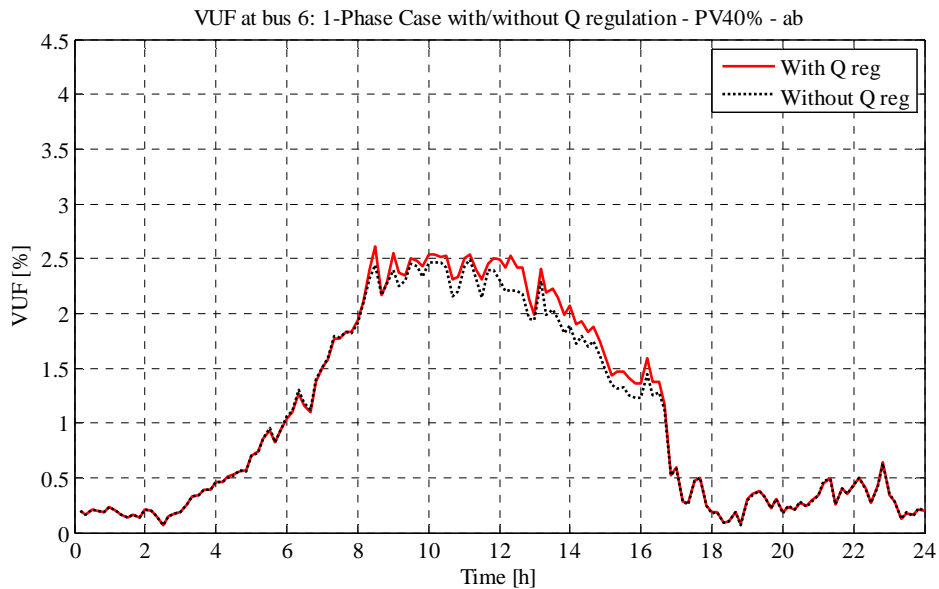


Figure 4.117. VUF at bus 6 – 1-Phase Case – With/Without Q regulation comparison in the scenario with 140 kW of PV connected to phase a and b

Both the total power loss and the power loss ratio get a bit reduced thanks to the reactive power regulation, as it can be noticed from Figure 4.118 and Figure 4.119.

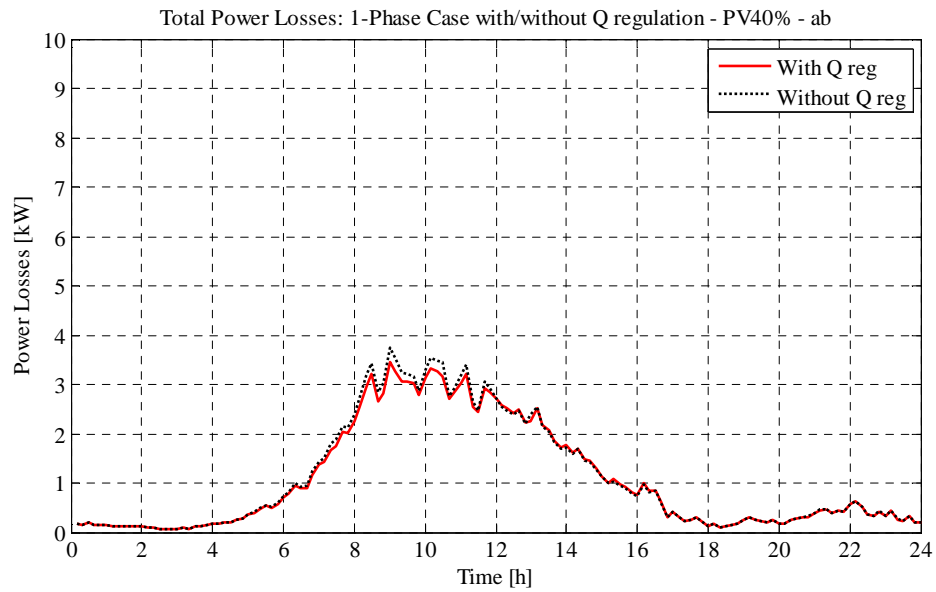


Figure 4.118. Total Power Losses – 1-Phase Case – With/Without Q regulation comparison in the scenario with 140 kW of PV connected to phase a and b

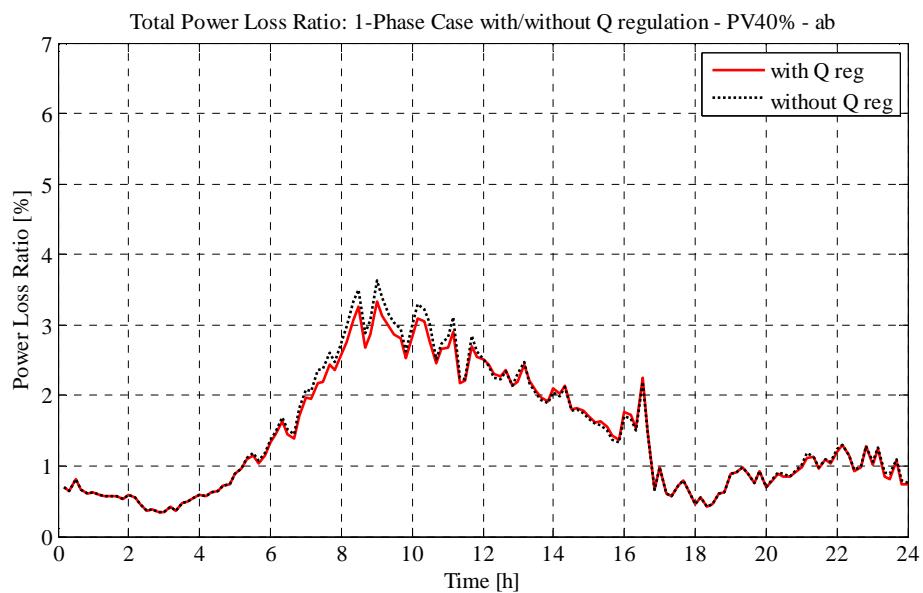


Figure 4.119. Total Power Loss Ratio – 1-Phase Case – With/Without Q regulation comparison in the scenario with 140 kW of PV connected to phase a and b

In Table 4.20 the total energy amounts absorbed by loads, injected by PVs and the amount through the transformer are reported together with the absolute energy loss and the energy loss deviations from the case without any Q regulation.

| Case | Total Energy absorbed by loads [kWh] | Total Energy injected by PV [kWh] | Energy through the trafo [kWh] | Energy Loss [kWh] | Energy Loss Deviation [%, compared to the case without Q regulation] |
|----------------------|--------------------------------------|-----------------------------------|--------------------------------|-------------------|--|
| Without Q regulation | 763.71 | 970.58 | -180.62 | 26.25 | +0.00% |
| With Q regulation | 757.74 | 974.70 | -192.48 | 24.48 | -6.74% |

Table 4.20. PV40% ab scenario 1-phase case – with/without Q regulation energy analysis comparison

4.3.2. PV50% – 175 kW – phases a and b

All the three phase-neutral voltages at the worst bus (bus 6) from 1-phase case without any reactive power regulation and the one with it, get closer to 1 p.u. Phase-neutral voltages and tap positions are depicted respectively in Figure 4.120 and in Figure 4.121.

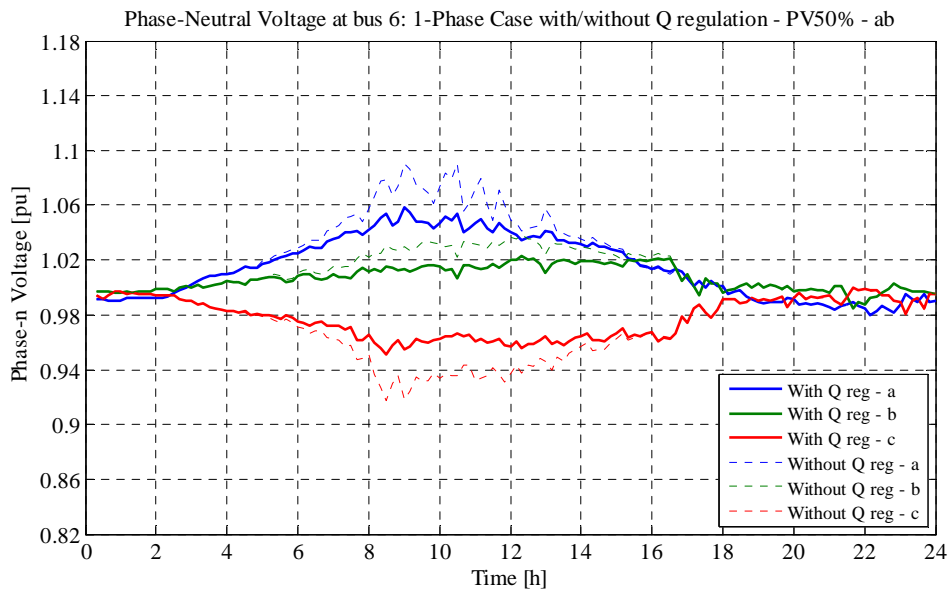


Figure 4.120. Phase-Neutral Voltage at bus 6 – 1-Phase Case – With/Without Q regulation comparison in the scenario with 175 kW of PV connected to phase a and b

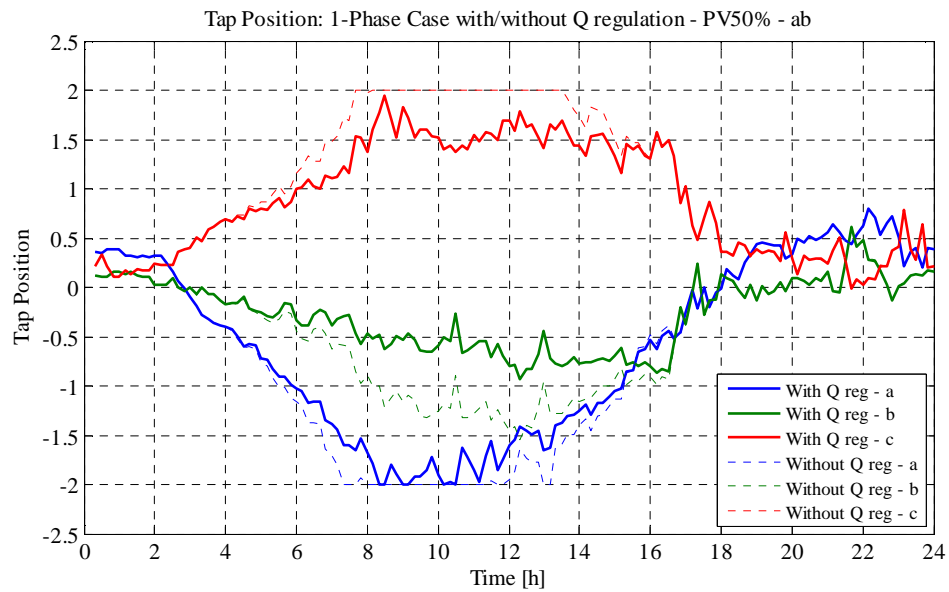


Figure 4.121. Tap Position – 1-Phase Case – With/Without Q regulation comparison in the scenario with 175 kW of PV connected to phase a and b

About the phase-ground voltages at the MV side of the transformer, it can be said that they all reduce because of the Q regulation (Figure 4.122). On the other hand, at the LV side only the one at phases a and reduce, while the other one increase: it can be seen from Figure 4.123. It has to be noticed that phase a reduces even below the -5% limit: almost till -6%.

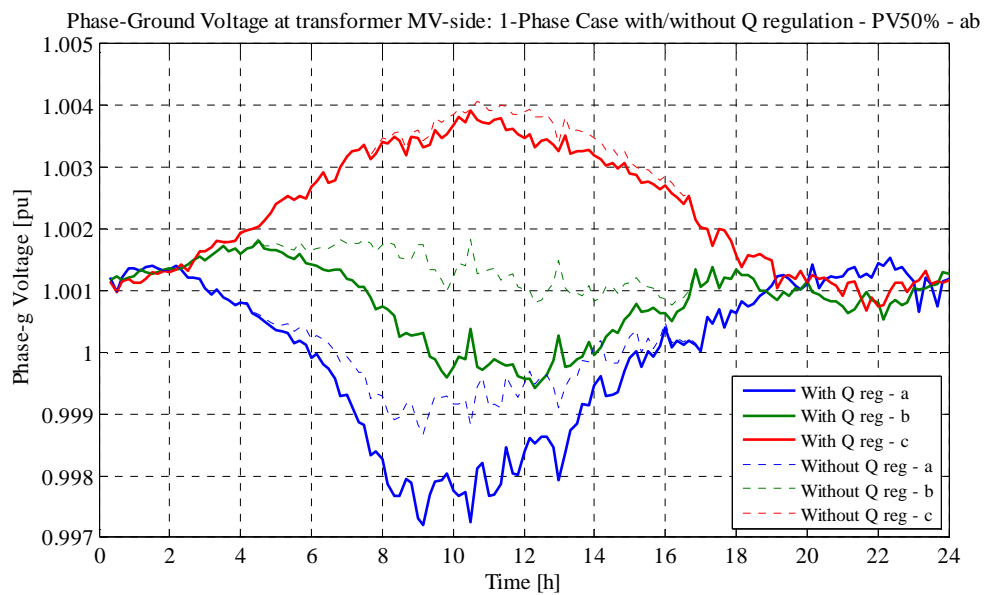


Figure 4.122. Phase-Ground Voltage at transformer MV-side – 1-Phase Case – With/Without Q regulation comparison in the scenario with 175 kW of PV connected to phase a and b

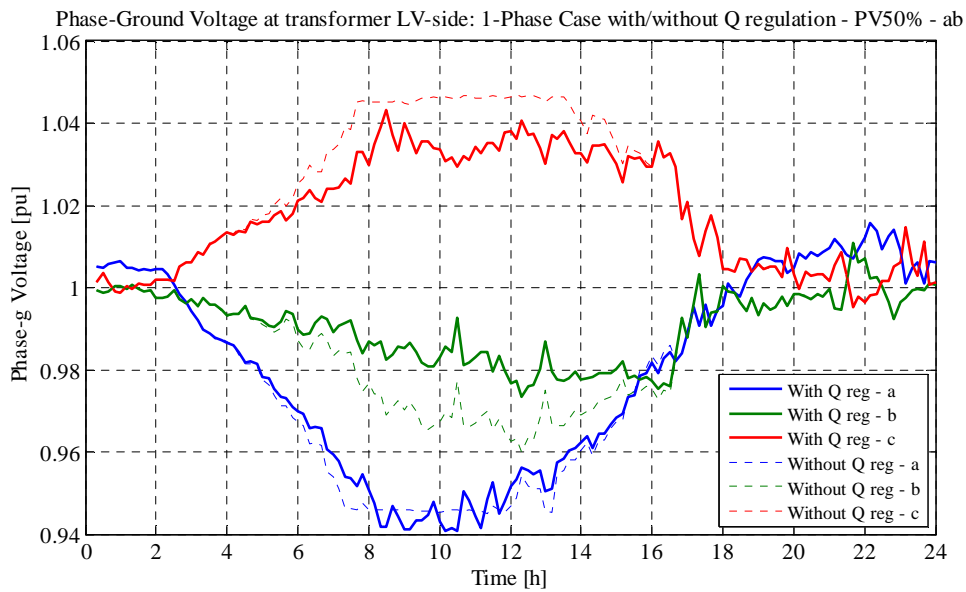


Figure 4.123. Phase-Ground Voltage at transformer LV-side – 1-Phase Case – With/Without Q regulation comparison in the scenario with 175 kW of PV connected to phase a and b

As depicted in Figure 4.124 the Q regulation makes the neutral-ground voltage at the worst bus gets closer: peaks decrease from 7% to 5%.

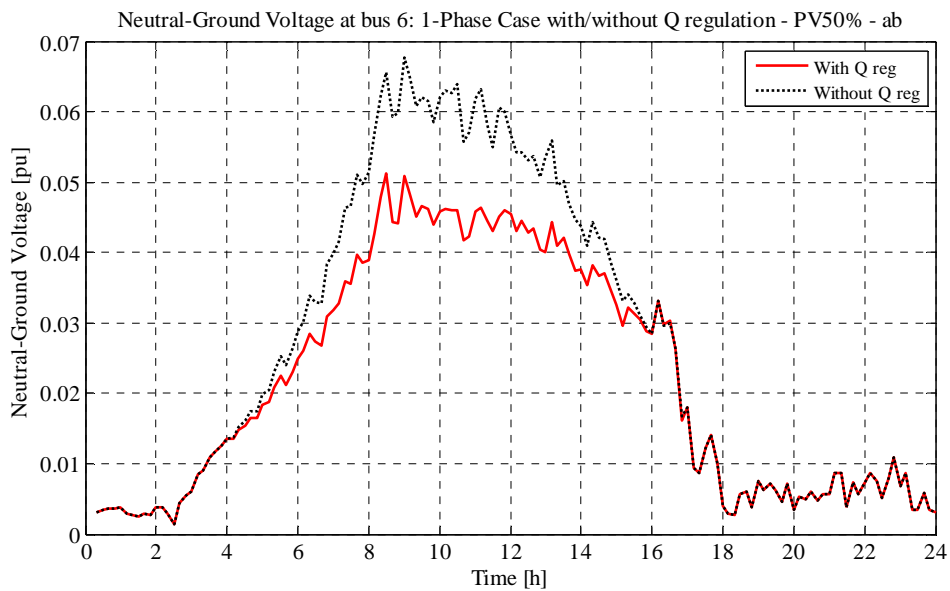


Figure 4.124. Neutral-Ground Voltage at bus 6 – 1-Phase Case – With/Without Q regulation comparison in the scenario with 175 kW of PV connected to phase a and b

From Figure 4.125 it can be deduced that the Q regulation is not able to reduce the VUF at bus 6: on the other hand it makes it bigger, since peaks grow from 2.7% to 3.5%.

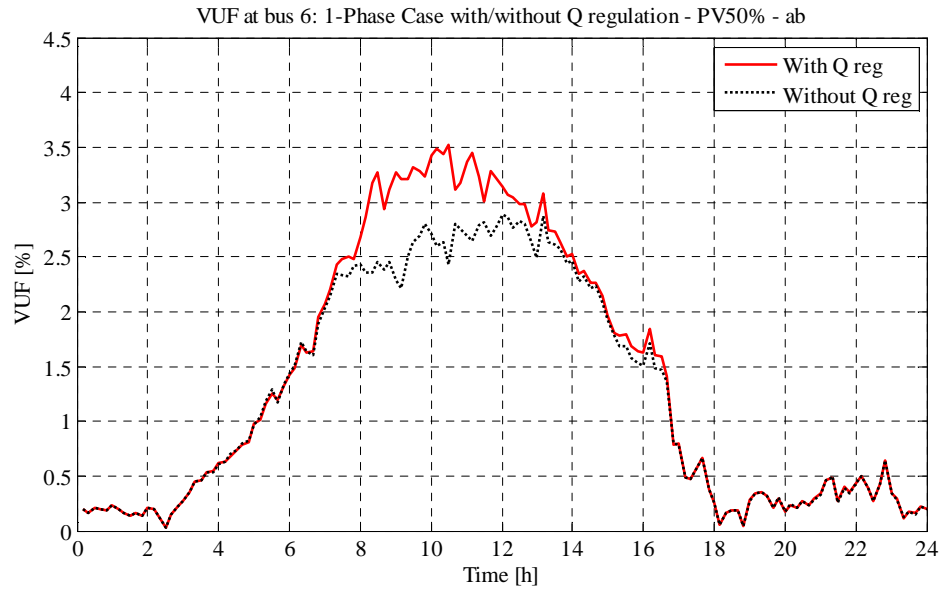


Figure 4.125. VUF at bus 6 – 1-Phase Case – With/Without Q regulation comparison in the scenario with 175 kW of PV connected to phase a and b

Both the total power loss and the power loss ratio get a bit reduced thanks to the reactive power regulation, as it can be noticed from Figure 4.126 and Figure 4.127.

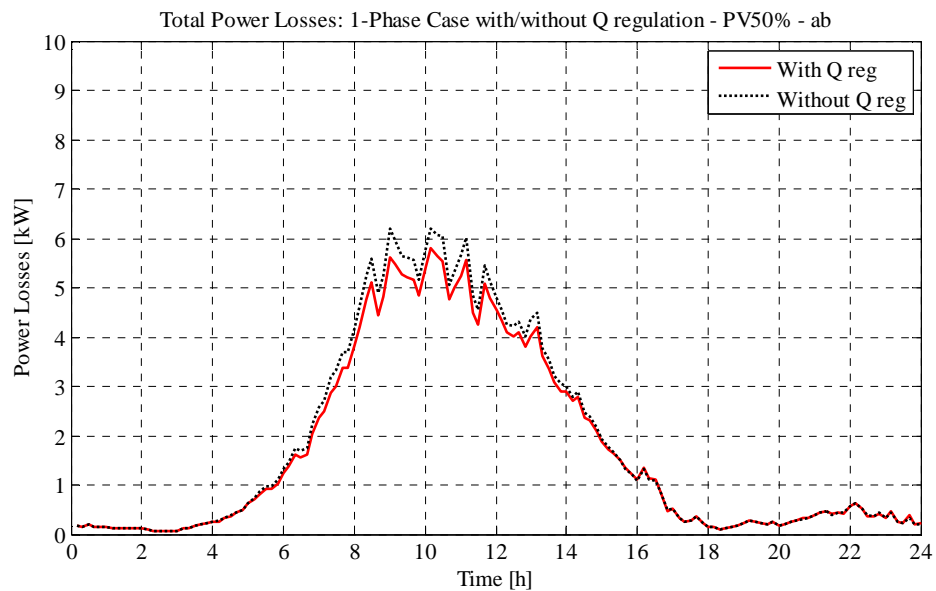


Figure 4.126. Total Power Losses – 1-Phase Case – With/Without Q regulation comparison in the scenario with 175 kW of PV connected to phase a and b

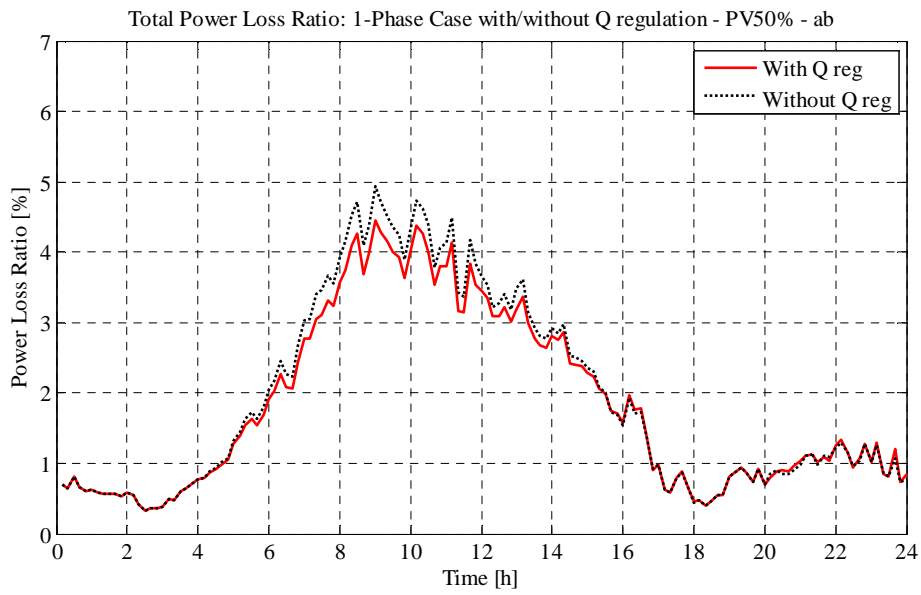


Figure 4.127. Total power Loss Ratio – 1-Phase Case – With/Without Q regulation comparison in the scenario with 175 kW of PV connected to phase a and b

In Table 4.21 the total energy amounts absorbed by loads, injected by PVs and the amount through the transformer are reported together with the absolute energy loss and the energy loss deviations from the case without any Q regulation.

| Case | Total Energy absorbed by loads [kWh] | Total Energy injected by PV [kWh] | Energy through the trafo [kWh] | Energy Loss [kWh] | Energy Loss Deviation [%, compared to the case without Q regulation] |
|----------------------|--------------------------------------|-----------------------------------|--------------------------------|-------------------|--|
| Without Q regulation | 765.04 | 1207.02 | -398.23 | 43.75 | +0.00% |
| With Q regulation | 764.03 | 1213.41 | -408.23 | 41.15 | -5.94% |

Table 4.21. PV50% ab scenario 1-phase case – with/without Q regulation energy analysis comparison

4.3.3. PV70% – 245 kW – phases a, b and c

All the three phase-neutral voltages at the worst bus (bus 6) from 1-phase case without any reactive power regulation and the one with it, get closer to 1 p.u. Phase-neutral voltages and tap positions are depicted respectively in Figure 4.128 and in Figure 4.129.

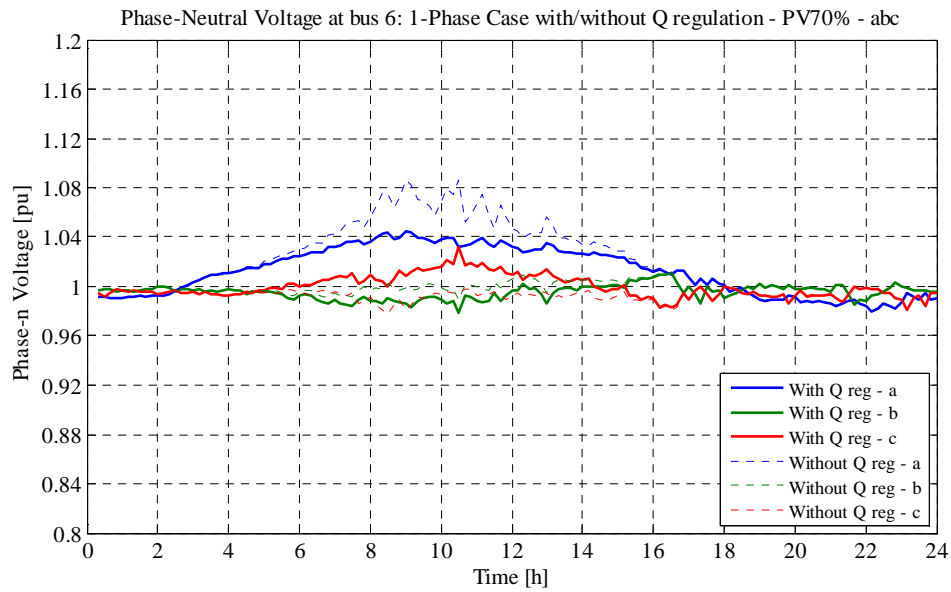


Figure 4.128. Phase-Neutral Voltage at bus 6 – 1-Phase Case – With/Without Q regulation comparison in the scenario with 245 kW of PV connected to phase a and b

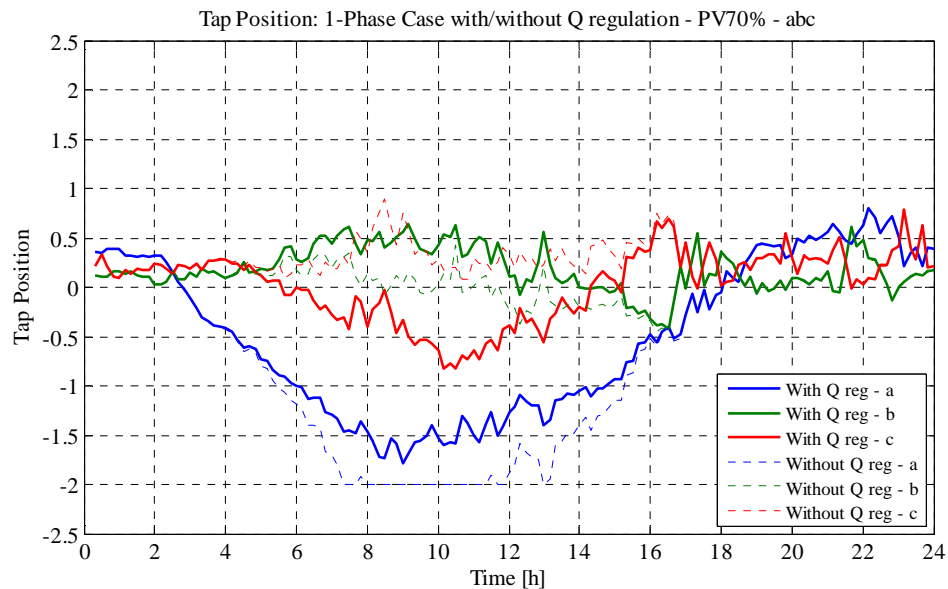


Figure 4.129. Tap Position – 1-Phase Case – With/Without Q regulation comparison in the scenario with 245 kW of PV connected to phase a and b

About the phase-ground voltages at the MV side of the transformer, it can be said that the ones at phases a and b reduce, while at phase c it is almost the same (Figure 4.130). On the other hand, at the LV side only the one at phase c gets reduced, while the other two increase: it can be seen from Figure 4.131.

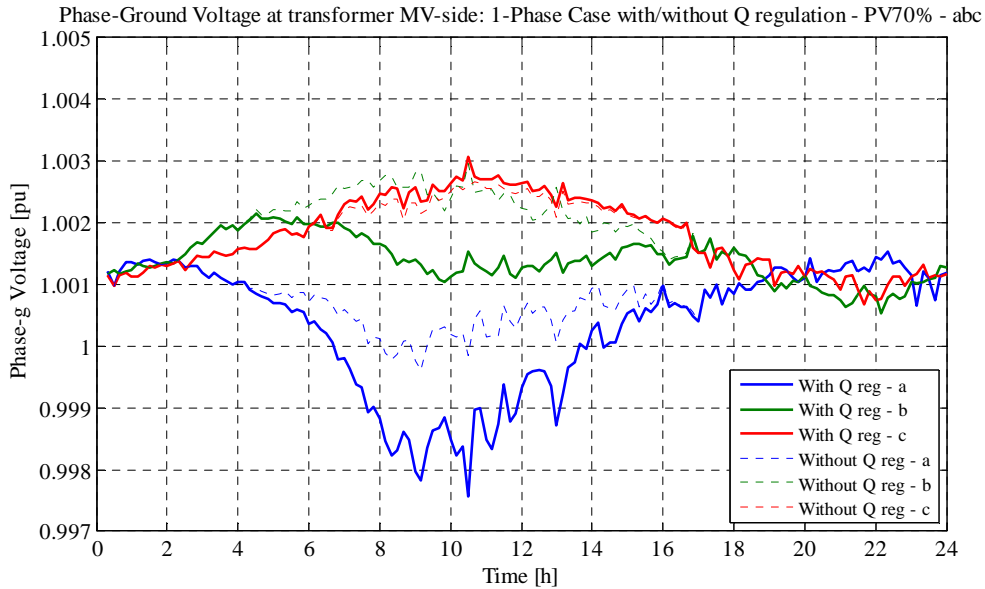


Figure 4.130. Phase-Ground Voltage at transformer MV-side – 1-Phase Case – With/Without Q regulation comparison in the scenario with 245 kW of PV connected to phase a and b

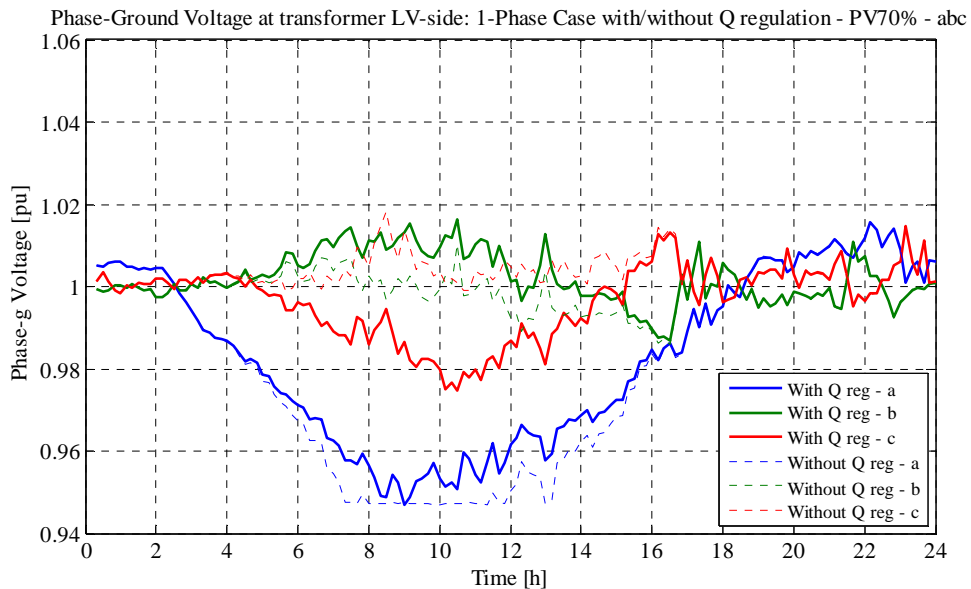


Figure 4.131. Phase-Ground Voltage at transformer LV-side – 1-Phase Case – With/Without Q regulation comparison in the scenario with 245 kW of PV connected to phase a and b

As depicted in Figure 4.132 the Q regulation makes the neutral-ground voltage at the worst bus gets closer: peaks decrease from 4.5% to 4%.

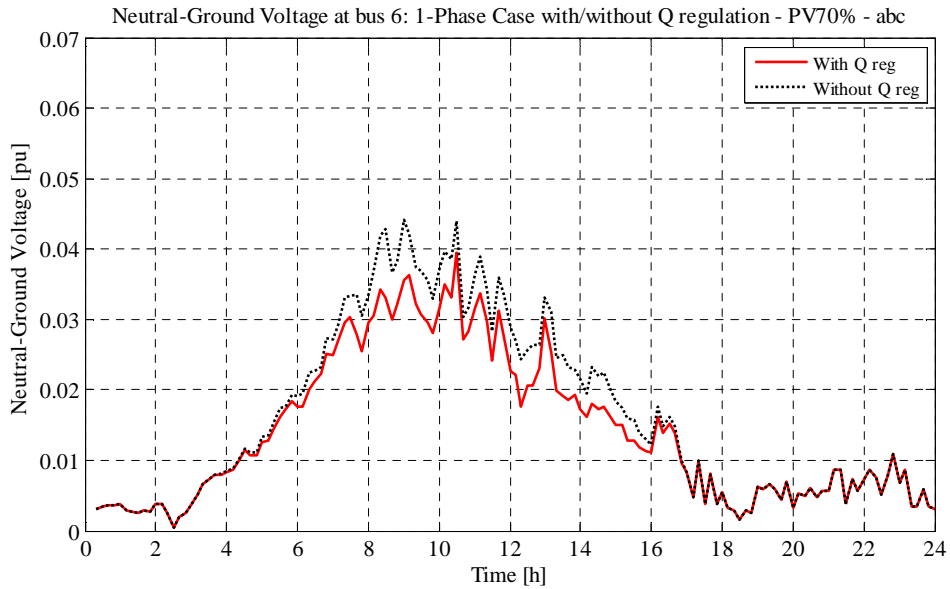


Figure 4.132. Neutral-Ground Voltage at bus 6 – 1-Phase Case – With/Without Q regulation comparison in the scenario with 245 kW of PV connected to phase a and b

From Figure 4.133 it can be deduced that the Q regulation is not able to reduce the VUF at bus 6: on the other hand it makes it bigger, since peaks grow from 2% to 4%.

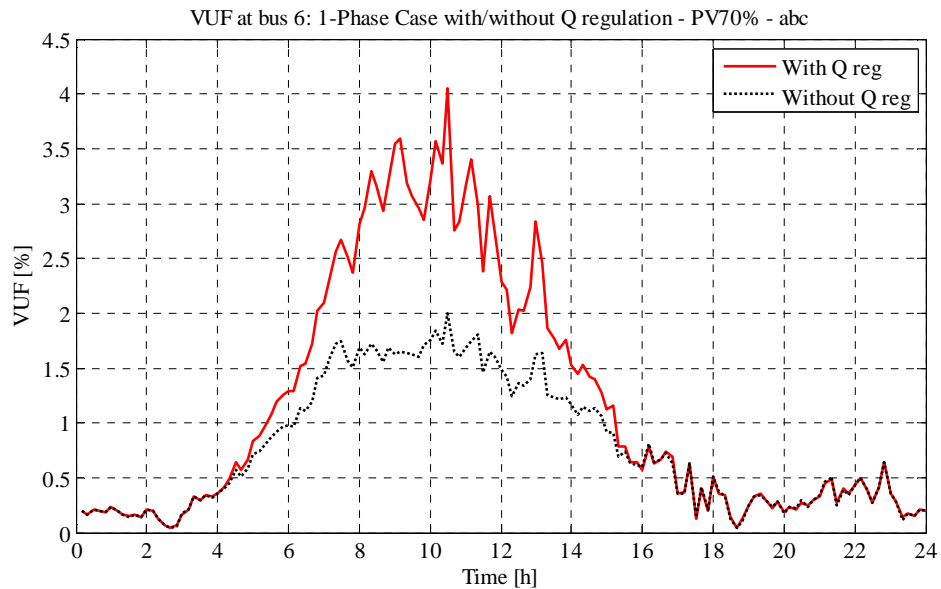


Figure 4.133. VUF at bus 6 – 1-Phase Case – With/Without Q regulation comparison in the scenario with 245 kW of PV connected to phase a and b

Both the total power loss and the power loss ratio get a bit increased due to the reactive power regulation, as it can be noticed from Figure 4.134 and Figure 4.135.

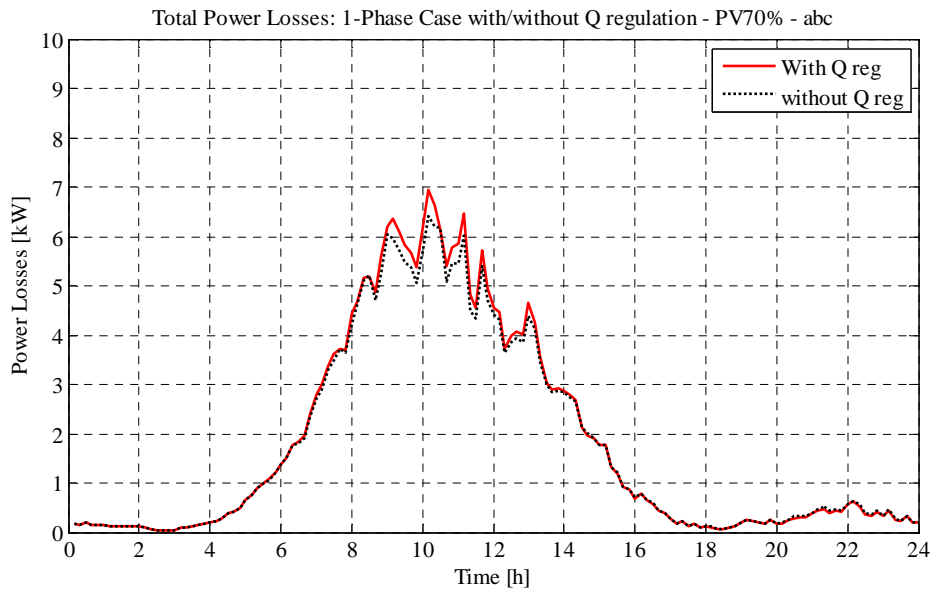


Figure 4.134. Total Power Losses – 1-Phase Case – With/Without Q regulation comparison in the scenario with 245 kW of PV connected to phase a and b

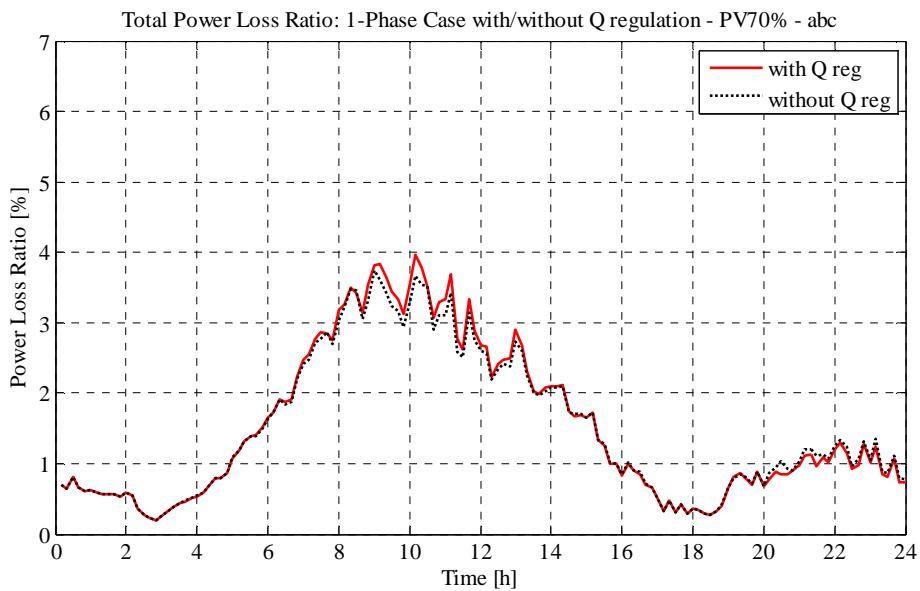


Figure 4.135. Total Power Loss Ratio – 1-Phase Case – With/Without Q regulation comparison in the scenario with 245 kW of PV connected to phase a and b

In Table 4.22 the total energy amounts absorbed by loads, injected by PVs and the amount through the transformer are reported together with the absolute energy loss and the energy loss deviations from the case without any Q regulation.

| Case | Total Energy absorbed by loads [kWh] | Total Energy injected by PV [kWh] | Energy through the trafo [kWh] | Energy Loss [kWh] | Energy Loss Deviation [%, compared to the case without Q regulation] |
|----------------------|--------------------------------------|-----------------------------------|--------------------------------|-------------------|--|
| Without Q regulation | 769.12 | 1713.54 | -902.70 | 41.72 | +0.00% |
| With Q regulation | 767.34 | 1715.44 | -904.88 | 43.22 | +3.60% |

Table 4.22. PV70% abc scenario 1-phase case – with/without Q regulation energy analysis comparison

4.3.4. PV80% – 280 kW – phases a, b and c

As it can be seen in Figure 4.136, the phase-neutral voltages at bus 6 are characterized by many fluctuations, which of course are not desired.

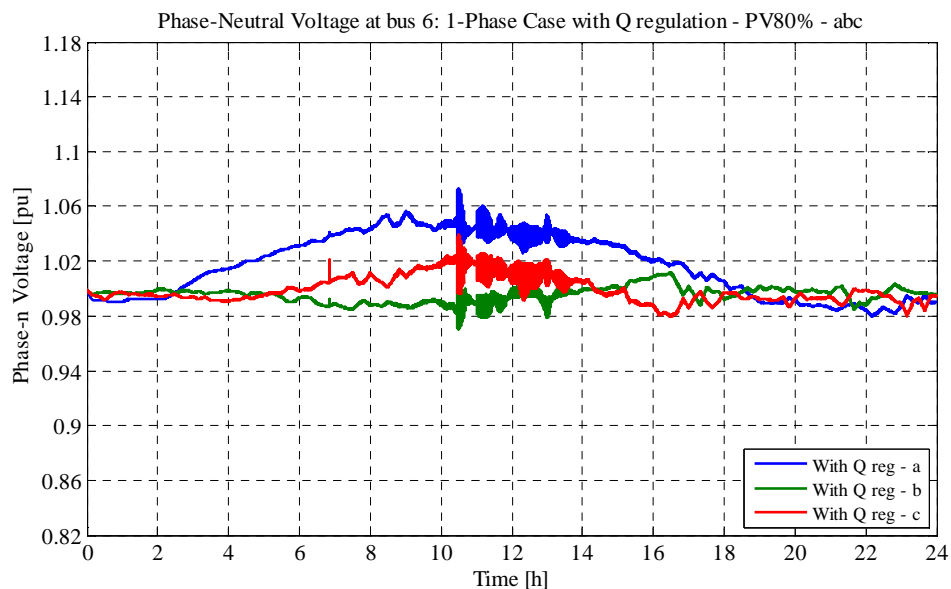


Figure 4.136. Phase-Neutral Voltage at bus 6 – 1-Phase Case – With/Without Q regulation comparison in the scenario with 280 kW of PV connected to phase a and b

The cause is due to the too high gain of reactive power regulation law (described in Chapter 3.3), which makes the control system unstable.

Due to this, it has been decided to consider a different $Q=f(V,P)$ law, which is shown in Figure 4.137. Compared to the previous one (Figure 3.3), it presents the same dead band but a different gain: there is a continuous growth/decrease from the limit voltage values of the dead band to the extreme voltage values of the regulation algorithm.

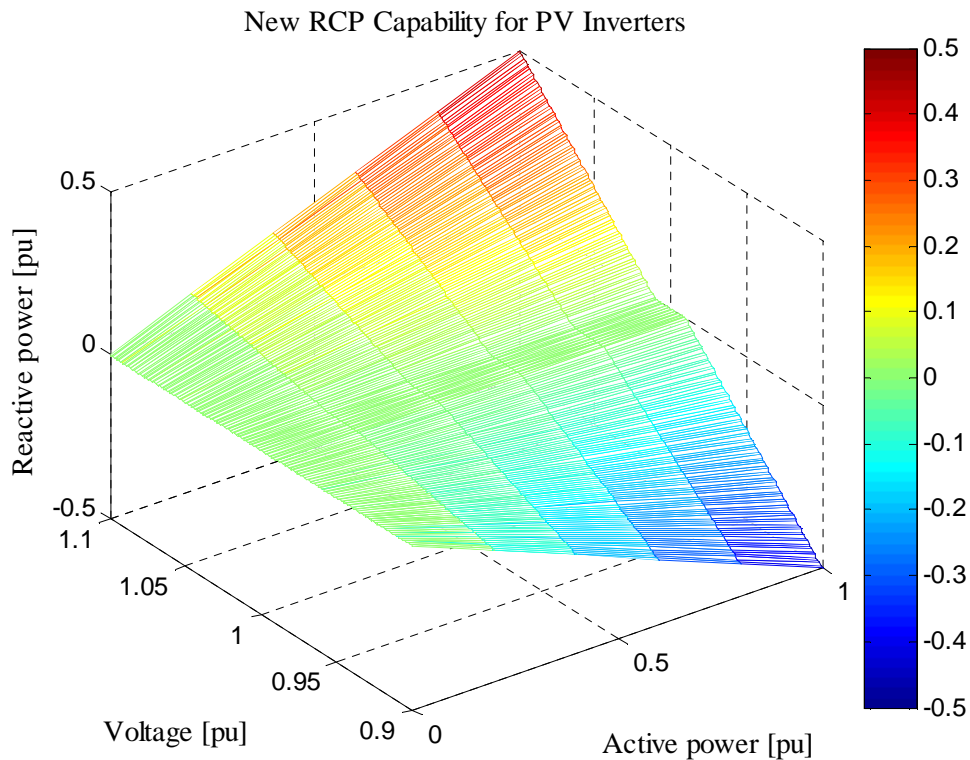


Figure 4.137. New Reactive Power Control capability for PV inverter

Thanks to this expedient, it has been possible to avoid the undesired fluctuations.

According to this new regulation law, plots and numerical results are now reported below.

All the three phase-neutral voltages at the worst bus (bus 6) from 1-phase case without any reactive power regulation to the one with it, get closer to 1 p.u: the voltage at phase a is now within the limit. Phase-neutral voltages and tap positions are depicted respectively in Figure 4.138 and in Figure 4.139.

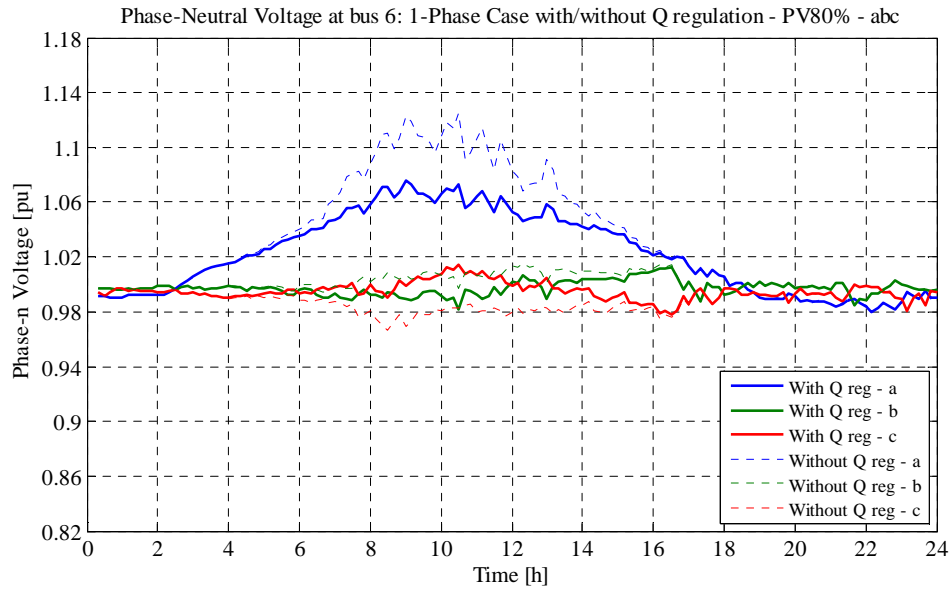


Figure 4.138. Phase-Neutral Voltage at bus 6 – 1-Phase Case – With/Without Q regulation comparison in the scenario with 280 kW of PV connected to phase a and b

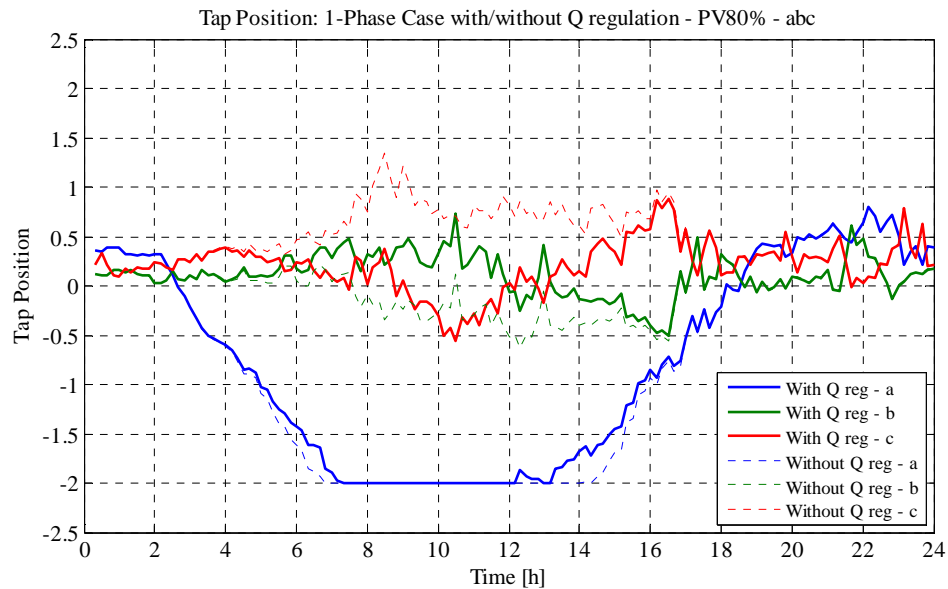


Figure 4.139. Tap Position – 1-Phase Case – With/Without Q regulation comparison in the scenario with 280 kW of PV connected to phase a and b

About the phase-ground voltages at the MV side of the transformer, it can be said that the ones at phases a and b reduce, while at phase c it is almost the same (Figure 4.140). On the other hand, at the LV side the ones at phases a and c get reduced, while the other one increase: it can be seen from Figure 4.141. It has to be noticed that phase a reduces even below the -5% limit: almost till -6%.

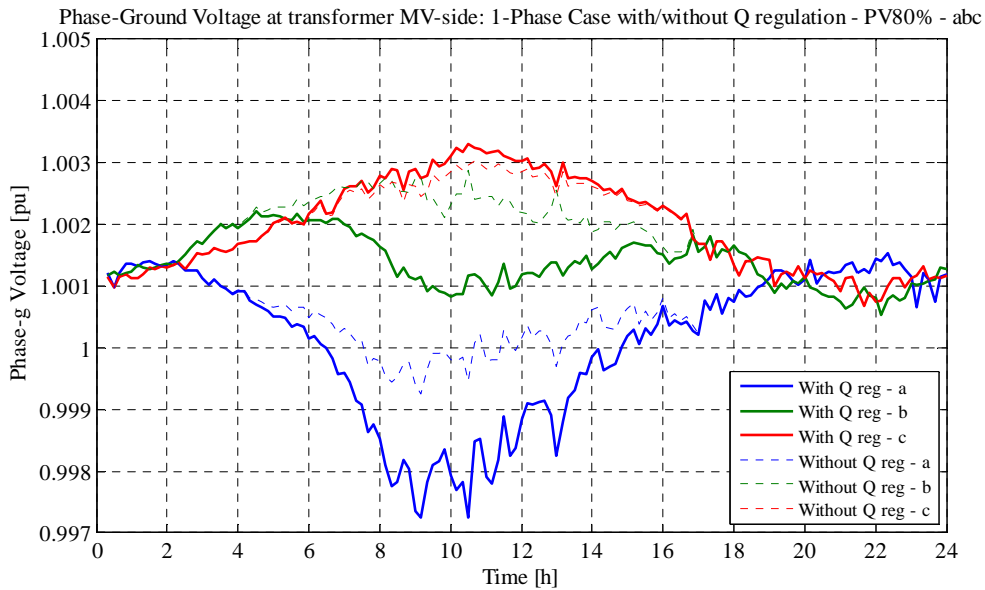


Figure 4.140. Phase-Ground Voltage at transformer MV-side – 1-Phase Case – With/Without Q regulation comparison in the scenario with 280 kW of PV connected to phase a and b

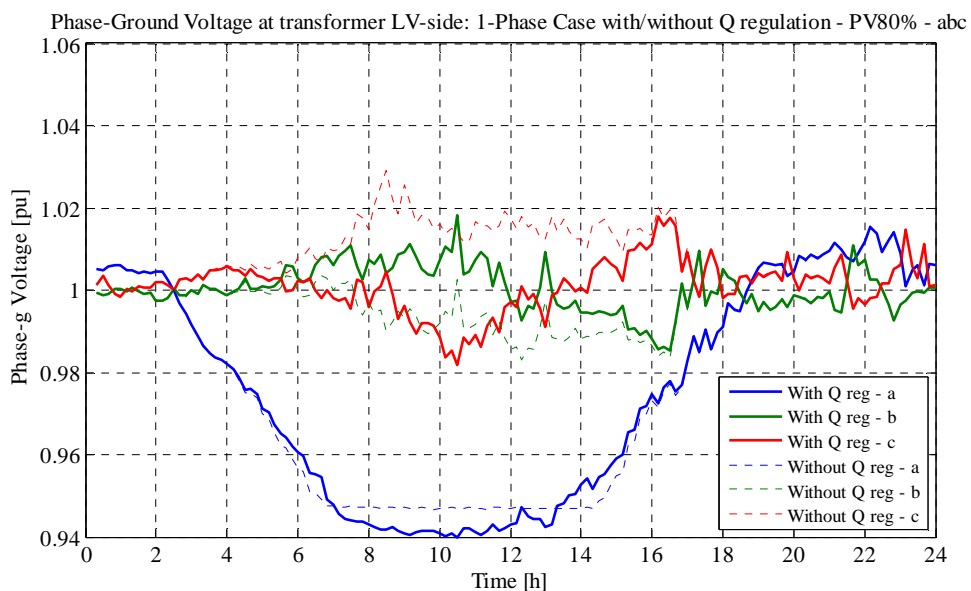


Figure 4.141. Phase-Ground Voltage at transformer LV-side – 1-Phase Case – With/Without Q regulation comparison in the scenario with 280 kW of PV connected to phase a and b

As depicted in Figure 4.142 the Q regulation makes the neutral-ground voltage at the worst bus gets closer: peaks decrease from 6% to 5%.

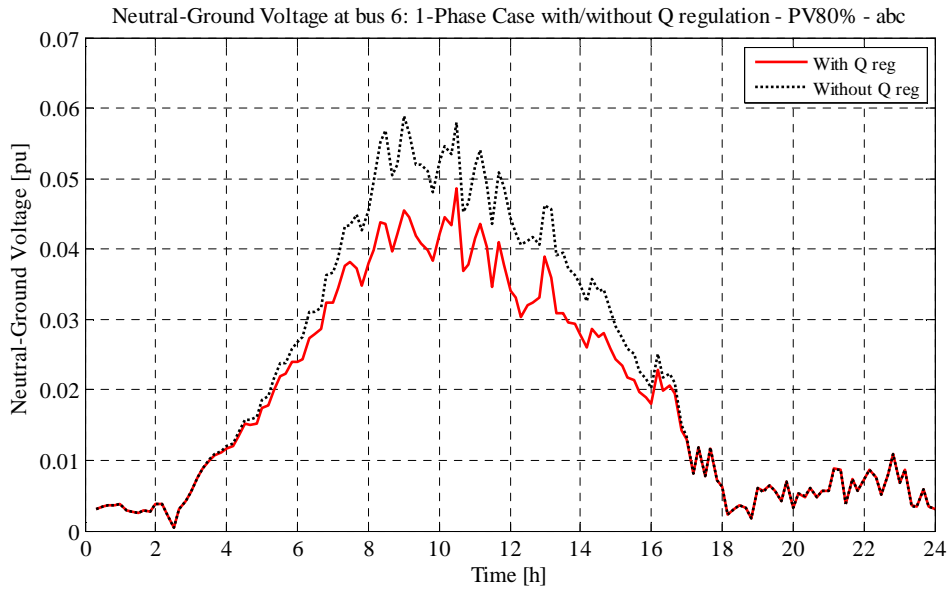


Figure 4.142. Neutral-Ground Voltage at bus 6 – 1-Phase Case – With/Without Q regulation comparison in the scenario with 280 kW of PV connected to phase a and b

From Figure 4.143 it can be deduced that the Q regulation is not able to reduce the VUF at bus 6: on the other hand it makes it bigger, since peaks grow from 2% to 4.5%.

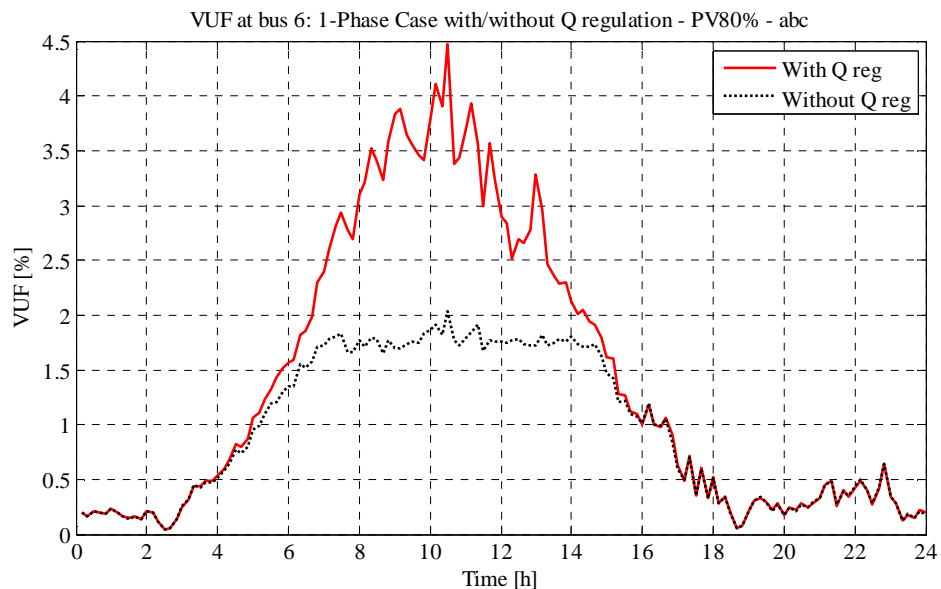


Figure 4.143. VUF at bus 6 – 1-Phase Case – With/Without Q regulation comparison in the scenario with 280 kW of PV connected to phase a and b

Both the total power loss and the power loss ratio do not present relevant differences due to the reactive power regulation, as it can be noticed from Figure 4.144 and Figure 4.145.

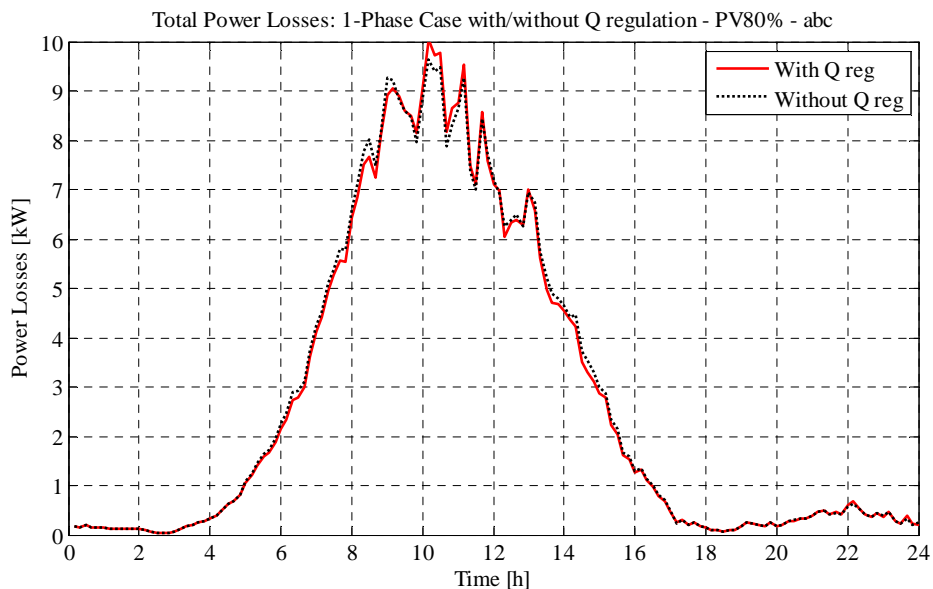


Figure 4.144. Total Power Losses – 1-Phase Case – With/Without Q regulation comparison in the scenario with 280 kW of PV connected to phase a and b

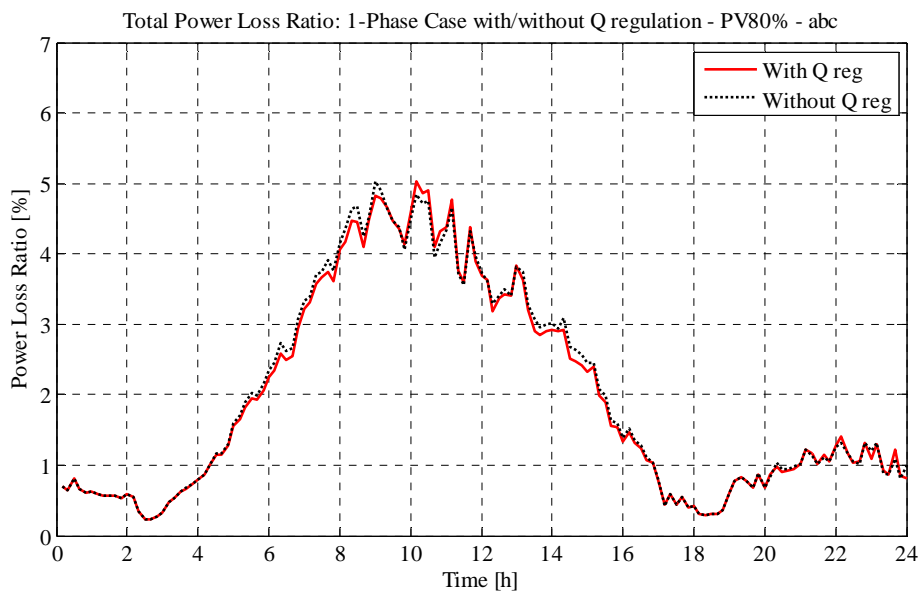


Figure 4.145. Total Power Loss Ratio – 1-Phase Case – With/Without Q regulation comparison in the scenario with 280 kW of PV connected to phase a and b

In Table 4.23 the total energy amounts absorbed by loads, injected by PVs and the amount through the transformer are reported together with the absolute energy loss and the energy loss deviations from the case without any Q regulation.

| Case | Total Energy absorbed by loads [kWh] | Total Energy injected by PV [kWh] | Energy through the trafo [kWh] | Energy Loss [kWh] | Energy Loss Deviation [%, compared to the case without Q regulation] |
|----------------------|--------------------------------------|-----------------------------------|--------------------------------|-------------------|--|
| Without Q regulation | 774.00 | 1952.04 | -1114.53 | 63.69 | +0.00% |
| With Q regulation | 769.04 | 1956.51 | -1122.65 | 64.82 | +1.77% |

Table 4.23. PV80% abc scenario 1-phase case – with/without Q regulation energy analysis comparison

4.4. With Q regulation cases: results comments and analysis

The second set of simulations are based on the consideration of inductive-capacitive reactive power injection from the photovoltaic inverters according to the $Q=f(V,P)$ law, previously described in detail in Chapter 3.3.

As said at the end of Chapter 4.2, the cases re-considered with this additional control algorithm have been the 40% and 50% ab cases and the ones with highest PV power injection, i.e. the 70% and the 80% abc cases. Comparisons between the 1-phase cases in the scenarios with and without Q regulation have been performed.

40% and 50% ab cases

The overall results of both the 40% and the 50% case show that positive benefits have been improved upon the phase-neutral voltages at the final bus, the neutral ground voltage at the same one and the total and relative power loss amounts. Not any relevant difference has been found at the phase-neutral voltages at the MV side of the transformer, but on the other hand in the 50% case at the LV side the voltage peaks at phase a has been decreased below the lower limit of -5%. About the VUF at the final bus, it has been found that it has not been reduced with the Q regulation: in the 50% case it has been even increased. Finally the energy losses in these two cases have been decreased of a few percentage points thanks to the reactive power control system.

In the 40% ab scenario, i.e. the one with 140kW connected to phases a and b, the 1-phase case results with the reactive power regulation control system are:

- phase-neutral voltages at the final bus within the range -4%/+4.5%;
- phase-ground voltages at the transformer level practically at the nominal values;
- neutral-ground voltage peaks at the final bus at around 4.5% of the phase-ground nominal value (230 V);
- VUF peaks around 2.5%;

- amount of energy losses of about 24.48 kWh, i.e. around -6.74% compared to the case without reactive power regulation;
- maximum power loss ratio of about 3.5%.

The situation is very similar to the one without Q regulation, with the main difference that now the neutral conductor potential at the worst bus stays below 4.5%. The phase-neutral voltages at the same bus got closer to 1 p.u. and the VUF has practically not changed.

What have changed have been the analyzed energy amounts, whose analysis and comparisons are reported in Table 4.24.

| Case | Total Energy absorbed by loads [kWh] | Total Energy injected by PV [kWh] | Energy through the trafo [kWh] | Energy Loss [kWh] | Energy Loss Deviation [%, compared to the case without Q regulation] |
|----------------------|--------------------------------------|-----------------------------------|--------------------------------|-------------------|--|
| Without Q regulation | 763.71 | 970.58 | -180.62 | 26.25 | +0.00% |
| With Q regulation | 757.74 | 974.70 | -192.48 | 24.48 | -6.74% |

Table 4.24. PV40% ab scenario 1-phase case – with/without Q regulation energy analysis comparison

In the 50% ab scenario, i.e. the one with 175 kW connected to phases a and b, the 1-phase case results with the reactive power regulation control system are:

- phase-neutral voltages at the final bus within the range -4%/+6%;
- phase-ground voltages at the transformer level within the range -6%/+5%;
- neutral-ground voltage peaks at the final bus at around 5% of the nominal value;
- VUF peaks around 3.5%;
- amount of energy losses of about 41.15 kWh, i.e. around -5.94% compared to the case without reactive power regulation;
- maximum power loss ratio of about 4.5%.

The situation is quite different to the one without Q regulation, because now, in addition to the fact that the phase-neutral voltages at the worst bus are much closer to the nominal value,

the neutral potential peaks at the same bus decreased a lot (from 7% to 5%). Again negative effects have been found about the VUF at bus 6: its peaks increased over 3%.

Energy amounts analysis and comparisons are reported in Table 4.25.

| Case | Total Energy absorbed by loads [kWh] | Total Energy injected by PV [kWh] | Energy through the trafo [kWh] | Energy Loss [kWh] | Energy Loss Deviation [%, compared to the case without Q regulation] |
|----------------------|--------------------------------------|-----------------------------------|--------------------------------|-------------------|--|
| Without Q regulation | 765.04 | 1207.02 | -398.23 | 43.75 | +0.00% |
| With Q regulation | 764.03 | 1213.41 | -408.23 | 41.15 | -5.94% |

Table 4.25. PV50% ab scenario 1-phase case – with/without Q regulation energy analysis comparison

70% Case

In the 70% case, which refers to a PV power connection of 245 kW, the following two positive effects have been found: the phase-neutral voltages at the worst bus gets closer to the nominal value and the neutral conductor potential at the same bus got reduced. On the other hand the same negative effect on the VUF appeared.

About the energy losses, it can be said that in this case the reactive power control system led to a few percentage points increase.

The results of this case are:

- phase-neutral voltages at the final bus within the range -2%/+4.5%;
- phase-ground voltages at the transformer level within the range -5%/+2%;
- neutral-ground voltage peaks at the final bus at around 4% of the nominal value;
- VUF peaks around 4%;
- amount of energy losses of about 43.22 kWh, i.e. around +3.60% compared to the case without reactive power regulation;
- maximum power loss ratio of about 4%.

Energy amounts analysis and comparisons are reported in Table 4.26.

| Case | Total Energy absorbed by loads [kWh] | Total Energy injected by PV [kWh] | Energy through the trafo [kWh] | Energy Loss [kWh] | Energy Loss Deviation [%, compared to the case without Q regulation] |
|----------------------|--------------------------------------|-----------------------------------|--------------------------------|-------------------|--|
| Without Q regulation | 769.12 | 1713.54 | -902.70 | 41.72 | +0.00% |
| With Q regulation | 767.34 | 1715.44 | -904.88 | 43.22 | +3.60% |

Table 4.26. PV70% abc scenario 1-phase case – with/without Q regulation energy analysis comparison

80% Case

In the 80% case, which refers to a PV power connection of 280 kW, as it could be seen in Figure 4.136, the phase-neutral voltages at bus 6 are characterized by many fluctuations, which of course are not desired at all. The cause is due to the too high gain of reactive power regulation law (described in Chapter 3.3), which makes the control system unstable.

As previously said in Chapter 4.3.4, it has been decided to consider a different $Q=f(V,P)$ law (Figure 4.146), which, compared to the previous one, presents the same dead band but a different gain: there is a continuous growth/decrease from the limit voltage values of the dead band to the extreme voltage values of the regulation algorithm.

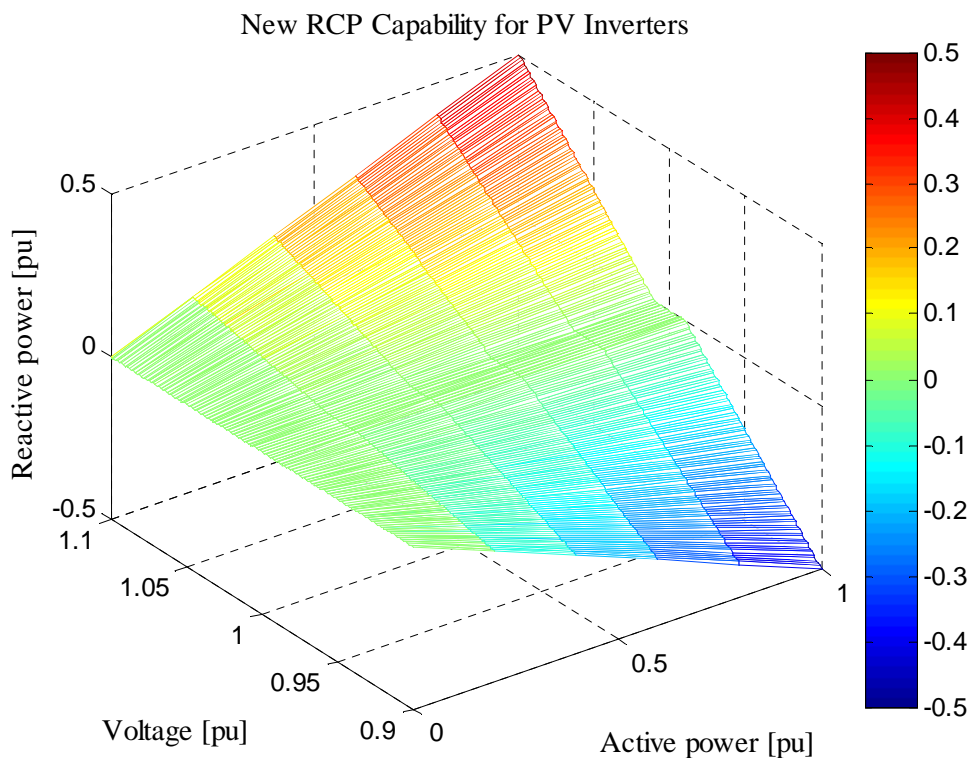


Figure 4.146. New Reactive Power Control capability for PV inverter

Thanks to this expedient, it has been possible to avoid the undesired fluctuations.

According to these considerations, it could be concluded that the fluctuations take place in presence of high PV power injection on one single phase (the 50% of the total amount of the energy in this case – 64.82 kWh – is injected only into one phase, i.e. 32.41 kWh injected into phase a), which is much bigger than the one absorbed by loads at phase a, i.e. 295.5 kWh.

A conclusion to this is that the DSO should take into account that if it issues reactive power regulation laws with a so high gain as in the first case, it could happen that fluctuations take place if a so high PV power amount is connected to the grid; in this case it should provide regulation laws with a smaller gain, so that it could be possible to accept such a high PV penetration.

In this case, considering as said the new Q regulation law, the following two positive effects have been found: the phase-neutral voltages at the worst bus gets closer to the nominal value and are now within the limit range, and the neutral conductor potential at the same bus got reduced. On the other hand the same negative effect on the VUF appeared.

About the energy losses, it can be said that in this case the reactive power control system led to a few percentage points increase.

The results of this case are:

- phase-neutral voltages at the final bus within the range -2%/+8%;
- phase-ground voltages at the transformer level within the range -6%/+2%;
- neutral-ground voltage peaks at the final bus at around 5% of the nominal value;
- VUF peaks around 4.5%;
- amount of energy losses of about 64.82 kWh, i.e. around +1.7% compared to the case without reactive power regulation;
- maximum power loss ratio of about 5%.

Energy amounts analysis and comparisons are reported in Table 4.27.

| Case | Total Energy absorbed by loads [kWh] | Total Energy injected by PV [kWh] | Energy through the trafo [kWh] | Energy Loss [kWh] | Energy Loss Deviation [%, compared to the case without Q regulation] |
|----------------------|--------------------------------------|-----------------------------------|--------------------------------|-------------------|--|
| Without Q regulation | 774.00 | 1952.04 | -1114.53 | 63.69 | +0.00% |
| With Q regulation | 769.04 | 1956.51 | -1122.65 | 64.82 | +1.77% |

Table 4.27. PV80% abc scenario 1-phase case – with/without Q regulation energy analysis comparison

Finally it can be concluded that both the two reactive power regulation algorithms brought real great benefits on the phase-neutral voltages, reducing their deviations to the nominal 1 p.u. value. Moreover it leded positive effects also upon the neutral-ground potential, which has always been reduced: even sometimes permitting to get below the 5% limit when it was higher. Not too relevant variations – few percentage points – have been caused to the total energy loss amount.

What has highly been changed in a negative way has been the level of voltage unbalance at the final bus, i.e. the VUF index, since its value grew in all the cases characterized by the reactive power control system.

The reason is naturally related to the positive and negative sequences amounts.

Since the algorithm is just based on active power and phase-neutral voltage measurements, it is clear that the implemented reactive power control law does not absolutely take into account any sequence-related index.

Therefore it could be concluded that the acceptable limit case is the 80% case (i.e. a PV penetration of 280 kW), since the phase-neutral voltages at bus 6 and the neutral conductor potential are within the respective limits and since the energy loss are still acceptable. The situation could be considered infeasible if the VUF at bus 6 is considered, since it exceeds the extreme limit of 3%. Actually this index is not supposed to be controlled by the tap logic system, neither by the reactive power one: for this reason the DSO is supposed to consider this aspect and look for other expedients.

At the end it can be concluded that the algorithm works well, since its proper regulation goal is the approach of the three phase-neutral voltages to the nominal value. Its operations also permit to obtain very positive effects to the neutral voltage too. Any relevant negative effect is caused on the energy loss amounts and to the voltages at the transformer level. The mentioned negative effects on the VUF amounts have to be considered and taken into

account by the DSO, which has to guarantee that it lies below the limits issued by the national and European technical standards. The DSO should so consider this VUF increase and decide if it needs to be controlled and monitored directly from the same reactive power algorithm, or if it should be managed by other control algorithms in other points of the distribution grids.

Nevertheless it should be remembered that all these analyzed cases are characterized by very high unbalanced conditions and by very high active power injection amounts, which very improbable could be found practically in the reality.

All the comparisons of the analyzed scenarios are simply summarized in Table 4.28:

| PV 40% ab Scenario: 140 kW PV connected to phases a and b | | |
|--|-----------------------------|--------------------------|
| | Without Q regulation | With Q regulation |
| Voltages deviation (an, bn, cn) at bus 6 | -6.5%/+5% | -4%/+4.5% |
| Max VUF at bus 6 | 2.5% | 2.5% |
| Max neutral potential | 5.5% | 4.5% |
| Total losses [kWh] | 26.25 | 24.48 (-6.74%) |
| PV 50% ab Scenario: 175 kW PV connected to phases a and b | | |
| | Without Q regulation | With Q regulation |
| Voltages deviation (an, bn, cn) at bus 6 | -8%/+9% | -4%/+6% |
| Max VUF at bus 6 | 2.9% | 3.5% |
| Max neutral potential | 7% | 5% |
| Total losses [kWh] | 43.75 | 41.15 (-5.94%) |
| PV 70% Scenario: : 245 kW PV connected to phases a, b and c | | |
| | Without Q regulation | With Q regulation |
| Voltages deviation (an, bn, cn) at bus 6 | -2%/+8.8% | -2%/+4.5% |
| Max VUF at bus 6 | 2.05% | 4% |
| Max neutral potential | 4.5% | 4% |
| Total losses [kWh] | 41.72 | 43.22 (+3.60%) |
| PV 80% Scenario: 280 kW PV connected to phases a, b and c | | |
| | Without Q regulation | With Q regulation |
| Voltages deviation (an, bn, cn) at bus 6 | -3%/+12% | -2%/+8% |
| Max VUF at bus 6 | 2.05% | 4.5% |
| Max neutral potential | 6% | 5% |
| Total losses [kWh] | 63.69 | 64.82 (+1.77%) |

Table 4.28. Overall comparisons summary

Chapter 5

Conclusions

This work has presented the simulation studies carried out in a project in collaboration with the Danish counselling company ‘PSS Energy’ where the aim was to develop and test the feasibility of a decoupled three-phase OLTC transformer in the distribution system with the objective of improving the distribution network power quality.

Further simulations and analysis have been run considering an additional control system, based on the management of the reactive power provision by the PV plants according to local real time voltage and active power measurements; investigations on coordinated control solutions between the OLTC control and reactive power provision by PVs have been performed. The reactive control provision logic has been set according to a specific $Q=f(V,P)$ 3D-curve, which includes topics both of the Italian and the German technical guidelines for distributed generation plants connected to MV or LV grids.

A real Danish low voltage network with characterizing real measurement data of the loads and realistic PV generation profiles have been used to apply the proposed control systems.

To perform the RMS (root mean square) simulation, the grid elements behavior and the control scheme for both the OLTC and the reactive power controller have been modelled with the software DigSilent PowerFactory.

For each scenario and case considered, several indexes have been directly – or after calculations – monitored: phase-voltage magnitudes at the worst bus, phase-ground magnitudes at both the sides of the MV/VL transformer, neutral potential at the worst bus, voltage unbalance factor at the worst bus and finally the relative and absolute system losses.

The simulation process involved the definition of several PV penetration percentage scenarios, under which three control options for the OLTC have been implemented: no control, 3-phase synchronous control and 1-phase decoupled control.

As first analysis several very unbalanced PV connection cases have been studied and it has been found out that the decoupled OLTC is able to improve the PV hosting capacity of the grid, since acceptable voltages, voltage unbalance factors and energy losses have been guaranteed.

After all more realistic PV connection configurations have been considered: the 50% of the total PV installed power connected to phase a, 30% to phase b and 20% to phase c. With this not too heavy unbalanced configuration, thanks to the decoupled phase-wise tap control, the maximum acceptable PV hosting capacity has grown from 140 kW (i.e. the 40%abc scenario) to 245 kW (i.e. the 70%abc scenario). In the process, the voltage unbalance factor has shown to be growing respect to the Base case as a result of the opposite trends in the positive and negative sequences magnitudes.

The second set of simulations are based on the consideration of inductive-capacitive reactive power injection from the photovoltaic inverters according to a particular $Q=f(V,P)$ law. Comparisons between the 1-phase cases in the scenarios with and without Q regulation have been performed: it has been found that if the PV power is too high (i.e. in the case of 280 kW, 80%abc case) the situation presents many undesired fluctuations, which make the control system unstable. The cause is due to the too high gain of reactive power regulation law, so that it has been decided to consider a different $Q=f(V,P)$ law, which compared to the previous one presents the same dead band but a different gain.

In general this PV reactive power control system brought benefits on the phase-neutral voltage deviations and on the neutral potential, but, since its control logic does not consider any voltage sequences analysis, it also involved undesired increases of the voltage unbalance factor.

A conclusion to this is that the DSO should take into account that if it issues reactive power regulation laws with a so high gain as in the first case, it could happen that fluctuations take place if a so important PV power amount is connected to the grid; in this case it should provide regulation laws with a smaller gain, so that it could be possible to accept such a high PV penetration.

About the increasing of the VUF, since in the extreme case it exceeds the limit of 3%, it should be remembered that it is not supposed to be controlled by the tap logic system, neither by the reactive power one. These negative effects on the VUF amounts have to be considered and taken into account by the DSO, which has to guarantee that it lies below the limits issued by the national and European technical standards, looking for other expedients.

The objective of future works is to extend the simulations analysis over a longer time period (weeks) and to run practical tests: the decoupled three-phase on load tap changer transformer will be experimentally tested using the SYSLAB-PowerLab.DK experimental facility at the DTU Risø Campus in 2015.

Chapter 6

Bibliography

- [1] “European Technical Standard EN 50160,” 2011.
- [2] M. Braun, T. Stetz, R. Bründlinger, C. Mayr, K. Ogimoto, H. Hatta, H. Kobayashi, B. Kroposki, B. Mather, and M. Coddington, “Is the distribution grid ready to accept large-scale photovoltaic deployment? State of the art, progress, and future prospects,” *Prog. photovoltaics Res. Appl.*, vol. 20, no. 6, pp. 681–697, 2012.
- [3] R. Caldon, M. Coppo, and R. Turri, “Distributed voltage control strategy for LV networks with inverter-interfaced generators,” *Electr. Power Syst. Res.*, vol. 107, no. 0, pp. 85–92, Feb. 2014.
- [4] B. Meersman, B. Renders, L. Degroote, T. Vandoorn, and L. Vandeveldel, “Three-phase inverter-connected DG-units and voltage unbalance,” *Electr. Power Syst. Res.*, vol. 81, no. 4, pp. 899–906, Apr. 2011.
- [5] T. Stetz, M. Kraiczy, M. Braun, and S. Schmidt, “Technical and economical assessment of voltage control strategies in distribution grids,” *Prog. Photovoltaics Res. Appl.*, vol. 21, no. 6, pp. 1292–1307, 2013.
- [6] Energinet.dk and DanishEnergyAssociaton, “Smart grid in Denmark 2.0,” 2012.
- [7] M. Stifter, R. Schwalbe, W. Tremmel, S. Henein, H. Brunner, B. Bletterie, A. Abart, F. Herb, and R. Pointner, “DG DemoNet: Experiences from volt/var control field trials and control algorithm advancements,” in *2012 3rd IEEE PES Innovative Smart Grid Technologies Europe (ISGT Europe)*, 2012, pp. 1–7.
- [8] M. Stifter, B. Bletterie, and F. Herb, “DG DemoNet: Impact of VOLT/VAR control on increasing the voltage band reserve — Results from field trial validations,” in *Electricity Distribution (CIRED 2013), 22nd International Conference and Exhibition on*, 2013, no. 0508, pp. 1–4.

- [9] M. Stifter, B. Bletterie, H. Brunner, D. Burnier, H. Sawsan, F. Andren, R. Schwalbe, A. Abart, R. Nenning, and F. Herb, "DG DemoNet validation: Voltage control from simulation to field test," in *Innovative Smart Grid Technologies (ISGT Europe), 2011 2nd IEEE PES International Conference and Exhibition on*, 2011, pp. 1–8.
- [10] F. Kupzog, H. Brunner, W. Pruggler, T. Pfajfar, and A. Lugmaier, "DG DemoNet-Concept-A new algorithm for active distribution grid operation facilitating high DG penetration," in *Industrial Informatics, 2007 5th IEEE International Conference on*, 2007, vol. 2, pp. 1197–1202.
- [11] M. Chindri, A. Cziker, A. Miron, H. B, and A. Iacob, "Propagation of Unbalance in Electric Power Systems."
- [12] V. Gosbell, S. Perera, and V. Smith, "Voltage Unbalance," *Integr. Energy - Power Qual. Cent. - Univ. Wollongong*, 2002.
- [13] A. A. Ansari and D. M. Deshpande, "Investigaion of performance of 3-phase asynchronous machine under voltage unbalance," *J. Theor. Appl. Inf. Technol.*, 2009.
- [14] S. Chattopadhyay, M. Mitra, and S. Sengupta, "Electric Power Quality," in *Electric Power Quality*, Springer, Dordrecht: Springer Netherlands, 2011.
- [15] S. Kurt and F. Delincé, "The importance of good power quality," *ABB Power Qual. Prod. Belgium*, pp. 1–20.
- [16] D. Chapman, "Power Quality Application Guide - the Cost of Poor Power Quality," 2001.
- [17] D. Dohnal, "On-load tap changers for power transformers," 2013.
- [18] A. Einfalt, F. Kupzog, H. Brunner, and A. Lugmaier, "Control strategies for smart Low voltage grids – the project DG DemoNet – smart LV grid," in *Integration of Renewables into the Distribution Grid, CIRED 2012 Workshop*, 2012, no. 0238, pp. 1–4.
- [19] "GRIDCON® TRANSFORMER - Datasheet." Maschinenfabrik Reinhausen GmbH.
- [20] "FITformer® REG - Datasheet." Siemens.
- [21] "DONG Energy." [Online]. Available: <http://www.dongenergy.com/>.
- [22] M. Coppo, R. Turri, M. Marinelli, and X. Han, "Voltage Management in Unbalanced Low Voltage Networks Using a Decoupled Phase-Tap-Changer Transformer," 2014.
- [23] "DIgSILENT GmbH - PowerFactory 15." User Manual, Gomaringen, Germany.
- [24] A. Constantin, R. D. Lazar, and K. S. Bækthøj, "Voltage control in low voltage networks by Photovoltaic inverters-PVNET.dk," 2012.

- [25] “Italian Technical Standard CEI 0-21.” Norma Italiana, 2012.
- [26] “German Technical Standard VDE-AR-N 4105.” FNN - Forum Netztechnik / Netzbetrieb im VDE, 2011.
- [27] K. Knezović, M. Marinelli, R. J. Møller, P. B. Andersen, C. Træholt, and F. Sossan, “Analysis of Voltage Support by Electric Vehicles and Photovoltaic in a Real Danish Low Voltage Network,” 2014.